https://doi.org/10.35662/unine-thesis-3210

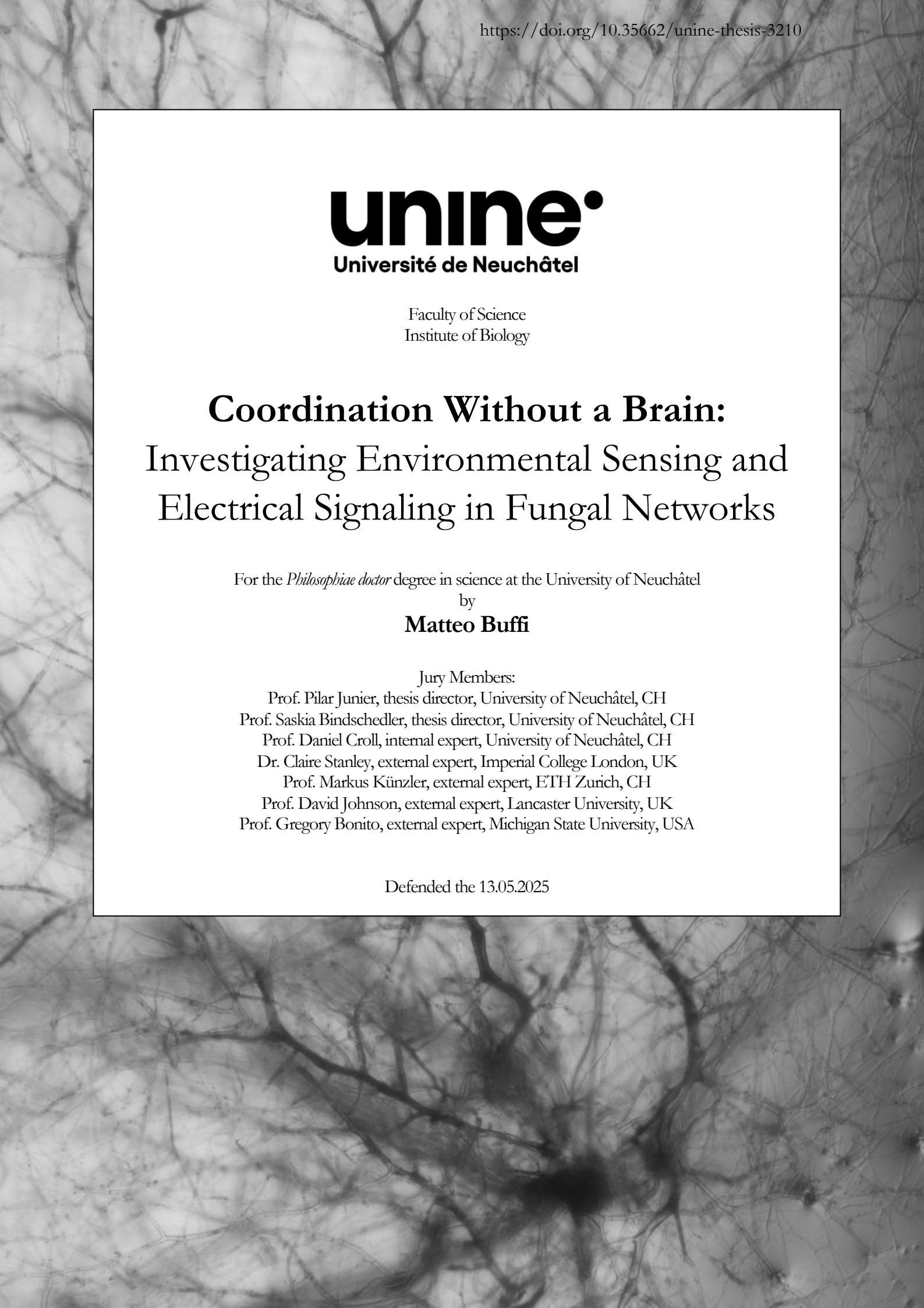

Université de Neuchâtel

Faculty of Science
Institute of Biology

Coordination Without a Brain: Investigating Environmental Sensing and Electrical Signaling in Fungal Networks

For the *Philosophiae doctor* degree in science at the University of Neuchâtel
by

Matteo Buffi

Jury Members:
Prof. Pilar Junier, thesis director, University of Neuchâtel, CH
Prof. Saskia Bindschedler, thesis director, University of Neuchâtel, CH
Prof. Daniel Croll, internal expert, University of Neuchâtel, CH
Dr. Claire Stanley, external expert, Imperial College London, UK
Prof. Markus Künzler, external expert, ETH Zurich, CH
Prof. David Johnson, external expert, Lancaster University, UK
Prof. Gregory Bonito, external expert, Michigan State University, USA

Defended the 13.05.2025

unine
Université de Neuchâtel
Faculté des sciences

Rue Emile-Argand 11
CH-2000 Neuchâtel
doctorat.sciences@unine.ch

IMPRIMATUR POUR THESE DE DOCTORAT

La Faculté des sciences de l'Université de Neuchâtel autorise l'impression de la présente thèse soutenue par

Monsieur Matteo BUFFI

Titre :

"Coordination Without a Brain: Investigating Environmental Sensing and Electrical Signalling in Fungal Networks"

sur le rapport des membres du jury composé comme suit :

- **Prof. Pilar Junier,** directrice de thèse, Université de Neuchâtel, Suisse
- **Prof. tit. Saskia Bindschedler,** co-directrice de thèse, Université de Neuchâtel, Suisse
- **Dr Claire Stanley,** Imperial College London, UK
- **Prof. Daniel Croll**, Université de Neuchâtel, Suisse
- **Prof. Markus Kuenzler,** ETHZ, Suisse
- **Prof. Gregory Bonito,** Michigan State University, USA
- **Prof. David Johnson**, Lancaster University, UK

Neuchâtel, le 2 octobre 2025

Le Doyen, Prof. P. Brunner

Dedico questa tesi di dottorato alla mia famiglia, senza la quale non avrei mai potuto arrivare fino a qui…

Acknowledgements

First and foremost, I would like to thank the University of Neuchâtel for providing me with the tools and opportunities to complete my doctoral studies. I am also deeply grateful to the entire university staff for fostering a pleasant and supportive work environment throughout these years.

I would like to express my deepest gratitude to my two thesis supervisors, Prof. Saskia Bindschedler and Prof. Pilar Junier. Thank you for believing in this project and allowing me to transition from my Master's to a PhD. Thank you for answering the thousands of questions—relevant or not—that I've thrown your way over the years. I am especially grateful for your honesty and candor, and for helping me not only grow as a researcher, but also as a person.

I would like to express my sincere gratitude to the Bioscience Division of Los Alamos National Laboratory for their financial support and invaluable assistance throughout the preparation of the manuscripts included in this thesis.

I would like to extend my heartfelt thanks to my thesis committee: Prof. Pilar Junier, Prof. Saskia Bindschedler, Dr. Claire E. Stanley, Prof. Markus Künzler, Prof. Gregory Bonito, Prof. Daniel Croll, and Prof. David Johnson. **To finish after defence - before printing**

I would like to thank my mid-thesis reviewers: Dr. Claire E Stanley, Prof. Markus Künzler, and Dr. Lukas Y Wick. Your insights and encouragement were essential in refocusing my project and gave me the motivation to move forward. In particular I thank:

Lukas: thanks for helping me set my priorities and your precious feedback directly inspired the development of my fourth chapter.

Markus: thank you for believing in my project and for the open exchanges we shared—I felt recognized and encouraged by our conversations.

Claire: thank you for your generous support, for helping with publications, and for the engaging moments shared with you and your team during our discussions about your fascinating research.

Many thanks to Dr. Guillaume Cailleau for your help in publications and the fruitful discussions.

A heartfelt thank you as well to Prof. Xiang-Yi Li Richter for the collaboration, and for motivating me and recognizing the value of my work. I truly appreciated it.

A huge thank you to Dr. Thierry Khun for your collaboration, and for all the time we spent problem-solving and developing new methods together. Your cheerfulness brought a joyful energy to many long workdays.

A heartfelt thank you to Prof. Lorenzo Pirrami and Prof. Daniel Oberson for your invaluable advice, assistance, and genuine interest in my research. I am grateful for the time and experience you shared with me.

Special thanks to Silvia Giangaspero for her help with data analysis and for the many fun and insightful conversations.

An infinite thank you to Maëlle Gross for our beautiful art-mycology collaboration and for lending me the equipment that turned out to be essential for completing this thesis. I look forward to more discussions and potential future collaborations.

A huge thank you to the entire Microbiology Laboratory at the University of Neuchâtel for creating such a welcoming environment. Special thanks to Ilona Palmieri for her help with experiments and for the hard work she puts into keeping such a large lab running smoothly. A heartfelt thank you as well to Matys Constantino—it was a pleasure working with you on various projects. Despite your young age, I learned a great deal from you.

My heartfelt thanks go to my office mates and dear friends, Danae Bregnard and Fabio Palmieri. These past years have undoubtedly been made brighter by your presence, your help, and the immense moral support you've given me. Thank you also for proofreading my documents throughout my thesis, and especially for the final revision of this manuscript. You are both wonderful people. Thank you for bearing with me.

A special thank you to Aislinn Estoppey, for teaching me so much both inside and outside the lab. Your help and our many long discussions have greatly enriched both my work and my personal development.

I also extend my warmest thanks to my colleagues in the B-office, Dr. Andrea Corona and Dr. Isha Ashmi. It was a pleasure to share this experience with you—thank you for your help, encouragement, and many thought-provoking conversations.

A profound thank you to my life partner, Aurora Ruggeri, not only for her many edits and corrections, but for being an unwavering supporter and true fan of my work. Your presence has helped me through the toughest moments. Our discussions contributed significantly to my research, including the development of the method used in my first chapter.

A sincere thanks to my great friend Geremia Losa, for mentoring me in the lab during my Master's, for your moral support, your contagious passion for fungi. An extended thanks to Mycocene, that gifted us colonized substrate with gourmet fungi to test our methods

My deepest gratitude to Valerio Foiada and Loïc Puthod, two incredible friends who came through in a moment of despair and helped me bring to life something I can truly be proud of. Thank you for the long days of work, for staying up late with me until 1 a.m. to finish an analysis and celebrate with champagne—those moments were priceless. Thank you as well for introducing me to your network of contacts, which was instrumental in developing my fourth chapter and to lend me your expertise and materials for my analyses.

To all my friends: thank you for listening to me over and over again, and for helping me put my failures into perspective. You kept me afloat when I needed it most.

To my mother, father, brother, and all my family: thank you for your constant support and encouragement. A special thank you to my parents—despite many sacrifices, you never let me lack for anything, and I owe much of where I am today to you.

A very special thank you to Polina To and Lili Po, my cats, for their companionship during long work sessions and for helping me manage the stress that came with this endeavor.

Abstract

Filamentous fungi form complex, highly adaptable mycelial networks capable of responding dynamically to their environment. These networks serve crucial ecological roles in nutrient cycling, organic matter decomposition, and maintaining soil health. Recent studies reveal that fungi utilize sophisticated regulatory mechanisms to optimize nutrient transport and communication across their extensive hyphal systems. This thesis explores how filamentous fungi regulate their mycelium in response to environmental stimuli, focusing on nutrient availability, electrical signalling pathways, and interactions with bacterial communities.

Through comprehensive literature review and experimental methodologies, this work examines how fungi integrate electrical signals to rapidly coordinate resource distribution and structural responses within their networks. Special attention is given to the concept of fungal electrical signalling as a communication method, highlighting its ecological significance and potential applications in biotechnology. Additionally, the development and application of innovative experimental platforms, such as the Fungal-Potential-Cards, are presented to demonstrate novel approaches for studying fungal signalling and mycelial behavior in controlled settings.

The findings emphasize the ecological and biotechnological implications of understanding fungal network organization, revealing potential for advancements in agriculture, environmental management, and bioengineering. Ultimately, this thesis contributes to a deeper understanding of fungal biology, highlighting the sophisticated capabilities of filamentous fungi as intelligent and responsive organisms within their ecological niches.

Keywords: Filamentous fungi; Mycelial network regulation; Bioelectrical signaling; Fungal–bacterial interactions; Fungal-Potential-Cards (experimental platform).

Résumé

Les champignons filamenteux forment des réseaux mycéliens complexes et très adaptables capables de répondre dynamiquement à leur environnement. Ces réseaux jouent des rôles écologiques essentiels dans le cycle des nutriments, la décomposition de la matière organique et le maintien de la santé des sols. Des études récentes montrent que les champignons utilisent des mécanismes régulateurs sophistiqués pour optimiser le transport des nutriments et la communication au sein de leurs systèmes hyphaux étendus. Cette thèse explore comment les champignons filamenteux régulent leur mycélium en réponse aux stimuli environnementaux, en se concentrant sur la disponibilité des nutriments, les voies de signalisation électrique et les interactions avec les communautés bactériennes.

À travers une revue exhaustive de la littérature et des méthodologies expérimentales, ce travail examine comment les champignons intègrent des signaux électriques pour coordonner rapidement la distribution des ressources et les réponses structurelles au sein de leurs réseaux. Une attention particulière est portée au concept de signalisation électrique fongique en tant que méthode de communication, soulignant son importance écologique et ses potentielles applications biotechnologiques. De plus, le développement et l'application de plateformes expérimentales innovantes, telles que les Fungal-Potential-Cards, sont présentés afin de démontrer de nouvelles approches pour étudier la signalisation fongique et le comportement du mycélium dans des conditions contrôlées.

Les résultats mettent en avant les implications écologiques et biotechnologiques liées à la compréhension de l'organisation des réseaux fongiques, révélant ainsi des potentiels de développement dans l'agriculture, la gestion environnementale et la bio-ingénierie. En fin de compte, cette thèse contribue à une compréhension approfondie de la biologie fongique, mettant en évidence les capacités sophistiquées des champignons filamenteux en tant qu'organismes intelligents et réactifs au sein de leurs niches écologiques.

Mots-clés : Champignons filamenteux ; Régulation des réseaux mycéliens ; Signalisation bioélectrique (électrique) ; Interactions fongiques–bactériennes ; Fungal-Potential-Cards (plateforme expérimentale).

Sommario

I funghi filamentosi formano reti miceliali complesse e altamente adattabili capaci di rispondere dinamicamente all'ambiente circostante. Queste reti svolgono ruoli ecologici cruciali nel ciclo dei nutrienti, nella decomposizione della materia organica e nel mantenimento della salute del suolo. Studi recenti rivelano che i funghi utilizzano sofisticati meccanismi regolatori per ottimizzare il trasporto dei nutrienti e la comunicazione attraverso i loro estesi sistemi ifali. Questa tesi esplora come i funghi filamentosi regolino il loro micelio in risposta agli stimoli ambientali, concentrandosi sui meccanismi di trasporto dei nutrienti, sulle vie di segnalazione elettrica e sulle interazioni con le comunità batteriche.

Attraverso una revisione completa della letteratura e metodologie sperimentali, questo lavoro esamina come i funghi integrino segnali elettrici per coordinare rapidamente la distribuzione delle risorse e le risposte strutturali all'interno delle loro reti. Particolare attenzione è dedicata al concetto di segnalazione elettrica fungina come metodo di comunicazione, evidenziandone l'importanza ecologica e le potenziali applicazioni biotecnologiche. Inoltre, lo sviluppo e l'applicazione di piattaforme sperimentali innovative, come le Fungal-Potential-Cards, vengono presentati per dimostrare nuovi approcci allo studio della segnalazione fungina e del comportamento del micelio in ambienti controllati.

I risultati sottolineano le implicazioni ecologiche e biotecnologiche derivanti dalla comprensione dell'organizzazione delle reti fungine, rivelando potenziali progressi in agricoltura, gestione ambientale e bioingegneria. In definitiva, questa tesi contribuisce a una più profonda comprensione della biologia fungina, evidenziando le sofisticate capacità dei funghi filamentosi come organismi intelligenti e reattivi all'interno delle loro nicchie ecologiche.

Parole chiave: Funghi filamentosi; Regolazione delle reti miceliari; Segnalazione bioelettrica (elettrica); Interazioni fungo–batteriche; Fungal-Potential-Cards (piattaforma sperimentale).

Zusammenfassung

Filamentöse Pilze bilden komplexe, hoch anpassungsfähige Myzel-Netzwerke, die dynamisch auf ihre Umgebung reagieren können. Diese Netzwerke erfüllen entscheidende ökologische Funktionen bei der Nährstoffzirkulation, dem Abbau organischer Stoffe und der Erhaltung der Bodengesundheit. Neuere Studien zeigen, dass Pilze ausgeklügelte regulatorische Mechanismen einsetzen, um den Nährstofftransport und die Kommunikation innerhalb ihrer ausgedehnten Hyphensysteme zu optimieren. Diese Arbeit untersucht, wie filamentöse Pilze ihr Myzel als Reaktion auf Umweltreize regulieren, mit besonderem Fokus auf Nährstofftransportmechanismen, elektrische Signalwege und Interaktionen mit bakteriellen Gemeinschaften.

Durch eine umfassende Literaturrecherche und experimentelle Methoden untersucht diese Arbeit, wie Pilze elektrische Signale integrieren, um die Ressourcenverteilung und strukturelle Anpassungen innerhalb ihrer Netzwerke schnell zu koordinieren. Besonderes Augenmerk liegt auf dem Konzept der elektrischen Signalübertragung bei Pilzen als Kommunikationsmethode, wobei deren ökologische Bedeutung und potenzielle Anwendungen in der Biotechnologie hervorgehoben werden. Zudem werden innovative experimentelle Plattformen, wie die „Fungal-Potential-Cards“, vorgestellt, die neue Möglichkeiten bieten, die pilzliche Signalübertragung und das Verhalten von Myzelien unter kontrollierten Bedingungen zu erforschen.

Die Ergebnisse verdeutlichen die ökologischen und biotechnologischen Implikationen eines vertieften Verständnisses der Organisation pilzlicher Netzwerke und zeigen Potenziale für Fortschritte in Landwirtschaft, Umweltmanagement und Bioengineering auf. Letztendlich trägt diese Arbeit zu einem tieferen Verständnis der Biologie filamentöser Pilze bei, indem sie deren hochentwickelte Fähigkeiten als intelligente und reaktionsfähige Organismen innerhalb ihrer ökologischen Nischen hervorhebt.

Keywords: Filamentöse Pilze; Regulation von Myzelnetzwerken; Bioelektrische Signalgebung; Pilz–Bakterien-Interaktionen; Fungal-Potential-Cards (experimentelle Plattform).

Table of Content

General introduction

Coordination Without a Brain: Investigating Environmental Sensing and Signaling in Fungal Networks

Strolling through the woods early in the morning, when the forest floor is still ruled by humidity, everyone has surely come across a cheerful and sometimes colourful, oddly shaped structure that—aside from a few exceptions—is easily recognizable as a mushroom. Yet, not everyone stops to wonder what it actually is: a plant? Even fewer realize that what they see is only the tip of the iceberg and that beneath their feet lies a vast and complex network, crucial not only to ecosystems but also to our society.

Through this thesis, I followed my curiosity to venture, even if only slightly, into the microscopic world where everything happens. Because from my point of view, it is not fungi that are microscopic; rather, we are too large, and by scaling everything from our own perspective, we often underestimate the importance of things we do not directly see or perceive.

1. Why Study Fungal Network Organization?

Fungi are among the most ancient, species-rich, and functionally diverse organisms on Earth, yet they remain one of the least explored kingdoms of life (Bengtson et al., 2017; Blackwell, 2011; Richards et al., 2017). Their influence extends across ecosystem dynamics, human health, and biotechnology, where they play crucial roles as decomposers, symbionts, pathogens, and biochemical innovators (Dighton, 2016; Grimm et al., 2005; Hyde et al., 2019; Meyer et al., 2016; Shah & Pell, 2003; Singh & Singh, 2014; Thatoi et al., 2013). Despite their ubiquity and ecological importance, our understanding of fungal biology is still in its infancy, particularly regarding their network organization, interactions with other organisms, and adaptations to terrestrial life.

From my point of view, one major reason for this underrepresentation in research is the lack of methods for observing fungi *in vivo*, a challenge largely due to their hidden lifestyle, dynamic behaviour, and structural plasticity. Many fungal species exist underground or within other organisms, making direct observation difficult. Their constantly evolving networks defy conventional models used to study other life forms, and as a distinct kingdom, they lack clear parallels with plants, animals, or bacteria, further complicating their

classification and study. Despite these challenges, fungi play a critical role in shaping ecosystems, influencing biodiversity, nutrient cycles, and symbiotic relationships. Their study thus contributes significantly to a deeper understanding of ecological resilience and sheds light on processes that help sustain life on Earth.

2. Fungi as Ecosystem Engineers: Understanding Their Ecological Roles

The ecological importance of fungi extends far beyond decomposition. They actively shape ecosystems, participating in nutrient cycling, symbiotic interactions, and even population control through parasitism. Their role as decomposers is fundamental, breaking down complex organic material like lignin and cellulose, facilitating nutrient release, and sustaining the carbon, nitrogen, and phosphorus cycles (Dighton, 2016; Newbound et al., 2010; Thatoi et al., 2013). Without fungi, for example, the accumulation of undecomposed organic matter would disrupt the balance of ecosystems, reducing nutrient availability for other organisms.

Fungi are also key symbionts, forming mutualistic associations with plants, animals, and microbes (Abeysinghe et al., 2020; Boddy, 2000; Evelin et al., 2009; Hart & Klironomos, 2003; Junier et al., 2021; Wood & Thomas, 1989). Mycorrhizal fungi, for example, enhance plant nutrient uptake, increase drought resistance, and are hypothesized to facilitate plant-to-plant communication via underground networks (Bonfante & Genre, 2010; Evelin et al., 2009; Gilbert & Johnson, 2017; Simard & Durall, 2011). Fungal endophytes, that live within plant tissues, often increase host resistance to environmental stressors, including drought, pathogens, and herbivory(Bruisson et al., 2019; de Lamo & Takken, 2020). These interactions make fungi essential for maintaining ecosystem stability and resilience, as they help organisms adapt to changing environmental conditions.

Even parasitic and pathogenic fungi, often perceived negatively, contribute to biodiversity regulation. Entomopathogenic fungi play a crucial role in controlling insect populations (Gielen et al., 2024), while fungal pathogens of plants and other fungi help shape species composition by preventing monoculture dominance (Ampt et al., 2022). Although parasitism can have destructive effects, particularly in human-managed environments (Fisher et al., 2020), in natural systems, it is a key driver of evolutionary pressure and ecosystem balance and resilience. Understanding fungal ecology is therefore crucial not only for defining their ecosystem services but also for identifying the conditions that allow fungi to shift between beneficial and harmful roles.

This perspective is also relevant for increasing awareness about fungi as commensal organisms in animals, highlighting the need for deeper knowledge regarding their role in animal health, disease, and within the animal holobiont. Such fungal contributions are often overlooked or underestimated, emphasizing the importance of further investigation.

3. The Double-Edged Impact of Fungi on Human Activities

Beyond their ecological functions, fungi have a profound and complex relationship with human activities, acting both as devastating pathogens and powerful industrial tools. Fungal diseases in plants, animals, and humans pose significant challenges to agriculture, food security, and public health (Almeida et al., 2019; Bongomin et al., 2017; Fisher et al., 2022), while fungal-derived products drive major innovations in medicine, biotechnology, and environmental sustainability. The growing impact of fungal pathogens is a major concern, particularly as climate change accelerates their spread and adaptability (Almeida et al., 2019; Casadevall, 2017, 2018; Garcia-Solache & Casadevall, 2010). Fungal infections already cause catastrophic losses in agriculture, with some estimates suggesting that around 15% of global food production is affected by fungal diseases annually, without considering post-harvest damage. Fungal pathogens were also the cause of famine and death in the past (Anand & Rajeshkumar, 2022).

In human health, thermal adaptation of fungi could bridge the temperature gap that has historically limited fungal infections in mammals (Garcia-Solache & Casadevall, 2010), increasing the risk of novel opportunistic pathogens. The development of antifungal drugs has also slowed, leaving limited treatment options for emerging fungal threats (Fisher et al., 2022; The Lancet Infectious Diseases, 2023). Understanding the mechanisms behind fungal persistence, immune evasion, and phenotypic plasticity is therefore critical for developing new antifungal strategies. Investigating fungal signaling and network coordination, particularly through ion channel regulation and electrical communication, could provide new avenues for antifungal drug discovery, potentially allowing for the repurposing of existing pharmaceuticals.

While fungi present challenges as pathogens, they are equally valuable as drivers of industrial and biotechnological innovation (Adrio & Demain, 2003; Grimm et al., 2005; Meyer, 2022; Meyer et al., 2020). Their ability to produce bioactive compounds has led to life-saving pharmaceuticals such as penicillin, cyclosporine, and statins, which collectively generate billions of dollars annually (Penicillin 11 Bil, *Penicillium spp.*, Cyclosporine A 2 Bil *Tolypocladium*

nivenum, and statins 30 Bil *Aspergillus terreus*) (Demain & Martens, 2016). In environmental applications, fungi are being explored for bioremediation, breaking down pollutants, heavy metals, and plastics. Some species can even contribute to electricity production through microbial fuel cells (Sekrecka-Belniak & Toczyłowska-Mamińska, 2018), harnessing their metabolic processes for sustainable energy solutions.

In food industries, fungal fermentation is essential for the production of staples like beer, cheese, soy sauce, and bread, demonstrating their widespread economic and cultural significance (Venturini Copetti, 2019). Furthermore, mushrooms, or fruiting bodies, are the most recognizable fungal forms and are valued for their culinary, medicinal, and economic importance, with species like white truffles (*Tuber magnatum*) reaching market values of up to 7,000 USD/kg (Čejka et al., 2023). They are also widely used in traditional medicine (Rizzo et al., 2021).

4. Bridging Fundamental Research with Future Applications

Despite their immense importance, fungi remain one of the least understood biological groups, with an estimated 95% of species still undiscovered (Hawksworth & Lücking, 2017). Advancing fungal research will require new methodologies for studying fungi in their natural environments, particularly in soil ecosystems, where they play critical roles in nutrient cycling, plant health, and microbial interactions(Akter et al., 2025; Ritz & Young, 2004). Investigating fungal signaling pathways, network organization, and adaptive mechanisms will not only improve our understanding of their ecological impact but also unlock new applications in human health, agriculture, and environmental technology.

By integrating ecological, microbiological, and biophysical perspectives, the study of fungi holds the potential to address major global challenges, from food security and climate resilience to disease control and biotechnological innovation. Though historically overlooked, fungi represent one of the most promising frontiers in science, offering unparalleled opportunities for discovery and application. Understanding their vast ecological roles and industrial potential is not just an academic pursuit—it is a necessity for shaping a more sustainable and resilient future.

5. Complexity for a Complex Environment: Soil

Fungi are found virtually everywhere. Yet, among the many ecosystems they inhabit, I would like to focus on what I consider the most important—and arguably the most complex—terrestrial ecosystem: soil.

Soils play a vital role in ecosystem services, from air and water purification to climate regulation and, most crucially, food production. A significant portion of nutrient cycling, particularly involving carbon, nitrogen, and phosphorus, takes place here. In many ways, we could argue that almost everything was, at some point, part of the soil—whether it be the food that nourishes us, the fibres that clothe us, or the elements that compose our bodies. Like fungi, soils are still vastly underexplored despite their recognized ecological importance, which continues to grow as new insights emerge (Pereira et al., 2018).

Described as the most complex biomaterial on Earth (Young & Crawford, 2004), soil is teeming with life. It is hypothesized that a single gram of healthy soil may contain more living organisms than there are humans who have ever lived. Rich in micro- and mesofauna, soil acts as a vast reservoir of microbial diversity (Fitter et al., 2005; Nannipieri et al., 2003; Phillips, 2017; Senesi & Wilkinson, 2008; Tiedje et al., 2009). Its structure is highly dynamic—constantly shifting in chemical composition—and physically heterogeneous, forming a three-dimensional matrix filled with diverse microniches (Ettema & Wardle, 2002; Tiedje et al., 2009).

Fungi, believed to be among the first organisms to adopt a terrestrial lifestyle, are also among the oldest living organisms still present today. They are thought to have dominated the terrestrial landscape around 500 million years ago (Moore, 2013). But what are the characteristics that have led to their success? How have they become ubiquitous in ecosystems? How did they colonize land and become essential parts, in concert with all the other organisms, of the resilience and utility of soils?

I do not yet claim to have personal answers to these fundamental questions. However, in this work, we focus on the fundamental organization of networks in filamentous fungi, as we believe this is central to the bio-socio architecture of soils.

6. The Filamentous Strategy: Growth Beyond the Cell

Filamentous fungi—perhaps less familiar than yeasts, their unicellular relatives—comprise the majority of molds and multicellular fungi. Their filamentous growth strategy, while not

exclusive to fungi, likely evolved as a fundamental adaptation to terrestrial environments (Moore, 2013). By extending narrow, branching tubes known as hyphae into the surrounding environment, these organisms overcome spatial limitations imposed by their immediate surroundings and can access resources dispersed across the complex three-dimensional matrix of soil.

This mode of growth is more than a strategy for nutrient acquisition—it is a way of being. The three-dimensional expansion of the mycelium serves not only exploration and colonization but also plays a crucial role in ecological interactions. As osmotrophs, fungi degrade complex organic compounds outside their bodies before absorption, a trait that has opened evolutionary pathways for cooperation, competition, and even exploitation by other organisms (Nagy et al., 2017; Richards et al., 2017). These externalized digestive and metabolic strategies position fungi as both architects and inhabitants of the intricate web of life in soils.

7. Building Networks: Architecture and Adaptability

The growth of filamentous fungi occurs through tip extension, leading to a three-dimensional radial expansion of hyphae—tube-like, branched structures that form extensive mycelial networks. These networks, which can range from millimetres to metres in scale, enable fungi to efficiently explore and colonize their environment, a strategy particularly well-suited, as mentioned above, for soil ecosystems (Grove & Bracker, 1970). Similar growth patterns are observed in other microorganisms with fungal-like characteristics, including certain bacteria and protists (Geisen et al., 2018; Wolf et al., 2013).

Adaptability to the complex 3D architecture of soils is a defining feature of filamentous fungi. This is facilitated by secondary hyphal growth through branching and by hyphal anastomosis, a process of cell-to-cell fusion that enhances network connectivity. Additionally, fungi dynamically regulate resource distribution within their mycelium, reallocating nutrients to specific regions while leaving other hyphae nearly devoid of cytoplasmic content. Over time, some sections of the network undergo autolysis, allowing them to be repurposed as a nutrient source (Jiang et al., 2022). These interconnected processes—branching, anastomosis, and autolysis—enable continuous reorganization of the mycelial network, optimizing nutrient acquisition and redistribution (Fischer & Glass, 2019; Harris, 2008; Rayner et al., 1995).

Recent work has shown that mycorrhizal fungi actively rewire their networks to improve bidirectional transport within the mycelium, facilitating efficient nutrient and carbon

exchange between the foraging point and the host root (Oyarte Galvez et al., 2025). This dynamic restructuring enhances fungal symbiosis with plants by optimizing resource allocation within the network, further underscoring the adaptability and complexity of fungal growth in soil environments (M. Fricker et al., 2007; Harris, 2008).

8. Architects of the Underground: Fungal Contributions to Soil Structure

Fungal colonization doesn't just occur in soil—it actively shapes it. The presence of fungal mycelia influences soil structure by aggregating particles, creating porous networks, and enhancing water and gas exchange. Their architecture transforms the soil environment, making it more hospitable to other life forms (Akter et al., 2025).

In this crowded and dynamic underground world, fungi act as engineers, predators, prey, and partners. Their networks serve as scaffolds for the movement and interaction of other organisms. One particularly striking example is the "fungal highway," where bacteria use the liquid film on hyphae as a dispersal medium, gaining access to otherwise unreachable regions of the soil (Junier et al., 2021; Losa & Bindschedler, 2018; Ritz & Young, 2004). This phenomenon contributes to microniche formation and increased biodiversity.

These interactions may also indirectly involve viruses (Périat et al., 2024; You et al., 2021), and likely include nematodes and other soil microfauna, further expanding the ecological connectivity of the underground environment. The extent to which different species can engage in such interactions is still being explored, particularly regarding what enables bacterial access to hyphae. Nevertheless, these relationships highlight the importance of fungal network organization and coordination—not just for fungal success, but for the structure and function of entire soil ecosystems.

9. Beneath the Surface: Nutrient Transport and Mycelial Coordination

The success of filamentous fungi lies not only in their expansive growth but also in their ability to coordinate activity across their networks. In a three-dimensional and resource-heterogeneous environment like soil, efficient transport of nutrients is essential—not just for survival, but for competition, symbiosis, and long-term resilience.

Short-distance transport can be sustained through direct uptake and intrahyphal diffusion, especially in resource-rich zones or in slow-growing fungi (Ashford & Allaway, 2007; Darrah et al., 2006; M. D. Fricker et al., 2017; Olsson, 2001; Olsson & Jennings, 1991a, 1991b). However, when the mycelium spans larger distances, more complex and energetically costly

redistribution mechanisms may be required (Cairney, 1992; Heaton et al., 2012; Jennings, 1994).

Passive transport via mass flow from water influx and efflux offers a low-cost alternative, but it comes with trade-offs: the large surface area of the mycelium increases the risk of water loss through evaporation (M. D. Fricker et al., 2017). Moreover, passive mechanisms alone cannot explain reversed nutrient flow in specialized fungal structures such as cords (Olsson & Gray, 1998) and trunk hyphae (Schmieder et al., 2019), which are involved in long-distance transport.

Recent studies on *Rhizophagus* species have shown bidirectional flow in nearly all hyphae, an essential feature for connecting foraging zones with plant hosts. Flow velocity also appears to scale with hyphal diameter—suggesting that fungi actively regulate transport speed within the network to optimize exchange (Oyarte Galvez et al., 2025). Pressure-driven redistribution, however, still struggles to explain how fungi coordinate activity across spatially distant regions (Roper & Seminara, 2019).

These findings suggest that filamentous fungi may employ a controlled cytoplasmic flow mechanism—especially in large, established networks or when acting as exchange hubs in symbiosis. A greater number of auxiliary hyphae connected to larger trunk hyphae might enhance transport flow, but such coordination would require precise network organization, for which data is still lacking. Overall, these observations point to the need for an additional or alternative process governing long-distance integration and modular behaviour in fungal networks.

10. Signaling Through Silence: Electrical Communication in Fungi

The ability to perceive and respond to environmental stimuli is fundamental to all living organisms, and electrical signaling serves as a rapid and efficient communication mechanism across diverse biological systems (Katz, 1961; Keener & Sneyd, 2009). While extensively studied in animals—where action potentials coordinate nervous system functions—evidence suggests that electrical signaling is widespread across all domains of life, including plants and bacteria (Brenner et al., 2006; Humphries et al., 2017; Prindle et al., 2015).

In fungi, early electrophysiological studies demonstrated action potential-like signals and electrical currents at hyphal tips (Armbruster & Weisenseel, 1983; Gow, 1984; Horwitz et al., 1984; Slayman et al., 1976; Slayman & Slayman, 1962; Stump et al., 1980) as reviewed in

Chapter 1, but the functional significance of these findings remained uncertain. Recent research has reignited interest in fungal electrical signaling, particularly in the context of soil ecosystems, where filamentous fungi play a critical role in nutrient cycling and plant interactions (Hunter, 2023).

Given the constraints of cytoplasmic flow and septal compartmentalization, electrical signaling could provide an alternative mechanism for long-distance coordination within mycelial networks—akin to systemic electrical responses in plants (Vodeneev et al., 2015). The structural properties of fungal hyphae, including hydrophobin-coated cell walls and melanin, may further influence their electrical conductivity, potentially playing a role in internal or external signal transmission (Kulkarni et al., 2017). The controversial "Wood Wide Web" hypothesis proposes that plants communicate via common mycorrhizal networks (CMNs) using electrical signals, based on observed changes in electrical activity at plant–fungus interfaces (Simard & Durall, 2011). However, the existence and ecological relevance of such communication remain debated (Karst et al., 2023).

Beyond their ecological roles, fungal electrical properties have garnered interest for biotechnological applications, including bioelectronic materials, fungal-based sensors, and "fungal computing", due to the apparent ability of mycelium to be induced to generate action potential-like signals (Hyde et al., 2024; Jo et al., 2023). However, significant challenges remain in applying traditional electrophysiological techniques to fungi, given the microscopic scale of hyphae and the complexity of mycelial networks. As research continues, understanding fungal electrical signaling alongside their dynamic structural adaptations may provide deeper insights into their role in ecosystems and their potential in technological innovation.

11. Exploring Intelligence Without a Brain: Toward a New Mycological Frontier

If fungal networks can detect, interpret, and respond to spatial stimuli across their bodies—without neurons or centralized control—then their behaviour borders on what some describe as "basal cognition." While the term remains debated, it emphasizes the challenges fungi pose to conventional models of intelligence and coordination.

This thesis explores how filamentous fungi perceive and process environmental cues through a combination of ecological realism and precise experimentation. Using a droplet-based

system, I introduced defined spatial stimuli and bacterial colonies to investigate fungal decision-making, interspecific interactions, and intra-mycelial signaling.

In parallel, I adapted and combined methods from microbiology, microscopy, biophysics, and electrophysiology to measure voltage potential across fungal networks—contributing to the growing field of fungal electrophysiology and offering new tools to probe long-distance coordination and network plasticity.

These investigations not only deepen our understanding of fungal biology but also highlight the extraordinary adaptability and complexity of these organisms. By uncovering how fungi integrate information and maintain coherence across vast networks, this work opens new avenues for applying fungal systems in biotechnology, health, and environmental sustainability—domains where fungi continue to shape life on Earth.

12. Thesis Outline and Research Questions

The central research question guiding this thesis is: do fungi communicate through electrical means in soils? To address this, I have defined specific objectives for each chapter. In Chapter 1, I explore the feasibility of visualizing electrical signals in fungal mycelia using recent, non-invasive techniques and investigate potential mechanisms underlying these signals to inform subsequent work. Chapter 2 examines whether fungi exhibit organized network architectures—assessing directional growth and probing the spatial distribution of any electrical activity under controlled conditions. Building on these insights, Chapter 3 introduces and refines methods for generating and controlling electrical signals, applying the system to inter-specific interactions between fungi and bacteria. Finally, Chapter 4 synthesizes the knowledge acquired in Chapters 1–3: evaluating the ubiquity of electrical signals within the mycelium, demonstrating the need for a novel detection approach, and establishing frequency-coding analysis as a more effective framework than traditional action-potential searches to understand how these signals contribute to fungal growth, environmental sensing, and inter-organismal communication.

Bibliography

Abeysinghe, G., Kuchira, M., Kudo, G., Masuo, S., Ninomiya, A., Takahashi, K., Utad, A. S., Hagiwara, D., Nomura, N., Takaya, N., Obana, N., & Takeshita, N. (2020). Fungal mycelia and bacterial thiamine establish a mutualistic growth mechanism. *Life Science Alliance*, *3*(12). https://doi.org/10.26508/LSA.202000878

Adrio, J. L., & Demain, A. L. (2003). Fungal biotechnology. *International Microbiology*, *6*(3), 191–199. https://doi.org/10.1007/S10123-003-0133-0/FIGURES/1

Akter, S., Mahmud, U., Shoumik, B. A. Al, & Khan, Md. Z. (2025). Although invisible, fungi are recognized as the engines of a microbial powerhouse that drives soil ecosystem services. *Archives of Microbiology 2025 207:4*, *207*(4), 1–28. https://doi.org/10.1007/S00203-025-04285-4

Almeida, F., Rodrigues, M. L., & Coelho, C. (2019). The Still Underestimated Problem of Fungal Diseases Worldwide. *Frontiers in Microbiology*, *10*(214). https://doi.org/10.3389/fmicb.2019.00214

Ampt, E. A., Francioli, D., van Ruijven, J., Gomes, S. I. F., Maciá-Vicente, J. G., Termorshuizen, A. J., Bakker, L. M., & Mommer, L. (2022). Deciphering the interactions between plant species and their main fungal root pathogens in mixed grassland communities. *Journal of Ecology*, *110*, 3039–3052. https://doi.org/10.1111/1365-2745.14012

Anand, G., & Rajeshkumar, K. C. (2022). *Challenges and Threats Posed by Plant Pathogenic Fungi on Agricultural Productivity and Economy* (pp. 483–493). https://doi.org/10.1007/978-981-16-8877-5_23

Armbruster, B. L., & Weisenseel, M. H. (1983). Ionic currents traverse growing hyphae and sporangia of the mycelial water moldAchlya debaryana. *Protoplasma*, *115*(1), 65–69. https://doi.org/10.1007/BF01293582

Ashford, A. E., & Allaway, W. G. (2007). Motile Tubular Vacuole Systems. *Biology of the Fungal Cell*, 49–86. https://doi.org/10.1007/978-3-540-70618-2_2

Bengtson, S., Rasmussen, B., Ivarsson, M., Muhling, J., Broman, C., Marone, F., Stampanoni, M., & Bekker, A. (2017). Fungus-like mycelial fossils in 2.4-billion-year-old vesicular basalt. *Nature Ecology and Evolution*, *1*. https://doi.org/10.1038/s41559-017-0141

Blackwell, M. (2011). The fungi: 1, 2, 3 ... 5.1 million species? *American Journal of Botany*, *98*, 426–438. https://doi.org/10.3732/ajb.1000298

Boddy, L. (2000). Interspecific combative interactions between wood-decaying basidiomycetes. *FEMS Microbiology Ecology*, *31*(3), 185–194. https://doi.org/10.1111/J.1574-6941.2000.TB00683.X

Bonfante, P., & Genre, A. (2010). Mechanisms underlying beneficial plant–fungus interactions in mycorrhizal symbiosis. *Nature Communications 2010 1:1*, *1*(1), 1–11. https://doi.org/10.1038/ncomms1046

Bongomin, F., Gago, S., Oladele, R. O., & Denning, D. W. (2017). Global and Multi-National Prevalence of Fungal Diseases—Estimate Precision. *Journal of Fungi*, *3*(4), 57. https://www.mdpi.com/2309-608X/3/4/57

Brenner, E. D., Stahlberg, R., Mancuso, S., Vivanco, J., Baluška, F., & Van Volkenburgh, E. (2006). Plant neurobiology: an integrated view of plant signaling. *Trends in Plant Science*, *11*(8), 413–419.

Bruisson, S., Zufferey, M., L'Haridon, F., Trutmann, E., Anand, A., Dutartre, A., De Vrieze, M., & Weisskopf, L. (2019). Endophytes and Epiphytes From the Grapevine Leaf Microbiome as Potential Biocontrol Agents Against Phytopathogens. *Frontiers in Microbiology*, *10*, 2726. https://doi.org/10.3389/fmicb.2019.02726

Cairney, J. W. G. (1992). Translocation of solutes in ectomycorrhizal and saprotrophic rhizomorphs. *Mycological Research*, *96*(2), 135–141. https://doi.org/10.1016/S0953-7562(09)80928-3

Casadevall, A. (2017). Don't forget the fungi when considering global catastrophic biorisks. *Health Security*, *15*(4), 341–342.

Casadevall, A. (2018). Fungal diseases in the 21st Century: the near and far horizons. *Pathogens & Immunity*, *3*(2), 183.

Čejka, T., Trnka, M., & Büntgen, U. (2023). Sustainable cultivation of the white truffle (Tuber magnatum) requires ecological understanding. *Mycorrhiza*, *33*(5–6), 291–302. https://doi.org/10.1007/S00572-023-01120-W/FIGURES/5

Darrah, P. R., Tlalka, M., Ashford, A., Watkinson, S. C., & Fricker, M. D. (2006). The vacuole system is a significant intracellular pathway for longitudinal solute transport in basidiomycete

fungi. *Eukaryotic Cell*, *5*(7), 1111–1125. https://doi.org/10.1128/EC.00026-06/SUPPL_FILE/SUPPLEMENTARY2.ZIP

de Lamo, F. J., & Takken, F. L. W. (2020). Biocontrol by Fusarium oxysporum Using Endophyte-Mediated Resistance. *Frontiers in Plant Science*, *11*, 1. https://doi.org/10.3389/FPLS.2020.00037

Demain, A. L., & Martens, E. (2016). Production of valuable compounds by molds and yeasts. *The Journal of Antibiotics 2017 70:4*, *70*(4), 347–360. https://doi.org/10.1038/ja.2016.121

Dighton, J. (2016). *Fungi in ecosystem processes* (Vol. 31). CRC press.

Ettema, C. H., & Wardle, D. A. (2002). Spatial soil ecology. In *Trends in Ecology and Evolution* (Vol. 17, Issue 4, pp. 177–183). Elsevier Ltd. https://doi.org/10.1016/S0169-5347(02)02496-5

Evelin, H., Kapoor, R., & Giri, B. (2009). Arbuscular mycorrhizal fungi in alleviation of salt stress: a review. *Annals of Botany*, *104*(7), 1263–1280. https://doi.org/10.1093/aob/mcp251

Fischer, M. S., & Glass, N. L. (2019). Communicate and Fuse: How Filamentous Fungi Establish and Maintain an Interconnected Mycelial Network. *Frontiers in Microbiology*, *10*(619). https://doi.org/10.3389/fmicb.2019.00619

Fisher, M. C., Alastruey-Izquierdo, A., Berman, J., Bicanic, T., Bignell, E. M., Bowyer, P., Bromley, M., Brüggemann, R., Garber, G., Cornely, O. A., Gurr, S. J., Harrison, T. S., Kuijper, E., Rhodes, J., Sheppard, D. C., Warris, A., White, P. L., Xu, J., Zwaan, B., & Verweij, P. E. (2022). Tackling the emerging threat of antifungal resistance to human health. *Nature Reviews Microbiology 2022 20:9*, *20*(9), 557–571. https://doi.org/10.1038/s41579-022-00720-1

Fisher, M. C., Gurr, S. J., Cuomo, C. A., Blehert, D. S., Jin, H., Stukenbrock, E. H., Stajich, J. E., Kahmann, R., Boone, C., Denning, D. W., Gow, N. A. R., Klein, B. S., Kronstad, J. W., Sheppard, D. C., Taylor, J. W., Wright, G. D., Heitman, J., Casadevall, A., & Cowen, L. E. (2020). Threats posed by the fungal kingdom to humans, wildlife, and agriculture. *MBio*, *11*(3). https://doi.org/10.1128/MBIO.00449-20/ASSET/84576E88-C8E9-466A-8318-793BA32AF729/ASSETS/GRAPHIC/MBIO.00449-20-F0001.JPEG

Fitter, A. H., Gilligan, C. A., Hollingworth, K., Kleczkowski, A., Twyman, R. M., & Pitchford, J. W. (2005). Biodiversity and ecosystem function in soil. *Functional Ecology*, *19*(3), 369–377. https://doi.org/10.1111/J.0269-8463.2005.00969.X

Fricker, M., Boddy, L., & Bebber, D. (2007). Network Organisation of Mycelial Fungi. In R. J. Howard & N. A. R. Gow (Eds.), *Biology of the Fungal Cell* (pp. 309–330). Springer Berlin Heidelberg. https://doi.org/10.1007/978-3-540-70618-2_13

Fricker, M. D., Heaton, L. L. M., Jones, N. S., & Boddy, L. (2017). The Mycelium as a Network. In *The Fungal Kingdom*. American Society of Microbiology. https://doi.org/doi:https://doi.org/10.1128/microbiolspec.FUNK-0033-2017

Garcia-Solache, M. A., & Casadevall, A. (2010). Global warming will bring new fungal diseases for mammals. *MBio*, *1*(1), e00061-10.

Geisen, S., Mitchell, E. A. D., Adl, S., Bonkowski, M., Dunthorn, M., Ekelund, F., Fernández, L. D., Jousset, A., Krashevska, V., Singer, D., Spiegel, F. W., Walochnik, J., & Lara, E. (2018). Soil protists: a fertile frontier in soil biology research. *FEMS Microbiology Reviews*, *42*(3), 293–323. https://doi.org/10.1093/FEMSRE/FUY006

Gielen, R., Ude, K., Kaasik, A., Põldmaa, K., Teder, T., & Tammaru, T. (2024). Entomopathogenic Fungi as Mortality Agents in Insect Populations: A Review. *Ecology and Evolution*, *14*, e70666. https://doi.org/10.1002/ece3.70666

Gilbert, L., & Johnson, D. (2017). Plant–plant communication through common mycorrhizal networks. In *Advances in Botanical Research* (Vol. 82, pp. 83–97). Elsevier.

Gow, N. A. (1984). Transhyphal electrical currents in fungi. *J Gen Microbiol*, *130*(12), 3313–3318. https://doi.org/10.1099/00221287-130-12-3313

Grimm, L. H., Kelly, S., Krull, R., & Hempel, D. C. (2005). Morphology and productivity of filamentous fungi. In *Applied Microbiology and Biotechnology* (Vol. 69, Issue 4, pp. 375–384). Springer. https://doi.org/10.1007/s00253-005-0213-5

Grove, S. N., & Bracker, C. E. (1970). Protoplasmic organization of hyphal tips among fungi: vesicles and Spitzenkörper. *Journal of Bacteriology*, *104*(2), 989–1009. https://doi.org/10.1128/JB.104.2.989-1009.1970

Harris, S. D. (2008). Branching of fungal hyphae: regulation, mechanisms and comparison with other branching systems. *Mycologia*, *100*(6), 823–832. https://doi.org/10.3852/08-177

Hart, M. M., & Klironomos, J. N. (2003). Diversity of arbuscular mycorrhizal fungi and ecosystem functioning. In *Mycorrhizal ecology* (pp. 225–242). Springer.

Hawksworth, D. L., & Lücking, R. (2017). Fungal Diversity Revisited: 2.2 to 3.8 Million Species. *Microbiology Spectrum*, *5*(4). https://doi.org/10.1128/MICROBIOLSPEC.FUNK-0052-2016/ASSET/A56131C0-D4D3-43FE-85ED-8C479B914E39/ASSETS/GRAPHIC/FUNK-0052-2016-FIG3.GIF

Heaton, L., Obara, B., Grau, V., Jones, N., Nakagaki, T., Boddy, L., & Fricker, M. D. (2012). Analysis of fungal networks. *Fungal Biology Reviews*, *26*(1), 12–29. https://doi.org/10.1016/J.FBR.2012.02.001

Horwitz, B. A., Weisenseel, M. H., Dorn, A., & Gressel, J. (1984). Electric Currents around Growing Trichoderma Hyphae, before and after Photoinduction of Conidiation. *Plant Physiology*, *74*(4), 912–916. https://doi.org/10.1104/pp.74.4.912

Humphries, J., Xiong, L., Liu, J., Prindle, A., Yuan, F., Arjes, H. A., Tsimring, L., & Süel, G. M. (2017). Species-Independent Attraction to Biofilms through Electrical Signaling. *Cell*, *168*(1–2), 200-209.e12. https://doi.org/10.1016/j.cell.2016.12.014

Hunter, P. (2023). The fungal grid. *EMBO Reports*, *24*(5). https://doi.org/10.15252/EMBR.202357255

Hyde, K. D., Baldrian, P., Chen, Y., Thilini Chethana, K. W., De Hoog, S., Doilom, M., de Farias, A. R. G., Gonçalves, M. F. M., Gonkhom, D., Gui, H., Hilário, S., Hu, Y., Jayawardena, R. S., Khyaju, S., Kirk, P. M., Kohout, P., Luangharn, T., Maharachchikumbura, S. S. N., Manawasinghe, I. S., … Walker, A. (2024). Current trends, limitations and future research in the fungi? *Fungal Diversity 2024 125:1*, *125*(1), 1–71. https://doi.org/10.1007/S13225-023-00532-5

Hyde, K. D., Xu, J., Rapior, S., Jeewon, R., Lumyong, S., Niego, A. G. T., Abeywickrama, P. D., Aluthmuhandiram, J. V. S., Brahamanage, R. S., & Brooks, S. (2019). The amazing potential of fungi: 50 ways we can exploit fungi industrially. *Fungal Diversity*, 1–136.

Jennings, D. H. (1994). Translocation in Mycelia. In *Growth, Differentiation and Sexuality* (pp. 163–173). Springer Berlin Heidelberg. https://doi.org/10.1007/978-3-662-11908-2_9

Jiang, L., Pettitt, T. R., Buenfeld, N., & Smith, S. R. (2022). A critical review of the physiological, ecological, physical and chemical factors influencing the microbial degradation

of concrete by fungi. *Building and Environment*, *214*, 108925. https://doi.org/10.1016/J.BUILDENV.2022.108925

Jo, C., Zhang, J., Tam, J. M., Church, G. M., Khalil, A. S., Segrè, D., & Tang, T. C. (2023). Unlocking the magic in mycelium: Using synthetic biology to optimize filamentous fungi for biomanufacturing and sustainability. *Materials Today Bio*, *19*, 100560. https://doi.org/10.1016/J.MTBIO.2023.100560

Junier, P., Cailleau, G., Palmieri, I., Vallotton, C., Trautschold, O. C., Junier, T., Paul, C., Bregnard, D., Palmieri, F., Estoppey, A., Buffi, M., Lohberger, A., Robinson, A., Kelliher, J. M., Davenport, K., House, G. L., Morales, D., Gallegos-Graves, L. V., Dichosa, A. E. K., … Chain, P. S. G. (2021). Democratization of fungal highway columns as a tool to investigate bacteria associated with soil fungi. *FEMS Microbiology Ecology*, *97*(2). https://doi.org/10.1093/FEMSEC/FIAB003

Karst, J., Jones, M. D., & Hoeksema, J. D. (2023). Positive citation bias and overinterpreted results lead to misinformation on common mycorrhizal networks in forests. *Nature Ecology & Evolution 2023 7:4*, *7*(4), 501–511. https://doi.org/10.1038/s41559-023-01986-1

Katz, B. (1961). How Cells Communicate. *Scientific American*, *205*(3), 209–221. http://www.jstor.org/stable/24937075

Keener, J., & Sneyd, J. (2009). Intercellular Communication. In J. Keener & J. Sneyd (Eds.), *Mathematical Physiology: I: Cellular Physiology* (pp. 347–384). Springer New York. https://doi.org/10.1007/978-0-387-75847-3_8

Kulkarni, S., Nene, S., & Joshi, K. (2017). Production of Hydrophobins from fungi. *Process Biochemistry*, *61*, 1–11. https://doi.org/https://doi.org/10.1016/j.procbio.2017.06.012

Losa, G., & Bindschedler, S. (2018). Enhanced tolerance to cadmium in bacterial-fungal Co-cultures as a strategy for metal biorecovery from e-waste. *Minerals*, *8*(4), 121.

Meyer, V. (2022). Connecting materials sciences with fungal biology: a sea of possibilities. *Fungal Biology and Biotechnology*, *9*(1), 1–4. https://doi.org/10.1186/S40694-022-00137-8/FIGURES/1

Meyer, V., Andersen, M. R., Brakhage, A. A., Braus, G. H., Caddick, M. X., Cairns, T. C., de Vries, R. P., Haarmann, T., Hansen, K., Hertz-fowler, C., Krappmann, S., Mortensen, U. H., Peñalva, M. A., Ram, A. F. J., & Head, R. M. (2016). Current challenges of research on

filamentous fungi in relation to human welfare and a sustainable bio-economy: A white paper. *Fungal Biology and Biotechnology*, *3*(1), 1–17. https://doi.org/10.1186/S40694-016-0024-8/TABLES/3

Meyer, V., Basenko, E. Y., Benz, J. P., Braus, G. H., Caddick, M. X., Csukai, M., De Vries, R. P., Endy, D., Frisvad, J. C., Gunde-Cimerman, N., Haarmann, T., Hadar, Y., Hansen, K., Johnson, R. I., Keller, N. P., Kraševec, N., Mortensen, U. H., Perez, R., Ram, A. F. J., … Wösten, H. A. B. (2020). Growing a circular economy with fungal biotechnology: a white paper. *Fungal Biology and Biotechnology 2020 7:1*, *7*(1), 1–23. https://doi.org/10.1186/S40694-020-00095-Z

Moore, D. (2013). Rise of the fungi. *Fungal Biology in the Origin and Emergence of Life*, 157–179. https://doi.org/10.1017/CBO9781139524049.012

Nagy, L. G., Toth, R., Kiss, E., Slot, J., Gacser, A., & Kovacs, G. M. (2017). Six Key Traits of Fungi: Their Evolutionary Origins and Genetic Bases. *The Fungal Kingdom*, 35–56. https://doi.org/10.1128/9781555819583.CH2

Nannipieri, P., Ascher, J., Ceccherini, M. T., Landi, L., Pietramellara, G., & Renella, G. (2003). Microbial diversity and soil functions. In *European Journal of Soil Science* (Vol. 54, Issue 4, pp. 655–670). John Wiley & Sons, Ltd. https://doi.org/10.1046/j.1351-0754.2003.0556.x

Newbound, M., Mccarthy, M. A., & Lebel, T. (2010). Fungi and the urban environment: A review. *Landscape and Urban Planning*, *96*(3), 138–145.

Olsson, S. (2001). Colonial Growth of Fungi. *Biology of the Fungal Cell*, 125–141. https://doi.org/10.1007/978-3-662-06101-5_6

Olsson, S., & Gray, S. N. (1998). Patterns and dynamics of 32P-phosphate and labelled 2-aminoisobutyric acid (14C-AIB) translocation in intact basidiomycete mycelia. *FEMS Microbiology Ecology*, *26*(2), 109–120.

Olsson, S., & Jennings, D. H. (1991a). A glass fiber filter technique for studying nutrient uptake by fungi: The technique used on colonies grown on nutrient gradients of carbon and phosphorus. *Experimental Mycology*, *15*(4), 292–301. https://doi.org/10.1016/0147-5975(91)90032-9

Olsson, S., & Jennings, D. H. (1991b). Evidence for diffusion being the mechanism of translocation in the hyphae of three molds. *Experimental Mycology*, *15*(4), 302–309. https://doi.org/10.1016/0147-5975(91)90033-A

Oyarte Galvez, L., Bisot, C., Bourrianne, P., Cargill, R., Klein, M., van Son, M., van Krugten, J., Caldas, V., Clerc, T., Lin, K. K., Kahane, F., van Staalduine, S., Stewart, J. D., Terry, V., Turcu, B., van Otterdijk, S., Babu, A., Kamp, M., Seynen, M., … Shimizu, T. S. (2025). A travelling-wave strategy for plant–fungal trade. *Nature 2025 639:8053*, *639*(8053), 172–180. https://doi.org/10.1038/s41586-025-08614-x

Pereira, P., Bogunovic, I., Muñoz-Rojas, M., & Brevik, E. C. (2018). Soil ecosystem services, sustainability, valuation and management. *Current Opinion in Environmental Science & Health*, *5*, 7–13. https://doi.org/10.1016/J.COESH.2017.12.003

Périat, C., Kuhn, T., Buffi, M., Corona-Ramirez, A., Fatton, M., Cailleau, G., Chain, P. S., Stanley, C. E., Wick, L. Y., Bindschedler, S., Gonzalez, D., Richter, X. Y. L., & Junier, P. (2024). Host and nonhost bacteria support bacteriophage dissemination along mycelia and abiotic dispersal networks. *MicroLife*, *5*. https://doi.org/10.1093/femsml/uqae004

Phillips, J. D. (2017). Soil Complexity and Pedogenesis. *Soil Science*, *182*(4), 117–127. https://doi.org/10.1097/SS.0000000000000204

Prindle, A., Liu, J., Asally, M., Ly, S., Garcia-Ojalvo, J., & Süel, G. M. (2015). Ion channels enable electrical communication in bacterial communities. *Nature*, *527*, 59. https://doi.org/10.1038/nature15709
https://www.nature.com/articles/nature15709#supplementary-information

Rayner, A. D. M., Griffith, G. S., & Ainsworth, A. M. (1995). Mycelial interconnectedness. In *The growing fungus* (pp. 21–40). Springer.

Richards, T. A., Leonard, G., & Wideman, J. G. (2017). What Defines the "Kingdom" Fungi? *The Fungal Kingdom*, 57–77. https://doi.org/10.1128/9781555819583.CH3

Ritz, K., & Young, I. M. (2004). Interactions between soil structure and fungi. *Mycologist*, *18*(2), 52–59. https://doi.org/10.1017/S0269915X04002010

Rizzo, G., Goggi, S., Giampieri, F., & Baroni, L. (2021). A review of mushrooms in human nutrition and health. *Trends in Food Science & Technology*, *117*, 60–73. https://doi.org/10.1016/J.TIFS.2020.12.025

Roper, M., & Seminara, A. (2019). Mycofluidics: the fluid mechanics of fungal adaptation. *Annual Review of Fluid Mechanics*, *51*, 511–538.

Schmieder, S. S., Stanley, C. E., Rzepiela, A., van Swaay, D., Sabotič, J., Nørrelykke, S. F., deMello, A. J., Aebi, M., & Künzler, M. (2019). Bidirectional Propagation of Signals and Nutrients in Fungal Networks via Specialized Hyphae. *Current Biology*, *29*(2), 217-228.e4. https://doi.org/https://doi.org/10.1016/j.cub.2018.11.058

Sekrecka-Belniak, A., & Toczyłowska-Mamińska, R. (2018). *Fungi-Based Microbial Fuel Cells*. *11*(10), 2827. http://www.mdpi.com/1996-1073/11/10/2827

Senesi, N., & Wilkinson, K. J. (2008). Biophysical chemistry of fractal structures and processes in environmental systems. In *Biophysical Chemistry of Fractal Structures and Processes in Environmental Systems* (Vol. 11). Wiley,. https://doi.org/10.1002/9780470511206

Shah, P. A., & Pell, J. K. (2003). Entomopathogenic fungi as biological control agents. *Applied Microbiology and Biotechnology*, *61*(5–6), 413–423. https://doi.org/10.1007/S00253-003-1240-8/TABLES/1

Simard, S. W., & Durall, D. M. (2011). Mycorrhizal networks: a review of their extent, function, and importance. *Https://Doi.Org/10.1139/B04-116*, *82*(8), 1140–1165. https://doi.org/10.1139/B04-116

Singh, A. P., & Singh, T. (2014). Biotechnological applications of wood-rotting fungi: A review. *Biomass and Bioenergy*, *62*, 198–206.

Slayman, C. L., Scott Long, W., & Gradmann, D. (1976). "Action potentials" in NEUROSPORA CRASSA, a mycelial fungus. *Biochimica et Biophysica Acta (BBA) - Biomembranes*, *426*(4), 732–744. https://doi.org/https://doi.org/10.1016/0005-2736(76)90138-3

Slayman, C. L., & Slayman, C. W. (1962). Measurement of Membrane Potentials in Neurospora. *Science*, *136*(3519), 876–877. https://doi.org/10.1126/SCIENCE.136.3519.876

Stump, R. F., Robinson, K. R., Harold, R. L., & Harold, F. M. (1980). Endogenous electrical currents in the water mold Blastocladiella emersonii during growth and sporulation. *Proceedings of the National Academy of Sciences*, *77*(11), 6673–6677.

Thatoi, H., Behera, B. C., & Mishra, R. R. (2013). Ecological role and biotechnological potential of mangrove fungi: a review. *Mycology*, *4*(1), 54–71.

The Lancet Infectious Diseases. (2023). An exciting time for antifungal therapy. *The Lancet. Infectious Diseases*, *23*(7), 763. https://doi.org/10.1016/S1473-3099(23)00380-8

Tiedje, J. M., Cho, J. C., Murray, A., Treves, D., Xia, B., & Zhou, J. (2009). Soil teeming with life: new frontiers for soil science. In *Sustainable management of soil organic matter* (pp. 393–425). CABI. https://doi.org/10.1079/9780851994659.0393

Venturini Copetti, M. (2019). Yeasts and molds in fermented food production: an ancient bioprocess. *Current Opinion in Food Science*, *25*, 57–61. https://doi.org/10.1016/J.COFS.2019.02.014

Vodeneev, V., Akinchits, E., & Sukhov, V. (2015). Variation potential in higher plants: Mechanisms of generation and propagation. *Plant Signaling & Behavior*, *10*(9), e1057365. https://doi.org/10.1080/15592324.2015.1057365

Wolf, A. B., Vos, M., De Boer, W., & Kowalchuk, G. A. (2013). Impact of Matric Potential and Pore Size Distribution on Growth Dynamics of Filamentous and Non-Filamentous Soil Bacteria. *PLOS ONE*, *8*(12), e83661. https://doi.org/10.1371/JOURNAL.PONE.0083661

Wood, T. G., & Thomas, R. J. (1989). *The mutualistic association between Macrotermitinae and Termitomyces*. 69–92.

You, X., Kallies, R., Kühn, I., Schmidt, M., Harms, H., Chatzinotas, A., & Wick, L. Y. (2021). Phage co-transport with hyphal-riding bacteria fuels bacterial invasion in a water-unsaturated microbial model system. *The ISME Journal 2021 16:5*, *16*(5), 1275–1283. https://doi.org/10.1038/s41396-021-01155-x

Young, I. M., & Crawford, J. W. (2004). Interactions and self-organization in the soil-microbe complex. *Science*, *304*(5677), 1634–1637.

https://doi.org/10.1126/SCIENCE.1097394/SUPPL_FILE/1097394S2.MOV

Chapter 1

Electrical signaling in fungi: past and present challenges

Published: 21 March 2025

FEMS Microbiology Reviews

DOI: https://doi.org/10.1093/femsre/fuaf009

Contributions:

Matteo Buffi, contributed to the study conception and design. Material preparation, data collection and analysis and to the writing of the manuscript.

FEMS Microbiology Reviews, 2025, **45**, fuaf009

DOI: 10.1093/femsre/fuaf009
Advance access publication date: 21 March 2025
Review Article

Electrical signaling in fungi: past and present challenges

Matteo Buffi[1], Julia M. Kelliher[2,3], Aaron J. Robinson[2], Diego Gonzalez[1], Guillaume Cailleau[1], Justine A. Macalindong[2], Eleonora Frau[4], Silvia Schintke[4], Patrick S.G. Chain[2], Claire E. Stanley[5], Markus Künzler[6], Saskia Bindschedler[1], Pilar Junier[1,*]

[1]Laboratory of Microbiology, Institute of Biology, University of Neuchâtel, CH-2000, Neuchâtel, Switzerland
[2]Bioscience Division, Los Alamos National Laboratory, Los Alamos, NM 87545, United States
[3]Microbiology, Genetics, and Immunology Department, Michigan State University, East Lansing, MI 48824, United States
[4]Laboratory of Applied NanoSciences (COMATEC-LANS), University of Applied Sciences and Arts Western Switzerland (HES-SO), CH-1401, Yverdon-les-Bains, Switzerland
[5]Department of Bioengineering, Imperial College London, SW7 2AZ, London, United Kingdom
[6]Institute of Microbiology, Department of Biology, ETH Zürich, CH-8093, Zürich, Switzerland
*Corresponding author. E-mail: Laboratory of Microbiology, Institute of Biology, University of Neuchâtel, CH-2000, Neuchâtel, Switzerland, pilar.junier@unine.ch
Editor: [Bart Thomma]

Abstract

Electrical signaling is a fundamental mechanism for integrating environmental stimuli and coordinating responses in living organisms. While extensively studied in animals and plants, the role of electrical signaling in fungi remains a largely underexplored field. Early studies suggested that filamentous fungi generate action potential-like signals and electrical currents at hyphal tips, yet their function in intracellular communication remained unclear. Renewed interest in fungal electrical activity has fueled developments such as the hypothesis that mycorrhizal networks facilitate electrical communication between plants and the emerging field of fungal-based electronic materials. Given their continuous plasma membrane, specialized septal pores, and insulating cell wall structures, filamentous fungi possess architectural features that could support electrical signaling over long distances. However, studying electrical phenomena in fungal networks presents unique challenges due to the microscopic dimensions of hyphae, the structural complexity of highly modular mycelial networks, and the limitations of traditional electrophysiological methods. This review synthesizes current evidence for electrical signaling in filamentous fungi, evaluates methodological approaches, and highlights experimental challenges. By addressing these challenges and identifying best practices, we aim to advance research in this field and provide a foundation for future studies exploring the role of electrical signaling in fungal biology.

Keywords: electrical signaling; modularity; filamentous fungi; ion channels; mycelium

Introduction

For all living organisms, sensing environmental stimuli and integrating this information to generate a response are fundamental processes for survival. There are several mechanisms that organisms use for this coordination, including electrical signaling. Electrical signaling constitutes a rapid and reliable way of intra- and intercellular communication (Katz 1961, Keener and Sneyd 2009).

Speculation about the importance of electricity in the functioning of a living organism dates back to 1780, following Luigi Galvani's seminal observation of muscle contraction in response to electrical currents (Piccolino 1998). Since this discovery, the connection between electricity and biology has been extensively investigated (Piccolino 1998, Canales et al. 2018). The role of electricity in cellular communication has been primarily investigated in animals, in particular mammals, given its importance for the functioning of the nervous system. In animal models, the transmission of an electrical signal between cells is driven by action potentials that result from specific stimuli. Briefly, action potentials are defined as a response to changes in voltage across the cell membrane, which result from ion (e.g. Na^+, Ca^{2+}, or K^+) redistribution across the membrane. Depolarization that causes the cell to reach a certain voltage threshold generates a "spike" that is characteristic of these action potentials, which can then propagate along a cell and pass between adjacent cells (Häusser 2000).

Electrical signaling is now recognized to be ubiquitous across all domains of life, from bacteria to animals and plants (Piccolino 1998, Brenner et al. 2006, Prindle et al. 2015). However, the mechanisms and outcomes of electrical signaling vary across these domains. For instance, processes mediated by electrical signaling for cell-to-cell communication include the excitation of muscles by nerves in animals (Piccolino 1998), the rapid closing of stomata or leaf traps in *Dionaea muscipula* (the Venus flytrap plant) (Böhm et al. 2016, Blatt 2024), and tissue regeneration and organization in plants (Nuccitelli 1988, 2003, Brenner et al. 2006, Clarke et al. 2013, Beagle and Lockless 2015, Prindle et al. 2015, Levin et al. 2017, Szechyńska-Hebda et al. 2017, McLaughlin and Levin 2018) and animals (Harris 2021). Unicellular organisms, such as bacteria found in biofilms, also utilize electrical signaling to aid in community coordination and response to environmental changes (Prindle et al. 2015).

In fungi, diverse electrophysiological behaviors, including the generation of action potential-like signals (Olsson and Hansson 1995) or the generation of currents in the hyphal tips (Stump et al. 1980, Gow 1984, Horwitz et al. 1984) were shown in studies conducted in the late 20th century. However, the role of electrical sig-

Received 31 January 2025; **revised** 13 March 2025; **accepted** 20 March 2025

naling as a mechanism of intracellular communication was not irrefutably shown in these early studies, and progress in the field stalled. Recent studies have sparked renewed interest in the topic, particularly in relation to the importance of filamentous fungi in soil ecosystems (Hunter 2023). The hypothesis of a "Wood Wide Web" considers plants being connected to each other via the common mycorrhizal network (CMN) (Simard and Durall 2011) and being able to communicate with each other using electrical signaling. This hypothesis is partly based on measurements of electrical currents in the plant–fungus interaction zone in roots, as well as the induction of changes in transmembrane potentials in germ tubes of mycorrhizal fungi exposed to plant root extracts (Berbara et al. 1995, Ayling et al. 2000). Although this highlights the potential importance of fungal electrical signaling at the level of ecosystems, the existence of the CMN and its role in interspecies communication is still highly debated (Karst et al. 2023). On the other hand, the proposed use of fungal mycelium for the generation of innovative materials with electric conductive properties such as sensors or so-called fungal computers (Li et al. 2022, Meyer 2022, Jo et al. 2023, Mayne et al. 2023, Hyde et al. 2024, Jones et al. 2024) has also contributed to the renewed interest in the area.

Fungi are a clade of eukaryotic microorganisms with remarkably diverse physiologies and metabolisms and can perform numerous ecological functions. Morphologically, fungi range from unicellular yeast to multicellular forms such as molds and mushrooms (James et al. 2020). Regardless of the apparent morphological complexity of one or the other growth mode, yeast and filamentous fungi are important models to study fundamental processes of eukaryotic cells (van der Klei and Veenhuis 2006). Moreover, filamentous fungi have been used by humankind as versatile and robust cell factories, but to exploit their full potential we need to overcome the limited knowledge of fungal biology (Meyer et al. 2016).

Multicellular filamentous fungi are tip growing organisms showing a radial three-dimensional growth of tube-like structures called hyphae. This morphology can be considered ideally suited for electrical signaling as hyphae contain a continuous plasma membrane and cell wall. Furthermore, the cell wall can be coated with hydrophobins (i.e. surface active amphiphile proteins) (Wösten and de Vocht 2000, Linder et al. 2005, Kulkarni et al. 2017) and other compounds such as melanin. These structural components and the cell wall polysaccharides could have a potential role in insulating the interior of the fungal cell, preventing electrical leaking, a function carried out by myelin in neurons (Morell and Quarles 1999). Filamentous fungi from basal clades (i.e. Mucoromycota) often have coenocytic (continuous cytoplasm) hyphae, but higher fungi (Dikarya) utilize septal pores to compartmentalize their hyphae continuum (Rayner et al. 1995, Fricker et al. 2007, Harris 2008). These pores regulate the exchange and transport of nutrients, macromolecules, organelles, and play a role in cellular differentiation and reproduction (Fischer 1999, Abadeh and Lew 2013). Septa can be closed by plugging to prevent loss of cytoplasm content after hyphal damage (Markham 1994, Steinberg et al. 2017), or in response to deleterious biological interactions such as mycoparasitism (Gimeno et al. 2021). This means that the cytoplasm in Dikarya is not always continuous and the propagation of chemical signals via cytoplasmic bulk flow can be inefficient. Conversely, plasma membrane continuity and, thus, electrical signaling, are not affected by septal pore plugging (Gow and Morris 1995, Roper and Seminara 2019). In this way, electrical signaling could still allow for communication between distant hyphae within a mycelial network, even during times of distress or physical disruption.

A fascinating feature of multicellular fungi is the formation of a mycelium, consisting of a network of interconnected hyphae that can grow, branch, fuse, and adapt dynamically to environmental conditions (Fricker et al. 2017). The formation of such networks allows filamentous fungi to improve nutrient acquisition and translocation (Rayner et al. 1995, Harris 2008, Fricker et al. 2017, Fischer and Glass 2019). The mycelial network is a highly dynamic structure and its plasticity in space and time allows fungi to cope with uneven or ephemeral distribution of resources in complex environments such as soils (Hutchings et al. 2000). The mycelium is inherently modular and provides an architecture that results in the adaptability needed to exploit resources and thrive in heterogeneous environments (Fig. 1). Each hyphal segment functions semiindependently, enabling the organism to allocate resources flexibly and respond locally to stimuli such as nutrient availability or stress. Experiments performed with wood rotting fungi have shown that network structure can change very rapidly when new resources are discovered by a foraging mycelial front (Wood et al. 2006). The speed and extent of the reorganization depend not only on the foraging strategy, but also on the size and quality of the new resource, and the presence of competitors (Wood et al. 2006). This observed capability to rapidly reorganize suggests the existence of one or several systems to integrate information from different areas in a mycelial network.

Direct uptake and intrahyphal nutrient diffusion are considered sufficient to sustain short-range local growth when resources are abundant (Olsson 2001) or in slow-growing fungal species (Olsson and Jennings 1991a, b, Darrah et al. 2006, Ashford and Allaway 2007, Fricker et al. 2017). In other conditions, multiple transport pathways (Jennings 1987, Cairney 1992, Heaton et al. 2012) or pressure-driven delocalization of resources have been suggested as mechanisms behind nutrient redistribution (Lew 2011). The cost of these strategies is expected to increase the longer the distance (i.e. meters) to be covered in the mycelial network (Fricker et al. 2017). Passive movement with the mass flow resulting from the influx–efflux of water could provide a less costly alternative. However, this creates a risk of excessive evaporation given the high surface area resulting from an extensive mycelial network (Fricker et al. 2017). Moreover, passive movement cannot explain the inversed flux of nutrients observed in fungal structures such as fungal cords (Olsson and Gray 1998), which are specialized structures made of densely packed hyphae used for transport of nutrients and water over long distances (Townsend 1954). Inversed cytoplasmic movement has also been observed in other specialized hyphae such as trunk hyphae (Schmieder et al. 2019). Recent work mapped and observed bidirectional flow in almost all hyphae of *Rhizophagus irregularis* A5, *R. irregularis* C2, and *Rhizophagus aggregatum*. The fungal partners exchange nutrients with roots and thus bidirectional flow is essential to connecting the foraging point to the plant host. A higher flow speed in larger hyphae suggest the control of speed by the fungus to increase the volume exchanged in larger and more direct trunk hyphae (Oyarte Galvez et al. 2025). Pressure-driven delocalization is also difficult to reconcile with behaviors performed in distant areas of the mycelium (Roper and Seminara 2019). These examples suggest that filamentous fungi need a mechanism to control cytoplasmic flow, especially when the mycelium is extended and/or when it acts as an exchange channel between two points. A larger volume from a higher number of auxiliary hyphae connected to larger trunk hyphae could explain an increased flow. However, this requires a fine

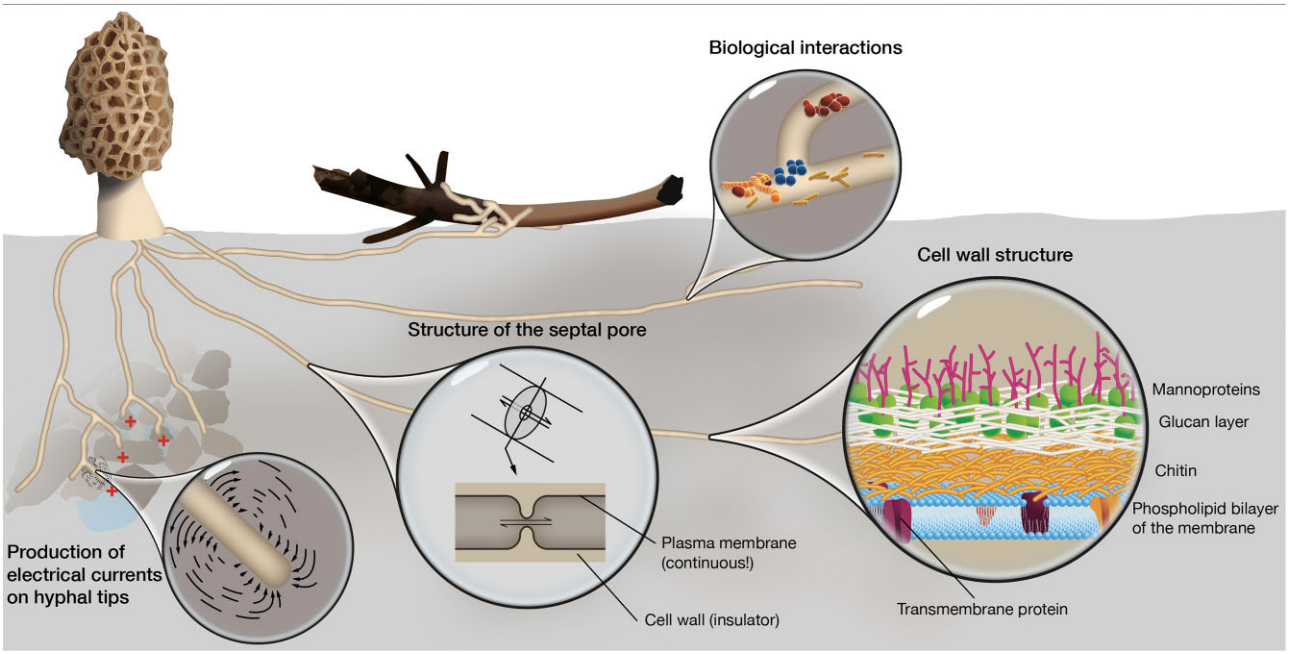

Figure 1. Organization of a mycelial network. In soils, the mycelium needs to integrate a multitude of stimuli to coordinate the reorganization of its hyphal network. This allows to improve nutrient acquisition and exploration and colonization of complex habitats. This decentralized growth strategy underpins many unique features of fungal biology, including interactions with other organisms. Studying how mycelial networks integrate information across multiple spatial and temporal scales presents unique challenges, including the high spatial heterogeneity of actively growing structures such as hyphal tips, where electrical currents are known to be produced. Moreover, morphological elements such as septal pores, as well as the structure and composition of the cell, appear ideally suited for electrical signaling.

control of network organization, and there is no data available for the moment that supports this hypothesis. All of the above pledges in favor of a different process for long-distance network coordination as well as for coordinating the modular behavior of the mycelial network.

In other organisms such as animals, integration and response to environmental stimuli is coordinated by the nervous system, which uses electrical signaling for fast responses. However, the use of electrical signaling for communication and coordination of responses to environmental stimuli in plants shows that a central nervous system is not a requirement. In plants, electrical signaling regulates slower responses (e.g. response time in minutes to hours) primarily for adapting to environmental stresses and regulating physiological processes, but it is also used in faster processes such as the closing of the Venus' fly trap or mimosa leaves. Electrical signaling in plants is mediated by the production of action potentials with the same key characteristics of those in animals, but with important differences in the molecular components of depolarization. While Na^+ ions are important in the generation of action potentials in animals, plants are thought to require Ca^{2+} and Cl^-, probably due to the high toxicity of sodium. Resting membrane potentials for plants are around −120 mV compared to the −70 mV for animals. Lastly, the speed of signal propagation in plants is typically slower than that in animals (for instance, 5–25 cm s^{-1} in the Venus flytrap versus 0.1–100 m s^{-1} in nerves) (Lee and Calvo 2023). In addition, electrical signaling in plants also includes the generation of variation and systemic potentials (Zimmermann et al. 2009, Vodeneev et al. 2015). Variation potentials are long-distance intercellular electrical signals to coordinate functional responses under stressors. Like in the case of action potentials, variation potentials are created by transient membrane depolarization, although the dynamics of membrane potential changes are different (Vodeneev et al. 2015). Similar to plants, fungi are sessile organisms that cannot escape stressors such as predators or nutrient scarcity, but must adapt locally. Accordingly, electrical signaling such as variation and systemic potentials could be some of the mechanisms behind the coordinated behavior of mycelial networks (Vodeneev et al. 2015).

The goal of this review is to provide an overview of the current evidence for the existence of electrical signaling in filamentous fungi and the challenges of applying traditional electrophysiological techniques for this specific type of microorganism. These challenges are not only due to the small dimensions of individual hyphae and the differentiation of cells (e.g. hyphal tip), but also to the spatial complexity of modular mycelial networks. In the second part of this review, we present a critical assessment of current methods and expose experimental caveats that we have encountered while trying to obtain novel evidence for electrical signaling in filamentous fungi. The objective of this second part is to help other research groups to avoid costly pitfalls and to encourage future studies in the area.

Electrophysiological phenomena in fungi

In electrophysiology, one distinguishes two kinds of measurements, voltage and current. Voltage, or electrical potential, corresponds to a measure of the difference in charge between two points in an electrical field. In biological systems, this is often the membrane potential created by the differences in ion concentrations inside and outside of a cell (i.e. across membranes) (Kamada 1934, Curtis and Cole 1942). Monitoring changes in the membrane potential allows for the characterization of the process of depolarization and repolarization that occur during an action potential (Curtis and Cole 1942). In contrast, current is the flow of electrical charge per unit of time (per second). In biological systems, this can correspond to the movement of ions across membranes (e.g.

through ion channels) or, in some cases, charge conduction along cells via electrons, ions, or specialized structures such as those observed in cable bacteria (Boschker et al. 2021). Overall, the studies published so far suggest that the currents transmitted along fungal hyphae are either of low intensity (μA cm^{-2}) (Gow and Morris 1995) or low voltage (nV to μV), resulting in values lower than those that have been observed along animal neurons that are in the mV range (Olsson and Hansson 1995). Accordingly, a recording method needs to be not only adapted to the magnitude of currents to be measured, but it also requires spatial awareness as to where to perform the recordings given the potential complexity and diversity of mycelial networks. For instance, multiple studies have demonstrated that specific areas of the mycelium are active upon predator attack (Schmieder et al. 2019) or during the nutritional exchange with plant hosts in mycorrhizal fungi (Oyarte Galvez et al. 2025). The latter study also showed highly dynamic network remodeling. Accordingly, it can be supposed that electrical signaling will not occur equally in all areas of the mycelial network, nor that all hyphae or even hyphal segments are equally involved in the conduction of the signal. Thus, it is essential to understand and control where and what should be measured to avoid the creation or measurement of artifacts or to generalize the behavior from single point observations to the entire modular organism as in the case of filamentous fungi. In this section, we will first present studies focusing on measuring electrical potential in fungi, and then address the existence of ion channels in this microbial group. An overall summary of relevant studies related to measuring electrical signaling and their findings is presented chronologically in Table 1. However, in the next sections, the discussion of the results was organized accordingly to the approach used or the electrophysiological process investigated.

Electrical measurements in microscopic fungal structures

The study of electrical signaling in microscopic fungal structures has been difficult due to technical challenges, particularly in recording internal currents in hyphae. Two of the most traditional methods to record action potentials are the voltage or current clamp. The patch clamp method, introduced by Neher and Sakmann in 1974 (Neher and Sakmann 1976) using frog muscle fibers, enabled the direct measurement of ion channel activity. This method involves forming a high-resistance seal between a glass pipette and a small patch of the cell membrane, allowing for the measurement of membrane potential and ionic currents with high precision (Neher and Sakmann 1992). Traditional patch-clamp techniques are reliable and widely applied in biological systems (Hamill et al. 1981, Zhao et al. 2008), but face limitations in fungal hyphae mainly due to their size (2–10 μm), but also to the presence of a cell wall and its associated proteins (Martinac et al. 2008). Accordingly, measurements with this approach have been mainly conducted in protoplasts obtained through enzymatic digestion on fungi-like cells of the oomycete *Saprolegnia ferax* (Garrill et al. 1992, 1993, Garrill and Davies 1994), or by laser ablation of the cell wall in *Aspergillus niger* (Roberts et al. 1997). Very recently, a novel method was utilized for nano-surgical ablation of the cell wall across multiple locations, which provides a new approach for protoplast generation in living hyphae that can be amenable to future patch-clamp studies of ion channels and their properties in filamentous fungi (Pajić et al. 2024).

In spite of all the challenges, electrophysiological behaviors have been studied since the late 20th century in several fungal species (Gow 1984, Harold et al. 1985, Gow and Morris 1995). The first studies were based on the use of intracellular glass microelectrodes. For this, sharp electrodes are used to penetrate the cell membrane, allowing researchers to record voltage (differential between two points in the colony or between the inside and outside of the cell membrane). This type of approach has been particularly useful for measuring the resting membrane potential and action potentials in neurons, providing insights into cellular excitability (Brette and Destexhe). The method can be applied to several types of microorganisms, and the first intracellular electrical recording ever made was the measurement of the resting membrane potential in *Paramecium* (Takeo Kamada 1934). The first example of their use in fungi was the detection of electrical currents in the apex of growing hyphae in *Neurospora crassa*. Differences in membrane potential between the colony border (i.e. apex region) and the area toward the center of the colony were linked to polarized growth (Slayman and Slayman 1962). Glass microelectrodes inserted with micromanipulators to penetrate the fungal cell wall were also used for recording spontaneous voltage fluctuations resembling action potentials in fungi (Slayman et al. 1976, Olsson and Hansson 1995). Conventional glass microelectrodes were directly inserted into the hyphae of *N. crassa*. The spontaneous action potential-like behavior in this species involved depolarization and repolarization of the membrane with an apparent refractory period, similar to action potentials (Slayman et al. 1976). In another study with cords of *Armillaria bulbosa*, similar action potential-like signals were induced when the growing mycelium contacted a piece of beech wood that was initially placed 1–2 cm away from the colony (Olsson and Hansson 1995). The signals recorded in cords were measured using a glass microelectrode that was inserted among the mycelial strands, with a reference electrode inserted into the agar medium. *Pleurotus ostreatus* was tested with the same approach, and similar results (i.e. recording of action potential-like signals) were obtained in so-called "looser" tissue located at the edges of the colony. In both cases, the rate of spontaneous firing was very similar (frequency of 0.5–5 Hz and amplitude of 5–50 mV) to that recorded in animal sensory systems. However, this invasive approach could have altered fungal behavior, potentially compromising the validity of the data. In addition, as shown by this pioneering work, this approach cannot be generalized to all cell types of filamentous fungi, as the recordings were unsuccessful with undifferentiated hyphae (Olsson and Hansson 1995).

Further studies were possible thanks to the development of extracellular vibrating electrodes that allow the extracellular recording of hyphae-generated currents (Jaffe and Nuccitelli 1974, Nuccitelli 1990). Vibrating microelectrodes are used primarily to measure extracellular ion flow and electric fields. This technique involves the vibration of a microelectrode at a fixed frequency, which helps to detect small changes in voltage related to ionic movement in tissues. This approach is particularly useful in studying bioelectric fields generated by excitable tissues such as the heart and nervous system in a less invasive manner (Dorn and Weisenseel 1982, Nuccitelli 1990). Vibrating microelectrodes have been employed in various studies to measure currents around growing hyphal tips, during sporulation, and in response to light stimuli (Stump et al. 1980, Gow 1984, Horwitz et al. 1984). The first studies in fungi were inspired by the measurements of a positive current entering the rhizoid and leaving by the thallus in the aquatic fungus *Blastocladiella emersonii*, in which the current was believed to be carried by protons (Stump et al. 1980). Similar studies with the oomycete *Achyla* showed that currents were driven by a proton flow (inwards in the tip and outwards in the region away from it and toward the center of the colony) (Armbruster and Weisenseel 1983, Kropf et al. 1984). In *Achlya*, the use of intracellular microelectrodes afterwards helped

Table 1. Summary of relevant studies related to measuring electrical signaling and their findings is presented chronologically.

Year	Author(s)	Fungus or fungi investigated	Other organisms	Method used	Studied structure	Key observations	Proposed function (when applicable)
1962	Slayman and Slayman	*Neurospora crassa*		Microelectrodes	Hyphae	Membrane potential changes induced by potassium. Reduction of membrane potential in response to sodium azide or nystatin	Membrane potential could be at the basis of foraging and environmental sensing
1974	Jaffe and Nuccitelli		Fucoid embryo	Development of extracellular vibrating microelectrodes	Embryo	Measurements of current in a developping embryo	Methological milestone allowing for a less invasive extracellular method to measure currents
1976	Slayman et al.	*Neurospora crassa*		Glass microelectrodes	Hyphae	Detection of autonomous action potentials	Undefined function
1976	Neher and Sakmann		Frog muscle fibers	Development of the patchclamp method	Muscle cells	Study of single transmembrane channels in neuromuscle signal transmission	Methodological milestone allowing to study the role of transmembrane ion-gated channels in signal transmission
1980	Stump et al.	*Blastocladiella emersonii*		Extracellular vibrating microelectrodes	Mycelium	Current patterns appear to play a role in the spatial localization of fungal growth and development	Possible function in growth and development
1983	Barbara, Armbruster and Weisenseel		*Achlya debaryana* (Oomycete)*	Extracellular vibrating microelectrodes	Hyphae and sporangia	Relationship between currents and the formation of asexual sporangia	Involvement of currents in development
1984	Kropf et al.		*Achlya bisexualis* (Oomycete)*	Extracellular vibrating microelectrodes	Hyphae	Transcellular electric currents associated to a proton/amino acid symporter	Amino acid (nutrient) absorbtion and hyphal polarization during growth
1984	Gow	*Neurospora crassa*, *Aspergillus nidulans*, *Schizophyllum commune*, *Mucor mucedo*, and *Coprinopsis cinerea*		Extracellular vibrating microelectrodes	Hyphae	All growing hyphae tested produced currents, but not hyphae that were not growing. The signal was proportional to the size of hyphae	Involvement of electrical current in growth of different fungi

Table 1. Continued

Year	Author(s)	Fungus or fungi investigated	Other organisms	Method used	Studied structure	Key observations	Proposed function (when applicable)
1984	Horwitz et al.	*Trichoderma harzianum*		Extracellular vibrating microelectrodes	Hyphae	Light stimulated formation of conidia. Inward currents at the tip and outer currents along hyphae.	Early biophysical reaction to light
1984	Potapova et al.	*Neurospora crassa*		Microelectrodes	Hyphae	Membrane potential responds to blue light illumination	Response to blue light
1986	Kropf		*Achlya bisexualis* (Oomycete)*	Microelectrodes	Hyphae	Depolarization caused by respiratory inhibitors	Intra cellular communication in response to stressors
1986	McGillivray and Gow	*Neurospora crassa*, *Aspergillus nidulans*, *Mucor mucedo*, and *Trichoderma harzianum*	*Achlya bisexualis* (Oomycete)*	Electrophoresis machine	Mycelium	Electrical fields affect the polarity of growth including germ tube formation and branching, the direction of hyphal extension and the frequency of branching and germination	Polarity of hyphal growth may be under electrical control
1988	Youatt et al	*Allomyces macrogynus*		Extracellular vibrating microelectrodes	Rhizoids and hyphae	Outward flow of positive electrical current behind the apex and inward flow around rhizoids	Localized nutrient transport linking symport of nutrients (e.g. amino acids or phosphate) with protons
1989	Gow	*Allomyces macrogynus* and *Basidiobolus ranarum*	*Achlya bisexualis* (Oomycete)*	Extracellular vibrating microelectrodes	Rhizoids and hyphae	Electrical currents are driving the expansion of the hyphal apex or maintaining cell polarity	Inward electrical current reflects local nutrient transport and not local cell growth
1992	Garril et al.		*Saprolegnia ferax* (Oomycete)*	Patch clamp	Protoplasts in different areas of the hyphae and hyphal tips	Presence of large Stretch-activated Ca^{2+} and K^+ permeable channels and a small Mg^{2+} in the hyphal tip, and the first two along the hyphae	Participation of Strech-activated channels in tip growth and Ca^{2+}-activated K^+ channels in turgor pressure

Table 1. Continued

Year	Author(s)	Fungus or fungi investigated	Other organisms	Method used	Studied structure	Key observations	Proposed function (when applicable)
1993	Garril et al.		*Saprolegnia ferax* (Oomycete)*	Patch clamp	Protoplasts in different areas of the hyphae and hyphal tips	Inhibitory effect of gadolinium on growth and on Stretch-activated Ca^{2+} channels at the tips. Inhibtion of Ca^{2+}-activated K^+ channels along hyphae by tetraethylammonium, causing a rapid but transient decrease in growth	Stretch-activated Ca^{2+} permeable channels as sensors for hyphal tip mechanical stress. Entry of Ca^{2+} at the tip is foundamental for growth
1994	Garrill and Davies		*Saprolegnia ferax* (Oomycete)*	Patch clamp	Protoplasts in different areas of the hyphae and hyphal tips	Direct measurement of ion channels on the membrane	Cell signaling, cell polarity, pH regulation, growth and differentiation, reproduction, nutrient uptake, turgor regulation, and pathology
1995	Olsson and Hansson	*Armillaria bulbosa* and *Pleourotus ostreatus*		Glass microelectrodes	Cords and "loose" tissue	Recording action potential-like signals in response to external stimuli	Sensing and communication in distant areas of the mycelium
1995	Berbara et al.	*Gigaspora margarita*	*Trifolium repens* and *Daucus carota*	One dimensional vibrating probe	Hyphae	Electrophysiological dimension to the plant fungus interaction and modulation of ion transport in the early events iof a mycorrhizal symbiosis	Modulating mycorrhizal interaction with roots and spore germination
1997	Roberts et al	*Aspergillus niger*		Patch clamp	Ablated hyphae	Description of an anion-selective efflux channel in the plasma membrane	Role of Cl^- efflux on tip growth and pH homeostasis
2018	Adamatzky	*Pleurotus djamor*		Subdermal needle electrodes	Fruiting bodies	Recording of trains of spikes (action potential-like signals) in fruit bodies that was correlated with translocation of nutrients and relocation of products of metabolism	Use of action potentials in physiology and communication

Table 1. Continued

Year	Author(s)	Fungus or fungi investigated	Other organisms	Method used	Studied structure	Key observations	Proposed function (when applicable)
2021	Adamatzky and Gandia	*Ganoderma resinaceum*		Subdermal needle electrodes	Fruiting bodies	Similarities between trains of spikes in another mushroom-forming species	Action potential-like spikes may correspond to fungal language
2022	Adamatzky	*Omphalotus nidiformis*, *Flammulina velutipes*, *Schizophyllum commune*, and *Cordyceps militaris*		Subdermal needle electrodes	Fruiting bodies	Species-specific spikes patterns	Action-potential-like spikes resemble human speech
2022	Thomas and Cooper	*Glomus intraradices*, *Glomus aggregatum*, *Glomus mosseae*, and *Glomus etunicatum*	*Pisum sativum* and *Cucumis sativus*	Glass microelectrodes (in the plant stems)	Interface plant–fungi	Transfer of electrical signals from one plant to the other	Interspecies communication
2024	Fukasawa et al.	*Pholiota brunnescens*		Six subdermal electrodes around a Petri dish	Mycelium	Electrical signal transfer and whole-body integration in fungal mycelia	Participation of electrical currents in fungal behavior
2024	Jones et al.	*Curvularia lunata*		Copper electrodes	Mycelium	Tissues from the fungus could potentially serve as a component in low-frequency biosensors for signal transmission	Mycelium as a biosensor
2024	Pajić et al.	*Phycomyces blakesleeanus*		Nano surgical ablation of cell wall + patch clamp	Hyphae	New faster and less invasive laser for laser ablation of the cell wall	Methodological milestone allowing future studies on the role of transmembrane ion-gated channels in signal transmission

*Oomycetes were classified at the time as fungi.

to demonstrate that respiratory inhibitors produce the rapid depolarization of the membrane, indicating that membrane potential is governed by an electrogenic ion pump (Kropf 1986). The initial work with vibrating microelectrodes in *B. emersonii* and *Achlya* was later replicated with filamentous fungi including *N. crassa*, *Aspergillus nidulans*, *Schizophyllum commune*, *Mucor mucedo*, and *Coprinopsis cinerea*, all of which generated electrical currents (varying between 0.05 and 0.60 μA cm^{-2}) around their hyphal tips (Gow 1984). Furthermore, the formation of light-stimulated conidia in *Trichoderma harzianum* was also proposed to be the result of electrical currents of different intensities applied along the hyphae. The modification of the currents in the membrane (outwards current in the sites stimulated by the light) was recorded 1–2 h after photoinduction (Horwitz et al. 1984). Similar experiments performed with microelectrodes and using blue light as stimulus suggested light-induced responses in *N. crassa*. The response in this case may not occur in every cell but the signal can be transmitted to the adjacent cells by means of electrical or chemical communication (Potapova et al. 1984).

The generation of inward electrical currents in the apex was initially linked to the regulation of the direction of growth of hyphae. The proposed model suggested that currents in the apex helped the directional growth of hyphae by providing a mechanism (i.e. establishing intracellular electrophoretic fields) explaining the movement of vesicles from the hyphal tip to the apex (Gow 1984). Accordingly, a study applying an external electric field showed that sites of germ tube formation and branching, the direction of hyphal extension, and the frequency of branching and germination can be affected by electric fields in some filamentous fungi including *N. crassa*, *A. nidulans*, *M. mucedo*, and *T. harzianum* (McGillivray and Gow 1986). However, another study measuring electrical currents with vibrating electrodes using the aquatic fungus *Allomyces macrogynus*, which produces true hyphae and rhizoids, presupposed a different behavior given its unique mechanism of cell wall deposition. Consequently, measurements with extracellular vibrating electrodes showed outward positive electrical currents around hyphae regardless of their growth status (extending or nonextending). In contrast, inward currents were detected in the rhizoids. The authors also did not find evidence indicating the role of calcium, while sites of nutrient uptake were correlated with inward electrical currents (Youatt et al. 1988). A follow-up study including *A. macrogynus* together with the soil fungus *Basidiobolus ranarum*, and the oomycete *Achyla bisexualis*, showed that inward electrical currents reflect local nutrient transport and not local cell growth, by linking together proton and nutrient symport (Gow 1989). Overall, these studies suggest that the role of electric currents on the hyphal tips in the redirection of growth cannot be generalized (Potapova 2012).

The use of vibrating microelectrodes is not without drawbacks. They are difficult to build and to operate correctly. Furthermore, the vibrating nature of the electrode can disturb biological processes (Jaffe and Nuccitelli 1974). Moreover, as the recordings are done extracellularly, they are often susceptible to background noise interference, thus requiring the inclusion of carefully designed controls and the use of systems such as a Faraday cage, which has been included in some but not all studies published so far. Recording signals in single hyphae does not only pose a problem due to the small size of individual hyphae relative to the electrode (usually on the order of 5 μm), but also by the complex organization of the fungal mycelium. When grown on a solid substrate such as an agar-based medium, it is virtually impossible to study individual hyphae, which can differ in their signaling activity, due to factors such as age or conditions of the local environment. This has been clearly shown, for instance, in experiments investigating the coordination of the response of *C. cinerea* to attacks by fungivorous nematodes. In this case, only specialized hyphae (called trunk hyphae) were shown to propagate chemical defense signals, while no activity was observed for a large fraction of the rest of the mycelial network (Schmieder et al. 2019).

The initial discovery of endogenous electrical fields at the hyphal tips prompted follow-up studies evaluating the effect of external electrical fields on the polarity of fungal growth as mentioned previously (McGillivray and Gow 1986). Fungi have shown both galvanotropic behavior, i.e. change of the direction of growth in response to an electrical field (Lever et al. 1994, Brand and Gow 2009) and electrotactic behaviors, i.e. active movement of a motile cell (e.g. zoospores) in response to an electrical field (Morris and Gow 1993, Swafford and Oakley 2018). The model organism *Candida albicans* has been fundamental to understanding the mechanism by which electrical fields affect the direction of growth. Germination experiments have shown that electrical fields modify the position of germ tubes likely by inducing the influx of Ca^{2+} via the voltage-gated channel Cch1. This is supported by deletion of Cch1 or in medium containing a pharmacological Ca^{2+}-channel blocker (i.e. BAPTA), which resulted in a severe attenuation of galvanotropism. Reciprocally, the response was enhanced in media with high extracellular Ca^{2+} concentration (Brand et al. 2007). The galvanotropic response of hyphae of *A. nidulans*, *N. crassa*, and *C. cinerea* was pH- and Ca^{2+}-dependent, suggesting also the implication of voltage-gated channels (Lever et al. 1994), as in the case of *C. albicans*.

Electrotaxis of zoospores of fungi-like oomycetes such as *Pythium* was triggered by electric fields of the same magnitude as those measured in plant roots (Morris and Gow 1993). Likewise, electrotaxis could be among the sensory mechanisms directing the movement of motile zoospores in zoosporic fungi. Wounding is known to generate an endogenous electric field in both plants and animals. In animals, this endogenous electric field serves to guide the movement of epithelial cells and other cells involved in wound healing to the wound site. In plants, these currents can lead to local hydraulic pressure and to a systemic potential trough the phloem to activate defenses (Tyler 2017). In accordance with the existence of this endogenous electric fields in their potential hosts, electrotaxis could participate in the localization of a suitable site for plant infection such as wounded areas. Zoosporic fungi are typically characterized as saprobes or parasites of both plant and animal hosts. Their zoospores have a finite amount of endogenous energy reserves and must locate quickly a suitable substrate or host. During dispersal of the zoosporic life stage, interpretation of environmental cues is critical for the survival and success of the future colony, and enhanced germination has been shown in weak electric fields (Moratto et al. 2023). Recently, an experimental system has been developed using zoospores of the saprotroph *Allomyces arbusculus*. This system demonstrated the combined role of photo and chemotaxis as part of a multisensory system acting during dispersal and settlement of zoospores (Swafford and Oakley 2018). This model could be used in future studies to evaluate the role of characteristic endogenous electric fields of a root or epidermis wounds (Jia et al. 2021) in guiding zoospore movement. The mechanisms explaining electrotaxis have not been elucidated in detail, but as in the case of galvanotropism, earlier studies suggest that this electro-guided movement is associated with Ca^{2+} transport across the membrane (Morris and Gow 1993).

Moreover, fungi have been found to display thigmotropism (Jaffe et al. 2002, Stephenson et al. 2014), which is a direc-

tional growth movement in response to a touch stimulus. Thigmotropism is modulated by electric signaling in other organisms such as plants and animals (Sibaoka 1966, Jaffe et al. 2002). In *C. albicans*, thigmotropism, like galvanotropism, is attenuated by decreased Ca^{2+} availability. Deletion of *CCH1* or the genes encoding two other transmembrane Ca^{2+} channels (i.e. Fig. 1 or Mid1—a mechanosensor channel that activates calcium influx via Cch1), reduces the sensitivity of hyphal tips to topographical features in the substratum. These observations suggest that a localized Ca^{2+} signal modulated by specific plasma-membrane Ca^{2+} channels relay topologic information to direct tip growth (Brand et al. 2007, Kumamoto 2008, Brand and Gow 2009). In other fungi, the mechanism is still unclear but a change in membrane potential can be observed at the tip of the *N. crassa* during thigmotropic responses (Stephenson et al. 2014).

Electrical currents at the interface with other organisms

Measurements of electrical currents at the interface between roots of *Trifolium repens* (L. cv. New Zealand White), *Daucus carota* (L. cv. Nantes), and the mycorrhizal fungus *Gigaspora margarita* (Berbara et al. 1995) suggested a potential role of electrical signaling in interspecies communication. This mechanism of communication could provide a basis for plant-to-plant interactions via the connecting mycelium (Gilbert and Johnson 2017). Electrical signals may be produced by plants in response to mechanical damage (Mousavi et al. 2013, Johnson and Gilbert 2015) and be propagated by the mycelium, making the fungal network act as a "communication cable" between plants (Johnson and Gilbert 2015). A more recent paper attempted to demonstrate this experimentally using mycorrhizae (Thomas and Cooper 2022). For this, two plants (*Pisum sativum* and *Cucumis sativus*) were linked via a mycorrhizal network creating a bridge that connected two separate agar plugs. The plugs were inoculated with a commercial inoculum containing several species of the *Glomus* genus (*Glomus intraradices*, *Glomus aggregatum*, *Glomus mosseae*, and *Glomus etunicatum*). The electrical recording was made by inserting glass microelectrodes into the stems of the plants. The authors concluded that electrical signals were reliably conducted across the mycelial bridges from one plant to the other upon the induction of a wound response (Thomas and Cooper 2022). The method and the interpretation of the data has generated criticism, mostly on the lack of evidence of the biological origin of the voltage changes measured and on the need for a better mechanistic understanding of the processes that would give rise to these currents (Blatt et al. 2023). Also, it is not possible to rule out the conversion of an electrical signal into a chemical signal in the connecting mycelium. In addition, the use of an agar-based system can result in the generation of so-called Donnan potentials. A Donnan potential refers to the electrical potential difference that arises across a semipermeable membrane when charged particles are distributed asymmetrically due to the presence of impermeable ions (Petsev 2004). This occurs typically when using agar, which acts as a semipermeable membrane in combination with an ionic solution (e.g. culture media). The gel-like nature of agar enhances this effect, allowing the development of electrochemical gradients that produce Donnan potentials. Moreover, another aspect that was problematic in the experimental design is the recording of an electrical current when the mycelium was replaced by a thread, hinting to a physical phenomenon rather than to a biological one (Blatt et al. 2023). Nonetheless, despite the criticisms on these experiments, electrical communication is still postulated as one of the mechanisms for interspecies communication in soils (Hunter 2023).

Another area in which interspecies interactions could be mediated by electrical signaling is plant–pathogen interactions. Experiments performed with motile zoospores of the fungus-like Oomycete *Phytophthora palmivora* and *Arabidopsis thaliana* and *Medicago truncatula* showed that the external application of a weak electric field can alter the attachment of the zoospores to the roots. These findings and understanding the underlying mechanisms can be important to provide future paths to co-opt those mechanisms to protect crops (Moratto and Sena 2023, Moratto et al. 2024). Similar mechanisms could affect the interaction of both beneficial and pathogenic fungi with plant roots.

Electrical measurements with macroscopic structures

Since 2018, several studies have investigated the production of action potential-like electrical currents in mushrooms. These studies were inspired by work performed on slime molds with the overall goal of developing sensing and computing systems based on filamentous fungi (Adamatzky 2018b). In the first of these studies, electrical potentials were recorded in fruiting bodies of *Pleurotus djamor*. Electrical activity was measured with subdermal needle electrodes that were inserted into the stalk and the translocation zone of the cap. Electrical activity (voltage potential) was recorded with a high-resolution data logger (ADC24, Pico Technology) with technical features that were touted to reduce noise (twisted cables for electrodes). The measurements made suggested that fruiting bodies exhibit spontaneous "spiking" behavior. This spontaneous behavior corresponded to a slow drift from a base voltage potential, combined with relatively fast (starting 3 s after stimulation) oscillations of the potential. In addition, the impact of chemical and thermal stimulation was investigated. Negative or positive spikes (i.e. depolarization and hyperpolarization) were detected upon stimulation (Adamatzky 2018a). In a follow-up study, the same approach was used to measure electrical activity in *Ganoderma resinaceum* (Adamatzky and Gandia 2021). Further tests using four fungal species (*Omphalotus nidiformis*, *Flammulina velutipes*, *S. commune*, and *Cordyceps militaris*) resulted in differences in the patterns obtained. This prompted the authors to propose that those differences convey species-specific information and the existence of a language derived from electrical activity (Adamatzky 2022). Although the methodology applied appeared to be promising for the advancement of the field, some aspects of the experimental design and the interpretation of the results have been criticized by some authors (Blatt et al. 2024). A considerable element of criticism is the fact that part of the electrical activity likely originates from voltage fluctuations that do not have a biological origin. For instance, the use of stainless-steel needles is prone to the recording of Donnan potentials (Blatt et al. 2024). A similar approach has been used recently to measure electrical responses in the basidiomycete *Pholiota brunnescens* during growth in agar plates over a long period of time (100 days). Electrical potentials were measured extracellularly with electrodes inserted in the plates and the results were analyzed based on the colonization of areas of electrodes. The authors claimed to have recorded the longest electric oscillation on this system (1 week oscillation cycle) (Fukasawa et al. 2024). Considering the methodology used (agar-based cultivation and extracellular electrodes), this study presents potentially similar experimental flaws as other studies in which abiotic fluctuations cannot be ruled out (Blatt et al. 2023). A different kind of study in which a fungal mycelial mat of the ascomycete *Curvularia lunata* was placed between two electrodes suggested that fungal biomass can serve as a low-speed data transmission medium (Jones et al. 2024). All these studies at-

test as to the potential for the generation of novel materials with electric conductive properties using mycelium.

Given the promising results and ease of design proposed to study mushrooms with needle electrodes (Adamatzky 2022), we attempted to replicate this experimental system and assessed some of the caveats indicated by other authors (Blatt et al. 2024). To do so, we used a related mushroom-producing Basidiomycete, *Pleurotus pulmonarius*, because of its fast growth and ease of fructification. The goal of these experiments was the independent replication of the method. Accordingly, we used the same recording device (ADC-20 with a ADC20/24 Terminal Board; Pico Technology Ltd) and subdermal needle electrodes with twisted cables (Neurodart, spes Medica) (Fig. 2A–D). Additional information on the growth conditions of the fungus is presented in the Supplementary information. We inserted the needles into newly formed fructifications (Fig. 2E) and, as a control, we placed one of the differential electrode pairs into uncolonized substrate (Fig. 2F). Additionally, we cut one of the fructifications (Fig. 2G) and observed the evolution of the voltage potential recording (Fig. 2H and I). In the fruiting bodies, multiple positive and negative spikes were observed (blue, pink, and gray lines; ranging from above 50 to up to −300 mV). After detaching one of the fructifications (gray line), the signal resembled those recorded in the uncolonized substrate (dark violet), which corresponded to a cyclic signal with an amplitude of around 0.005 Hz (Fig. 2I). This suggested that the spikes were produced only while the fruiting body was attached to the fungus. This experiment confirmed the reproducibility of the recording method for fruiting bodies (Adamatzky 2022). However, we also observed signal changes due to the opening of the incubator door, the presence of people walking near the incubator or even the automatic closing of window shades behind the incubator in both the fungus and the control (i.e. positive and negative spike recorded at 18 and 42 h). This agrees with some of the criticisms of the method, in particular regarding the potential for recording of noise. Thus, a more controlled setting, such as a Faraday cage, is essential to improving this approach.

Another aspect that needs to be considered in future studies for the measurement of electrical currents with macroscopic structures, at the interface of organisms, or even when using extracellular electrodes in cultures growing on solid media is the importance of the positioning of the electrodes and their reference. The electrodes used in these studies can be considered as "proximity" electrodes that record electrical field potentials. Those correspond to voltage that can arise passively from either biological (i.e. the fungus or plants) and nonbiological sources (e.g. movement of ions on a matrix), and the precise origin cannot be distinguished between these sources (Blatt et al. 2023). Moreover, the interpretation of the recorded data as action potential-like signals based on extracellular measurements of changes in voltage can be misleading. Action potentials are transmembrane potentials arising between the intracellular and extracellular space, and are generally measured with microelectrodes placed inside living cells. Instead, the use of surface and extracellular electrodes to record local voltages when placed close to or in contact with excitable cells, rather reflects synchronous behavior of multiple cells (Buzsáki et al. 2012, Blatt et al. 2024). Therefore, validating the measurements using intracellular electrodes, improving the analysis of the signal, or identifying methods to reduce the nonbiological noise is important to advance in this area.

Ion channels in fungi

As indicated previously, resting membrane potentials are maintained actively in the cell by controlling the movement of ions across the membrane with the help of selective channels and/or ion pumps (Martinac et al. 2008). These transmembrane proteins allow the selective movement of ions (for instance, Na^+, Ca^{2+}, and K^+) across the membrane, but can also have functions other than electrical signaling (Catterall et al. 2017).

Early studies in fungal electrical signaling postulated the involvement of proton pumps (H^+) and other ion channels (Ca^{2+} and Cl^-) (Slayman et al. 1976, Harold et al. 1985, Gow and Morris 1995). Spontaneous action potential-like behavior in *Neurospora* was proposed to be due to an electrogenic H^+ pump, or a change in the selectivity of the membrane to ions. From the various ions that were evaluated in this early study, H^+ and Cl^- were identified as the most likely ions responsible for carrying the inward current during action potential firings (Slayman et al. 1976). Moreover, the response of spontaneous action potential-like firing activity in *A. bulbosa* and *P. ostreatus* to current injection differed from the response in classical animal models (Olsson and Hansson 1995). In these two fungi, the injection of negative currents increased the amplitude of the signals, whereas injection of negative currents inhibits the activity of neurons. This suggested that the ions and ion channels involved in the generation and maintenance of action potentials in fungi are different from those in classical animal models (Olsson and Hansson 1995). In contrast, and as indicated previously, galvanotropism and thigmotropism in *C. albicans* appear to be regulated by the movement of Ca^{2+} via the voltage-gated channel Cch1 (Brand et al. 2007). More recently, a study in *A. nidulans* showed Ca^{2+} signaling intracellularly in response to a localized stress. The movement of Ca^{2+} was highly localized and caused a wave of voltage measurements with variable frequency (Itani et al. 2023).

Different types of ion and voltage-gated channels have been described in fungi based mainly on the study of yeasts. However, more recently, specific families of these channels have also been identified in filamentous fungi (Houdinet et al. 2023), including voltage-gated proton channels that displayed shared features to animal counterparts, but that were sufficiently different to confer specific functional adaptations unique to filamentous fungi (e.g. voltage range of activation or pH sensitivity) (Zhao and Tombola 2021). Moreover, the analysis of whole-genome sequencing projects allowed to identify genes likely to encode homologues of K^+, Ca^{2+}, transient receptor potential (Trp), and mitochondrial Ca^{2+} uniporter channels (Prole and Taylor 2012). To expand this knowledge beyond pathogens, we performed a homology search for known ion and voltage-gated channels in available fungal proteomes based on human voltage-gated channel subunits (additional information is provided as the Supplementary information). The distribution of the hits and their presence in different fungal clades were analyzed (Fig. 3). The results of this search indicated the presence of putative voltage-gated channels in response to multiple ions (Ca^{2+}, Cl^-, K^+, Na^+, and H^+) and the signal molecule glutamate. Most of the identified channels were present in all eight fungal phyla. However, the different subunits of the voltage-dependent K^+ channel KCN were less represented in Ascomycota, despite the fact that most of the proteomes screened corresponded to this phylum (1283 out of 1942 proteomes screened). In contrast, those were among the only type of channels found in Cryptomycota (three proteomes available). In Basidiomycota and Blastocladiomycota (390 and 2 proteomes screened, respectively), all the types of channels were detected, but some subunits were more common than others. In Mucoromycota and Chrytridiomycota, (84 and 23 proteomes, respectively), Cl^- channels were rare (5–11 and 1, respectively). In Olpidiomycota, for which a single proteome was available, only the

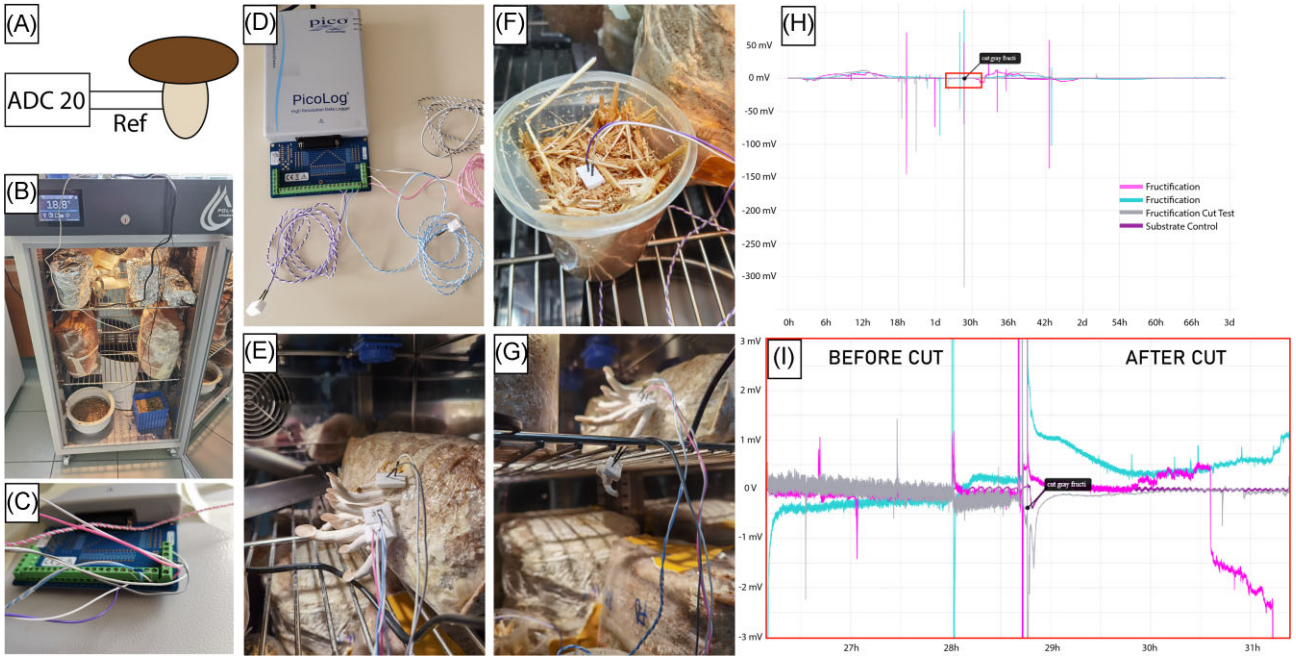

Figure 2. Measurement of voltage fluctuations with needle electrodes inserted in fruiting bodies of the agaricomycete *P. pulmonarius*: (A) Scheme illustrating the insertion of the needle electrode into the foot of the *P. pulmonarius* fructification. (B) Images of the open incubator (POL-EKO-APARATURA sp.j, type: st 3C SMART) in which the experiments were performed; an aquarium lamp (Dennerle nanolight, 11 W) was located at the top. A humidifier (Stylies Alaze SC21011) and a recipient with moist vermiculite were placed at the bottom to maintain humidity. (C) ADC20/24 Terminal Board (Pico Technology Ltd) used to connect the cables to the datalogger. (D) Image of the data logger ADC-20 (Pico Technology Ltd) with four pairs of differential neurological subdermal needles with twisted cables (Neurodart, spes Medica). Needles were inserted through polystyrene pieces to ensure that the needles were located at a fixed distance (1 cm from one another). (E) Needle electrodes attached to three different fructifications of one fructifying bag of *P. pulmonarius*. (F) One pair of needle electrodes was inserted in the substrate without fungus as a control. (G) Fructification with inserted electrodes cut from the fructifying bag (1 day after insertion of the electrodes). (H) Raw signal recorded on the Picolog 6 software (Pico Technology Ldt). The red box represents the zoomed area shown in (I), in which we observed the effect of cutting off the fructification shown in (G). (I) Magnification of the red box from (H). Comparison of a signal for a fructification before and after cutting. Lines in blue, pink, and gray correspond to three different fructifications, while the uncolonized control corresponds to a dark violet line visible after the cut of the fruiting body in (G). After the cut, it is possible to observe the signal from the cut fruiting body (gray) resembling that of substrate control (dark violet).

receptor for glutamate was detected. Finally, in Zoopagomycota, K^+ channels were more commonly found (details provided in the Supplementary information).

The homology search performed here suggests the widespread presence of potential ion- and voltage-gated channels in different fungal clades. However, ultimately, this type of analysis needs to be validated by structural modeling and functional characterization experiments to confirm their role on electrical signaling. The characterization of fungus-specific K^+ channels is an example of this type of validation (Houdinet et al. 2023). These channels were initially identified using the patch-clamp method in fungal spheroplasts and protoplasts (Gustin et al. 1986, Bertl et al. 1993). This led to the description of the *Sc*TOK1, the first member of a new family of K^+ channels to be described in *S. cerevisiae* (Houdinet et al. 2023). This channel was shown to elicit mainly outwardly rectifying K^+ currents upon membrane depolarization in yeast and when expressed in *Xenopus laevis* oocytes. This rectifying function is not directly involved in generating action potentials. Instead, it helps maintain ionic balance in yeast cells. (Gustin et al. 1986, Zhou et al. 1991, 1995, Bertl et al. 1993, Ketchum et al. 1995, Lesage et al. 1996, Loukin et al. 1997). Similar experimental studies would strongly contribute to the field.

Evaluation of innovative recording techniques and potential improvements

In this second part of the review, we will present the evaluation of innovative recording methods that we explored to investigate electrical signaling in fungi. The goal was to expose experimental caveats that we have encountered, as well as present new methods that have the potential to provide novel evidence for electrical signaling in fungi. We hope this will promote future studies in the area and avoid costly mistakes by other researchers aiming to enter the field.

Resistivity measurements

Studies with giant squid neurons showed a decrease in resistance, and thus an increase in conductivity, when neurons fire action potentials (Cole and Curtis 1939). Theoretical models of action potentials, such as the Hodgkin–Huxley model, rely on changes in ion conductance (which inversely affects resistivity) across the cell membrane to describe how action potentials are generated and propagated (Häusser 2000). Although animal neurons are often used as a model, action potentials in other organisms like plants show the same 3-fold defining phases: depolarization, repolarization, and hyperpolarization. In plants, such as *Nitella flexilis*, a decrease in resistivity has also been measured during action potential events (Cole and Curtis 1938). This suggest that electrical signaling in biological systems can be often correlated with changes in resistivity. Accordingly, one way to assess the existence of action potentials in fungi is to assess a change in resistivity in the mycelium in response to stimuli. To test this, we used Mibots (Imina technology), which are piezo-driven micromanipulators that support conductivity-measurements with precise contact needle micropositioning under a camera or a microscope. The

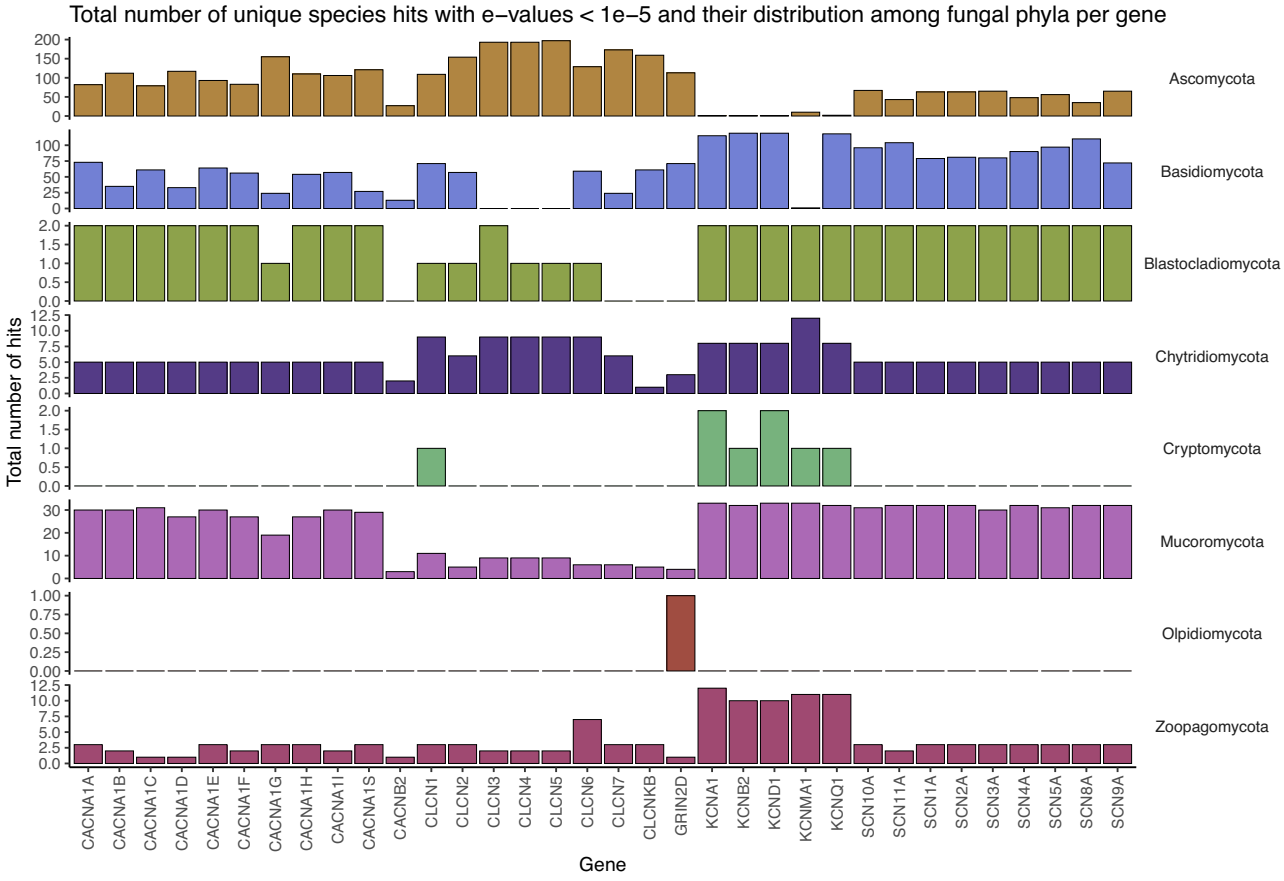

Figure 3. Distribution of PSI-BLAST hits for homologues to voltage-gated ion channels in different fungal clades. The total number of PSI-BLAST hits with e-values < 1e-5 and the number of hits per phylum for each gene was calculated and is displayed as unstacked bar plots. The number of hits per phylum was variable.

electrical measurements were performed using a Keithley 2400 source meter for the recording of current–voltage data. Three different fungi were tested: *Fusarium oxysporum*, *C. cinerea*, and *P. ostreatus* (Fig. 4). Conductivity was measured using the piezoelectric actuators connected in the Mibots (Fig. 4A and B). These piezoelectric actuators were used to measure resistance on indium tin oxide (ITO) stripes on uninoculated glass slides (Fig. 4C) or on slides on which the fungi were grown (Fig. 4D). Resistance can be measured by placing the actuators on the same stripe at variable distances (e.g. Fig. 4C). In the uninoculated glass slide covered with ITO stripes, the resistance was between 45 and 128 ohms, depending on the distance at which the actuators were placed (distance in mm indicated in Fig. 4E). In contrast, in the glass slides colonized by the three fungi, the presence of the mycelium resulted in an increase in resistance (Fig. 4E). In the case of the mycelium of *F. oxysporum*, a resistance value could be obtained in a variable number of stripes (seven ITO stripes per slide as shown in Fig. 4C) in four independent tests. In the case of slides colonized by *C. cinerea* and *P. ostreatus*, the resistance was so high that measurements could only be obtained in the last stripe that contained the lowest biomass (resistance above 5×10^8 ohms; Fig. 4E). We ascribed the increase in resistance to the growth of the mycelium on the ITO stripes and the resulting insulation from the production of hydrophobins, as has been suggested previously (Gow and Morris 1995). Therefore, this method, which was easy to implement, could be used in the future to evaluate the effect of components of the cell wall on insulation and to validate the role of cell wall components on preventing ion leakage (Morell and Quarles 1999). For this, future experiments could employ mutants devoid of a cell wall such as the *N. crassa* slime mutant (Levina et al. 2002) or diverse *Penicillium expansum* mutant strains that lack hydrophobins (Luciano-Rosario et al. 2022). The use of such mutants should circumvent the measurement impairments thought to be caused by the cell wall and prove its role as an insulator. Mycelial growth in the slime mutant can be challenging, but a combination of this type of recording method with the use of, for instance, microfluidic devices to provide structural support could help to circumvent this issue.

Multielectrode arrays

Studies in human neuronal networks have led to recent technical advancements that allow the extracellular recording of voltage fluctuations. The use of a similar approach for mycelial networks could confirm previous results from vibrating microelectrodes where external currents were measured around the apex (Stump et al. 1980, Horwitz et al. 1984). We attempted this by using a high-density multielectrode array (MEA) from 3Brain (3Brain.com, Switzerland) developed to record electrical activity of neuronal networks *in vitro*. The MEA microchip consists of an array of more than 4000 electrodes of micrometer size (20×20 μm^2 sensing area, 80 μm pitch) that register voltage fluctuations with a sensitivity of few tens of μV (Fig. 5A and B). The voltage fluctuations result from extracellular ionic flows occurring when ion channels and transporters of the cell membrane open. The signals collected

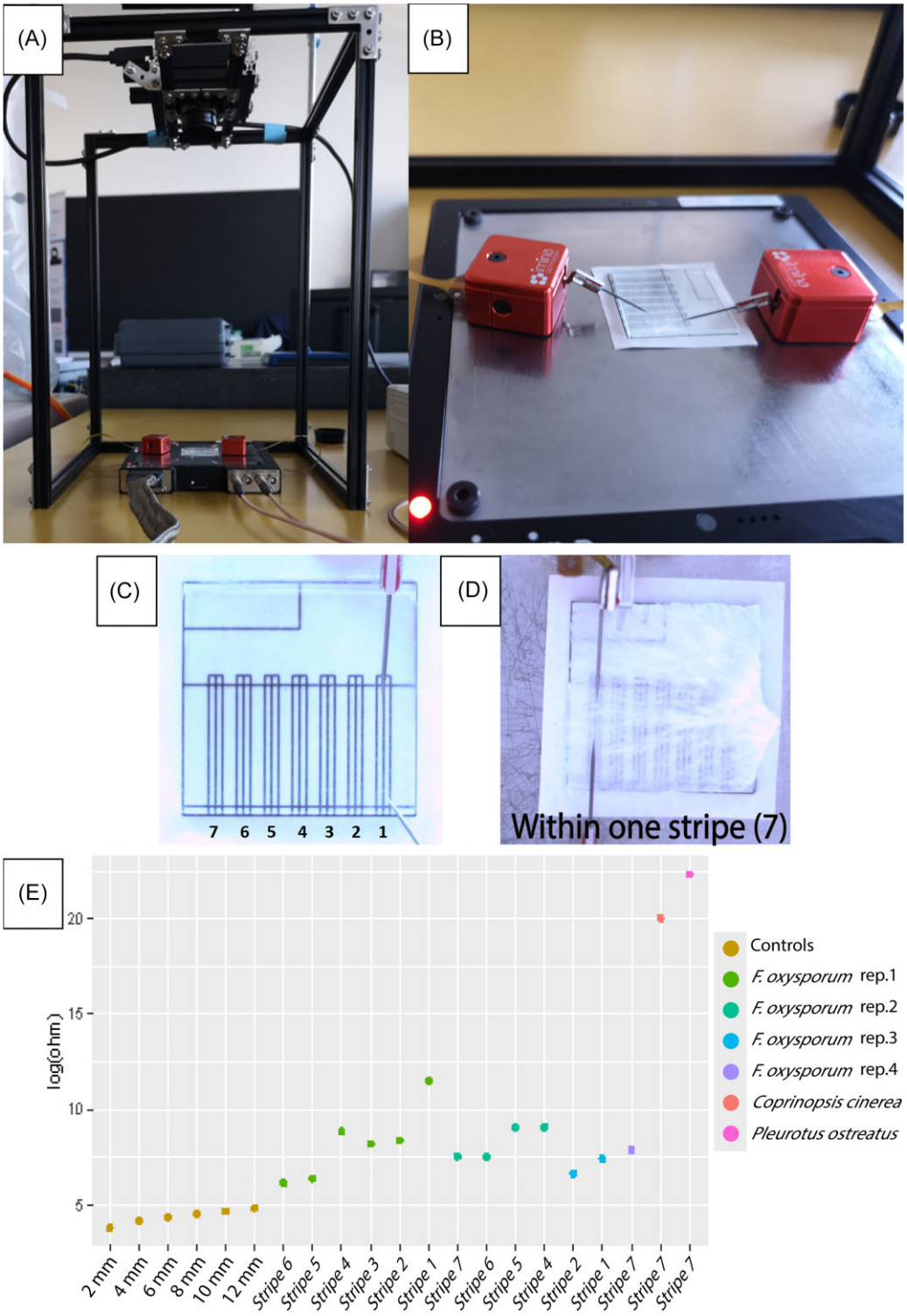

Figure 4. Conductivity measurement of fungal mycelia with MiBots (Imina technologies): for this experiment, we tested *F. oxysporum*, *P. ostreatus*, and *C. cinerea*. The three fungi were cultivated on malt agar medium, where glass slides covered by stripes of ITO were placed next to the inoculum. Once the fungus had grown onto the slide, it was placed onto the MiBots arena to conduct measurements. (A) Camera system mounted in order to visualize the probes for more accurate measurements with the MiBots piezoelectric actuators. (B) Example of a measurement on a slide colonized by *F. oxysporum* hyphae. (C) Details of ITO-covered glass slide. The ITO stripes are transparent and therefore, a mask is placed underneath to indicate their position and to guide the measurements. The position of the ITO stripes corresponds to the middle lines in the three-line marks highlighted by the numbers 1–7. The slide is about 2.5 cm × 2.5 cm, with the stripes being separated by around 2 mm. In the top left part, there is a rectangular area covered by ITO that can be used as a positive control. In this example, the distance between the electrode probes, positioned using the piezoelectric actuators, corresponds to 12 mm. (D) Example of measurement on stripe 7 on a slide colonized by *P. ostreatus*. (E) Plotting of the resistance measurements (logarithmic Ohm—for the detailed measurements, please see the Supplementary information). The controls correspond to measurements in an uninoculated slide on stripe 1 with the electrodes positioned at different distances along the stripe (2 mm, 4 mm, 6 mm, 8 mm, and 12 mm, respectively). For *F. oxysporum*, four individual slides were measured and only the values on the stripes that could be measured are reported in different stripes. For *C. cinerea* and *P. ostreatus*, recordings were only possible on stripe 7.

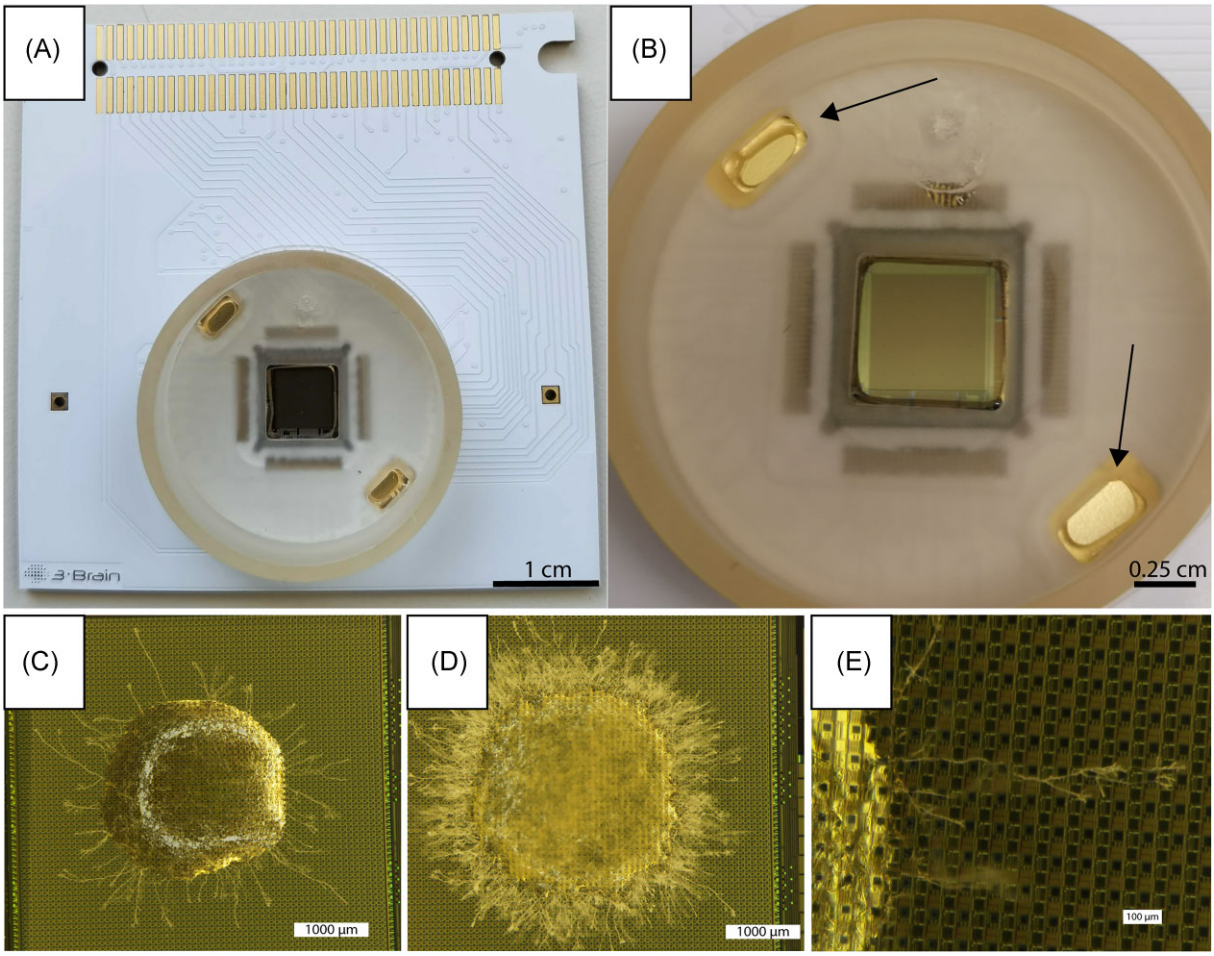

Figure 5. Measuring voltage fluctuations in a mycelial network using a high-density MEA from 3Brain. (A) MEA chip used (~1 cm^2). The microchip (gold square in the middle) is surrounded by a plastic container acting as a reservoir for medium and organism growth. (B) Close-up image of the microchip chamber. The chip contains 4096 electrodes for measuring electrical activity. On the sides, the two large gold electrodes (outside the chip) act as references for the differential measurement. (C) Image showing the growth of *F. oxysporum* inoculated using the spore drop method in Dulbecco's modified eagle medium (DMEM; GiBCO) liquid medium. Image taken 2 days postinoculation. (D) *Fusarium oxysporum* at 3 days postinoculation (before measurements). For the measurements, the chamber (B) was flooded with medium (required for the measurements). (E) Magnified image showing *F. oxysporum* hyphae that have grown from the point of inoculation and are attached to the electrodes.

simultaneously by each of the thousands of electrodes can be visualized as functional activity images, allowing for tracking of electrical impulses propagating inside an electrogenic tissue with micrometer resolution. Multiple tests for recording the propagation of electrical impulses in a mycelial network were conducted using *F. oxysporum*. First, the fungus was inoculated by placing a small agar plug on the surface of liquid medium overlying the electrodes. This method did not yield any results because the fungus grew on the surface of the medium at the air–medium interface and never made physical contact with the electrodes. Therefore, we developed a second inoculation method (Buffi et al. 2023), to be able to place and cultivate the fungus directly onto the chip's surface (Fig. 5C–E). This second approach resulted in a recording. An oscillation signal in the range of ± 50 µV was recorded. However, the signal remained constant after induction with a calcium ionophore, which is known to induce a physiological reaction in *F. oxysporum* (Hoshino et al. 1991). Also, killing the fungus with the antifungal agent cycloheximide did not affect the signal. Upon discussion with the chip developers, it became evident that the signal recorded corresponded to background noise. MEA chips were originally designed to measure relatively high frequency signals (from 5–10 to 2–3k Hz), while in most of the existing literature, fungal signals have temporal dynamics of tens of seconds up to hours resulting in a signal spectral frequency in the order of 0.0003–0.1 Hz. This major difference makes the recording using the commercial chip design inappropriate and would require major modifications of the design and the analysis software to be suitable. Nevertheless, this type of electrode array could provide a way to measure the propagation of an electrical signal within the complex spatial structure of a growing mycelium.

Visualization of membrane potentials using dyes

The last method tested here aimed to visualize changes in membrane potential in fungal hyphae by coupling the use of voltage sensitive dyes with fluorescence microscopy. Voltage sensitive dyes are molecules that bind to the cell membrane and whose fluorescence changes when a membrane potential fluctuation is detected (Fig. 6A). They have been mainly used for imaging of complex neuronal network behaviors (Ebner and Chen 1995, Chemla and Chavane 2010, Adams and Levin 2012, Kulkarni and Miller 2017). Thioflavin T (ThT) is a fluorescent dye usually used for

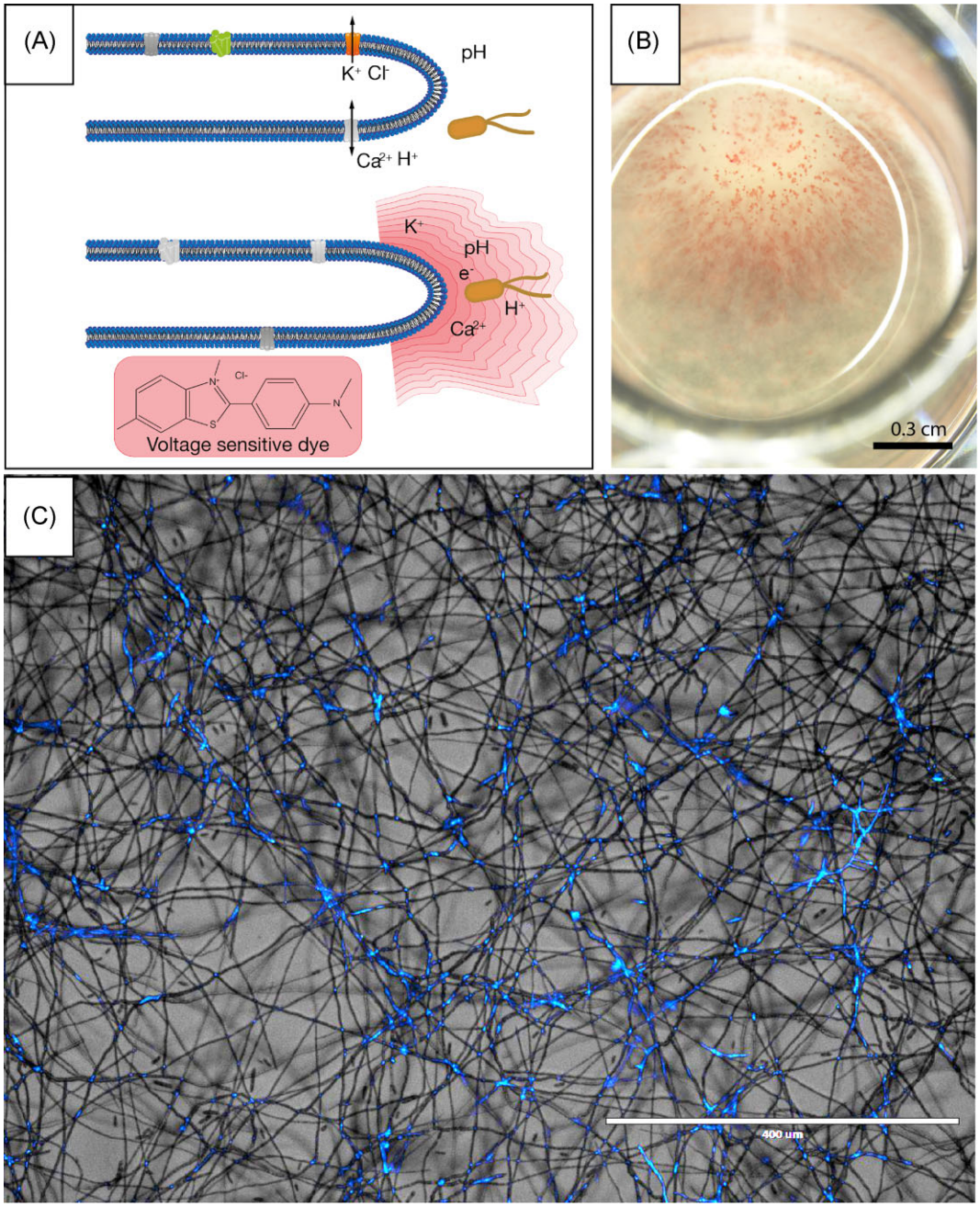

Figure 6. Visualization of membrane potential changes with the voltage sensitive dye ThT. (A) Scheme representing the mechanism behind the visualization of membrane potential using ThT. ThT is positively charged but it does not cross the fungal membrane. If the inner cell is negatively charged (e.g. efflux of positively charged ions), ThT will concentrate on the surface of the cell and fluorescence can then be detected (image in the bottom of the scheme). This can be the result of changes in the movement of specific ions across the membrane. (B) *Fusarium oxysporum* growing in Vogel-N-Medium in a 24-well cell culture plate (Corning incorporated). ThT was added in a final concentration of 30 µM, the plate was covered with dark paper and mixed gently for half an hour before performing imaging on an inverted microscope (EVOS FL imaging system, Invitrogen) with a DAPI filter. (C) Example of a picture overlying a DAPI image with a bright field image showing the inconsistent staining with ThT. Here part of the mycelium and spores of *F. oxysporum* were stained while others were not. Furthermore, the issue of imaging superposed stained hyphae can be observed.

staining amyloid fibrils (Biancalana and Koide 2010) that was previously used as a membrane potential dye for bacteria (Prindle et al. 2015). ThT does not cross the plasma membrane. The dye is positively charged and accumulates close to the membrane in response to changes in membrane potential (for instance if the plasma membrane becomes negatively charged). This makes ThT a good candidate for slow membrane potential changes. To test this, *F. oxysporum* was cultivated in liquid medium to which ThT was added at a final concentration of 30 µM (Fig. 6B). In the microscopic images, an uneven staining along hyphae and on spores was observed (Fig. 6C). Moreover, it was very difficult to distinguish between changes in staining resulting from variations in membrane potential or simply diffusion of the dye. Therefore, optimization of the set-up is required including additional controls

to test photobleaching or the comparison of alive versus dead hyphae. Combining fungal staining and cultivation on microfluidic devices would help confine single hyphae, thus eliminating issues related to hyphal superposition. Microfluidic devices have been used in the past in order to spatially separate single hyphae and observe different physiological interactions (Stanley et al. 2016). Microfluidic devices have emerged particularly valuable tools for studying hyphal growth dynamics, spore germination, and fungal network formation with spatial and temporal resolution (Richter et al. 2022). Although the compartments of the microfluidic devices are usually saturated with liquid medium, potentially impairing measurements, the use of the devices without fluid is also possible (Gimeno et al. 2021). Alternatively, the use of other methods for visualizing the hyphal network such as the drop method (Buffi et al. 2023) could be another possible solution.

Future directions

The challenges encountered so far underscore the complexity of accurately recording electrical signals in fungi. A recurrent challenge in the experimental systems described and evaluated above is the difficulty in effectively measuring electrical signals intra- or extracellularly due to the fungal cell wall. This obstacle is not unique to fungi; similar issues were encountered in plant studies. For intracellular measurements, this issue was partially overcome by using aphid stylets as probes for plants (Tjallingii 1985). However, translating this approach to fungi (for instance, using nematode stylets) could pose significant technical challenges due to the small size of individual hyphae. The use of internal microelectrodes in fungi has raised concerns about altering fungal behavior, such as causing membrane leakage, but new methods provide alternatives to those. For instance, the injection of nanopebbles coupled with a voltage sensitive dye (Koo Lee and Kopelman 2012) could be used to measure intracellular ionic currents. Nanopebbles are nanoparticles composed of an external inert coating and an active inner sensor that can be visualized by microscopy without interfering with the cell functioning. The injection of nanopebbles in fungal mycelia could be achieved using a microfluidic probe connected to an atomic force microscope (FluidFM). This approach has been used for instance to inject bacteria into fungal cells (Guillaume-Gentil et al. 2022, Giger et al. 2024), and could be used to inject the nanopebbles or to create ionic fluxes and investigate the propagation of an electrical signal in the mycelial network. Another approach involves the expression of intracellular reporters for specific ions such as Ca^{2+}. Indeed, the expression of genetically encoded Ca^{2+} indicators has been shown for different unicellular and multicellular fungi, but it is still challenging to achieve and optimize (Carbó et al. 2017, Barykina et al. 2020, Kim et al. 2021). The potential application of this technology for signaling in fungal composite materials has been recently reviewed elsewhere (Schyck et al. 2024).

Future research might also benefit from exploring innovative approaches, such as genetically encoded voltage indicators (GEVI) (Yang and St-Pierre 2016). Such fluorescent proteins could provide a less invasive way of tracking changes in membrane potential, similar to techniques used in neuronal studies. For this, identifying good models is crucial. For instance, *C. cinerea* (a saprotrophic fungus), which has served as a model organism for homobasidiomycete fungi, is a good candidate to study the effect of electrical signaling during fruiting body formation (Navarro-González et al. 2011). Moreover, this fungus is amenable to genetic manipulation and it has been modified to express fluorescent metabolic reporters in response to biotic stress like nematode attacks (Schmieder et al. 2019). By expressing voltage-sensitive fluorescent proteins in *C. cinerea* and coupling this with fluorescently marked analogues (e.g. 2-NBDG glucose or labeled phosphorus and carbon), electrical signaling could be coupled to physiological and behavioral responses. Such an approach could reveal how fungi coordinate mycelial responses to biological (e.g. attacks by mycoparasitic fungi or nematodes) or abiotic (e.g. fruiting body formation in response to electrical signals) stimuli. Furthermore, finding a good model organism could help further improve the use of GEVI in complex networks with low voltage changes.

Conclusion

Demonstrating the biological origin of electrical signals and improving our understanding of the mechanisms and roles of electrical communication in fungi has implications reaching beyond mycology. For instance, parallels and differences have been highlighted as part of the polar growth and intracellular communication of neurons and hyphae, in which mutual progress can lead, for instance, to a better understanding of mechanisms of neural diseases. Reciprocally, neurons could serve as a model to study tip-to-nucleus communication in hyphae (Etxebeste and Espeso 2016). In ecology, it could reshape our understanding of fungal physiology and interactions with other organisms. This has implications in diverse areas and can provide new ways to tackle the emerging problem of fungal diseases in both agriculture and medicine (Rickerts 2019, Fisher et al. 2022, The Lancet Infectious Diseases 2023). Moreover, in the field of biotechnology, leveraging fungal electrical properties could pave the way for innovative applications, such as the use of fungi in biosensors or as components in biological computing systems (Adamatzky 2018b).

Funding

This research was supported by a Science Focus Area Grant from the U.S. Department of Energy (DOE), Biological and Environmental Research (BER), Biological System Science Division (BSSD) under the grant number LANLF59T to P.S.C. and the Swiss National Science Foundation grant 310030_212435 to M.K.

Acknowledgments

We would like to thank Gilles Weder and Sarah Heub (CSEM), and Alessando Maccione (3Brain.com) for their help during the experiments with MEA chips.

Supplementary data

Supplementary Data is available at *FEMSRE Journal* Online.

Conflict of interest: None declared.

References

Abadeh A, Lew RR. Mass flow and velocity profiles in *Neurospora* hyphae: partial plug flow dominates intra-hyphal transport. *Microbiology* 2013;**159**:2386–94. https://doi.org/10.1099/MIC.0.071191-0/CITE/REFWORKS.

Adamatzky A, Gandia A. On electrical spiking of *Ganoderma resinaceum*. *Biophys Rev Lett* 2021;**16**:133–41. https://doi.org/10.1142/S1793048021500089.

Adamatzky A. Language of fungi derived from their electrical spiking activity. *R Soc Open Sci* 2022;**9**. https://doi.org/10.1098/RSOS.211926.

Adamatzky A. On spiking behaviour of oyster fungi *Pleurotus djamor*. *Sci Rep* 2018a;**8**:7873.

Adamatzky A. Towards fungal computer. *Interface Focus* 2018b;**8**. https://doi.org/10.1098/RSFS.2018.0029.

Adams DS, Levin M. Measuring resting membrane potential using the fluorescent voltage reporters DiBAC4 (3) and CC2-DMPE. *Cold Spring Harb Protoc* 2012;**2012**:459–64.

Armbruster BL, Weisenseel MH. Ionic currents traverse growing hyphae and sporangia of the mycelial water mold *Achlya debaryana*. *Protoplasma* 1983;**115**:65–69. https://doi.org/10.1007/BF01293582.

Ashford AE, Allaway WG. Motile tubular vacuole systems. In: *Biology of the Fungal Cell*. Berlin: Springer, 2007, 49–86. https://doi.org/10.1007/978-3-540-70618-2_2.

Ayling SM, Smith SE, Smith FA. Transmembrane electric potential difference of germ tubes of arbuscular mycorrhizal fungi responds to external stimuli. *New Phytologist* 2000;**147**:631–9.

Barykina NV, Sotskov VP, Gruzdeva AM *et al*. FGCaMP7, an improved version of fungi-based ratiometric calcium indicator for in vivo visualization of neuronal activity. *Int J Mol Sci* 2020;**21**:3012. https://doi.org/10.3390/IJMS21083012.

Beagle SD, Lockless SW. Electrical signalling goes bacterial. *Nature* 2015;**527**:44. https://doi.org/10.1038/nature15641.

Berbara RLL, Morris BM, Fonseca HMAC *et al*. Electrical currents associated with arbuscular mycorrhizal interactions. *New Phytol* 1995;**129**:433–8. https://doi.org/10.1111/J.1469-8137.1995.TB04314.X.

Bertl A, Slayman CL, Gradmann D. Gating and conductance in an outward-rectifying K^+ channel from the plasma membrane of *Saccharomyces cerevisiae*. *J Membr Biol* 1993;**132**:183–99. https://doi.org/10.1007/BF00235737/METRICS.

Biancalana M, Koide S. Molecular mechanism of thioflavin-T binding to amyloid fibrils. *Biochim Biophys Acta Proteins Proteomics* 2010;**1804**:1405–12.

Blatt MR, Draguhn A, Taiz L *et al*. A challenge to claims for mycorrhizal-transmitted wound signaling. *Plant Signal Behav* 2023;**18**. https://doi.org/10.1080/15592324.2023.2222957.

Blatt MR, Pullum GK, Draguhn A *et al*. Does electrical activity in fungi function as a language?. *Fungal Ecol* 2024;**68**:101326. https://doi.org/10.1016/J.FUNECO.2023.101326.

Blatt MR. A charged existence: a century of transmembrane ion transport in plants. *Plant Physiol* 2024;**195**:79–110. https://doi.org/10.1093/PLPHYS/KIAD630.

Böhm J, Scherzer S, Krol E *et al*. The Venus flytrap *Dionaea muscipula* counts prey-induced action potentials to induce sodium uptake. *Curr Biol* 2016;**26**:286–95. https://doi.org/10.1016/j.cub.2015.11.057.

Boschker HTS, Cook PLM, Polerecky L *et al*. Efficient long-range conduction in cable bacteria through nickel protein wires. *Nat Commun* 2021;**12**:1–12. https://doi.org/10.1038/s41467-021-24312-4.

Brand A, Gow NAR. Mechanisms of hypha orientation of fungi. *Curr Opin Microbiol* 2009;**12**:350. https://doi.org/10.1016/J.MIB.2009.05.007.

Brand A, Shanks S, Duncan VMS *et al*. Hyphal orientation of *Candida albicans* is regulated by a calcium-dependent mechanism. *Curr Biol* 2007;**17**:347–52. https://doi.org/10.1016/j.cub.2006.12.043.

Brenner ED, Stahlberg R, Mancuso S *et al*. Plant neurobiology: an integrated view of plant signaling. *Trends Plant Sci* 2006;**11**:413–9.

Brette R., Destexhe A.. Handbook of Neural Activity Measurement. In: Brette R. Destexhe A. (Eds.), *Intracellular recording*. Cambridge: Cambridge University Press, 2012, 44–91.

Buffi M, Cailleau G, Kuhn T *et al*. Fungal drops: a novel approach for macro- and microscopic analyses of fungal mycelial growth. *MicroLife* 2023;**4**:1–13. https://doi.org/10.1093/FEMSML/UQAD042.

Buzsáki G, Anastassiou CA, Koch C. The origin of extracellular fields and currents—EEG, ECoG, LFP and spikes. *Nat Rev Neurosci* 2012;**13**:407–20. https://doi.org/10.1038/nrn3241.

Cairney JWG. Translocation of solutes in ectomycorrhizal and saprotrophic rhizomorphs. *Mycol Res* 1992;**96**:135–41. https://doi.org/10.1016/S0953-7562(09)80928-3.

Canales J, Henriquez-Valencia C, Brauchi S. The integration of electrical signals originating in the root of vascular plants. *Front Plant Sci* 2018;**8**. https://doi.org/10.3389/fpls.2017.02173.

Carbó N, Tarkowski N, Ipiña EP *et al*. Sexual pheromone modulates the frequency of cytosolic $Ca2^+$ bursts in *Saccharomyces cerevisiae*. *Mol Biol Cell* 2017;**28**:501. https://doi.org/10.1091/MBC.E16-07-0481.

Catterall WA, Wisedchaisri G, Zheng N. The chemical basis for electrical signaling. *Nat Chem Biol* 2017;**13**:455. https://doi.org/10.1038/NCHEMBIO.2353.

Chemla S, Chavane F. Voltage-sensitive dye imaging: technique review and models. *J Physiol* 2010;**104**:40–50.

Clarke D, Whitney H, Sutton G *et al*. Detection and learning of floral electric fields by bumblebees. *Science* 2013;**340**:66–69.

Cole KS, Curtis HJ. Electric impedance of Nitella during activity. *J Gen Physiol* 1938;**22**:37–64. https://doi.org/10.1085/JGP.22.1.37.

Cole KS, Curtis HJ. Electric impedance of the squid giant axon during activity. *J Gen Physiol* 1939;**22**:649–70.

Curtis HJ, Cole KS. Membrane resting and action potentials from the squid giant axon. *J Cell Comp Physiol* 1942;**19**:135–44.

Darrah PR, Tlalka M, Ashford A *et al*. The vacuole system is a significant intracellular pathway for longitudinal solute transport in basidiomycete fungi. *Eukaryot Cell* 2006;**5**:1111–25. https://doi.org/10.1128.

Dorn A, Weisenseel MH. Advances in vibrating probe techniques. *Protoplasma* 1982;**113**:89–96. https://doi.org/10.1007/BF01281996.

Ebner TJ, Chen G. Use of voltage-sensitive dyes and optical recordings in the central nervous system. *Prog Neurobiol* 1995;**46**:463–506.

Etxebeste O, Espeso EA. Neurons show the path: tip-to-nucleus communication in filamentous fungal development and pathogenesis. *FEMS Microbiol Rev* 2016;**40**:610–24. https://doi.org/10.1093/FEMSRE/FUW021.

Fischer MS, Glass NL. Communicate and fuse: how filamentous fungi establish and maintain an interconnected mycelial network. *Front Microbiol* 2019;**10**. https://doi.org/10.3389/fmicb.2019.00619.

Fischer R. Nuclear movement in filamentous fungi. *FEMS Microbiol Rev* 1999;**23**:39–68. https://doi.org/10.1111/J.1574-6976.1999.TB00391.X.

Fisher MC, Alastruey-Izquierdo A, Berman J *et al*. Tackling the emerging threat of antifungal resistance to human health. *Nat Rev Microbiol* 2022;**20**:557–71. https://doi.org/10.1038/s41579-022-00720-1.

Fricker M, Boddy L, Bebber D. Network organisation of mycelial fungi. In: Howard RJ, Gow NAR (eds), *Biology of the Fungal Cell*. Berlin: Springer, 2007, 309–30. https://doi.org/10.1007/978-3-540-70618-2_13.

Fricker MD, Heaton LLM, Jones NS *et al*. The mycelium as a network. In: *The Fungal Kingdom*. Washington, DC: American Society of Microbiology, 2017. https://doi.org/10.1128/microbiolspec.FUNK-0033-2017.

Fukasawa Y, Akai D, Takehi T *et al.* Electrical integrity and week-long oscillation in fungal mycelia. *Sci Rep* 2024;**14**:1–7. https://doi.org/10.1038/s41598-024-66223-6.

Garrill A, Davies JM. Patch clamping fungal membranes: a new perspective on ion transport. *Mycol Res* 1994;**98**:257–63. https://doi.org/10.1016/S0953-7562(09)80452-8.

Garrill A, Jackson SL, Lew RR *et al.* Ion channel activity and tip growth: tip-localized stretch-activated channels generate an essential $Ca2^+$ gradient in the oomycete *Saprolegnia ferax*. *Eur J Cell Biol* 1993;**60**:358–65. http://europepmc.org/abstract/MED/7687216.

Garrill A, Lew RR, Heath IB. Stretch-activated $Ca2^+$ and $Ca2^+$-activated K+ channels in the hyphal tip plasma membrane of the oomycete *Saprolegnia ferax*. *J Cell Sci* 1992;**101**:721–30. https://doi.org/10.1242/JCS.101.3.721.

Giger GH, Ernst C, Richter I *et al.* Inducing novel endosymbioses by implanting bacteria in fungi. *Nature* 2024;**635**:415–22. https://doi.org/10.1038/s41586-024-08010-x.

Gilbert L, Johnson D. Plant–plant communication through common mycorrhizal networks. In: *Advances in Botanical Research*. Vol. **82**, Amsterdam: Elsevier, 2017, 83–97.

Gimeno A, Stanley CE, Ngamenie Z *et al.* A versatile microfluidic platform measures hyphal interactions between *Fusarium graminearum* and *Clonostachys rosea* in real-time. *Commun Biol* 2021;**4**:1–10. https://doi.org/10.1038/s42003-021-01767-1.

Gow NA. Transhyphal electrical currents in fungi. *J Gen Microbiol* 1984;**130**:3313–8. https://doi.org/10.1099/00221287-130-12-3313.

Gow NAR, Morris BM. The electric fungus. *Botan J Scot* 1995;**47**:263–77. https://doi.org/10.1080/03746609508684833.

Gow NAR. Relationship between growth and the electrical current of fungal hyphae. *Biol Bull* 1989;**176**:31–35. https://doi.org/10.2307/1541645.

Guillaume-Gentil O, Gäbelein CG, Schmieder S *et al.* Injection into and extraction from single fungal cells. *Commun Biol* 2022;**5**:1–10. https://doi.org/10.1038/s42003-022-03127-z.

Gustin MC, Martinac B, Saimi Y *et al.* Ion channels in yeast. *Science* 1986;**233**:1195–7. https://doi.org/10.1126/SCIENCE.2426783.

Hamill OP, Marty A, Neher E *et al.* Improved patch-clamp techniques for high-resolution current recording from cells and cell-free membrane patches. *Pflügers Archiv* 1981;**391**:85–100. https://doi.org/10.1007/BF00656997.

Harold FM, Kropf DL, Caldwell JH. Why do fungi drive electric currents through themselves?. *Exp Mycol* 1985;**9**:3–86. https://doi.org/10.1016/0147-5975(85)90013-1.

Harris MP. Bioelectric signaling as a unique regulator of development and regeneration. *Development* 2021;**148**:dev180794. https://doi.org/10.1242/DEV.180794.

Harris SD. Branching of fungal hyphae: regulation, mechanisms and comparison with other branching systems. *Mycologia* 2008;**100**:823–32. https://doi.org/10.3852/08-177.

Häusser M. The Hodgkin-Huxley theory of the action potential. *Nat Neurosci* 2000;**3**:1165.

Heaton L, Obara B, Grau V *et al.* Analysis of fungal networks. *Fungal Biol Rev* 2012;**26**:12–29. https://doi.org/10.1016/J.FBR.2012.02.001.

Horwitz BA, Weisenseel MH, Dorn A *et al.* Electric currents around growing *Trichoderma* hyphae, before and after photoinduction of conidiation. *Plant Physiol* 1984;**74**:912–6. https://doi.org/10.1104/pp.74.4.912.

Hoshino T, Mizutani A, Shimizu S *et al.* Calcium ion regulates the release of lipase of *Fusarium oxysporum*. *J Biochem* 1991;**110**:457–61. https://doi.org/10.1093/oxfordjournals.jbchem.a123602.

Houdinet G, Guerrero-Galán C, Rose BD *et al.* Secrets of the fungus-specific potassium channel TOK family. *Trends Microbiol* 2023;**31**:511–20. https://doi.org/10.1016/j.tim.2022.11.007.

Hunter P. The fungal grid: fungal communication via electrical signals has inspired the hypothesis of a Wood Wide Web of plants and fungi: fungal communication via electrical signals has inspired the hypothesis of a Wood Wide Web of plants and fungi. *EMBO Rep* 2023;**24**. https://doi.org/10.15252/EMBR.202357255.

Hutchings MJ, Wijesinghe DK, John EA. The effects of heterogeneous nutrient supply on plant performance: a survey of responses, with special reference to clonal herbs. In: *The Ecological Consequences of Environmental Heterogeneity*. Cambridge: Cambridge University Press, 2000, 91–109.

Hyde KD, Baldrian P, Chen Y *et al.* Current trends, limitations and future research in the fungi?. *Fungal Diver* 2024;**125**:1–71. https://doi.org/10.1007/S13225-023-00532-5.

Itani A, Masuo S, Yamamoto R *et al.* Local calcium signal transmission in mycelial network exhibits decentralized stress responses. *PNAS Nexus* 2023;**2**:1–10. https://doi.org/10.1093/PNASNEXUS/PGAD012.

Jaffe LF, Nuccitelli R. An ultrasensitive vibrating probe for measuring steady extracellular currents. *J Cell Biol* 1974;**63**:614–28. https://doi.org/10.1083/jcb.63.2.614.

Jaffe MJ, Leopold AC, Staples RC. Thigmo responses in plants and fungi. *Am J Bot* 2002;**89**:375–82.

James TY, Stajich JE, Hittinger CT *et al.* Toward a fully resolved fungal tree of life. *Annu Rev Microbiol* 2020;**74**:291–313. https://doi.org/10.1146/ANNUREV-MICRO-022020-051835/1.

Jennings DH. Translocation of solutes in fungi. *Biol Rev* 1987;**62**:215–43. https://doi.org/10.1111/J.1469-185X.1987.TB00664.X.

Jia N, Yang J, Liu J *et al.* Electric field: a key signal in wound healing. *Chin J Plastic Reconstruc Surg* 2021;**3**:95–102. https://doi.org/10.1016/S2096-6911(21)00090-X.

Jo C, Zhang J, Tam JM *et al.* Unlocking the magic in mycelium: using synthetic biology to optimize filamentous fungi for biomanufacturing and sustainability. *Mater Tod Bio* 2023;**19**:100560. https://doi.org/10.1016/J.MTBIO.2023.100560.

Johnson D, Gilbert L. Interplant signalling through hyphal networks. *New Phytol* 2015;**205**:1448–53. https://doi.org/10.1111/NPH.13115.

Jones RM, Reynolds RW, Thurston AK *et al.* Fungal tissue as a medium for electrical signal transmission: a baseline assessment with melanized fungus *Curvularia Lunata*. *IEEE J Electromagnet RF Microwaves Med Biol* 2024;1–8. https://doi.org/10.1109/JERM.2024.3476444.

Karst J, Jones MD, Hoeksema JD. Positive citation bias and overinterpreted results lead to misinformation on common mycorrhizal networks in forests. *Nat Ecol Evol* 2023;**7**:501–11. https://doi.org/10.1038/s41559-023-01986-1.

Katz B. How cells communicate. *Sci Am* 1961;**205**:209–21. https://doi.org/10.1038/scientificamerican0961-209.

Keener J, Sneyd J. Intercellular communication. In Keener J, Sneyd J (eds), *Mathematical Physiology: I: Cellular Physiology*. New York, NY: Springer, 2009, 347–84. https://doi.org/10.1007/978-0-387-75847-3_8.

Ketchum KA, Joiner WJ, Sellers AJ *et al.* A new family of outwardly rectifying potassium channel proteins with two pore domains in tandem. *Nature* 1995;**376**:690–5. https://doi.org/10.1038/376690a0.

Kim HS, Kim JE, Hwangbo A *et al.* Evaluation of multi-color genetically encoded $Ca2^+$ indicators in filamentous fungi. *Fungal Genet Biol* 2021;**149**:103540. https://doi.org/10.1016/J.FGB.2021.103540.

Koo Lee YE, Kopelman R. Nanoparticle PEBBLE sensors in live cells. *Methods Enzymol* 2012;**504**:419–70. https://doi.org/10.1016/B978-0-12-391857-4.00021-5.

Kropf DL, Caldwell JH, Gow NAR *et al.* Transcellular ion currents in the water mold Achlya. Amino acid proton symport as a mech-

anism of current entry. *J Cell Biol* 1984;**99**:486–96. https://doi.org/10.1083/JCB.99.2.486.

Kropf DL. Electrophysiological properties of Achlya hyphae: ionic currents studied by intracellular potential recording. *J Cell Biol* 1986;**102**:1209–16. https://doi.org/10.1083/jcb.102.4.1209%J.

Kulkarni RU, Miller EW. Voltage imaging: pitfalls and potential. *Biochemistry* 2017;**56**:5171–7.

Kulkarni S, Nene S, Joshi K. Production of hydrophobins from fungi. *Process Biochem* 2017;**61**:1–11. https://doi.org/10.1016/j.procbio.2017.06.012.

Kumamoto CA. Molecular mechanisms of mechanosensing and their roles in fungal contact sensing. *Nat Rev Microbiol* 2008;**6**:667–73. https://doi.org/10.1038/nrmicro1960.

Lee J, Calvo P. The potential of plant action potentials. *Synthese* 2023;**202**:1–30. https://doi.org/10.1007/S11229-023-04398-7/METRICS.

Lesage F, Guillemare E, Fink M *et al.* A pH-sensitive yeast outward rectifier K^+ channel with two pore domains and novel gating properties. *J Biol Chem* 1996;**271**:4183–7. https://doi.org/10.1074/jbc.271.8.4183.

Lever MC, Robertson BEM, Buchan ADB *et al.* pH and $Ca2^+$ dependent galvanotropism of filamentous fungi: implications and mechanisms. *Mycol Res* 1994;**98**:301–6. https://doi.org/10.1016/S0953-7562(09)80458-9.

Levin M, Pezzulo G, Finkelstein JM. Endogenous bioelectric signaling networks: exploiting voltage gradients for control of growth and form. *Annu Rev Biomed Eng* 2017;**19**:353–87. https://doi.org/10.1146/annurev-bioeng-071114-040647.

Levina NN, Dunina-Barkovskaya AY, Shabala S *et al.* Blue light modulation of ion transport in the slime mutant of *Neurospora crassa*. *J Membr Biol* 2002;**188**:213–26. https://doi.org/10.1007/s00232-001-0185-z.

Lew RR. How does a hypha grow? The biophysics of pressurized growth in fungi. *Nat Rev Microbiol* 2011;**9**:509–18.

Li K, Jia J, Wu N *et al.* Recent advances in the construction of biocomposites based on fungal mycelia. *Front Bioeng Biotechnol* 2022;**10**:1067869. https://doi.org/10.3389/FBIOE.2022.1067869/BIBTEX.

Linder MB, Szilvay GR, Nakari-Setälä T *et al.* Hydrophobins: the protein-amphiphiles of filamentous fungi. *FEMS Microbiol Rev* 2005;**29**:877–96. https://doi.org/10.1016/J.FEMSRE.2005.01.004.

Loukin SH, Vaillant B, Zhou XL *et al.* Random mutagenesis reveals a region important for gating of the yeast K^+ channel Ykc1. *EMBO J* 1997;**16**:4817–25. https://doi.org/10.1093/EMBOJ/16.16.4817.

Luciano-Rosario D, Eagan JL, Aryal N *et al.* The Hydrophobin gene family confers a fitness trade-off between spore dispersal and host colonization in *Penicillium expansum*. *mBio* 2022;**13**. https://doi.org/10.1128/MBIO.02754-22/SUPPL_FILE/MBIO.02754-22-S0007.TIF.

Markham P. Occlusions of septal pores in filamentous fungi. *Mycol Res* 1994;**98**:1089–106. https://doi.org/10.1016/S0953-7562(09)80195-0.

Martinac B, Saimi Y, Kung C. Ion channels in microbes. *Physiol Rev* 2008;**88**:1449. https://doi.org/10.1152/PHYSREV.00005.2008.

Mayne R, Roberts N, Phillips N *et al.* Propagation of electrical signals by fungi. *Biosystems* 2023;**229**:104933. https://doi.org/10.1016/J.BIOSYSTEMS.2023.104933.

McGillivray AM, Gow NAR. Applied electrical fields polarize the growth of mycelial fungi. *J Gen Microbiol* 1986;**132**:2515–25. https://doi.org/10.1099/00221287-132-9-2515/CITE/REFWORKS.

McLaughlin KA, Levin M. Bioelectric signaling in regeneration: mechanisms of ionic controls of growth and form. *Dev Biol* 2018;**433**:177–89.

Meyer V, Andersen MR, Brakhage AA *et al.* Current challenges of research on filamentous fungi in relation to human welfare and a sustainable bio-economy: a white paper. *Fungal Biol Biotechnol* 2016;**3**:1–17. https://doi.org/10.1186/S40694-016-0024-8/TABLES/3.

Meyer V. Connecting materials sciences with fungal biology: a sea of possibilities. *Fungal Biol Biotechnol* 2022;**9**:1–4. https://doi.org/10.1186/S40694-022-00137-8/FIGURES/1.

Moratto E, Rothery S, Bozkurt TO *et al.* Enhanced germination and electrotactic behaviour of *Phytophthora palmivora* zoospores in weak electric fields. *Phys Biol* 2023;**20**:056005. https://doi.org/10.1088/1478-3975/ACE751.

Moratto E, Sena G. The bioelectricity of plant–biotic interactions. *Bioelectricity* 2023;**5**:47–54. https://doi.org/10.1089/BIOE.2023.0001.

Moratto E, Tang Z, Bozkurt TO *et al.* Reduction of *Phytophthora palmivora* plant root infection in weak electric fields. *Sci Rep* 2024;**14**:1–10. https://doi.org/10.1038/s41598-024-68730-y.

Morell P, Quarles RH. Characteristic composition of myelin. In: *Basic Neurochemistry: Molecular, Cellular and Medical Aspects*. Vol. **6**. New York, NY: Raven Press, 1999.

Morris BM, Gow NAR. Mechanism of electrotaxis of zoospores of phytopathogenic fungi. *Physiol Biochem* 1993;**83**:877.

Mousavi SAR, Chauvin A, Pascaud F *et al.* Glutamate receptor-like genes mediate leaf-to-leaf wound signalling. *Nature* 2013;**500**:422–6. https://doi.org/10.1038/NATURE12478.

Navarro-González M, Arndt M, Zomorrodi M *et al.* Regulation of fruiting body formation in *Coprinopsis cinerea*. In: *Proceedings of the Seventh International Conference on Mushroom Biology and Mushroom Products (ICMBMP7) 2011*. Vol. **1**. Bordeaux: INRA Bordeaux, 2011, 175–87.

Neher E, Sakmann B. Single-channel currents recorded from membrane of denervated frog muscle fibres. *Nature* 1976;**260**:799–802. https://doi.org/10.1038/260799a0.

Neher E, Sakmann B. The patch clamp technique. *Sci Am* 1992;**266**:44–51. https://doi.org/10.1038/scientificamerican0392-44.

Nuccitelli R. A role for endogenous electric fields in wound healing. *Curr Top Dev Biol* 2003;**58**:1–26.

Nuccitelli R. Ionic currents in morphogenesis. *Experientia* 1988;**44**:657–66. https://doi.org/10.1007/BF01941026.

Nuccitelli R. Vibrating probe technique for studies of ion transport. *Modern Cell Biol* 1990;**9**:273–310.

Olsson S, Gray SN. Patterns and dynamics of ^{32}P-phosphate and labelled 2-aminoisobutyric acid (14C-AIB) translocation in intact basidiomycete mycelia. *FEMS Microbiol Ecol* 1998;**26**:109–20. https://doi.org/10.1016/S0168-6496(98)00026-9.

Olsson S, Hansson BS. Action potential-like activity found in fungal mycelia is sensitive to stimulation. *Naturwissenschaften* 1995;**82**:30–31. https://doi.org/10.1007/bf01167867.

Olsson S, Jennings DH. A glass fiber filter technique for studying nutrient uptake by fungi: the technique used on colonies grown on nutrient gradients of carbon and phosphorus. *Exp Mycol* 1991a;**15**:292–301. https://doi.org/10.1016/0147-5975(91)90032-9.

Olsson S, Jennings DH. Evidence for diffusion being the mechanism of translocation in the hyphae of three molds. *Exp Mycol* 1991b;**15**:302–9. https://doi.org/10.1016/0147-5975(91)90033-A.

Olsson S. Colonial growth of fungi. In: *Biology of the Fungal Cell*. Berlin: Springer, 2001, 125–41. https://doi.org/10.1007/978-3-662-06101-5_6.

Oyarte Galvez L, Bisot C, Bourrianne P *et al.* A travelling-wave strategy for plant–fungal trade. *Nature* 2025;**639**:172–80. https://doi.org/10.1038/s41586-025-08614-x.

Pajić T, Stevanović K, Todorović NV *et al.* In vivo femtosecond laser nanosurgery of the cell wall enabling patch-clamp measurements on filamentous fungi. *Microsyst Nanoeng* 2024;**10**:1–17. https://doi.org/10.1038/s41378-024-00664-x.

Petsev D. *Emulsions: Structure, Stability and Interactions*. Amsterdam: Elsevier, 2004. ISBN: 9780080472652.

Piccolino M. Animal electricity and the birth of electrophysiology: the legacy of Luigi Galvani. *Brain Res Bull* 1998;**46**:381–407. https://doi.org/10.1016/S0361-9230(98)00026-4.

Potapova T. Cell-to-Cell communication in the tip growth of mycelial fungi. In: Witzany G (ed.), *Biocommunication of Fungi*. Dordrecht: Springer, 2012, 103–14. https://doi.org/10.1007/978-94-007-4264-2_7 LB---Potapova2012.

Potapova TV, Levina NN, Belozerskaya TA *et al.* Investigation of electrophysiological responses of *Neurospora crassa* to blue light. *Arch Microbiol* 1984;**137**:262–5. https://doi.org/10.1007/BF00414555/METRICS.

Prindle A, Liu J, Asally M *et al.* Ion channels enable electrical communication in bacterial communities. *Nature* 2015;**527**:59. https://doi.org/10.1038/nature15709 https://www.nature.com/articles/nature15709#supplementary-information.

Prole DL, Taylor CW. Identification and analysis of cation channel homologues in Human pathogenic fungi. *PLoS One* 2012;**7**:e42404. https://doi.org/10.1371/JOURNAL.PONE.0042404.

Rayner ADM, Griffith GS, Ainsworth AM. Mycelial interconnectedness. In: *The Growing Fungus*. Berlin: Springer, 1995, 21–40.

Richter F, Bindschedler S, Calonne-Salmon M *et al.* Fungi-on-a-chip: microfluidic platforms for single-cell studies on fungi. *FEMS Microbiol Rev* 2022;**46**. https://doi.org/10.1093/FEMSRE/FUAC039.

Rickerts V. Climate change and systemic fungal infections. In: *Bundesgesundheitsblatt—Gesundheitsforschung—Gesundheitsschutz*. Vol. **62**. Berlin: Springer, 2019, 646–51. https://doi.org/10.1007/s00103-019-02931-z.

Roberts SK, Dixon GK, Dunbar SJ *et al.* Laser ablation of the cell wall and localized patch clamping of the plasma membrane in the filamentous fungus *Aspergillus*: characterization of an anion-selective efflux channel. *New Phytol* 1997;**137**:579–85. https://doi.org/10.1046/j.1469-8137.1997.00862.x.

Roper M, Seminara A. Mycofluidics: the fluid mechanics of fungal adaptation. *Annu Rev Fluid Mech* 2019;**51**:511–38. https://doi.org/10.1146/annurev-fluid-122316045308.

Schmieder SS, Stanley CE, Rzepiela A *et al.* Bidirectional propagation of signals and nutrients in fungal networks via specialized hyphae. *Curr Biol* 2019;**29**:217–28.e4. https://doi.org/10.1016/J.CUB.2018.11.058.

Schyck S, Marchese P, Amani M *et al.* Harnessing fungi signaling in living composites. *Global Challenges* 2024;**8**:2400104. https://doi.org/10.1002/GCH2.202400104.

Sibaoka T. Action potentials in plant organs. *Symp Soc Exp Biol* 1966;**20**:49–73.

Simard SW, Durall DM. Mycorrhizal networks: a review of their extent, function, and importance. *Can J Bot* 2011;**82**:1140–65. https://doi.org/10.1139/B04-116.

Slayman CL, Scott Long W, Gradmann D. "Action potentials" in *Neurospora crassa*, a mycelial fungus. *Biochim Biophys Acta Biomembr* 1976;**426**:732–44. https://doi.org/10.1016/0005-2736(76)90138-3.

Slayman CL, Slayman CW. Measurement of membrane potentials in *Neurospora*. *Science* 1962;**136**:876–7. https://doi.org/10.1126/SCIENCE.136.3519.876.

Stanley CE, Grossmann G, Casadevall i Solvas X *et al.* Soil-on-a-Chip: microfluidic platforms for environmental organismal studies. *Lab Chip* 2016;**16**:228–41. https://doi.org/10.1039/C5LC01285F.

Steinberg G, Harmer NJ, Schuster M *et al.* Woronin body-based sealing of septal pores. *Fungal Genet Biol* 2017;**109**:53–55. https://doi.org/10.1016/J.FGB.2017.10.006.

Stephenson KS, Gow NAR, Davidson FA *et al.* Regulation of vectorial supply of vesicles to the hyphal tip determines thigmotropism in *Neurospora crassa*. *Fungal Biol* 2014;**118**:287–94. https://doi.org/10.1016/j.funbio.2013.12.007.

Stump RF, Robinson KR, Harold RL *et al.* Endogenous electrical currents in the water mold *Blastocladiella emersonii* during growth and sporulation. *Proc Natl Acad Sci* 1980;**77**:6673–7.

Swafford AJM, Oakley TH. Multimodal sensorimotor system in unicellular zoospores of a fungus. *J Exp Biol* 2018;**221**:jeb163196. https://doi.org/10.1242/jeb.163196.

Szechyńska-Hebda M, Lewandowska M, Karpiński S. Electrical signaling, photosynthesis and systemic acquired acclimation. In: *Frontiers in Physiology*. Vol. **8**, Lausanne: Frontiers Media S.A., 2017, 684. https://doi.org/10.3389/fphys.2017.00684.

Takeo Kamada B. Some observations on potential differences across the ectoplasm membrane of paramecium. *J Exp Biol* 1934;**11**:94–102. https://doi.org/10.1242/JEB.11.1.94.

The Lancet Infectious Diseases. An exciting time for antifungal therapy. *Lancet Infect Dis* 2023;**23**:763. https://doi.org/10.1016/S1473-3099(23)00380-8.

Thomas MA, Cooper RL. Building bridges: mycelium–mediated plant–plant electrophysiological communication. *Plant Signal Behav* 2022;**17**. https://doi.org/10.1080/15592324.2022.2129291.

Tjallingii WF. Electrical nature of recorded signals during stylet penetration by aphids. *Entomol Exp Appl* 1985;**38**:177–86.

Townsend BB. Morphology and development of fungal rhizomorphs. *Trans Br Mycol Soc* 1954;**37**:222–33. https://doi.org/10.1016/S0007-1536(54)80004-0.

Tyler SEB. Nature's electric potential: a systematic review of the role of bioelectricity in wound healing and regenerative processes in animals, humans, and plants. *Front Physiol* 2017;**8**:251878. https://doi.org/10.3389/FPHYS.2017.00627/PDF.

van der Klei IJ, Veenhuis M. Yeast and filamentous fungi as model organisms in microbody research. *Biochim Biophys Acta Mol Cell Res* 2006;**1763**:1364–73. https://doi.org/10.1016/J.BBAMCR.2006.09.014.

Vodeneev V, Akinchits E, Sukhov V. Variation potential in higher plants: mechanisms of generation and propagation. *Plant Signal Behav* 2015;**10**:e1057365. https://doi.org/10.1080/15592324.2015.1057365.

Wood J, Tordoff GM, Jones TH *et al.* Reorganization of mycelial networks of *Phanerochaete velutina* in response to new woody resources and collembola (*Folsomia candida*) grazing. *Mycol Res* 2006;**110**:985–93. https://doi.org/10.1016/J.MYCRES.2006.05.013.

Wösten HAB, de Vocht ML. Hydrophobins, the fungal coat unravelled. *Biochim Biophys Acta Rev Biomembr* 2000;**1469**:79–86. https://doi.org/10.1016/S0304-4157(00)00002-2.

Yang HH, St-Pierre F. Genetically encoded voltage indicators: opportunities and challenges. *J Neurosci* 2016;**36**:9977–89. https://doi.org/10.1523/JNEUROSCI.1095-16.2016.

Youatt J, Gow NAR, Gooday GW. Bioelectric and biosynthetic aspects of cell polarity in *Allomyces macrogynus*. *Protoplasma* 1988;**146**:118–26. https://doi.org/10.1007/BF01405920/METRICS.

Zhao C, Tombola F. Voltage-gated proton channels from fungi highlight role of peripheral regions in channel activation. *Commun Biol* 2021;**4**:1–13. https://doi.org/10.1038/s42003-021-01792-0.

Zhao Y, Inayat S, Dikin DA *et al.* Patch clamp technique: review of the current state of the art and potential contributions from nanoengineering. *Proc Inst Mech Eng Part N J Nanoeng Nanosyst* 2008;**222**:1–11. https://doi.org/10.1243/17403499jnn149.

Zhou XL, Stumpf MA, Hoch HC *et al.* A mechanosensitive channel in whole cells and in membrane patches of the fungus Uromyces. *Science* 1991;**253**:1415–7. https://doi.org/10.1126/science.1716786.

Zhou XL, Vaillant B, Loukin SH *et al.* YKC1 encodes the depolarization-activated K^+ channel in the plasma membrane of yeast. *FEBS Lett* 1995;**373**:170–6. https://doi.org/10.1016/0014-5793(95)01035-D.

Zimmermann MR, Maischak H, Mithöfer A *et al.* System potentials, a novel electrical long-distance apoplastic signal in plants, induced by wounding. *Plant Physiol* 2009;**149**:1593–600. https://doi.org/10.1104/pp.108.133884.

Received 31 January 2025; **revised** 13 March 2025; **accepted** 20 March 2025

Supplementary Material Chapter 1

Electrical signaling in fungi: past and present challenges

Published: 21 March 2025

FEMS Microbiology Reviews

DOI: https://doi.org/10.1093/femsre/fuaf009

Title: Electrical signaling in fungi: past and present challenges

Authors: Matteo Buffi[1], Julia M. Kelliher[2,3], Aaron J. Robinson[2], Diego Gonzalez[1], Guillaume Cailleau[1], Justine A. Macalindong[2], Eleonora Frau[4], Silvia Schintke[4], Patrick, S.G. Chain[2], Claire E. Stanley[5], Markus Künzler[6], Saskia Bindschedler[1], Pilar Junier[1*]

[1]Laboratory of Microbiology, Institute of Biology, University of Neuchâtel, Neuchâtel, Switzerland
[2]Bioscience Division, Los Alamos National Laboratory, Los Alamos, NM, USA
[3]Microbiology, Genetics, & Immunology Department, Michigan State University, East Lansing, MI, USA
[4]Laboratory of Applied NanoSciences (COMATEC-LANS), University of Applied Sciences and Arts Western Switzerland (HES-SO), CH-1401 Yverdon-les-Bains, Switzerland
[5]Department of Bioengineering, Imperial College London, London, United Kingdom
[6]Institute for Microbiology, Department of Biology, ETH Zürich, Zurich, Switzerland

Supplementary information on experimental methods:

Organisms:

The fungi *Fusarium oxysporum, Coprinopsis cinerea, Pleurotus pulmonarius,* and *Pleurotus ostreatus* were obtained from the fungal collection of the laboratory of microbiology, university of Neuchâtel, Switzerland. For regular maintenance, the different strains were plated on Malt Extract Agar (MEA, 12 g/l malt extract [SIOS Homebrew], 15 g/l Agar [Biolife]) before inoculum preparation for the experiments.

Experimental evaluation:

Electrical measurements with macroscopic structures (Figure 2)

Fruiting bodies of *P. pulmonarius* were produced as follows: spawn was composed of 44.5% wet rye, 55.22% wet vermiculite, and 0.28% gypsum, which was autoclaved in zipper filter bags (https://saco2.com/) and inoculated when the bags were at room temperature by scraping the mycelium from a one-week-old Petri dish inoculated with *P. pulmonarius* on MEA medium. Once fully colonized, the spawn was used to inoculate fructifying bags by breaking the mycelium and pouring a part of it in fructifying bags composed of 40% wheat straw, 40% sawdust, 15.7% rye, 3% starch, 1.3% compost soil, with a final water content around 73-76%. The bags were then placed in an incubator (POL-EKO-APARATURA sp.j, type: st 3C SMART) maintained at 22 °C with nearly 100% relative humidity (Humifier Stylies Alaze SC21011). Electrodes were inserted in young fructifications as they emerged from the bag. The recordings were performed with an ADC20 (Pico technology Ltd, UK), with four pairs of differential neurological sub-dermal needles with twisted cables (Neurodart, spes Medica). One pair of differential electrodes was placed inside a non-inoculated fructifying medium, the other three pairs were inserted into fruiting bodies always keeping the reference electrode towards the base of the mushroom. To keep a constant distant between the electrodes, they were fixed trough a polystyrene cube with markings at 1 cm distance. After one day, one of the fruiting bodies was cut using a scalpel from the bag as an additional control.

Resistivity measurements (Figure 4)

All the measurements were performed in the laboratory of COMATEC-LANS in the school of engineering and management HEIG-VD in Yverdon (Vaud, Switzerland). Resistivity measurements were done using Microbots (mibots) from Imina technologies on glass slides covered by conductive Indium Tin Oxide (ITO) stripes. Three different fungi were tested: *F. oxysporum*, *C. cinerea*, and *P. ostreatus*. The three fungi were cultivated on a Petri dish with MEA medium on which a glass slides covered with ITO stripes was placed next to the inoculum. The goal was for the growing mycelium to cover the glass slides. The Petri dishes where then moved to the laboratory in which the recordings were performed, and then the ITO covered glass was detached from the rest of the mycelium with the aid of a scalpel.

A mask indicating the position of the different ITO stripes was placed under the glass to aid precise measurements. The measurements of resistance (Ω) was done following the Ohm law that states that a current (I) passing in a conductor between two points is directly proportional to the voltage (V) across the two points, and where the constant of this proportionality is resistance (Ω). Thus, by dividing the current (I) from the voltage (V), we obtain resistance (Ω). The measurements were made starting from the closest stripe to the fungal inoculum (Table SI1).

Table SI1. Result of the resistance measured in Ohm for Figure 4E.

Sample	Stripe	Ohm
Control 2 mm	1	45,63
Control 4 mm	1	65,13
Control 6 mm	1	78,91
Control 8 mm	1	92,07
Control 10 mm	1	108,2
Control 12 mm	1	128,6
F. oxysporum	6	477,4
F. oxysporum	5	600,1
F. oxysporum	4	7137,2
F. oxysporum	3	3691
F. oxysporum	2	4426,6
F. oxysporum	1	99679
F. oxysporum 2	7	1920,4
F. oxysporum 2	6	1836
F. oxysporum 2	5	8598,9
F. oxysporum 2	4	8794
F. oxysporum 3	1	1682,9
F. oxysporum 3	2	768,22
F. oxysporum 4	7	2689,3
C. cinerea	7	500000000
P. ostreatus	7	5000000000

Multi electrode arrays (Figure 5)

Fusarium oxysporum spore suspensions were produced and quantified as previously reported (Buffi et. Al., 2023). A drop of 20 microliters at a final concentration of 1-10 spores was placed at the centre of the gold plate for recordings. Measurements were run for 2 hours. All the measurements were performed by Sarah Heub (CSEM), and analysed by Alessando Maccione (3Brain.ch).

Visualization of membrane potentials using dyes (Figure 6)

Fusarium oxysporum was cultivated in wells of 400 µl media (LHC (GIBCO), DNMN (GIBCO), liquid malt and Vogel-N-Medium). Before total colonisation of the well by the fungus, Thioflavin T (ThT) was added at a final concentration of 30 µM to the medium. After 30 minutes of gently shaking in the dark, recordings of membrane potential changes were performed on an inverted microscope (EVOS FL imaging system, Invitrogen) with a DAPI filter. Time-lapse recording was performed on 24 h periods with a picture taken every 30 minutes. A representative image of the recordings is shown.

Supplementary information on bioinformatic methods:

Ion channels in fungi (Figure 3)

The human sequence of voltage-gated channel genes (Table SI2) was downloaded from UniProt and run through PSI-BLAST using the UniProtKB Fungi database. The PSI-BLAST results of each gene were then filtered for hits with e-values < 1e-5. Genes with PSI-BLAST results less than 50 hits with e-values < 1e-5 were then removed from the list of voltage-gated channel genes. The filtered PSI-BLAST results of each gene were measured for fungal diversity by counting the number of hits for each fungal phyla (Table SI3) and observing their distribution. FASTA files for each gene were created containing the sequence of each PSI-BLAST hit (e-value < 1e-5) downloaded from UniProt. Each gene FASTA file was aligned using Clustal Omega. The aligned FASTA files were made into hmm profiles using hmmbuild from HMMER.

Table SI2. List of genes tested

Gene	Subunits	Organism	Description
CACNA1	A-S	Homo sapiens	Voltage-sensitive calcium channels
CACNB2	B2	Homo sapiens	Beta subunit of voltage-dependent calcium channels.
CACNG8	G8	Homo sapiens	Regulates the trafficking and gating properties of AMPA-selective glutamate receptors (AMPARs).
CLCN1		Homo sapiens	Chloride voltage-gated channel
CLCN2-7		Homo sapiens	Chloride voltage-gated channel
CLCNKA-B		Homo sapiens	Chloride voltage-gated channel
GRIN2D		Homo sapiens	Receptor for glutamate.
HVCN1		Homo sapiens	Proton-selective channel through which protons may pass in accordance with their electrochemical gradient.
KCNA1		Homo sapiens	Potassium voltage-gated channel
KCNB2		Homo sapiens	Potassium voltage-gated channel
KCNMA1		Homo sapiens	Potassium calcium-activated channel
KCNQ1		Homo sapiens	Potassium voltage-gated channel
SCN1A-5A;8A-11A		Homo sapiens	Sodium voltage-gated channel subunits

Table SI2. List of genes tested with the number of hits for each fungal Phyla

Gene	Ascomycota	Basidiomycota	Blastocladiom	Chytridiomycot	Cryptomycota	Mucoromycota	Olpidiomycota	Zoopagomycot	Total ccount
CACNA1A	81	73	2	5	0	30	0	3	194
CACNA1B	111	34	2	5	0	30	0	2	184
CACNA1C	79	60	2	5	0	31	0	1	178
CACNA1D	117	32	2	5	0	27	0	1	184
CACNA1E	92	63	2	5	0	30	0	3	195
CACNA1F	83	55	2	5	0	27	0	2	174
CACNA1G	155	24	1	5	0	19	0	3	207
CACNA1H	110	53	2	5	0	27	0	3	200
CACNA1I	106	56	2	5	0	30	0	2	201
CACNA1S	120	27	2	5	0	29	0	3	186
CACNB2	26	12	0	2	0	3	0	1	44
CLCN1	109	71	1	9	1	11	0	3	205
CLCN2	154	57	1	6	0	5	0	3	226
CLCN3	191	0	2	9	0	9	0	2	213
CLCN4	191	0	1	9	0	9	0	2	212
CLCN5	196	0	1	9	0	9	0	2	217
CLCN6	128	59	1	9	0	6	0	7	210
CLCN7	172	24	0	6	0	6	0	3	211
CLCNKB	158	61	0	1	0	5	0	3	228
GRIN2D	113	71	0	3	0	4	1	1	193
KCNA1	1	115	2	8	2	33	0	12	173
KCNB2	1	119	2	8	1	32	0	10	173
KCND1	1	119	2	8	2	33	0	10	175
KCNMA1	10	1	2	12	1	33	0	11	70
KCNQ1	2	118	2	8	1	32	0	11	174
SCN10A	67	96	2	5	0	31	0	3	204
SCN11A	43	103	2	5	0	32	0	2	187
SCN1A	63	78	2	5	0	32	0	3	183
SCN2A	63	80	2	5	0	32	0	3	185
SCN3A	65	79	2	5	0	30	0	3	184
SCN4A	48	89	2	5	0	32	0	3	179
SCN5A	56	96	2	5	0	31	0	3	193
SCN8A	35	109	2	5	0	32	0	3	186
SCN9A	65	71	2	5	0	32	0	3	178

To observe how different e-value cut-offs affect the total number of unique species hits, the PSI-BLAST hits were filtered and visualized at several e-value cut-offs (e-value < 1e-5, 1e-10, 1e-15, and 1e-20; Figure SI1). In addition, the e-values of all PSI-BLAST hits were plotted using a boxplot to examine the distribution of e-values across all genes (Figure SI2). For the majority of genes investigated, altering the e-value cut-off did not alter the number of hits, motivating the selection of 1e-5 as presented in the main text. <

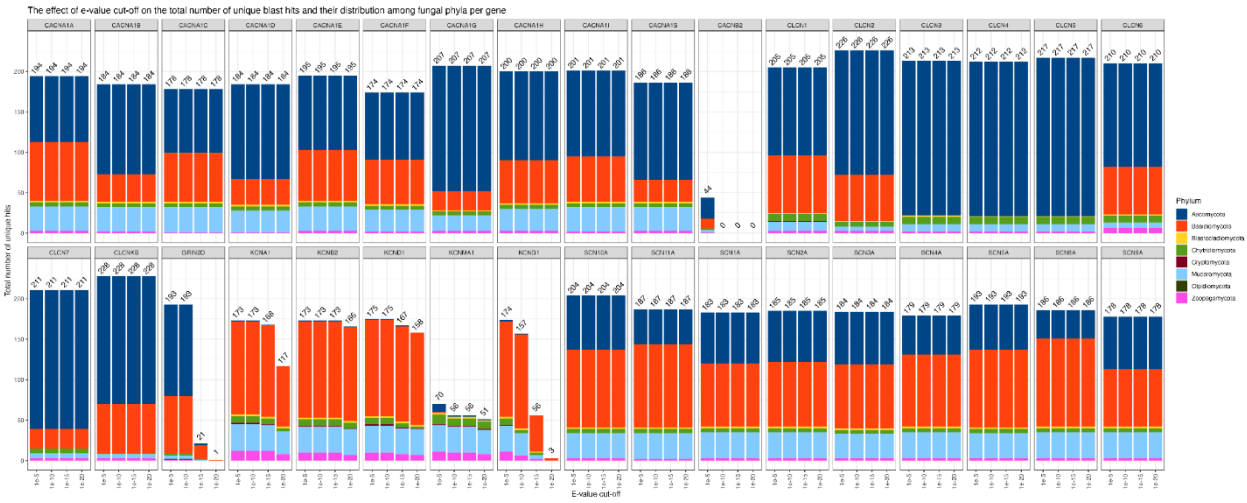

Figure SI1. The change in total number of PSI-BLAST hits and their distribution among fungal clades due to e-value cut-off. The total number of PSI-BLAST hits of unique species was measured after filtering at multiple e-value cut-offs (e-value < 1e-5, 1e-10, 1e-15, and 1e-20). The number above each bar represents the total number of unique species hits that remain after filtering by each respective e-value. In most genes, the total number of hits is not affected by e-value cut-off.

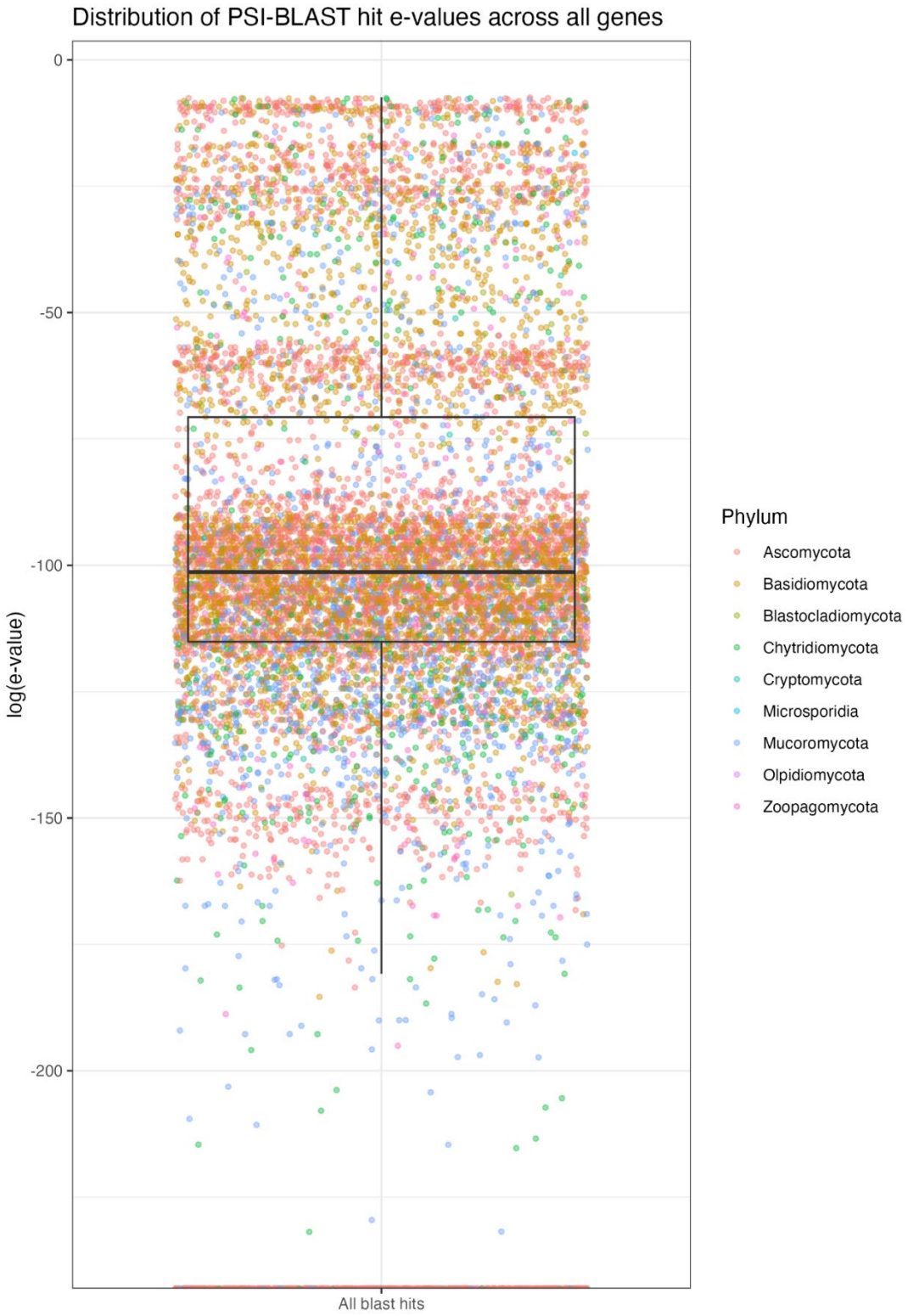

Figure SI2: The distribution of e-value of all PSI-BLAST hits. The e-values of all PSI-BLAST hits across all genes were plotted. Each point represents one PSI-BLAST hit and the color of the point represents the phylum it belongs to. E-value is represented on a log scale on the y-axis. The median determined the median determined e-value was above the selected cut-off threshold.

Chapter 2

Fungal drops: a novel approach for macro- and microscopic analyses of fungal mycelial growth

Published: 18 October 2023

FEMS μLife

DOI: https://doi.org/10.1093/femsml/uqad042

Contributions:

Matteo Buffi, contributed to the study conception and design. Material preparation, data collection and analysis and to the writing of the manuscript.

microLife, 2023, **4**, 1–13
DOI: 10.1093/femsml/uqad042
Advance access publication date: 18 October 2023
Research Article

Fungal drops: a novel approach for macro- and microscopic analyses of fungal mycelial growth

Matteo Buffi[1], Guillaume Cailleau[1], Thierry Kuhn[1,2], Xiang-Yi Li Richter[1,2,3], Claire E. Stanley[4], Lukas Y. Wick[5], Patrick S. Chain[6], Saskia Bindschedler[1,*], Pilar Junier[1,*]

[1]Laboratory of Microbiology, University of Neuchâtel, Rue Emile-Argand 11, 2000 Neuchâtel, Switzerland
[2]Laboratory of Eco-Ethology, University of Neuchâtel, Rue Emile-Argand 11, 2000 Neuchâtel, Switzerland
[3]Present address: Institute of Ecology and Evolution, University of Bern, Balterstrasse 6, 3012 Bern, Switzerland
[4]Department of Bioengineering, Imperial College London, B304, Bessemer Building, South Kensington Campus, SW7 2AZ, London, United Kingdom
[5]Department of Environmental Microbiology, Helmholtz Centre for Environmental Research - UFZ, Permoserstrasse 15, 04318 Leipzig, Germany
[6]Bioscience Division, Los Alamos National Laboratory, Los Alamos, P.O. Box 1663, NM 87545, United States
*Corresponding authors. Laboratory of Microbiology, University of Neuchâtel, Rue Emile-Argand 11, 2000 Neuchâtel, Switzerland.
E-mail: saskia.bindschedler@unine.ch; pilar.junier@unine.ch
Editor: [Axel Brakhage]

Abstract

This study presents an inexpensive approach for the macro- and microscopic observation of fungal mycelial growth. The 'fungal drops' method allows to investigate the development of a mycelial network in filamentous microorganisms at the colony and hyphal scales. A heterogeneous environment is created by depositing 15–20 μl drops on a hydrophobic surface at a fixed distance. This system is akin to a two-dimensional (2D) soil-like structure in which aqueous-pockets are intermixed with air-filled pores. The fungus (spores or mycelia) is inoculated into one of the drops, from which hyphal growth and exploration take place. Hyphal structures are assessed at different scales using stereoscopic and microscopic imaging. The former allows to evaluate the local response of regions within the colony (modular behaviour), while the latter can be used for fractal dimension analyses to describe the hyphal network architecture. The method was tested with several species to underpin the transferability to multiple species. In addition, two sets of experiments were carried out to demonstrate its use in fungal biology. First, mycelial reorganization of *Fusarium oxysporum* was assessed as a response to patches containing different nutrient concentrations. Second, the effect of interactions with the soil bacterium *Pseudomonas putida* on habitat colonization by the same fungus was assessed. This method appeared as fast and accessible, allowed for a high level of replication, and complements more complex experimental platforms. Coupled with image analysis, the fungal drops method provides new insights into the study of fungal modularity both macroscopically and at a single-hypha level.

Keywords: bacterial–fungal interactions; mycelium observation; quantification fractal dimension; fungal highways; mycological method; user-friendly

Introduction

Filamentous fungi are tip-growing organisms that display a three-dimensional (3D) radial growth of tube-like branched structures called hyphae (Grove and Bracker 1970). This growth pattern eventually leads to the formation of mycelial networks, which are structures observed from the millimetric to the metric-scale. This growth mechanism is ideal for the colonization of soils, and thus, it is observed in other fungi-like microorganisms including some bacteria and protists (Wolf et al. 2013, Geisen et al. 2018). Soils are considered as one of the most structurally and biologically complex ecosystems on Earth and a major reservoir of biodiversity (Nannipieri et al. 2003, Fitter et al. 2005, Senesi and Wilkinson 2008, Phillips 2017). In soils, shifting chemical properties and heterogeneity are exacerbated by an ever-changing physical matrix, which gives rise to a 3D structure with an arguably infinite combination of microniches (Ettema and Wardle 2002, Tiedje et al. 2009). Given the complexity of soils, fungi and fungi-like organisms need to be able to coordinate the behaviour of their mycelial network in order to cope with all the interactions and challenges encountered during colonization. Filamentous fungi have a remarkable ability to adapt to the variable 3D structure of soils. This is provided by the secondary growth of hyphae, called branching, and by the process of hyphal anastomosis, consisting in cell-to-cell fusion at the hyphal scale. In addition to this, filamentous fungi are also able to reallocate resources to regions of the mycelia where nutrients are required, leaving some hyphae almost devoid of cytoplasmic content. Eventually, some parts of the mycelial network may even be used as a nutrient source through autolysis (Jiang et al. 2022). All these processes allow fungi to reorganize their network in order to improve resource exploitation through nutrient acquisition and translocation (Rayner et al. 1995, Harris 2008, Fischer and Glass 2019). Network reorganization through branching, anastomosis, and autolysis are thus essential process that enable fungal survival and colonization of environments with a complex 3D structure (Fricker et al. 2007, Harris 2008).

To understand the process of network reorganization, the 3D structure and complexity of soils must be replicated. However, achieving this at a laboratory scale is highly challenging. Solid media is generally used for the growth and maintenance of fungal mycelia. Solid media can be modified to allow for the combination of multiple nutrient conditions or the separation of interacting organisms, for example in two-compartment Petri dishes (Hunziker

Received 7 July 2023; **revised** 11 October 2023; **accepted** 17 October 2023

et al. 2015). However, in solidified media (e.g. agar-based media), direct microscopical observation of individual hyphae is difficult due to extensive and overlapping mycelial growth. Cutting of a thin media layer and observation on a glass slide allows for the recognition of physiological structures such as sexual or asexual fructifications. But the spatial arrangement of the sample cannot be preserved during preparation of thin slices. Furthermore, nutrient heterogeneity, which is a defining feature of soils (Aleklett et al. 2018), is difficult to replicate in jellified media. Cultivation in liquid media is often used for the production of metabolites by fungi, but liquid media is an even poorer representation of soils. In fully mixed liquid cultures, emulating the patchiness of nutrient distribution is not possible and microscopic observations are also difficult. The use of microfluidic devices allows for spatial separation and confinement of single hyphae under nutrient-rich and deficient conditions, but provides only limited control of air-filled voids (Gimeno et al. 2021). Furthermore, microfluidic technologies often require specific equipment for their production. Other techniques are being developed to recreate soil in a 2D or 3D fashion (Otten et al. 2012, Aleklett et al. 2018), but experimental systems that allow to replicate more than one or two soil properties simultaneously are uncommon.

In this study, a novel and inexpensive approach for the macro- and microscopic observation of fungal mycelia is proposed. The approach aims to recreate the patchy structure of soil in a simple and straightforward manner. This provides a way to replicate niche heterogeneity associated with air gaps and assorted resource availability. By disposing drops of liquid media on a cell culture-treated Petri dish, it is possible to recreate a 2D patchy environment for the fungus to grow. The individual drops, each of a few microliters, allow for multistimuli testing on one mycelial colony at once. The control of distance between the drops allows for the observation of mycelial exploration at the colony (macroscopic) or single hyphal (microscopic) levels. Inoculation can be done either using spores or mycelial fragments, recreating a situation where a single propagule starts to explore its environment. Also, the system can be used for the characterization of different mycelial behaviours, such as branching, elongation-growth speed, surface hyphal proprieties (i.e. hydrophilicity or hydrophobicity), thigmotropism, formation of reproductive structures, or secondary growth. As the drops are not confined, the addition of other factors (organisms, stressors, and nutrients) is possible at any time during the experiment. This is particularly suited for observing response to an abiotic or trophic factor, and intraorganismal interactions. Furthermore, as continuous microscopic observations are feasible, it is possible to produce time-lapse images and evaluate the complexity of the mycelial network over time by quantifying the changes in the mycelial mass fractal dimension (FD). FD is an index that represents in a single value the complexity and space-filling efficiency of mycelial growth in response to different stimuli at a microscopic scale (Juge et al. 2009). This method is already used to quantify shape in corals (Martin-Garin et al. 2007), complexity during plants development (Corbit and Garbary 1995), and space-filling capabilities in filamentous microorganisms (Boddy et al. 1999, Papagianni 2006, Barry et al. 2009). The latter is particularly relevant for filamentous fungi in which a trade-off between apical and lateral hyphal growth is essential for resource exploitation, exploration, and colonization intensity of highly heterogeneous substrates (Camenzind et al. 2020). Moreover, the development and use of this method to extract information on the network features of mycelial growth has greatly facilitated the quantitative description of the complex behaviour of filamentous microorganisms and our ability to characterize these dynamic networks (Heaton et al. 2012). FD analysis requires high consistency in image collection and treatment within a given experiment, and is especially suited for describing complex structures on a flat surface (Juge et al. 2009). All of the former makes FD suitable as a quantitative approach to analyse the results generated with the spore drop method, which typically will consist in images of filamentous network with different levels of complexity. Herein, the validation of the approach is described by testing three different scenarios: (i) growth and features' observation for different filamentous fungal species and one oomycete, (ii) modulation of the mycelial network of a selected filamentous fungus to different nutrient concentrations, and (iii) bacterial–fungal interactions. The two latter scenarios were chosen to provide not only a proof-of-concept for the fungal drops method, but also to demonstrate its general application to obtain insights into the morphophysiological and ecological responses of fungi and other filamentous microbial species to changing trophic and biotic factors in a complex environment. Indeed, soil heterogeneity, both in terms of structure and resource distribution as well as bacterial–fungal interactions are known to be key to soil functioning and fungal ecology (Barron 1988, 2003, De Boer et al. 2005, Deveau et al. 2018). Hence, the scenarios chosen. Moreover, this new approach can be replicated with ease in any laboratory using basic microbiological equipment and without the need for specialized materials.

Materials and methods

Method validation

To initially test if the fungal drops method would function for different filamentous microbial species, five organisms were selected from our laboratory collection. Three Ascomycota fungi: the phenotypic plastic *Fusarium oxysporum*, the well-known gourmet mushroom *Morchella crassipes*, and the saprotrophic biocontrol agent *Trichoderma rossicum*; the fast growing and ubiquitous *Mucor moelleri* (Mucoromyctoa); and the pathogenic Oomycota *Pythium ultimum*. In all further experiments, *F. oxysporum* was used as main model organism. This fungus is commonly found in soils and its very large phenotypic plasticity makes it an interesting model to study fungal behaviour. Some strains are described as plant pathogens (Fravel et al. 2003, Gordon 2017, Joshi 2018), while others have been described as beneficial (or at least neutral) to plants (de Lamo and Takken 2020). Moreover, easy spore production was also an important factor in the choice of this organism. For the experiments testing bacterial–fungal interactions, the model soil bacterium *Pseudomonas putida* KT2440 (Nelson et al. 2002) was used. This bacterium has been used in previous experiments investigating interactions with soil fungi (Pion et al. 2013) or fungi-like soil dwellers (You et al. 2021). The strain used is constitutively tagged with green fluorescent protein (GFP). All the strains were obtained from the fungal and bacterial collection of the laboratory of microbiology, University of Neuchâtel, Switzerland. For the regular maintenance, all filamentous microorganism were plated on Malt Extract Agar (MEA; Table S1, Supporting Information), while the bacterium was maintained on Nutrient Agar (NA; Table S1, Supporting Information).

Inocula preparation

For experiments involving *P. ultimum*, *M. moelleri*, and *M. crassipes*, mycelial suspensions were used for drop inoculation due to the difficulty in producing and/or collecting asexual spores. *P. ultimum* and *M. moelleri* were inoculated in M9 mineral liquid

medium (Table S1, Supporting Information) while Malt Extract Broth (MEB; Table S1, Supporting Information) was used for *M. crassipes*. All fungi were then cultured at room temperature under agitation (Lab Shaker, Adolf Kühner AG) at 120 rpm for 5 days. The mycelium was then fragmented in a 50-ml Falcon tube (CORNING®) using an ULTRA-TURRAX® (IKA® T18 basic) at max speed for 10 seconds, and then washed three times with physiological water (0.9 g l^{-1} NaCl). Hyphal density was then assessed with a Neubauer chamber (BIOSYSTEMS® 0.01 mm) and resuspended at a final concentration of around 10 hyphal fragments l^{-1} in M9 mineral medium (Table S1, Supporting Information) for *P. ultimum* and *M. moelleri* and MEB for *M. crassipes*. For experiments involving *F. oxysporum* and *T. rossicum*, spore suspensions were used for drop inoculation. *Fusarium oxysporum* was grown on Potato Dextrose Agar (PDA; Table S1, Supporting Information) for 2 weeks in order to induce asexual spore formation. Spores were then collected following a method described previously (Bruisson et al. 2019) and stored in 500 µl MilliQ water at 4°C. Spores were quantified in a Neubauer Chamber (BIOSYSTEMS® 0.01 mm) and diluted to the desired concentration in MilliQ water or in the selected medium immediately before the start of the experiment. The same general method was used for *T. rossicum*, with the only difference being the induction of sporulation. For conidia production, *T. rossicum* was inoculated on MEA (Table S1, Supporting Information) and incubated at room temperature under the exposition to sunlight for 2 weeks in order to increase conidia production. The bacterium *P. putida* KT2440 was cultivated overnight in 5 ml of Nutrient Broth (NB; Table S1, Supporting Information), at 120 rpm room temperature. The culture was then washed three times with physiological water and diluted to ~2.2×10^4 cells in the target medium as a final inoculum.

Construction of the system

Tissue-culture treated Petri dishes (CORNING®, REF 430167) compatible with direct inverted microscopic observations were used. These Petri dishes are treated for optimal cell adhesion, and are often used for the culturing of mammal cells. Masks to facilitate the precise positioning of the drops were made beforehand with Adobe illustrator® and are provided as Supplementary Information (Figure S1, Supporting Information). Deposition of the drops (15–20 µl) was performed with a 20-µl pipette and with the aid of the mask placed underneath the Petri dish. To prevent drop desiccation a larger Petri dish with humidified cotton or an incubation chamber was prepared using either a desiccator containing moistened vermiculite at the bottom. In the desiccator humidity was measured using a hygrometer (GFTH200, Greisinger®). Air circulation was maintained using a hydrophobic filter allowing for gas exchange while retaining moisture inside.

Comparison of the fungal drops system to normal agar medium

To compare the growth and the utility of the fungal drops system to normal agar based solid media, spores of *F. oxysporum* were collected as mentioned above and suspended to 1–2 spores per 15 µl in liquid MEB (Table S1, Supporting Information). For this, 15 µl drops where then deposed either on solid PDA or on tissue culture-treated Petri dishes (CORNING®, REF 430167) and then incubated at room temperature. To compare the two systems, pictures were taken in the same time frame (8-day post inoculation or dpi). Additionally, a 24-hour time-lapse was performed between 1 and 2 dpi to show how the fungus escapes the drop environment and further colonizes the space between the drops.

Stereo- and microscopic analysis of the system

Whole Petri dish images were taken with a Canon Powershot SX230 HS camera. Macroscopic observations of single drops were performed with a stereoscope (NIKON SMZ18). Microscopical observations were performed with an inverted microscope (EVOS FL, EVOS M5000, Invitrogen) at room temperature and room relative humidity. For this, the Petri dish was positioned on the microscope and the focus was performed manually.

Measure of drop area for each media used at different volumes

In order to assess the reproducibility of the system, different drop volumes (5, 10, 15, and 20 µl) for each liquid medium used for this manuscript (Table S1, Supporting Information) were deposed in triplicates on a tissue culture-treated Petri dish (CORNING®, REF 430167), and then photographed with a Canon Powershot SX230 HS with the aid of a camera holder. The pictures were taken on a flat levelled surface to avoid the change in shape of the drop during visualization. The area in cm^2 was then measured with Image J and the results were plotted with R version 4.2.2 (R Core Team 2022).

Fluorescein trace test for assessing drop leakage on mycelium

To observe whether any hydraulic flow established from one drop to another trough fungal hyphae, *M. moelleri* was inoculated as mentioned above and 0.01% Fluoresceine sodium (MERCK Sigma-Aldrich, Germany, Ref: 518–47-8) was added either in the inoculum or the target drops. This molecule is often used as a fluorescent tracer for liquids. Images with a GFP filter were taken in order to follow the liquid movement. The same experiments were performed with *P. ultimum*.

Effect of target nutrient availability on mycelial growth of *F. oxysporum*

System set-up

In order to investigate the behaviour of *F. oxysporum* when confronted with different nutrient concentrations, asexual spores of the fungus were collected and quantified as described above and then diluted in MEB (Table S1, Supporting Information) to a concentration of about two spores μl^{-1}. The drop system was prepared using a flower-like design (mask provided in Figure S1, Supporting Information) in order to assess the effect of different nutrient concentrations on growth patterns. The central drop (15 µl inoculum) was surrounded by six drops (15 µl each) containing three different target media: potato dextrose broth (PDB; Table S1, Supporting Information), PDB diluted at a 1:2 ratio (PDB 1:2) or 1:10 ratio (PDB 1:10). Drops with the different media were all positioned 5 mm from the central drop and in duplicates for each flower. Positioning of the different target media were randomized three times in order to avoid experimental bias. Each Petri dish contained six identical flowers, for a total of six Petri dishes giving 36 replicates for each target media.

Image treatment and mass FD analysis

To assess mass FD of the mycelial network image treatment was performed using R version 4.2.2 (R Core Team 2022) and Image J (Schneider et al. 2012). FD was measured using the box counting method already used for mycelia (Obert et al. 1990, Boddy et

al. 1999, Senesi and Wilkinson 2008). This method involves overlapping the image with grids of scaling pixel sizes (i.e. 3, 6, 12, 24, 48, 96, 192, and 384). Mycelial presence for each grid box and at a given size was then assessed and FD was estimated as the slope of the logarithmic regression between the counted boxes and their scaling factor. For the mass FD, the images needed to be treated to extract the mycelium from the image and to remove unwanted noise around the fungal filaments. Step-wise treatment was performed as follows: (i) 8-bit images were hand-cropped in R to extract the region of interest removing the scalebar and drops from the image to be analysed, (ii) a Kuwahara smoothing filter (linear variant) was selected in ImageJ to perform an adaptive noise reduction to highlight the hyphae, (iii) a Sobel edge detector was used to detect drastic changes in image intensity (i.e. the hyphae), (iv) the output was converted to a binary mask that makes the fungal filament edge appear white and the background black, and (v) for each grid made of a given box size, each box covering a white pixel was counted. After repeating step five over the range of box sizes, the mass FD of the image was calculated. All the scripts used are provided as a detailed procedure (Supplementary Information S1). Statistical analyses were performed in RStudio (RStudio 2020). A two factor ANOVA was performed, and a *post hoc* Tukey contrast was used to obtain pair-wise comparisons between the different factors for the exploratory behaviour based on nutrient choice.

Image treatment and colour quantification

To quantify the red colouration in relation to different media concentrations, the images were processed using ImageJ software to isolate the red colour from the rest of the image. First, the images were converted into LAB colour space using the 'Lab stack' function in ImageJ. The 'a-chroma' stack was then duplicated and extracted from the stacks. Next, an automatic thresholding algorithm called the Huang Thresholding Algorithm was applied to all images to maximize the entropy between the pixels that needed to be counted (i.e. red colour) and the background pixels. The Polygon selection tool in ImageJ was used to define the border of the drops as the area of interest for analysis. To quantify the red pixels, the 'Analyse Particles' function in ImageJ was used for each defined drop. Drops that were not fully visible in the image were excluded from the analysis. Statistical analyses were performed as indicated above for the FD analysis.

Bacterial–fungal interactions

System set-up

In order to assess the interaction of *F. oxysporum* with the bacterium *P. putida*, asexual spores of the fungus and cells of *P. putida* KT2440 were prepared as described above and then resuspended in MEB to a final concentration of one spore μl^{-1} for *F. oxysporum* and 2×10^4 bacterial cells per drop for *P. putida* KT2440. The drop system was prepared as described above using lanes of four consecutive drops with a 5-mm gap between each drop. Three lanes were placed per Petri dish, each placed 2 cm apart from the other (mask provided in Figure S1, Supporting Information). The experimental setting included three different conditions: (i) simultaneous inoculation of both the spores and the bacterial cells in the same drop, (ii) inoculum of *F. oxysporum* alone, and (iii) inoculum of *P. putida* alone. To control for the change in volume upon bacterial coinoculation, 10 μl of sterile physiological water (0.9% NaCl in deionized water) were added to the fungus-alone condition.

Bacterial viability

To verify the dispersal and viability of bacteria, bacterial abundance in the drops was measured each day for 8 days in three independent replicates. For this, 4 μl were collected and suspended in 16 μl of NB. The resulting suspension was then diluted six times by resuspending each time 10 μl in 90 μl of NB (10x dilution series). A volume of 5 μl of each dilution were then plated on NA enriched with cycloheximide (500 mg l^{-1}) and incubated at 30°C. After 24 hours, bacterial abundance was assessed by counting colony forming units (CFU).

FD analysis

In order to quantify the effect of *P. putida* on the growth of *F . oxysporum* FD differences were measured as described above. Pictures from six replicates were taken in between the inoculum drop and the first target drop after 7 days for the conditions in which the fungus was inoculated alone and when coinoculated with the bacterium. A Student's *T*-test is used to compare the mean between the two groups. All the statistical analyses and plotting are performed on RStudio (RStudio 2020).

Results

Construction of the fungal drops system

The goal of the approach developed here was to recreate the heterogeneous structure and patchy resource distribution of soils in order to observe the exploratory behaviour and growth of filamentous microorganisms. For this, a variable number of drops were deposited at a fixed distance on a cell culture Petri dish treated to improve cell adhesion. The premise considered here is that given the radial and exploratory growth pattern of filamentous fungi, they will exit the initial drop and colonize adjacent drops. Multiple experimental configurations can easily be produced in the system as illustrated by the different tests performed (see specific experiments below). In addition, the approach is simple and allows for a high level of replication and throughput. In the cases described here, one of the drops corresponded to the inoculum and contained a suspension with spores (Fig. 1A-top). From this initial point, hyphae emerged and explored their surroundings in response to the trophic or biotic stimuli provided (Fig. 1A-bottom). Given the very small inoculation volume (usually 10–25 μl), one major issue that can limit the use of the system is fast desiccation. Two methods were tested to prevent the system from drying out during the experiments. For the incubation of individual Petri dishes, those were placed inside a nontreated 100 mm Petri dish with cotton filters at the bottom soaked in 2 ml of deionized water (Fig. 1B). This method was suitable if the system was to be moved or required continuous monitoring. Alternatively, an incubation chamber with moistened vermiculite at the bottom allowed the humidity of the system to be maintained at above 80% (Fig. 1C). This method was suitable for incubating several Petri dishes simultaneously and was used as the main incubation method for all the experiments with the drops. The time required by the drop to completely dry depended on the volume of the drop and the organism used. For instance, when inoculated alone, *F. oxysporum* drops remained moist for up to 1 month if kept in the humid chamber but dried out in a matter of days when left outside of the incubator.

In order to assess the reproducibility of the inoculation scheme, the final area of the drop (i.e. surface covering the bottom of the plate) was correlated to the inoculation volume. Well-defined drops (Fig. 1D) were obtained from a range of inoculation volumes

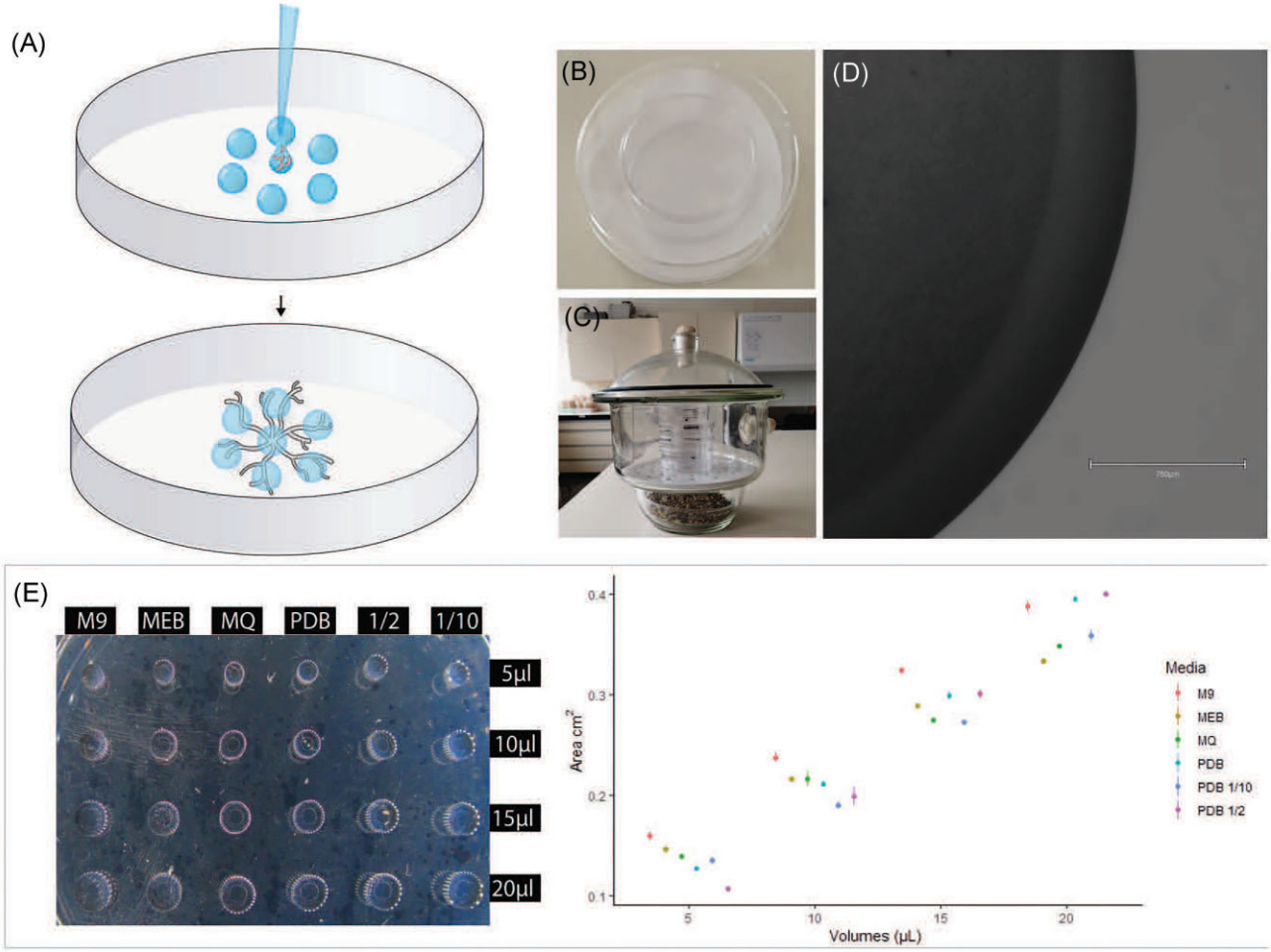

Figure 1. Experimental set-up of the drop system. (A) Schematic representation of the system: one or multiple drops consists of the spore or mycelial fragments' inoculum (here drop in the middle), which is surrounded by other drops to be colonized and monitored. In order to maintain humidity two different humidity-controlled chambers were used: (B) a 9-mm Petri dish with a cotton filter soaked in sterile water; or (C) a desiccator containing water-saturated vermiculite at the bottom and a hydrophobic air filter. (D) Microscopical image of noninoculated drop. In the image it is possible to observe the continuous border of the drop, showing no diffusion of the liquid on the treated surface. (E) Image showing drops of different volume (5, 10, 15, and 20 µl) of all the different media used in this work deposed on the cell culture-treated Petri dish (left); a plot relating the area (cm^2) measured for each different volume (three replicates for each volume) is shown on the right. Each coloured point represents the mean and standard deviation for three replicates of the same media, the different colours represent different media tested. Red: M9 mineral medium (M9); yellow: MEB; green: Milli Q water (MQ); light blue: PDB; dark blue: PDB 10 times diluted (PDB 1/10); and violet: PDB two times diluted (PDB 1/2).

between 5 and 20 µl and this was consistent for all the media tested (Fig. 1E). Although deposition was done manually, pipetting errors were negligible and the variation between multiple drops replicates was low. This was seen in the volume/area ratio of multiple individual replicates. For the duration of the experiments testing of the system (in our case 7–15 days) the optimal volume was 15–20 µl. This is mainly due to a trade-off between evaporation, which is inversely correlated to the volume, and stability of the drops during manipulation of the Petri dishes, which is more problematic with increasing volumes.

Growth of filamentous microorganisms in the drop system and liquid movement between the drops

Several organisms were compared to validate the performance of the fungal drops method. First, germination, growth, and exploration behaviour were assessed with *F. oxysporum* comparing the fungal drops system to normal agar plates (Fig. 2). In both systems the fungus was able to germinate, grow, and expand from multiple inoculation points (Fig. 2A and E). Images at different levels of magnification were taken to compare the performance of the two methods. In the macroscopic view of a single colony (Fig. 2B and F), single hyphae were distinguishable in the drop method but not in the solid medium. On solid media, as hyphae do not grow on a 2D plane, direct microscopy offered only limited information (Fig. 2C and D). In contrast, easy microscopic and stereoscopic observations were possible without the need for destructive sampling for the drop system, reaching a single hypha resolution (Fig. 2G and H). Furthermore, in the drop system it was possible to follow the habitat exploration strategies behaviour of *F. oxysporum* using time lapse microscopy (Fig. 2I; Supplementary Video).

Other filamentous organisms were also all able to germinate in the drop environment and then escape from the drop to explore the surroundings (Fig. 3 A–D). Furthermore, additional mycelial characteristic could be observed for specific organisms. For instance, in the case of the ascomycete *M. crassipes*, besides the observation of multiple hyphal structures, it was possible to observe the deposition of a black pigment at the edge between the drop and the air (Fig. 3A). In *M. moelleri* (Fig. 3B) and *T. rossicum* (Fig. 3C), the exploration beyond the edge of the drop coincided with the

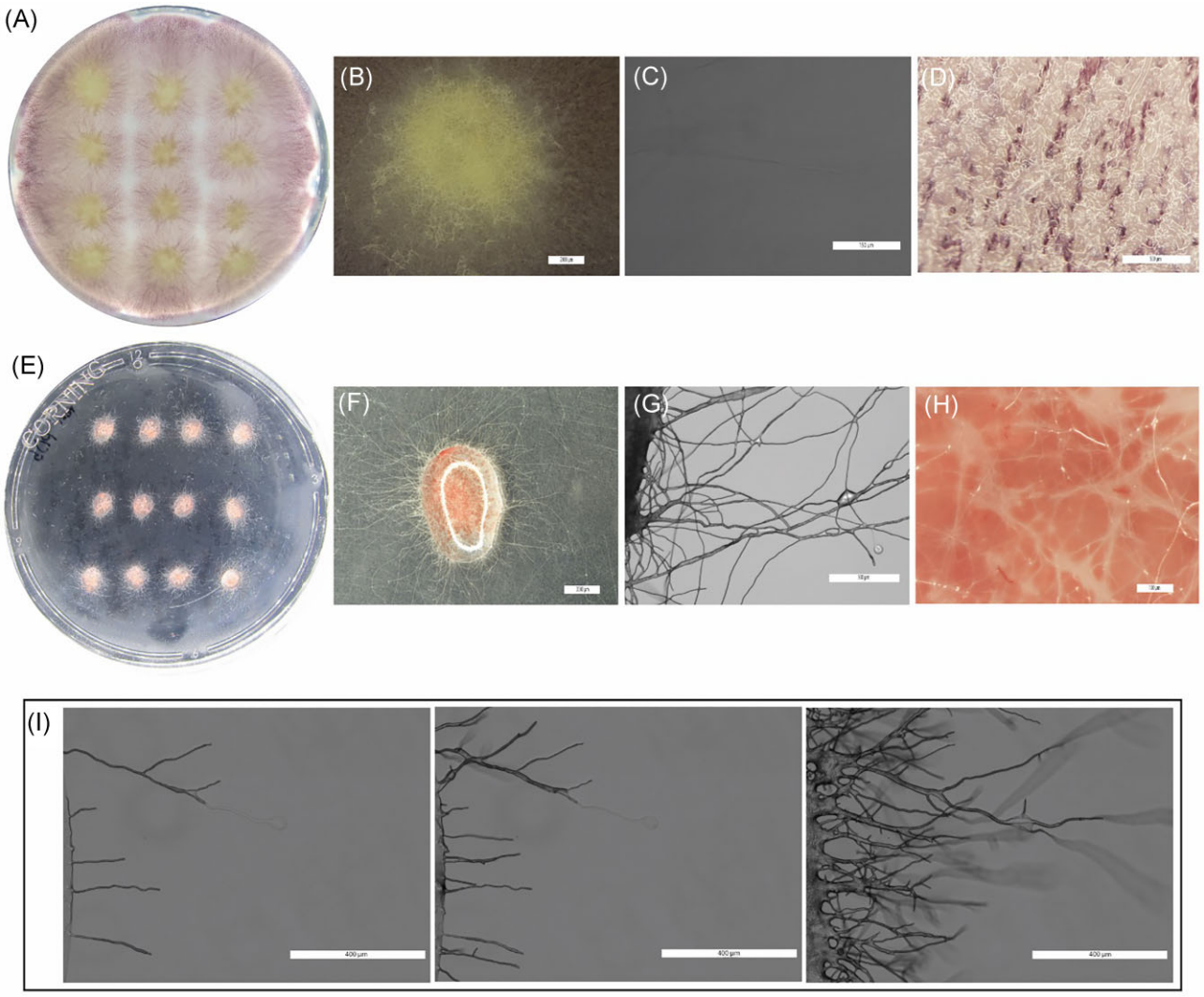

Figure 2. Growth of *F. oxysporum* in the drop system and comparison to normal agar media. Comparison of germination from spores and growth of *F. oxysporum* on PDA (A–D) versus germination and growth on drops with PDB (E–H). The images in (A) and (E) corresponded to the entire Petri dish (9 cm in diameter); Images (B) and (F) correspond to stereoscopic pictures of one replicate for the agar and the drop system, respectively. Images (C) and (G) correspond to images of the same area observed in (B) and (F) but taken with an inverted microscope. Images (D) and (H) show a close up of the colony surface in normal agar or in the drop system, respectively. (I) Snapshots of the supplementary video showing the growth (in MEB) of the mycelium of *F. oxysporum* out of the drop (drop edge visible on the left) in a 24-hour microscopical time lapse movie 1-day postinoculation.

production of asexual reproductive structures when in contact with air. The tests were not restricted to organisms of the fungal kingdom as we included the filamentous oomycete *P. ultimum*, which has previously been used as a model organism for the study of bacterial dispersal on mycelial networks (Wick et al. 2007). *Pythium ultimum* was also able to grow in and out the drops and we observed that the liquid film around the hyphae was thicker than for the other filamentous organism tested here (Fig. 3D). Moreover, with this method, a reduction of the thickness of the liquid film around the hyphae could be highlighted when *P. ultimum* was cocultured with a bacterium (Figure S2, Supporting Information). Finally, to assess whether any movement of liquid could be observed along the hyphae once the organism has exited a drop, we used fluorescein staining of the liquid phase. The comparison of white field and fluorescent images showed some fluorescent signals in hyphae outside the drops (Fig. 3E and F). However, this did not occur with all the hyphae exiting the drop (Fig. 3G and H). To test whether the signals corresponded to fluorescein being moved by the fungus existing the drop, the same experiments were conducted with *P. ultimum*. In the absence of fluorescein, fluorescent signals were observed in the mycelium, suggesting that autofluorescence can explain the fluorescence signals observed previously (Figure S3, Supporting Information). Moreover, in the presence of fluorescein, no movement of the dye was observed outside the drops, both in the presence or absence of bacteria (Figure S4, Supporting Information).

Effect of nutrient concentration on mycelial growth of *F. oxysporum*

To illustrate the use of the approach to investigate questions relevant to the biology of filamentous microorganisms we investigated the effect of variable concentration of nutrients on the habitat exploration strategies of an expanding mycelium. For this, a flower-like spatial arrangement was adopted inspired by previous studies performed to test the recruitment of entomopathogenic nematodes by ravaged plants (6-arm olfactometer) (Rasmann et al. 2005). This flower-like design allows for multiple stimuli to be tested at the same time (Fig. 4A and B). Macroscopic changes in

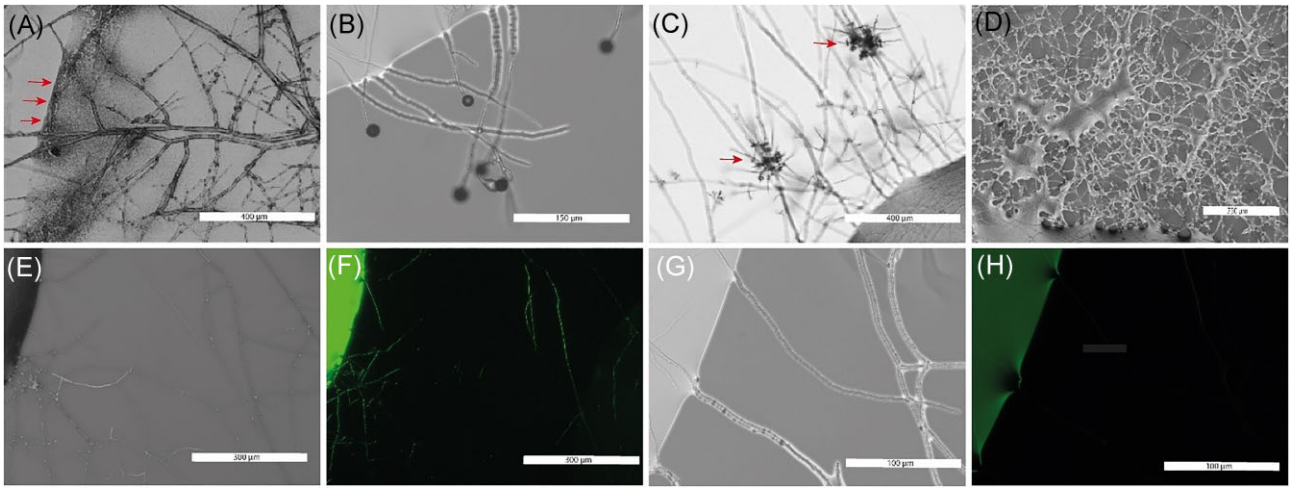

Figure 3. Growth of different filamentous microorganisms in and out the drops and liquid movement on the mycelium. (A) Observation of the production and deposition of a dark pigment at the edge of the drop (red arrows) by the Ascomycota *M. crassipes*. (B) Microscopical observation of *M. moelleri* exiting the drop and producing conidiophores; (C): microscopical observation of the asexual reproductive structures (conidiophores; red arrows) formed outside of the drop of the ascomycete *T. rossicum* cultivated in MEB; (D) stereoscopy image of the mycelium of the highly hydrophilic mycelium of the oomycete *P. ultimum* after existing the drop (visible on the bottom of the image). (E–H). White field and fluorescence images showing liquid redistribution by hyphae of *M. moelleri* exiting from the drop (visible on the left).

the colonies were observed and those were correlated with quantitative differences in the microscopic architecture and density of the mycelium. The mycelium of *F. oxysporum* was able to exit the inoculum drop and colonize all of the adjacent target drops (Fig. 4C). The exploratory behaviour of the emerging hyphae was already visible at 2 days postinoculation (dpi) with higher density towards the two times diluted medium (PDB 1/2; Fig. 4C). The difference in the hyphal density connecting drops with different media concentrations became more apparent at the macro and microscopic levels after 8 dpi (Fig. 4C). Moreover, the macroscopic overview of the experiment at 8 dpi revealed a difference in the concentration of a pigment secreted by the fungus in the target media (Fig. 4C). Analysis of the percentage covered by red colour in each drop (Fig. 4D), revealed a significant difference (P-value < .001; df: = 2) between the three different media concentrations. The full medium (PDB) being the most coloured (mean = 75.24, sd = 8.39, P-value < .001), then the two times diluted with an average colouration (mean = 47.74, sd = 9.49, P-value < .001), and last the 10 times diluted media with a slight colouration (mean = 11.54, sd = 3.5, P-value < .001).

Mass FD was used to compare the space-filling efficiency of mycelial growth between the inoculum drop and each of the six target drops (Fig. 5). The hypothesis tested was that once the fungus had made contact with drops of different nutrient content (stimuli), it will reallocate resources to occupy more efficiently the space in which nutrient concentration is highest. After image treatment (Fig. 5A–D), mass FD was measured from pictures taken at 2 or 8 dpi. Different grid sizes were tested for the analysis in order to assess the robustness of the method and to select the best settings for our experiment. Although the absolute FD value changed with a given combination of box sizes (Table S2, Supporting Information), the overall tendency of the results is maintained, as shown by the comparison of the statistical analysis performed with different box sizes (Table S3, Supporting Information). The series of box sizes 3, 6, 12, 24, 48, 96, 192, and 384 was selected for the analysis, as the starting point (box size 3) is representative of the smallest size object that is observed in the images, and the largest size (box size 384) excludes values in which FD does not change within the images (Table S2, Supporting Information). At 2 dpi, the highest mean FD (FD = 1.549) was observed for PDB 1/2, followed respectively by PDB (FD = 1.532), and PDB 1/10 (FD = 1.498) (Fig. 5E). The highest FD at 8 dpi was found in mycelium reaching the drops containing PDB (FD = 1.613), followed by PDB 1/2 (FD = 1.593) and PDB 1/10 (FD = 1.533) (Fig. 5E). The statistical analysis (Table S4, Supporting Information) showed that there was a statistical difference in FD between 2 and 8 dpi (F-value = 34.43; df = 1; P-value = < .001), regardless of the concentration of nutrients. For all nutrient concentrations, FD was higher at 8 dpi as compared to 2 dpi (PDB: P-value < .001; PDB ½: P-value: .002 and PDB 1/10: P-value = .0158). Statistically significant differences between target media were also observed (F-value = 7.5823, df = 2, P-value < .001). Specifically, the FD at 2 dpi in PDB 1/2 (mean = 1.549) was found to be statistically different to PDB 1/10 (mean = 1.498; P-value = .00165). FD was also higher for PDB (mean = 1.532) compared to PDB 1/10 (mean = 1.498), but this difference was not significant (P-value = .05). At 8 dpi, the FD was not statistically different between PDB (mean 1.613) and PDB 1/2 (mean 1.593), but a statistical difference was found between these two and PDB 1/10 (P-value < .001) (Table S4, Supporting Information).

Bacterial–fungal interactions

The system could further be used to study interactions of mycelium-forming organisms with other soil dwellers such as bacteria. To do this, a different spatial arrangement of drops was used. Specifically, multiple drops were deposited in a straight line equidistant from one another to form a 'lane', with the first drop containing the inoculum (Fig. 6A). Multiple lanes were placed in parallel to one another within a single Petri dish to allow direct comparison of multiple treatments. By maintaining a sufficient distance between each lane (in this case 2 cm, which is greater than the intradrop distance of 0.5 cm border to border within a lane), the successive colonization of the drops along the same lane was ensured, without interference from one lane to the next (Fig. 6B). With this setup, the effect of coculturing the bacterium *P. putida* KT2440 with *F. oxysporum* was evaluated. In a conventional confrontation experiment on MA, we observed

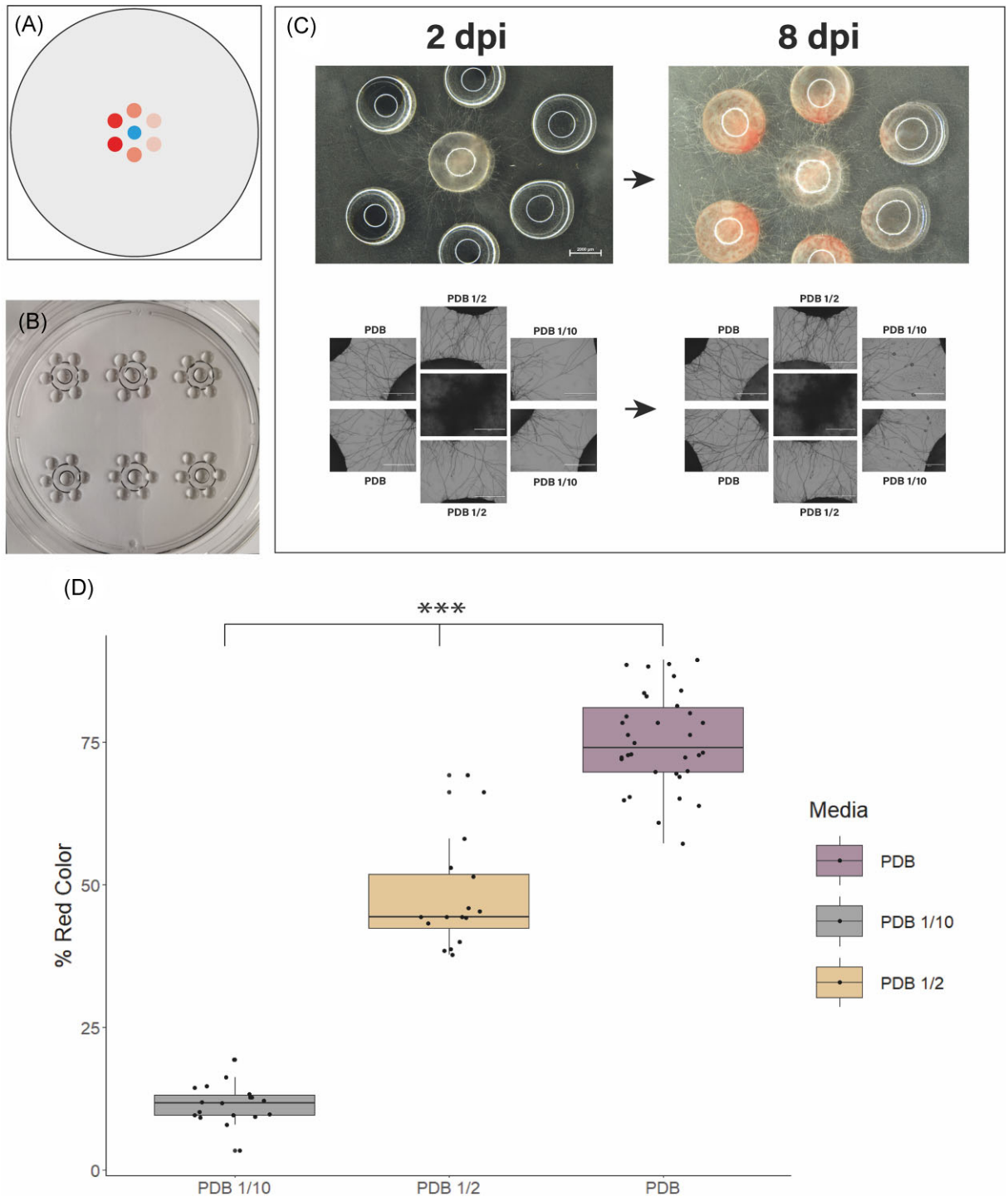

Figure 4. Effect of target nutrient concentration on mycelial growth. (A) Schematic representation of the flower-like disposition of drops in which the different shades of red represent different media or diluted versions of the same medium. In this case, the blue dot represents the inoculum in MEB and the red dots are technical duplicates for each medium: full strength PDB, two times diluted PDB (PDB 1/2) and 10 times diluted PDB (PDB 1/10). (B) Overview of the experiment after deposition and inoculation of six drops in a flower-like shape with a random disposition of the different target media for each flower of drops. (C) A stereoscopic overview of the inoculated system after 2 and 8 dpi is shown in the top part of panel (C). Stereoscopic images (40x) of the mycelium colonizing the different media at 2 and 8 dpi are shown on the bottom of panel (C). (D) Graphical boxplot and raw data representation of the percentage of red colour for each medium at 8 dpi (PDB violet, PDB ½ orange and PDB 1/10 in grey); for all conditions there is a statistically difference regarding the red colouration. Scale bars in (B) represent 15 mm; (C) (macroscopic pictures) 2 mm, (C) (microscopic pictures) 1 mm.

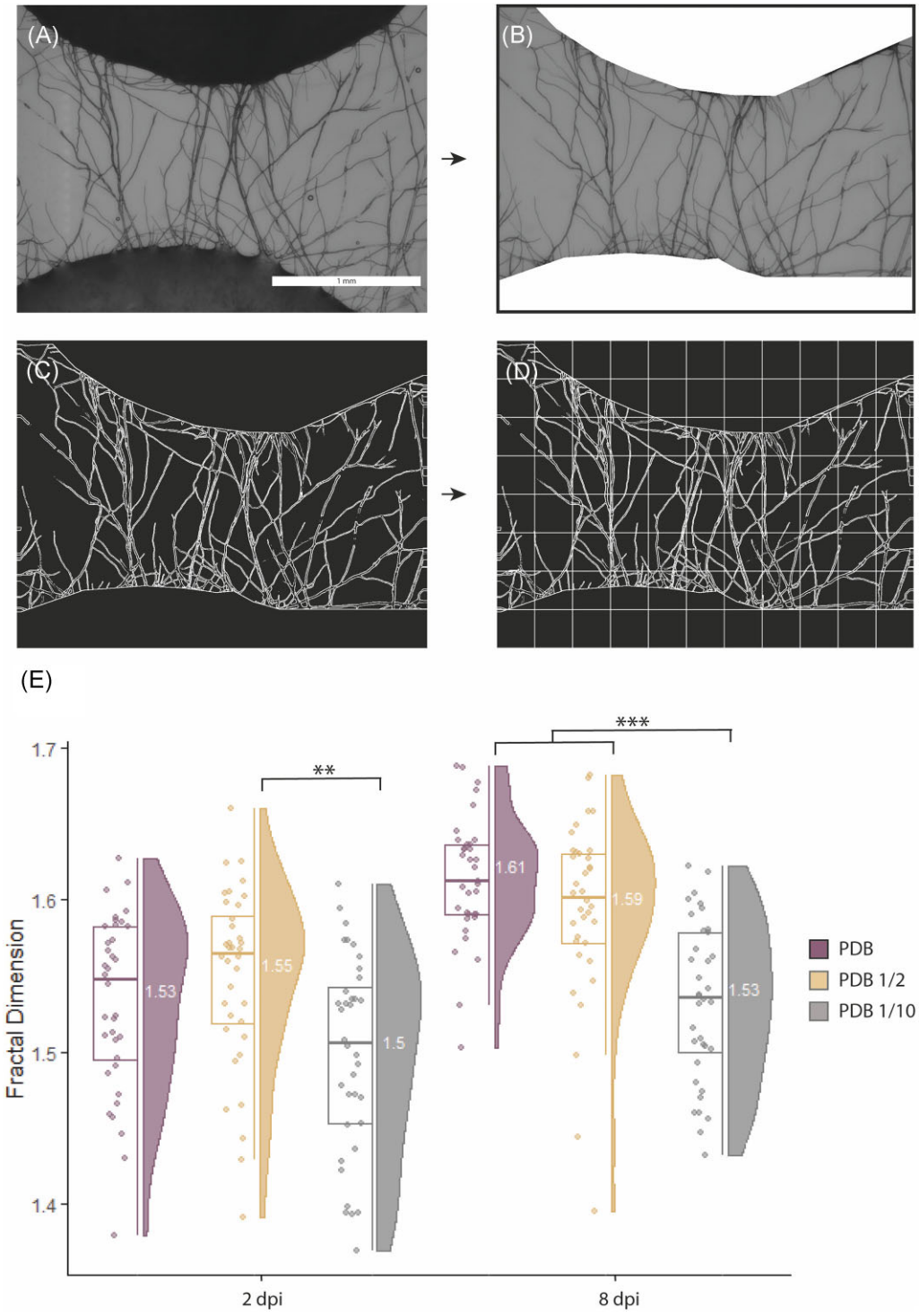

Figure 5. Image postprocessing and mass FD calculation to measure the effect of different nutrient concentration on the growth of *F. oxysporum* mycelium. (A) Example of an image taken between the inoculum drop (bottom) and a target drop with PDB (top) before postprocessing. (B) Same image as in panel (A) but processed using R to remove the pixel information contained in the drops and scale bar in order to obtain only the region of interest. (C) Application of the Kuwahara smoothing filter where the image is turned to black and white in order to keep only hyphae and reduce background noise. (D) Mass FD estimation using the box counting method with grids of scaling pixel sizes. (E) Raincloud plot of the mass FD estimation after image processing. The plot shows FD for each different condition tested (PDB, violet; PDB 1/2, orange; PDB 1/10, grey) after 2 and 8 dpi. For each condition the following information is highlighted: (i) raw data distribution ('rain') plus boxplot showing median, upper and lower quartile (left side) and (ii) data distribution ('cloud') labelled with the mean for each condition. At 2 dpi, the difference in mass FD between PDB and PDB 1/10 was statistically different, but not between PDB ½ and PDB 1/10. At 8 dpi, mass FD in both PBD and PBD 1/2 was statistically distinct from PBD 1/10. Pair-wise comparisons between 2 and 8 dpi were all significantly different, but the corresponding symbols were omitted from the graph for clarity reasons. For additional information see Table S2 (Supporting Information).The number of replicates for each media was 35 (PDB) or 36 (PDB 1/2 and PDB 1/10).

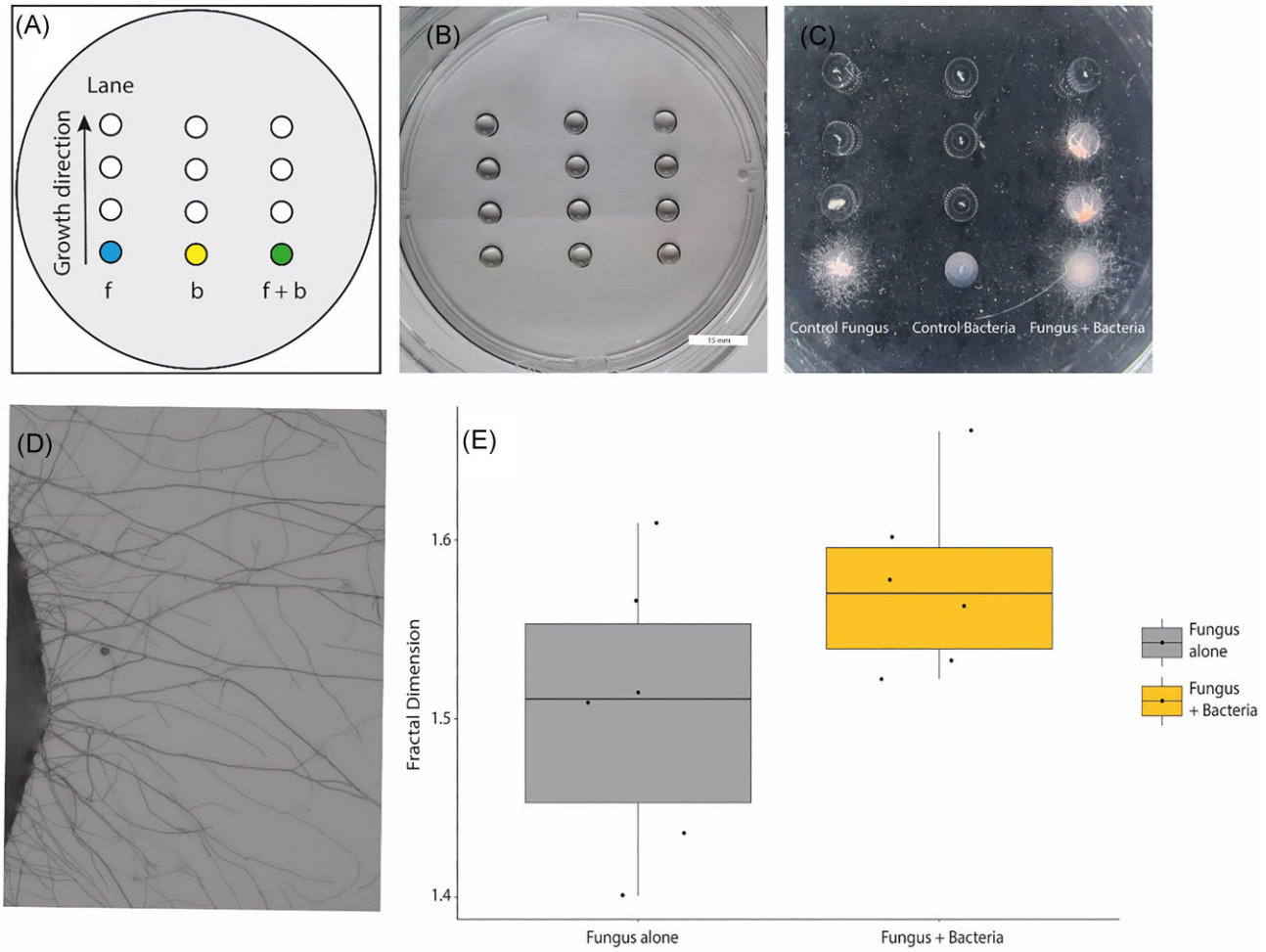

Figure 6. Example of a bacterial–fungal interaction. (A) Schematic representation of the system with the coloured drops representing inoculum drops at the start of a lane (vertical drops,). The arrow represents the growth direction for all conditions. The conditions corresponded to: (F) *F. oxysporum* alone (fungal control in blue), (B) *P. putida* KT2440 alone (bacterial control in yellow) and (F + B) *F. oxysporum* and *P. putida* coinoculated together (fungus + bacteria coinoculation in green). (B) Overview of the inoculated system at the start. (C) Macroscopic view of one of the systems as an example showing the effect of the bacteria on the growth and colonization pattern by the fungus (third lane vs. first lane). Picture taken after 8 days. (D) Example of images used for the calculation of the mass FD estimation. (E) Boxplot and raw data for the Mass FD estimation at 7 dpi of *F. oxysporum* alone (grey) and when coinoculated with *P. putida* (yellow). A trend towards an increasing FD in the coinoculated treatment was observed (*P*-value .08)

the deposition of a red pigment by *F. oxysporum* on the bacterial inoculum. Furthermore, we observed growth of the fungus on the bacterial inoculum, after which, bacteria were no longer viable (Figure S5, Supporting Information). This prompted us to use this bacterial–fungal couple to assess the interaction in the drops method. For this, three parallel treatments (i.e. lanes) were performed per plate with the fungus inoculated alone, the bacterium alone, or both organisms in a coculture. The coinoculation with *P. putida* changed both the growth and pattern of drop colonization by *F. oxysporum*. When coinoculated with *P. putida*, the fungus was able to colonize the second drop (Fig. 6C) in five out of six replicates (Figure S6, Supporting Information). In addition, the second drop was connected to the inoculum drop at 7 dpi in the cocultures, after which the fungus continued to colonize the successive drops, reaching the last drop at 15 dpi. In contrast, when the fungus was inoculated alone, *F. oxysporum* was only able to reach the second drop at 6 dpi in three out of six replicates (Figure S6, Supporting Information). To assess if there was an effect of the bacterium on mycelium space-filling efficiency and coverage of *F. oxysporum*, a mass FD estimation on microscopic was performed on pictures taken between the inoculum drop and the first target drop for the fungus inoculated alone and when coinoculated with the bacterium (Fig. 6D). A trend in which mass FD was higher (mean = 1.576, sd = 0.050, *P*-value = .098, df = 8.57) when the two organisms were coinoculated was observed compared to the FD when the fungus is alone (mean = 1.050, sd = 0.077; Fig. 6E). Finally, to assess bacterial viability, bacterial abundance was measured by colony forming counting in the drops overtime. In the controls with bacteria only, bacterial abundance fluctuated, but bacteria were detected throughout the entire duration of the incubation with over 1×10^9 cells μl^{-1} after 7 days (Figure S7, Supporting Information). In contrast, in the coinoculated drops the bacterial abundance declined after 5 days in the inoculum drop, with no detectable bacteria from day 7. Hence, as bacteria were no longer detectable in the inoculum drop, when the fungus reached the second drop bacteria were not detected to disperse to the second drop.

Discussion

This study presents an easy-to-use approach to observe mycelial development in response to different trophic or biotic habitat

conditions. This approach allows to observe different levels of organization, from mycelial colonies to individual hyphae. It is also fast and inexpensive, which allows generating numerous experimental designs with a high level of replication, minimal reagents, and using standard laboratory material. In addition to this, the drops were consistent in volume and area, ensuring highly similar conditions upon replication. Furthermore, the drops are deposited onto transparent surfaces treated for cell adhesion, thus rendering them compatible with direct microscopical observation, including fluorescence imaging. This allows the use of an inverted microscope in a nondestructive manner and without excessive manipulation enabling *in situ* observations. Finally, this method offers the opportunity for the production of time lapse movies allowing to assess the dynamics of fungal growth and response to different factors affecting exploration and growth on filamentous microorganisms.

The drops are placed on a cell-treated dry surface with a constant distance between them, mimicking an artificial 2D soil in which different stimuli surround a propagule of an organism. In this way, the drops recreate a situation in which an organism (represented by either as a spore or as a hyphal fragment) is confronted to an environment with a limited amount of nutrients, and thus is forced to explore the surroundings to find additional resources. Previous studies have shown the complex behaviour of filamentous fungi when thriving in the vast and heterogeneous niches in soils (Griffin 1972, Ritz and Young 2004), or when confronted with other organisms (Fricker et al. 2007, Wrzosek et al. 2016, Deveau et al. 2018, Hiscox et al. 2018). The conclusions of these studies are based on macroscopic observations of mycelia grown on agar/wood blocks (Boddy 1993) or by visualizing single hyphae with microfluidic devices (Schmieder et al. 2019). However, the simultaneous observation of mycelia at the macro and microscopic levels is hard to achieve in either of these approaches. This is one of the most significant advantages offered by the drop system. The combined macro- and microscopic analyses allow to bring new insights into how filamentous fungi manipulate their network architecture, something essential not only for survival and colonization in soil ecosystems (Nannipieri et al. 2003, Delgado-Baquerizo et al. 2016), but also in other ecosystems (Adrio and Demain 2003). Our approach, even if still far from a realistic reconstruction of a natural soil as compared to other methods (Boddy 1993, 2000), represents a simple and well-controlled microbial ecosystem in 2D. Compared to other methods, the nutrient supply is limited by the size of the drops, as compared to normal agar plates where the initial nutrient content is higher, or in microfluidics where a nutrient flow can be maintained. However, this allows for a precise control of the nutrient content and heterogeneous availability. This could be a better representation of a nonsaturated soil in which nutrients may be spaced, diverse, and limited.

The different tested organisms were all able to colonize and exit the drop (Fig. 2). Furthermore, we were able to observe additional features such as the formation of asexual reproductive structures in *T. rossicum* and *M. moelleri* and the production and deposition of melanin by *M. crassipes* (Fig. 3). The method should be of wide application with different media and conditions for specific organisms. The drops are mostly connected by the mycelium and its activity, and not by the liquid film formed on them, as little to no movement of the media was observable on the mycelium, and no fluorescence could be detected in the target drop in the experiments with fluoresceine. However, when different media and condition are tested, a control should be performed to validate this observation under different experimental conditions to avoid artefacts.

The usefulness of the fungal drop approach to study fungal biology was illustrated using two examples. In the first one, the approach was used to collect qualitative and quantitative data regarding mycelial growth in response to nutrient availability (Fig. 4). At the macroscopic level differences in mycelial pigmentation related to different nutrient concentrations were observed and the changes in colour were assessed quantitatively by image analysis. At the microscopic level, space-filling efficiency was measured quantitatively using mass FD analysis (Fig. 5). Our results with *F. oxysporum* demonstrate that network complexity and space-filling efficiency increased significantly when the mycelium connected patches with higher nutrient content (PDB; PDB1/2). This suggests that the fungus coordinates its network to increase efficiency with increasing nutrient conditions, as proposed in previous studies (Veresoglou et al. 2017). The increased network complexity might be the result from regrowth of the fungus from target drops towards the inoculation drops. However, this could not be controlled here. Moreover, the increasing difference in FD after 8 dpi supports the idea that fungi display learning and decision-making capabilities (Aleklett and Boddy 2021). In the future, other measurements of network complexity could be tested on the images generated by the method (Heaton et al. 2012).

Soil is not only composed of a heterogeneous matrix of nutrients, but it is also inhabited by an enormous number of living organisms (Fitter et al. 2005, Aleklett et al. 2018). Biotic interactions, hence are key in ecological processes including pollutant degradation and nutrient turnover (Kohlmeier et al. 2005, Khan et al. 2023). Therefore, the use of the approach was also illustrated by assessing multispecies interactions. Using the drop system, it was possible to observe the effect of bacteria on the colonization of a new habitat by the fungus *F. oxysporum* (Fig. 6). Fungal colonization was more effective in the cocultures, but it did not correlate with the colonization of the new drop by bacteria. Instead, bacterial populations collapsed prior to the colonization by the fungus of the new drop (Figure S7, Supporting Information). In this case, dead bacteria might be an additional nutritional source for the fungus (Barron 1988, Pion et al. 2013), which may be used to improve exploratory behaviour. This is supported by the observations showing that in the coinoculation condition the fungus was better able to reach a second drop, as compared to the control with the fungus alone (Fig. 6; Figure S7, Supporting Information). Furthermore, mass FD analysis between the first and second drop showed a trend towards higher complexity and coverage for the mycelium in the coinoculation treatment, compared to the conditions in which the fungus was inoculated alone. This suggests that the interaction was beneficial for the fungus in terms of environmental colonization. Another hypothesis may be that bacteria produced growth factors for the fungus, something that would explain the higher growth of the fungus when cocultured with *P. putida,* but it does not explain the death of the bacteria. Other studies have shown that *Pseudomonas* spp. can be used as a biocontrol agent against *Fusarium* wilt in plants (Tari and Anderson 1988, Bora et al. 2004). Although this suggests a possible negative relationship between the two organisms, this is likely highly strain specific and the outcome might be determined by the environment in which the interactions take place. In our experiment, bacteria appear to act as an additional nutrient source in agreement with the observations of the first experiment in which higher FD was correlated to higher nutrient content; and by the mycelial growth on the bacterial inoculum when the two organisms are confronted

on conventional agar media (Figure S5, Supporting Information). However, further experiments are required to test either hypothesis. Combining the drop system with methods such as proteomics or metabolomics could provide further insights into the mechanisms behind these observations. The combination of our approach with further improvements in the multiomics methods would certainly contribute to a better mechanistic understanding of the interactions observed here.

Conclusion

Given its simplicity, our approach could be used in the future to observe additional types of interactions in microorganisms with a filamentous growth (e.g. predation). Moreover, this approach can allow visualizing the specific areas of production and deposition of other important secondary metabolites in a complex mycelial network. Thanks to the possibility of generating time-lapse imaging coupled with fluorescent tagging, the system could enable the observation of complex fungal behaviours such as mating fusion between compatible strains. The ability to build a 2D heterogenous environment connected by a fungal network could become a very important tool to study bacterial–fungal interactions, as well as the interaction of fungi (and fungi-like microorganisms) with other soil organisms. In conclusion, the examples provided demonstrate how the drop system represents a valuable tool to study fungal biology, while maintaining low costs and requiring minimal expertise. This method, coupled with image analysis, provides new insights into the study of fungal behaviour macroscopically and at a single-hypha level. This approach complements in this way the use of more complex experimental platforms such as microfluidic devices.

Acknowledgements

This study was funded by the U.S. Department of Energy, Office of Science, Biological and Environmental Research Division, under award number LANLF59T; the Swiss National Science Foundation grants PZ00P3_180145 and 211549 to X-Y.L.R; and the Leverhulme Trust (RPG-2020–352 to C.E.S.).

Supplementary data

Supplementary data is available at *FEMSML Journal* online.

Conflict of interest: None declared.

References

Adrio JL, Demain AL. Fungal biotechnology. *Int Microbiol* 2003;**6**:191–9.

Aleklett K, Boddy L. Fungal behaviour: a new frontier in behavioural ecology. *Trends Ecol Evol* 2021;**36**:787–96.

Aleklett K, Kiers ET, Ohlsson P *et al.* Build your own soil: exploring microfluidics to create microbial habitat structures. *ISME J* 2018;**12**:312–9.

Barron GL. Microcolonies of bacteria as a nutrient source for lignicolous and other fungi. *Can J Bot* 1988;**66**:2505–10.

Barron GL. Predatory fungi, wood decay, and the carbon cycle. *Biodiversity* 2003;**4**:3–9.

Barry D, Ifeyinwa O, McGee S *et al.* Relating fractal dimension to branching behaviour in filamentous microorganisms. *ISAST Trans Electron Signal Process* 2009;**4**:71–6.

Boddy L, Wells JM, Culshaw C *et al.* Fractal analysis in studies of mycelium in soil. *Geoderma* 1999;**88**:301–28.

Boddy L. Interspecific combative interactions between wood-decaying basidiomycetes. *FEMS Microbiol Ecol* 2000;**31**:185–94.

Boddy L. Saprotrophic cord-forming fungi: warfare strategies and other ecological aspects. *Mycol Res* 1993;**97**:641–55.

Bora T, Özaktan H, Göre E *et al.* Biological control of *Fusarium oxysporum* f. sp. *melonis* by wettable powder formulations of the two strains of *Pseudomonas putida*. *J Phytopathol* 2004;**152**:471–5.

Bruisson S, Zufferey M, L'Haridon F *et al.* Endophytes and epiphytes from the grapevine leaf microbiome as potential biocontrol agents against phytopathogens. *Front Microbiol* 2019;**10**:2726.

Camenzind T, Lehmann A, Ahland J *et al.* Trait-based approaches reveal fungal adaptations to nutrient-limiting conditions. *Environ Microbiol* 2020;**22**:3548–60.

Corbit JD, Garbary DJ. Fractal dimension as a quantitative measure of complexity in plant development. *Proc R Soc Lond Ser B Biol Sci* 1995;**262**:1–6.

De Boer W, Folman LB, Summerbell RC *et al.* Living in a fungal world: impact of fungi on soil bacterial niche development. *FEMS Microbiol Rev* 2005;**29**:795–811.

de Lamo FJ, Takken FLW. Biocontrol by *Fusarium oxysporum* using endophyte-mediated resistance. *Front Plant Sci* 2020;**11**:1.

Delgado-Baquerizo M, Grinyer J, Reich PB *et al.* Relative importance of soil properties and microbial community for soil functionality: insights from a microbial swap experiment. *Funct Ecol* 2016;**30:** 1862–73.

Deveau A, Bonito G, Uehling J *et al.* Bacterial–fungal interactions: ecology, mechanisms and challenges. *FEMS Microbiol Rev* 2018;**42**:335–52.

Ettema CH, Wardle DA. Spatial soil ecology. *Trends Ecol Evol* 2002;**17**:177–83.

Fischer MS, Glass NL. Communicate and fuse: how filamentous fungi establish and maintain an interconnected mycelial network. *Front Microbiol* 2019;**10**. https://doi.org/10.3389/fmicb.2019.00619.

Fitter AH, Gilligan CA, Hollingworth K *et al.* Biodiversity and ecosystem function in soil. *Funct Ecol* 2005;**19**:369–77.

Fravel D, Olivain C, Alabouvette C. *Fusarium oxysporum* and its biocontrol. *New Phytol* 2003;**157**:493–502.

Fricker M, Boddy L, Bebber D. Network organisation of mycelial fungi. In: Howard RJ, Gow NAR (eds), *Biology of the Fungal Cell*. Berlin, Heidelberg: Springer, 2007, 309–30.

Geisen S, Mitchell EAD, Adl S *et al.* Soil protists: a fertile frontier in soil biology research. *FEMS Microbiol Rev* 2018;**42**:293–323.

Gimeno A, Stanley CE, Ngamenie Z *et al.* A versatile microfluidic platform measures hyphal interactions between *Fusarium graminearum* and *Clonostachys rosea* in real-time. *Commun Biol* 2021;**4**:1–10.

Gordon TR. *Fusarium oxysporum* and the *Fusarium* wilt syndrome. *Annu Rev Phytopathol* 2017;**55**:23–39.

Griffin DM. Ecology of soil fungi. *Nature* 1972;**141**:85.

Grove SN, Bracker CE. Protoplasmic organization of hyphal tips among fungi: vesicles and spitzenkörper. *J Bacteriol* 1970;**104**:989–1009.

Harris SD. Branching of fungal hyphae: regulation, mechanisms and comparison with other branching systems. *Mycologia* 2008;**100**:823–32.

Heaton L, Obara B, Grau V *et al.* Analysis of fungal networks. *Fung Biol Rev* 2012;**26:** 12–29.

Hiscox J, O'Leary J, Boddy L. Fungus wars: basidiomycete battles in wood decay. *Stud Mycol* 2018;**89**:117–24.

Hunziker L, Bönisch D, Groenhagen U *et al. Pseudomonas* strains naturally associated with potato plants produce volatiles with high

potential for inhibition of phytophthora infestans. *Appl Environ Microbiol* 2015;**81**:821–30.
Jiang L, Pettitt TR, Buenfeld N *et al.* A critical review of the physiological, ecological, physical and chemical factors influencing the microbial degradation of concrete by fungi. *Build Environ* 2022;**214**:108925.
Joshi R. A review of *Fusarium oxysporum* on its plant interaction and industrial use. *J Med Plants Stud* 2018;**6**:112–5.
Juge C, Champagne A, Coughlan AP *et al.* Quantifying the growth of arbuscular mycorrhizal fungi: usefulness of the fractal dimension. *Botany* 2009;**87**:387–400.
Khan N, Muge E, Mulaa FJ *et al.* Mycelial nutrient transfer promotes bacterial co-metabolic organochlorine pesticide degradation in nutrient-deprived environments. *ISME J* 2023;**17**:1–9.
Kohlmeier S, Smits THM, Ford RM *et al.* Taking the fungal highway: mobilization of pollutant-degrading bacteria by fungi. *Environ Sci Technol* 2005;**39**:4640–6.
Martin-Garin B, Lathuilière B, Verrecchia EP *et al.* Use of fractal dimensions to quantify coral shape. *Coral Reefs* 2007;**26**:541–50.
Nannipieri P, Ascher J, Ceccherini MT *et al.* Microbial diversity and soil functions. *Eur J Soil Sci* 2003;**54**:655–70.
Nelson KE, Weinel C, Paulsen IT *et al.* Complete genome sequence and comparative analysis of the metabolically versatile *Pseudomonas putida* KT2440. *Environ Microbiol* 2002;**4**:799–808.
Obert M, Pfeifer P, Sernetz M. Microbial growth patterns described by fractal geometry. *J Bacteriol* 1990;**172**:1180–5.
Otten W, Pajor R, Schmidt S *et al.* Combining X-ray CT and 3D printing technology to produce microcosms with replicable, complex pore geometries. *Soil Biol Biochem* 2012;**51**:53–5.
Papagianni M. Quantification of the fractal nature of mycelial aggregation in *Aspergillus niger* submerged cultures. *Microb Cell Fact* 2006;**5**:5.
Phillips JD. Soil complexity and pedogenesis. *Soil Sci* 2017;**182**:117–27.
Pion M, Spangenberg JE, Simon A *et al.* Bacterial farming by the fungus *Morchella crassipes*. *Proc R. Soc B Biol Sci* 2013;**280**:20132242.
R Core Team. R: a Language and Environment for Statistical ## Computing. 2022.
Rasmann S, Köllner TG, Degenhardt J *et al.* Recruitment of entomopathogenic nematodes by insect-damaged maize roots. *Nature* 2005;**434**:732–7.
Rayner ADM, Griffith GS, Ainsworth AM. Mycelial interconnectedness. In: *The Growing Fungus*. Berlin: Springer, 1995, 21–40.
Ritz K, Young IM. Interactions between soil structure and fungi. *Mycologist* 2004;**18**:52–9.
RStudio Team. RStudio: Integrated Development for R. RStudio, PBC, Boston, MA. 2020. http://www.rstudio.com/.
Schmieder SS, Stanley CE, Rzepiela A *et al.* Bidirectional propagation of signals and nutrients in fungal networks via specialized hyphae. *Curr Biol* 2019;**29**:217–28.
Schneider CA, Rasband WS, Eliceiri KW. NIH image to ImageJ: 25 years of image analysis. *Nat Methods* 2012;**9**:671–5.
Senesi N, Wilkinson KJ. *Biophysical Chemistry of Fractal Structures and Processes in Environmental Systems*. Chichester, Hoboken: Wiley, 2008.
Tari PH, Anderson AJ. *Fusarium* wilt suppression and agglutinability of *Pseudomonas putida*. *Appl Environ Microbiol* 1988;**54**:2037–41.
Tiedje JM, Cho JC, Murray A *et al.* Soil teeming with life: new frontiers for soil science. In: *Sustainable Management of Soil Organic Matter*. Wallingford: CABI, 2009, 393–425.
Veresoglou SD, Wang D, Andrade-Linares DR *et al.* Fungal decision to exploit or explore depends on growth rate. *Microb Ecol* 2017;**75**:289–92.
Wick LY, Remer R, Wurz B *et al.* Effect of fungal hyphae on the access of bacteria to phenanthrene in soil. *Environ Sci Technol* 2007;**41**:500–5.
Wolf AB, Vos M, De Boer W *et al.* Impact of matric potential and pore size distribution on growth dynamics of filamentous and non-filamentous soil bacteria. *PLoS ONE* 2013;**8**:e83661.
Wrzosek M, Ruszkiewicz-Michalska M, Sikora K *et al.* The plasticity of fungal interactions. *Mycol Prog* 2016;**16**:101–8.
You X, Kallies R, Kühn I *et al.* Phage co-transport with hyphal-riding bacteria fuels bacterial invasion in a water-unsaturated microbial model system. *ISME J* 2021;**16**:1275–83.

Received 31 January 2025; revised 13 March 2025; accepted 20 March 2025

Supplementary Material Chapter 2

Fungal drops: a novel approach for macro- and microscopic analyses of fungal mycelial growth

Published: 18 October 2023

FEMS µLife

DOI: https://doi.org/10.1093/femsml/uqad042

Fungal drops: a novel approach for macro- and microscopic analyses of fungal mycelial growth

Authors: Matteo Buffi[1], Guillaume Cailleau[1], Thierry Kuhn[1,2], Xiang-Yi Li Richter[1,2], Claire E. Stanley[3], Lukas Y. Wick[4], Patrick S. Chain[5], Saskia Bindschedler[1]*, Pilar Junier[1]*

Affiliations: 1. Laboratory of Microbiology, University of Neuchâtel, Neuchâtel, Switzerland. 2. Laboratory of Eco-ethology, University of Neuchâtel, Neuchâtel, Switzerland; 3. Department of Bioengineering, Imperial College London, London, United Kingdom. 4. Helmholtz Centre for Environmental Research, Department of Environmental Microbiology, Leipzig, Germany. 5. Bioscience Division, Los Alamos National Laboratory, Los Alamos, New Mexico, USA.
*Co-corresponding authors: saskia.bindschedler@unine.ch; pilar.junier@unine.ch

Running title (50 characters): Observation of fungal mycelial growth

Keywords (6): Bacterial-fungal interactions, mycelium observation, quantification fractal dimension, fungal highways, mycological method, user-friendly

Journal FEMS µlife

Supplementary Material

Supplementary Information Table S1. Media used in this study.

Name of the medium	abbreviation	composition
Malt Exctract Agar	MEA	12 g/l malt extract ["Support Is Our Success"; SIOS® Homebrew, Switzerland, Ref: XE201]; 15 g/l Technical Agar [Biolife, Japan, Ref: 4110254]; 1 l Deionized water.
Nutrient Broth	NB	25 g/l NB stock powder [CARLROTH®, Germany, Ref: AE92.2] containing: 15 g/l Peptone; 3 g/l Yeast Extract; 6 g/l Sodium Chloride; 1 g/l Glucose; pH 7.5; 1 l Deionized water.
Nutrient Agar	NA	25 g/l Nutrient Broth; 15 g/l Technical Agar [Biolife, Japan, Ref: 4110254]; 1 l Deionized water.
Potato Dextrose Agar	PDA	39 g/l of PDA stock powder [CARLROTH®, Germany, Ref: X931.2] containing: 4 g/l Potato Starch; 20 g/l Glucose; 15 g/l Agar; 1 l Deionized water.
Potato Dextrose Broth	PDB	4 g/l Potato infusion [MERCK Sigma-Aldrich, Germany , Ref: 52424]; 20 g/l D[+]Glucose monohydrate [CARLROTH®, Germany, Ref: 6887.1]; 1 l Deionized water.
Malt Extract Broth	MEB	6 g/l Malt Extract [SIOS® Homebrew, Switzerland, Ref: XE201]; 1.8 g/l Maltose (Honeywell Fluka®, North Carolina, US, Ref: 63420); 6 g/l D[+]Glucose Monohydrat [CARLROTH®, Germany, Ref: 6887.1]; 1.2 g/l yeast extract [LLG-labware, Germany, Ref: 6271004]; 1 l Deionized water.
M9 Mineral Medium	M9	Protocol was taken from Helmholtz Centre Munich German Research Centre for Environmental Health: https://static.igem.org/mediawiki/2019/2/20/T--Tuebingen--M9_recipe.pdf 1 l of M9 mineral medium contains: 100 ml M9 salt solution (10x); 20 ml D[+]Glucose monohydrate 20% (200g/l)[CARLROTH®, Germany, Ref: 6887.1]; 1 ml $MgSO_4$-$7H_2O$ 1M [MERCK Sigma-Aldrich, Germany , Ref: 63140]; 0.3 ml $CaCl_2$.$2H_2O$ 1M [CARLROTH®, Ref: HNO4.3]; 1 ml Biotin (1 mg/ml) [MERCK Sigma-Aldrich, Germany , Ref: 10740]; 1 ml Thiamin (1 mg/ml) [MERCK Sigma-Aldrich, Germany , Ref: 8181]; 10 ml trace elements solution (100x); 867 ml Dionized water; M9 salt solution (10x): 75.2 g/l Na_2HPO_4 -$2H_2O$ [CARLROTH®, Germany, Ref: T877.2]; 30 g/l KH_2PO_4 [CARLROTH®, Germany, Ref: 3904.1]; 5 g/l NaCl [CARLROTH®, Germany, Ref: 3957.2]; 5 g/l NH_4CL [Honeywell Fluka®, North Carolina, US, Ref: 9700]; 100X trace elements solution: 5 g/l EDTA [CARLROTH®, Ref: X986.1]; 0.83 g/l $FeCL_3$-$6H_2O$ [Honeywell Fluka®,North Carolina, US Ref: 9720]; 84 mg/l $ZnCl_2$ [Honeywell Fluka®, North Carolina, US, Ref: 96470]; 13 mg/l $CuCl_2$-$2H_2O$ [Honeywell Fluka®, North Carolina, US, Ref: 61175]; 10 mg/l $CoCl_2$-$6H_2O$ [MERCK Sigma-Aldrich, Germany , Ref: 7791-13-1];

Supplementary information Table S2: Example for the selection of the good box sizes for the Estimation of Fractal Dimension: On top, as an example, six different images were analysed (Label) using a box size of 3, 6, 12, 24, 48, 96, 192, 384, 768, 1536. In red (D10) the FD obtained by considering the counts of all box sizes (3 – 1536), In grey (D9) FD obtained by considering only the first 9 box sizes (3 – 768) and in blue (D8) FD obtained by considering the first 8 box sizes (3 – 384). Below, the mean FD values for multiple conditions is reported. For our analysis we decided to consider only the columns in which the number of counted boxes differed between samples (in this example, box size 384), however, the values calculated for 9 or 10 box sizes (D9 and D10) show the same tendency. In SI Table S3 it is possible to observe that the changes in the calculated FD values does not affect the statistical significance of the results obtained in the experiment.

Label	C3	C6	C12	C24	C48	C96	C192	C384	C768	C1536	D8	D9	D10
1A=1=31	16488	6017	2251	862	304	92	29	10	4	1	1.531	1.525	1.548
1A=1=32	15465	5662	2170	834	309	106	35	12	4	1	1.470	1.487	1.523
1A=2=31	15593	5654	2124	824	314	106	34	12	4	1	1.472	1.487	1.523
1A=2=32	15906	5696	2164	835	310	106	32	11	4	1	1.492	1.500	1.532
1A=3=31	14124	5140	1924	711	256	87	28	11	4	1	1.485	1.483	1.510
1A=3=32	18111	6603	2534	968	357	117	34	12	4	1	1.508	1.523	1.557

Sample	D8 mean	D9 Mean	D10 mean
PDB 2dpi	1.532	1.535	1.562
PDB/2 2dpi	1.549	1.556	1.582
PDB/10 2dpi	1.498	1.51	1.543
PDB 8dpi	1.613	1.607	1.625
PDB/2 8dpi	1.593	1.595	1.617
PDB/10 8dpi	1.533	1.545	1.575

Supplementary information Table S3: Different p-values obtained when comparing the statistical significance of the differences in fractal dimension measured using different box sizes for the box counting method. This comparison shows the robustness of the statistical significance for the comparisons performed within a single experiment.

Box sizes / Comparisons	1, 2, 4, 8, 16, 32, 64, 128, 256, 512	1, 2, 4, 8, 16, 32, 64, 128, 256	1, 2, 4, 8 16, 32, 64, 128	3, 6, 12, 24, 48, 96, 192, 384, 768	3, 6, 12, 24, 48, 96, 192, 384
2dpi – 8dpi	< 0.001 ***	< 0.001 ***	< 0.001 ***	< 0.001 ***	< 0.001 ***
PDB 2dpi – PDB 8dpi	< 0.001 ***	< 0.001 ***	0.00741 **	< 0.001 ***	< 0.001 ***
PDB 1:2 2dpi – PDB 1:2 8dpi	< 0.001 ***	0.005 **	0.005 **	0.0043 **	0.002 **
PDB 1:10 2dpi – PDB 1:10 8dpi	0.0158 *	0.0356 *	0.106	0.00931 **	0.0158 *
Target media	0.002 **	< 0.001 ***	0.001257 **	< 0.001 ***	< 0.001 ***
2dpi					
PDB – PDB 1:2	0.33	0.3412	0.384	0.24	0.468
PDB – PDB 1:10	0.15	0.0983	0.085	0.163	0.05
PDB 1:2 – PDB 1:10	0.00413 **	0.0020 **	0.002 **	0.002 **	0.00165 **
8dpi					
PDB – PDB 1:2	0.3	0.259	0.184	0.55	0.237
PDB – PDB 1:10	< 0.001 ***	< 0.001 ***	< 0.001 ***	< 0.001 ***	< 0.001 ***
PDB 1:2 – PDB 1:10	< 0.001 ***	< 0.001 ***	< 0.001 ***	< 0.001 ***	< 0.001 ***

Supplementary information Table S4: Results Fractal dimension estimation results coming from a two factor ANOVA and a post hoc-Tukey contrast for pair-wise comparison between the different factors. In a second table the Means and standard deviation for the FD value obtained. Box size used: 3, 6, 12, 24, 48, 96, 192, 384

Comparison	F-value	Degree of Freedom	p-value
2dpi – 8dpi	34.4397	1	< 0.001 ***
PDB 2dpi – PDB 8dpi			< 0.001 ***
PDB 1:2 2dpi – PDB 1:2 8dpi			0.002 **
PDB 1:10 2dpi – PDB 1:10 8dpi			0.0158 *
Target media	7.5823	2	< 0.001 ***
2dpi			
PDB – PDB 1:2			0.468
PDB – PDB 1:10			0.05
PDB 1:2 – PDB 1:10			0.00165 **
8dpi			
PDB – PDB 1:2			0.237
PDB – PDB 1:10			< 0.001 ***
PDB 1:2 – PDB 1:10			< 0.001 ***

Connection	Mean FD	Standard Deviation FD
PDB 2dpi	1.532	0.057
PDB 1:2 2dpi	1.549	0.059
PDB 1:10 2dpi	1.498	0.064
PDB 8dpi	1.613	0.04
PDB 1:2 8dpi	1.593	0.059
PDB 1:10 8dpi	1.533	0.052

Supplementary Figures Legends:

Figure S1: Masks used to place the drops for the different experiments. (A-B) Bacterial fungal interactions, dotted lines are used to keep the drops at a constant distance. (C) Choice of nutrients. Masks were created with Adobe Illustrator®

Figure S2: Comparison of the thickness of the liquid film surrounding hyphae of *Pythium ultimum* when grown alone (A-D) or co-inoculated with *Pseudomonas putida* KT2440 (E-H). Two close-up images (D and H) show the details of the variable thickness of the liquid film.

Figure S3: Evaluation of autofluorescence in the mycelium of *Pythium ultimum* when grown alone (A) or co-inoculated with *Pseudomonas putida* KT2440 (B). Images taken at different magnifications.

Figure S4: Evaluation of the movement of liquid from the drop on the mycelium of *Pythium ultimum* using fluorescein. (A) *Pythium ultimum* grown alone. (B) *P. ultimum* in co-inoculated with *Pseudomonas putida* KT2440. Images taken at different magnifications.

Figure S5: Confrontation assay on MA between *Fusarium oxysporum* and *Pseudomonas putida* KT2440. On the left the MA Petri dish with *F. oxysporum* inoculated in the centre and the inoculum with *P. putida* on top. The two organisms were inoculated at the same time and the image shows the interaction once the fungal growth front has reached the bacterial inoculum. The image on the right corresponds to a magnification of the bacterial inoculum area showing the overgrowth of *F. oxysporum* on bacteria. Upon fungal colonization bacteria viability was tested by trying to re-culture the red inoculum on NA with cycloheximide (500mg/L), but the bacteria were shown to be dead.

Figure S6: Overview of the individual replicates in the experiment testing fungal-bacterial interactions presented in Figure 4. For each replicate (3 drop lanes): first lane is the fungus inoculated alone, second line the bacteria inoculated alone and in the third line the fungus and the bacteria co-inoculated together.

Figure S7: Counting of viable bacteria over time. The grey line corresponds to the counting of viable bacteria in the control inoculated with bacteria only. The orange line corresponds to the counting of viable bacteria from drops that were co-inoculated with *F. oxysporum*. Error bars represent the standard deviation between three replicates.

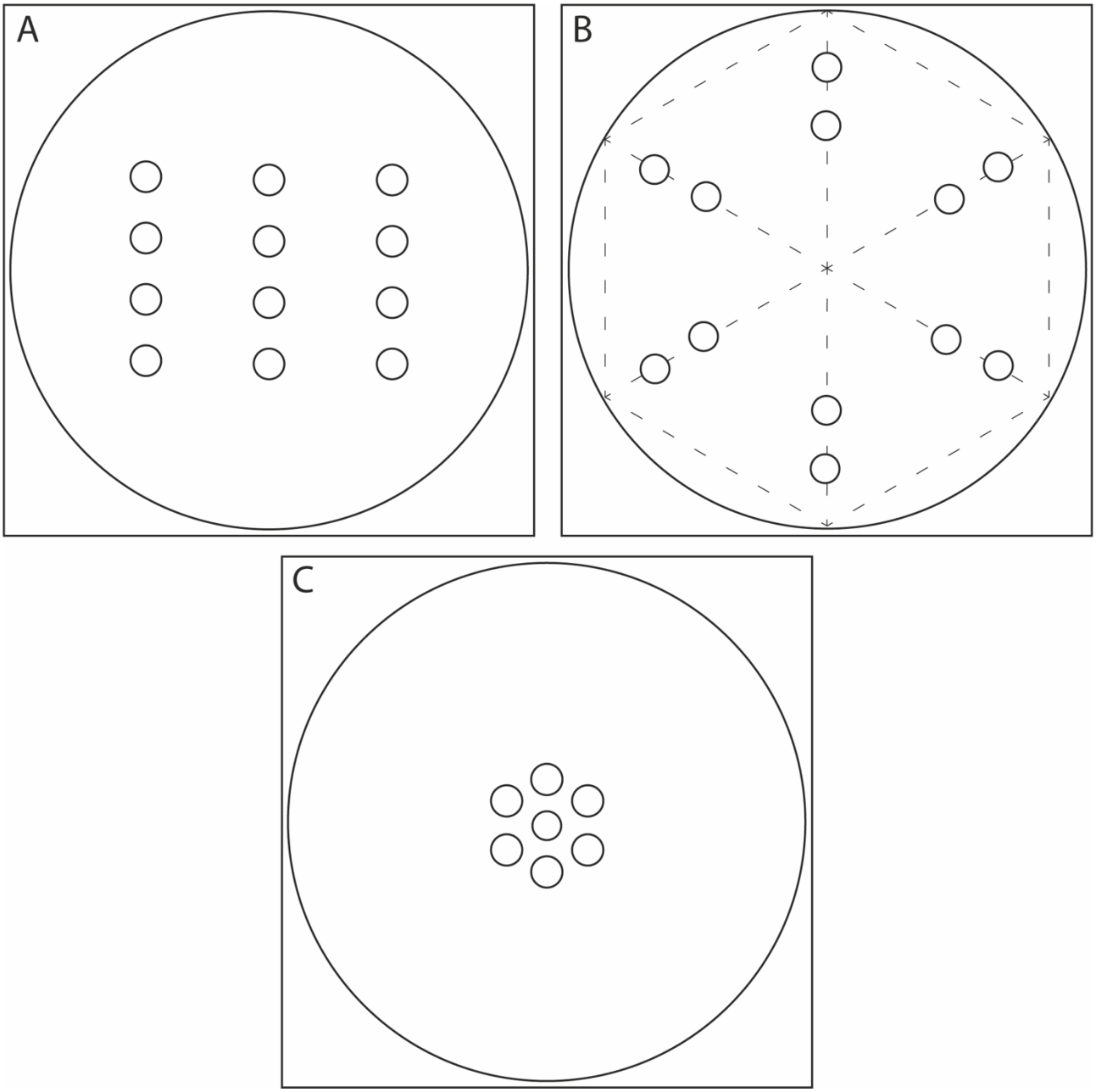

Figure S1

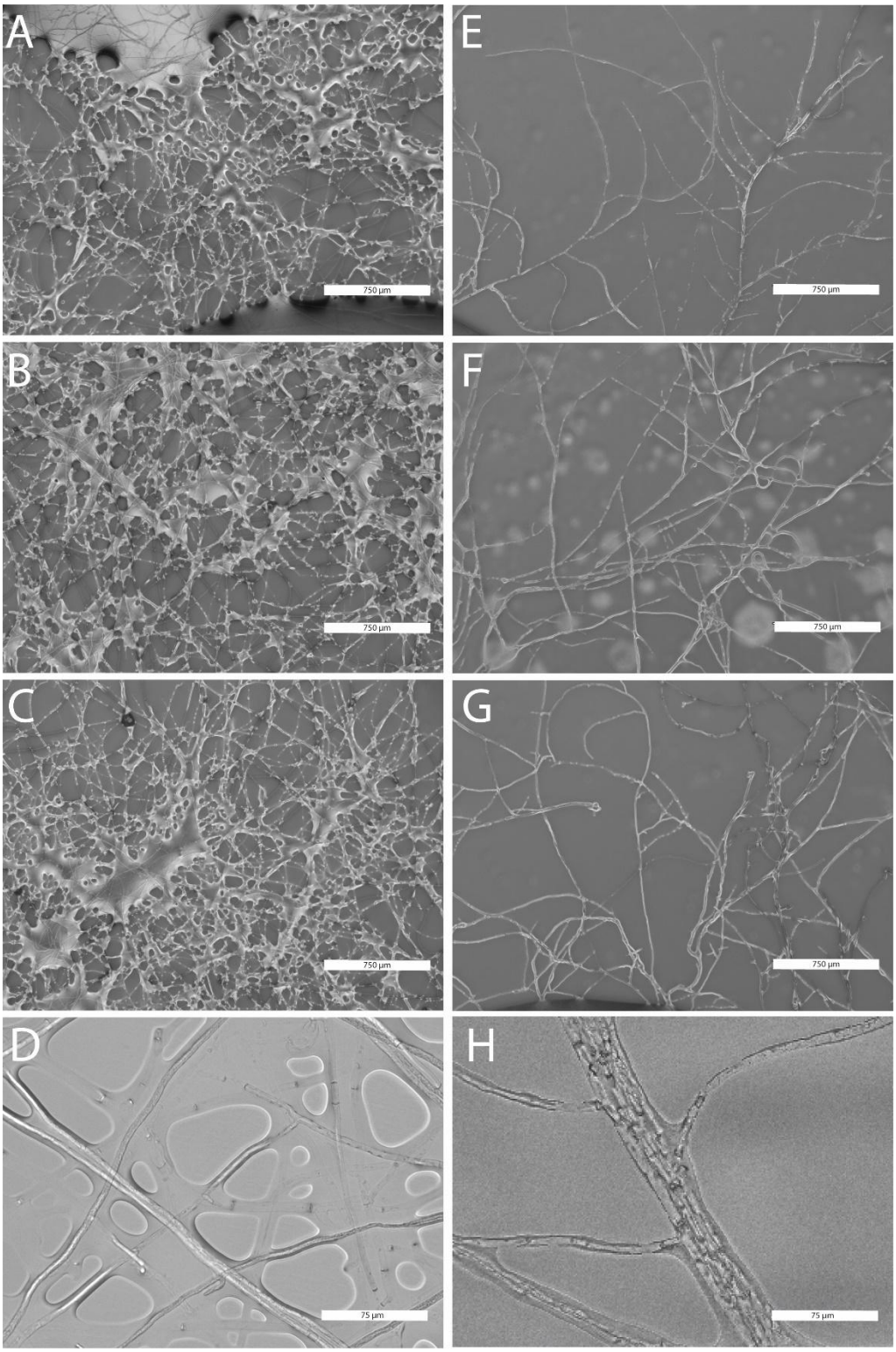

Figure S2

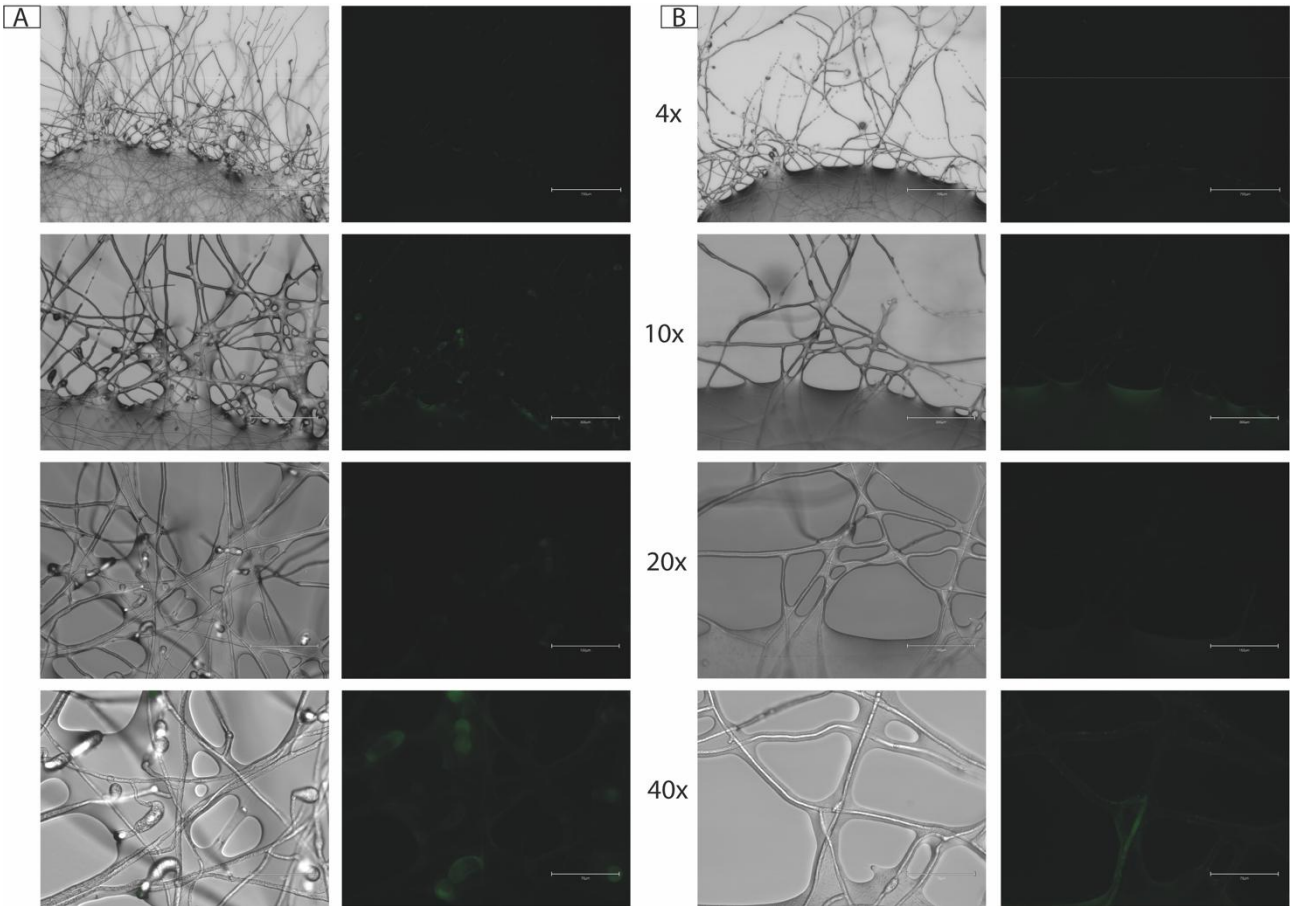

Figure S3

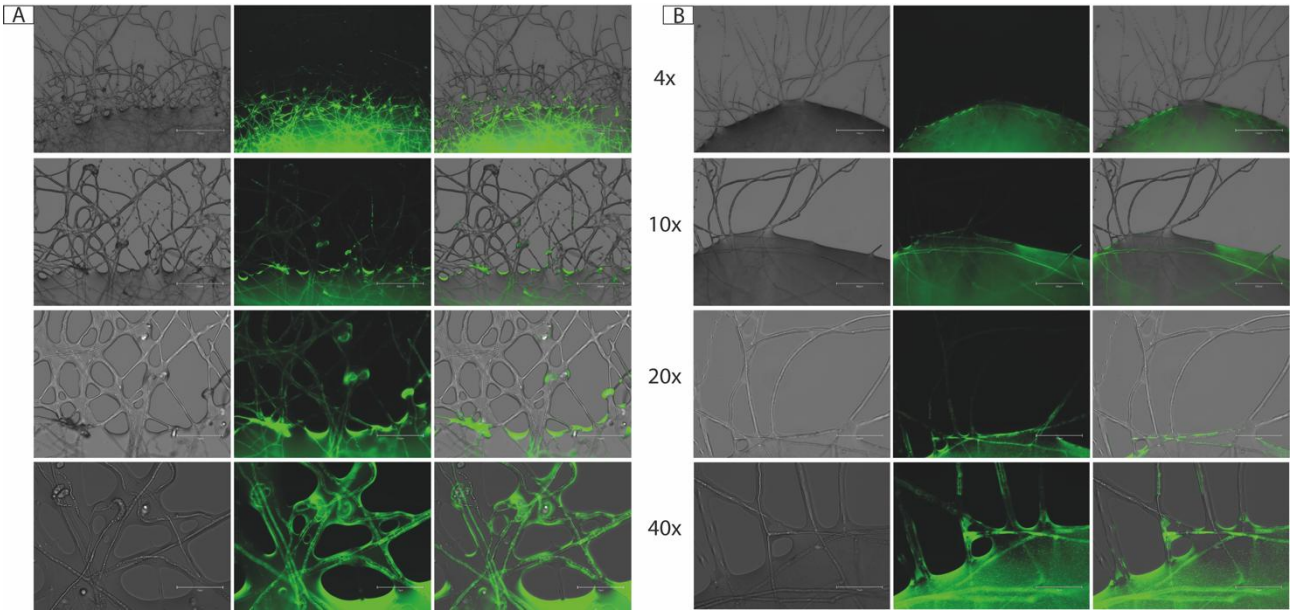

Figure S4

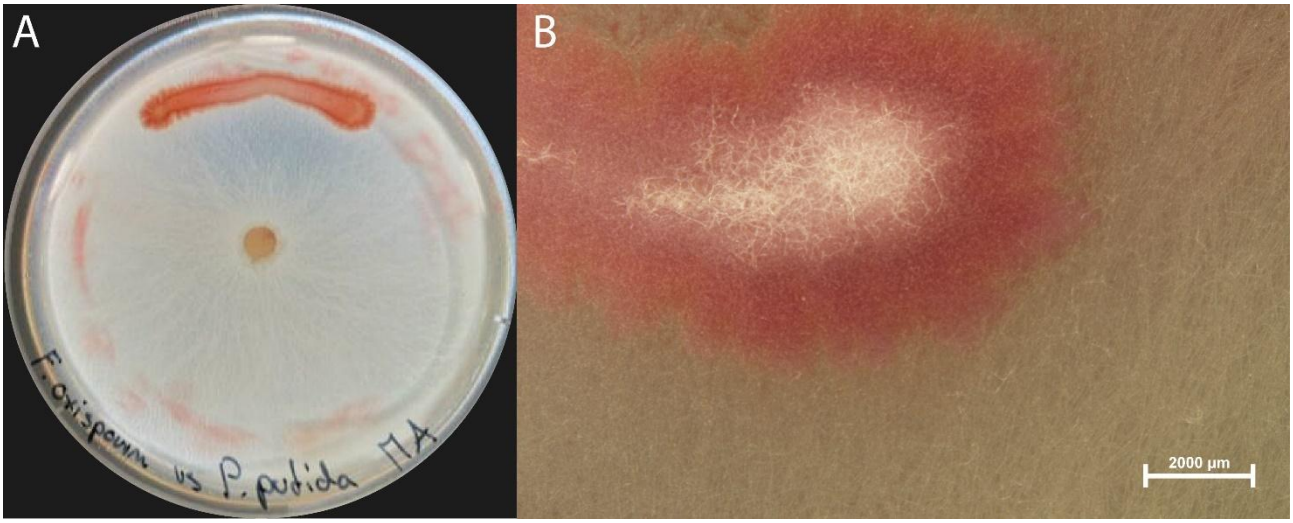

Figure S5

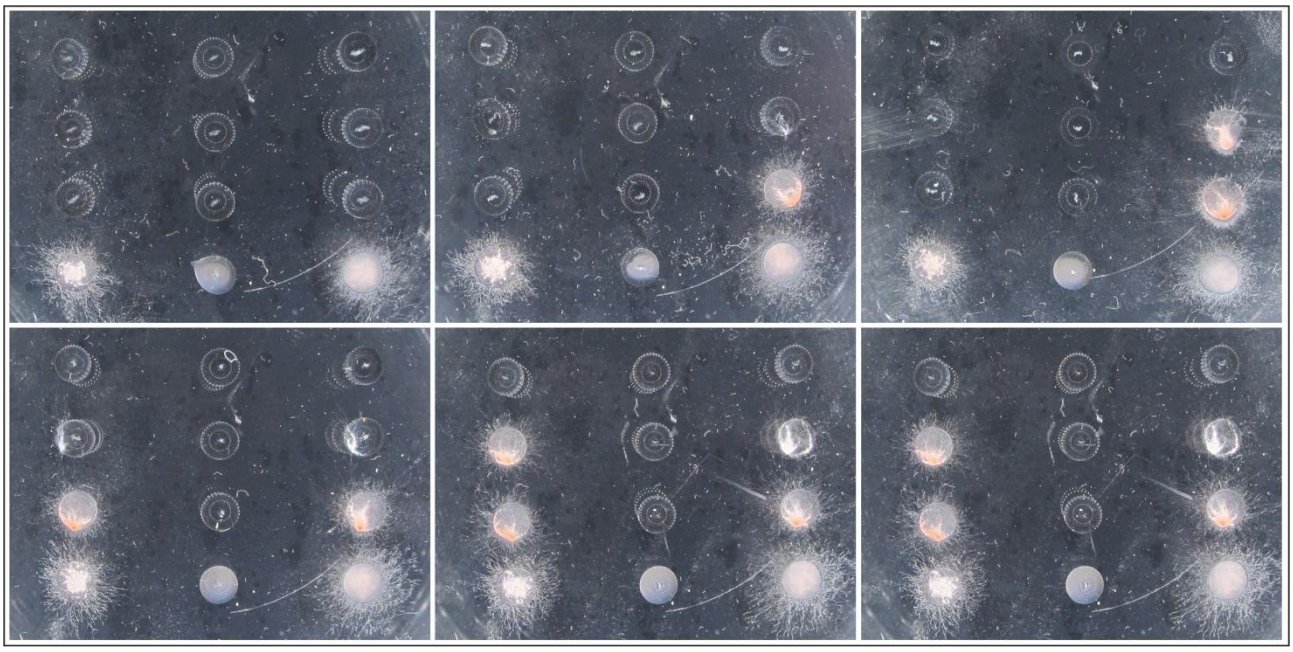

Figure S6

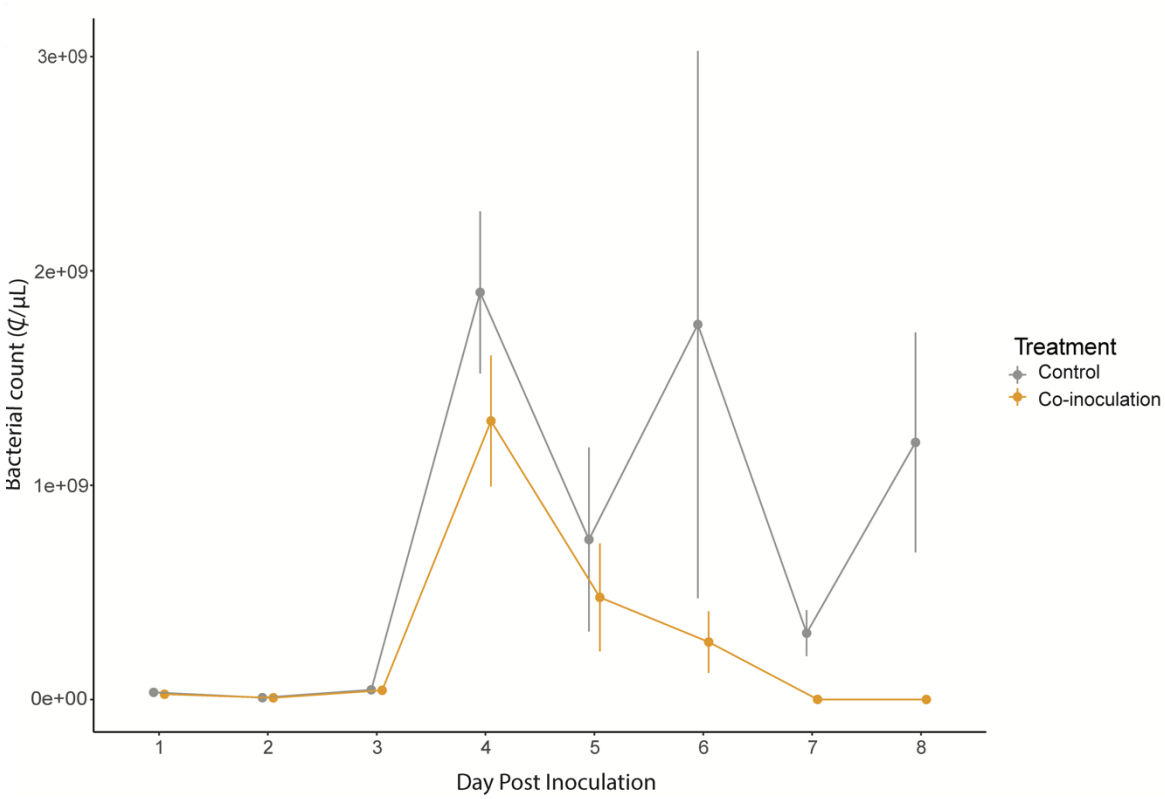
3e+09
2e+09
1e+09
0e+00
Bacterial count (₡/µL)
1
2
3
4
5
6
7
8
Day Post Inoculation
Treatment
Control
Co-inoculation

Figure S7

Supplementary Information

Image preparation in R

In order to remove the droplet in the microscope images we performed a two-modules treatment in R (R Core Team, 2017) using the scripts provided below.

Step 1: droplet removal preparation step

The first module, using the *png_crop_by_polygon_clean.R* script produces a hand-made polygon aiming at cropping each image (by clicking on the displayed image to exclude the droplet from the polygon) in a source folder (here 12 images per modality). This creates for each image treated a raster image, result of the cropping. These data are then stored for further use.

Step 2: droplet removal step

The second module, using the *Script_2crop_clean.R* script aims at cleaning the original image by importing the cropped raster previously created. This module sets the cropped area in pure white for easing further computation in ImageJ. These two modules are supported by the packages *imager* (Barthelme, 2020) and *magick* (Ooms, 2020) for image computation and *sp* (Pebesma and Bivand, 2005) and *raster* (Hijmans, 2021) for "spatial" data management.

Image analysis in ImageJ (Schindelin *et al.* 2012)

The whole process is available in a Macro used in Fiji (provided in a separate file).

The images, obtained from our 2-step pre-treatment, are first converted to 8-bit images, then a Kuwahara smoothing filter is used to reduce the noise in the image, which remove bubble artifacts while preserving the edges, i.e., the hyphae. Here we used a Kuwahara linear filter, which is a variant of this adaptive noise reduction filter. Then a Sobel edge detector is used to detect drastic changes in intensity, i.e., the hyphae. Then the "edge-image is converted into a binary mask that makes the fungal filament edge appear white and the background black. Finally, we run a fractal box count algorithm with box sizes of 1, 2, 4, 8, 16, 32, 64, 128, 256, 512 pixels wide. For each grid made of a given box size, each box covering a white pixel is counted. Repeated over the range of box size, the fractal dimension D of the image can be then calculated.

Note for using the Fiji Macro: The input folder contains all the cropped images, whatever the experimental modality. The output folder contains all the related images (saved at line 8 of the macro), on which the fractal box count algorithm is applied. At the end a "results data-sheet" is subsequently saved, storing the results of all images computed from the input folder.

When looking at the images in the output folder, one can see that the boundary resulting from the cropping step is identified as an edge. A test was performed (but not presented here) on 4 samples to define if this artefact influences the calculation of D or not. For such a test, the cropping hand-made polygons defined and saved for each image in R, was imported into imageJ. Then, by a single step of erosion of the polygon-based binary image we obtained, we were able to crop the edge-image (before it was created as a binary mask). The obtained image was free of the cropping artefact and can be compared to the same image with artefact. No fractal dimension difference was detected, so this time-consuming computing task was discarded.

Attached: files:

Script_2crop_clean.R first module in R

png_crop_by_polygon_clean.R second module in R

For_FD_with_Fiji.ijm macro program to run into Fiji (additional file)

References:

Barthelme, S. (2020). imager: Image Processing Library Based on 'CImg'. R package version 0.42.3. https://CRAN.R-project.org/package=imager

Hijmans, R.J. (2021). raster: Geographic Data Analysis and Modeling. R package version 3.4-10. https://CRAN.R-project.org/package=raster

Ooms, J. (2020). magick: Advanced Graphics and Image-Processing in R. R package version 2.3. https://CRAN.R-project.org/package=magick

Pebesma, E.J., R.S. Bivand, 2005. Classes and methods for spatial data in R. R News 5 (2), https://cran.r-project.org/doc/Rnews/

R Core Team (2017). R: A language and environment for statistical computing. R Foundation for Statistical Computing, Vienna, Austria. URL https://www.R-project.org/

Schindelin, J., Arganda-Carreras I., Frise E., Kaynig V., Longair M., Pietzsch T., Preibisch S., Rueden C., Saalfeld S., Schmid B., Tinevez J-Y, White D.J., Hartenstein V., Eliceiri K., Tomancak P., Cardona, A. (2012). Fiji: an open-source platform for biological-image analysis. Nature Methods, 9(7), 676–682. doi:10.1038/nmeth.2019

Script_2crop_clean.R first module in R

```
rm(list=ls())
library(imager)
library(magick)
library(raster)
library(sp)

# running with R 4.x
setwd("PUT_YOUR_FOLDER_PATH_HERE")
#here we have only tif images
Files <- list.files(pattern="tif$")
paths <- paste(getwd(), "/", Files, sep="")

for(i in 1:length(paths)){
      # read with imageMagick
      im_IMgck <- image_read(paths[i])%>% image_quantize(colorspace =
'gray')
      image_write(im_IMgck, path=gsub(".tif", ".png", paths[i]),
format="png")
      im <- load.image(gsub(".tif", ".png", paths[i]))

      #Manual removal of the droplets
      if(unlist(attributes(dev.cur()))!="null
device"){sapply(1:length(c(dev.list())), function(i)dev.off(dev.cur()))}
      plot(im)
      # hand-made polygon for cropping, you can make polygon as complex as
you want (no hole supported here)
      # add points by pressing the (first) mouse button,
      # end the polygon building by pressing any other mouse button (or esc
key for some graphic devices).
      Manual <- locator( type="l", col=2)
      xym <- do.call(cbind, Manual)
      p = Polygon(xym)
      ps = Polygons(list(p),1)
      MASK = SpatialPolygons(list(ps))

      # cropping image to obtain a raster
      im_IMgck_array <- as.integer(im_IMgck[[1]])
      int <- matrix(im_IMgck_array, ncol=dim(im)[1], byrow=F)
      data_raw <- raster(int)
      extent(data_raw)@xmax <- dim(im)[1]
      extent(data_raw)@xmin <- 1
      extent(data_raw)@ymax <- dim(im)[2]
      extent(data_raw)@ymin <- 1

      r <- raster()
      proj4string(r) <- CRS(sprintf("+proj=aeqd +lat_0=%s +lon_0=%s +x_0=0
+y_0=0 +R=6371000", as.integer(dim(data_raw)[2])/2,
as.integer(dim(data_raw)[1])/2))
      #r[is.na(r)] <- 1
      r[]<-NA
      extent(r)@xmin <- extent(data_raw)@xmin
      extent(r)@xmax <- extent(data_raw)@xmax
      extent(r)@ymin <- extent(data_raw)@ymin
      extent(r)@ymax <- extent(data_raw)@ymax
      r@ ncols <- as.integer(dim(data_raw)[2])
      r@ nrows <- as.integer(dim(data_raw)[1])
      rp <- rasterize(MASK, r)

      test <- as.matrix(rp)
```

```
246         fliplr = function(x) {
247          x[,ncol(x):1]
248         }
249         test <- t(test)
250         test <- fliplr(test)
251         Mask <- t(raster(test))
252         extent(Mask)@xmax <- dim(im)[1]
253         extent(Mask)@xmin <- 1
254         extent(Mask)@ymax <- dim(im)[2]
255         extent(Mask)@ymin <- 1
256         Clean_data <- mask(data_raw, Mask, matrix=NA)
257         plot(Clean_data)
258         Sys.sleep(1)
259         ############### end droplet cleaning
260
261         # save important data
262         DAT <- list(MASK, Clean_data, paths[i])
263         save(DAT, file=gsub(".tif", ".RData", gsub(paste(getwd(), "/",
264   sep=""), "", paths[i])))
265   }
266
267
268
```

png_crop_by_polygon_clean.R second module in R

```
library(stringr)
library(imager)
library(magick)

# running with R 4.x
PWD <- "PATH_TO_YOUR_FOLDERS"
setwd(PWD)
# get the folder with the images to analyse (HERE WE HAVE MANY FOLDER IN
PATH_TO_YOUR_FOLDERS)
folders <- "MY_FOLDER_OF_CHOICE"

OK <- sapply(1:length(folders), function(i){
      setwd(paste(getwd(), folders[i], sep="/"))
      #list RDA we created in the first step
      LIST_RData <- list.files(pattern="RData")

      OK <- sapply(1:length(LIST_RData), function(j){
            #open each to crop images or save raster as image format png
            load(LIST_RData[j])
            #conversion to png for imager
            im <- image_read(paste(getwd(), tail(unlist(str_split(DAT[[3]],
"\\/")), 1), sep="/"))
            tmpF <- tempfile(fileext=".png")
            im <- image_convert(im, format="png")
            image_write(im, path=tmpF, format="png", quality =100)

            #to work in imager
            im <- load.image(tmpF)
            FOR_mask <- !is.na(as.cimg(DAT[[2]])) %>% pixset
            #duplicate chanels for futher use
            final <- im* add.colour(FOR_mask)
            px <- add.colour(!FOR_mask)
            im <- final
            #make a uniform image of the same dimensions
            #using a background colour of R=1,G=1,B=1 (white)
            bg <- imfill(dim=dim(final),val=c(1,1,1))
            msk <- as.cimg(px)
            final <- bg*msk+(1-msk)*im
            save.image(final,file=gsub("tif$", "png", paste(getwd(),
tail(unlist(str_split(DAT[[3]], "\\/")), 1), sep="/")))
      })
      setwd(PWD)
})
```

Chapter 3

Assessing the speed of individual bacteria dispersing on mycelial networks

Published: 2 January 2025

Evolutionary Ecology

DOI: https://doi.org/10.1007/s10682-025-10329-4

Contributions:

Matteo Buffi, contributed to the study conception and design. Material preparation, data collection and interpretation and to the writing of the manuscript.

Evolutionary Ecology
https://doi.org/10.1007/s10682-025-10329-4

RESEARCH

Assessing the speed of individual bacteria dispersing on mycelial networks

Matteo Buffi[1] · Thierry Kuhn[1,2] · Diego Gonzalez[1] · Saskia Bindschedler[1] · Patrick S. Chain[3] · Xiang-Yi Li Richter[1,2,4,5] · Pilar Junier[1]

Received: 9 July 2024 / Accepted: 2 January 2025

Abstract

The movement of bacteria on the hyphae of fungi and other mycelial-forming organisms is an important process that determines their ability to actively disperse in water-unsaturated habitats. However, direct observation and characterization of bacterial cell movement on mycelial networks have been difficult to achieve. In this study, we developed a new method that uses high-speed video recording to track the dispersal of individual fluorescently tagged cells of two closely related strains of *Pseudomonas putida* (UWC1 and KT2440) over the mycelial network of the oomycete *Pythium ultimum*. We found high intra-population heterogeneity and between-population differences in dispersal speeds for the two bacterial strains. The fitting of the speed distribution functions led to the separation of speeds into two ranges (fast/slow) at an intersection of the fitted curves. In the lower speed range, the UWC1 strain dispersed faster, while the KT2440 strain moved faster in the higher speed range. This finding helps explain conflicting competition outcomes revealed in previous studies and suggests that population mean speed alone does not capture key aspects of bacterial dispersal in mycelial networks. Our new method opens the possibility of studying bacterial dispersal, competition, and other social interactions in spatially heterogeneous environments, such as soils.

Keywords *Pseudomonas putida* · *Pythium ultimum* · Fungal highways

✉ Xiang-Yi Li Richter
li@evolbio.mpg.de

✉ Pilar Junier
pilar.junier@unine.ch

[1] Laboratory of Microbiology, University of Neuchâtel, Rue Emile-Argand 11, 2000 Neuchâtel, Switzerland

[2] Laboratory of Eco-Ethology, University of Neuchâtel, Rue Emile-Argand 11, 2000 Neuchâtel, Switzerland

[3] Bioscience Division, Los Alamos National Laboratory, P.O. Box 1663, Los Alamos, NM 87545, USA

[4] Institute of Ecology and Evolution, University of Bern, Baltzerstrasse 6, 3012 Bern, Switzerland

[5] Department of Biology, University of Konstanz, Universitaetsstrasse 10, 78464 Constance, Germany

Published online: 25 January 2025

Introduction

The dispersal of bacteria plays an important role in ecosystem processes such as nutrient cycling, bioremediation of pollutants, or the biorecovery of valuable materials (Kohlmeier et al. 2005; Banitz et al. 2013; Losa and Bindschedler 2018; Custer et al. 2022). While fundamental knowledge regarding the mechanisms of bacterial motility is well-established (Kearns 2010), particularly in controlled laboratory conditions, there is still much to learn about the complexity of bacterial movement in natural ecosystems, especially spatially heterogeneous environments that are not saturated with water. In liquid media, where the majority of the studies have been performed, most bacteria use one or more rotatory flagella to swim. In other media, such as hydrated substrates, bacteria undergo hyperflagellation (increase in the number of flagella) and move collectively during swarming. Alternatively, other structures such as Type IV pili have been involved in twitching, especially on solid surfaces, while adhesins, located on the surface of the cells, have been involved in gliding motility (Wadhwa and Berg 2021). Regardless of the type of motility, one common aspect that limits bacterial dispersal in the environment is the level of water saturation or the presence of air-filled gaps (Or et al. 2007). A strategy that has been shown to allow bacteria to overcome dispersal limitation in spatially heterogeneous environments that are not saturated with water such as soils (Simon et al. 2017; Junier et al. 2021) or cheese rinds (Zhang et al. 2018) is the active movement of bacteria in the liquid film formed around hyphae of hyphae-forming organisms such as filamentous fungi or Oomycetes. The hyphae constitute in this way a network of "fungal highways" that serve as a physical pathway that bacteria can use to colonize areas that would be otherwise inaccessible (Kohlmeier et al. 2005; Simon et al. 2015). Fungi have also been shown to benefit from allowing bacteria to move on their hyphae by increasing their uptake of essential nutrients (Lohberger et al. 2019; Jiang et al. 2021). Fungal highways have been shown to be highly relevant for soil ecological functioning (Wick et al. 2007; Simon et al. 2017; Junier et al. 2021) or in processes such as food production (Zhang et al. 2018).

Other than the need for flagella (Pion et al. 2013) or the "hitchhiking" of non-flagellated bacteria on other flagellated bacteria (Warmink et al. 2011; Kuhn et al. 2022b) many aspects of fungal highways remain understudied. One of those is the level of control that hyphae-forming microorganisms exert on the bacteria moving on their hyphae. For instance, the thickness of the liquid film on the surface of hyphae is thought to restrict the free movement of individual cells (Or et al. 2007). This parameter depends not only on environmental conditions (Wong and Griffin 1976), but also varies among different taxa based on their ability to produce different surfactants or to modify the composition of the cell wall (Kohlmeier et al. 2005; Gow et al. 2017). Consequently, bacteria using hyphae to disperse may encounter areas with varying degrees of "crowding" or "traffic jams", influenced by the intrinsic properties of the species supporting dispersal, the environmental conditions, or a combination of both. Under these conditions, bacteria might adopt different strategies to overcome these limitations. Adaptations allowing the modification of speed, such as expressing different numbers of grappling-hook-like pili, have been observed in previous studies as a strategy to overcome crowding in *Pseudomonas aeruginosa* in collective movement across surfaces (Meacock et al. 2020). Given the complex spatial structure and diverse spatial niches in fungal highways, we could expect a bet-hedging strategy that favors plastic movement speeds to better use exploration and exploitation opportunities in the dispersal networks. We hypothesized that this adaptation applies to bacteria moving on fungal highways, but to test this, the speed of individual cells on fungal highways need to

be measured. Accomplishing this task is challenging because it requires an experimental system where the movement of individual bacteria can be observed with sufficient magnification and temporal resolution to enable accurate tracking of individual cells.

Therefore, in this study, we present an approach to observe the trajectory and measure the speed of individual cells moving in the liquid film surrounding hyphae. For this, we combine a recently developed method called the "fungal drops" that allows for establishing fungal highways at the laboratory scale (Buffi et al. 2023) with high-speed imaging and video analysis to achieve tracking of individual bacterial cells. Although this system does not fully capture the complexity and heterogeneity of real soil, it provides a feasible environment for measuring the movement of single cells in dispersal networks generated by mycelial-forming organisms. This is challenging to achieve in other systems used to model fungal highways, such as water-saturated microfluidic devices or agar cultures, as both hold continuous water films where bacteria can disperse independently from mycelial network (Pion et al. 2013; Buffi et al. 2023). Furthermore, as bacterial behavior can be heterogeneous (Xue et al. 2009), a detailed examination of the variation in speeds must be accomplished by measuring the distribution of instantaneous movement speeds of individual bacterial cells within a population. This approach provides insights into the strategies adopted by bacteria dispersing in spatially complex environments, such as mycelial networks in the soil, as such environments may select for bet-hedging strategies for exploring and exploiting different spatial niches.

Materials and methods

Preparation of mycelial suspensions

The filamentous oomycete *P. ultimum* was obtained from the microbial collection of the laboratory of microbiology, University of Neuchâtel, Switzerland, and was maintained on Malt Extract Agar (MEA, 12 g/l malt extract [SIOS, Homebrew], 15 g/l Agar [Biolife]). For the preparation of mycelial suspensions, *P. ultimum* was incubated in M9 minimal liquid medium at room temperature and under constant agitation (Lab Shaker, Adolf Kühner AG) at 120 rpm for 5 days. The mycelium was then fragmented and homogenized using an ULTRA-TURRAX® (IKA® T18 basic) at max speed for 10 s and then washed 3 times with physiological saline solution (0.9% NaCl). The resulting hyphal suspension was quantified with a Neubauer chamber (BIOSYSTEMS® 0.01 mm) and then resuspended at a final concentration of circa 10 hyphal fragments/µl in a M9 minimal liquid medium (64 g/l $Na_2HPO_4 \bullet 7H_2O$, 15 g/lKH_2PO_4 2.5 g/l NaCl, 5.0 g/l NH_4Cl).

Preparation of the bacterial inoculum

We used two closely related *Pseudomonas putida* strains deposited in the bacterial collection of the laboratory of microbiology, University of Neuchâtel, Switzerland: *P. putida* KT2440 and *P. putida* UWC1. Both strains are flagellated and have originally been isolated from a rhizospheric soil (Regenhardt et al. 2002). The two strains are constitutively tagged with fluorescent proteins via mini-Tn7 transposon insertions, KT2440 with a green fluorescent protein (GFP) and UWC1 with mCherry (Rochat et al. 2010; Dechesne et al. 2010). The different tags allowed us to identify the strains using epifluorescence microscopy. Bacterial suspensions were obtained from overnight cultures incubated in Nutrient Broth (NB,

25 g/L, Carl Roth, AE92.2) at room temperature and under constant agitation (120 rpm). The cells were then collected by centrifuging (5000 g for 5 min), washed 3 times in physiological saline solution, and then resuspended in M9 minimal liquid medium at an optical density of 1, corresponding to approximately 10^9 cells/ml.

Glass slides treatment

The "fungal drops" (Buffi et al. 2023) system was set on a rectangular (24 × 60 mm) glass cover slide with thickness #0 (0.08–0.130 mm; see Fig. 1). To foster *P. ultimum* growth and the formation of the liquid film associated with its hyphal network, the cover slides were treated with Poly-D-Lysine (0.1 mg/ml; GIBCO®) as follows. First, the cover slides were immersed in 37% HCl (Sigma ref.: 84,422) overnight, then thoroughly rinsed, and autoclaved in milli-Q H_2O. After this cleaning step, the cover slides were coated following the product manual (GIBCO®) and used once dried. When not used directly, the slides were stored at 4 °C and used in the coming weeks.

Inoculation

Two 15 µl drops were placed on the coated cover slide at a distance of 0.5 cm from each other. One of the drops consisted of the initial inoculum drop and contained the hyphal suspension, while the other contained sterile M9 minimal medium. The inoculated "fungal drops" systems were then incubated at room temperature in a humid chamber consisting of a glass bell containing moistened Vermiculite at the bottom (Buffi et al. 2023). *P. ultimum* was left to grow over five days until its network connected the two drops. At five days post inoculation (dpi), 2 µl of the bacterial suspension was added to the inoculum drop previously inoculated with *P. ultimum*. The experiments were performed in 5 replicates for each bacterial strain.

Recording

To observe and record bacteria moving along fungal highways, an inverted Nikon Ti2-E microscope equipped with an OkoLab box incubator to control relative humidity at > 80% and temperature at 24 °C was used. All observations were done using an oil immersed 40X objective at a numerical aperture (NA) of 1.45, a working distance (WD) of 0.13 mm, a Plan Apo lambda DIC (differential interference contrast) objective lens, a color camera (Orca Fusion BT 2304 × 2304 pixels, 6.5 µm × 6.5 µm), and a spectra III light engine (8-wavelength; GFP: 474/27 nm; mCherry-like: 578/21 nm). We ran the microscope in time-lapse imaging mode, with a frame rate acquisition speed of 0.024 s. The field of view was set to the mycelial network connecting the drops. The pictures obtained were then used to compile a video using the software Image J (Schneider et al. 2012). A total of 5 videos for each bacterial strain were produced and analyzed (details see next section).

Tracking

To track bacterial movement in the liquid films of the mycelial network of *P. ultimum*, we used the plugin TrackMate (Tinevez et al. 2017) of the software Fiji (version 1.8.0), which allows for the automated tracking of individual bacterial cells. TrackMate creates a file

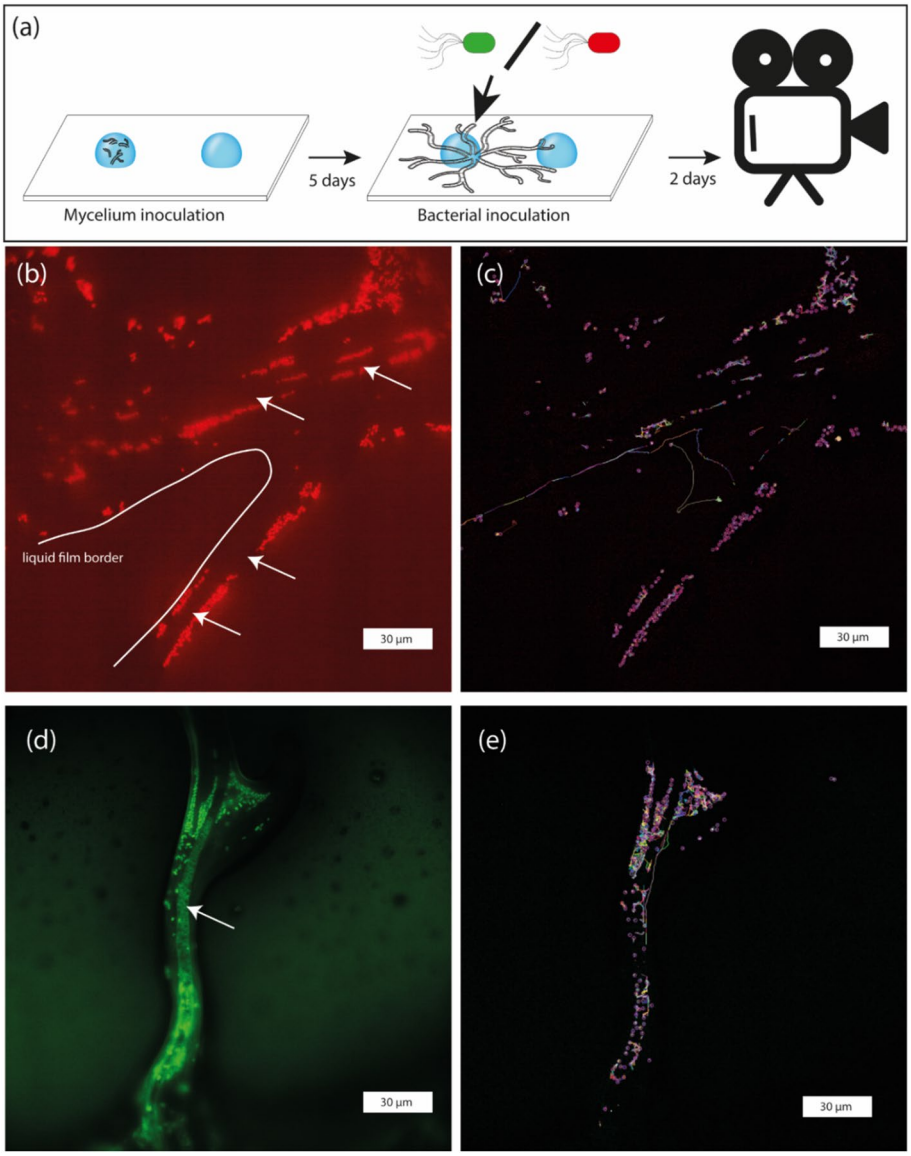

Fig. 1 Tracking the movement of bacteria in the *Pythium ultimum* mycelial network. Panel **a**: overview of the inoculation of drops with *P. ultimum* forming a mycelial network connecting the two drops; after 5 days post inoculum one of the two bacterial strains was added; bacteria moving along the hyphae network between the drops were filmed after 2 days. Panels **b** and **d**: snapshots of the microscopic videos of the liquid film around *P. ultimum* hyphae. Panels **c**, **e**: snapshots of the microscopic videos of bacterial movement on fungal hyphae. Panels **b** and **d** show the fluorescently labelled UWC1 (red) and KT2440 (green) strains of *Pseudomonas putida*, respectively. Panels **c** and **e** show the corresponding tracking results, where the magenta circles represent individual cells, and the coloured lines represent movement trajectories. The corresponding videos are provided in the Zenodo repository: https://zenodo.org/records/14163816; the frame-wise tracking trajectories are provided in the Zenodo repository: https://zenodo.org/records/14166198

with the coordinates of each cell at any time point. The tracking algorithm identified some very fast cells, which were suspected to be an artifact (e.g., a cell moving out of the focal plane followed by another one moving in). Those were excluded by manually checking the videos. After manual checking, the fastest instant speed of KT2440 and UWC1 cells was around 115 um/s. To be more stringent in the inclusion criteria and to avoid tracking artifacts, we set an upper cutoff of the speed at 100 um/s. This cutoff excluded 1.137% of the UWC1 speed measurement (Supplementary Information Appendix Section 1) and 0.741% of the KT2440 cells (Supplementary Information Appendix Section 2). We further excluded tracking trajectories shorter than 5 μm in distance from the analysis because they mainly correspond to cells inside mini-colonies. The movements were caused by cells pushing each other to rearrange positions, which does not lead to dispersal. We also excluded tracking trajectories shorter than 0.25 s because they correspond to cells entering the focal plane only transiently. The trajectories of these cells were often not parallel to the focal plane, which can cause errors when calculating their movement speeds. After cleaning up the data, we used the statistical software R (R Core Team (2022) to calculate the movement speed of cells by dividing the distance between a cell's coordinates in two consecutive frames with the time difference between the frames.

Statistical analysis

We fitted the speed distribution data recorded for the two bacterial strains to simple forms of continuous probability distributions and evaluated their goodness of fit based on a series of evaluation criteria, including the Bayesian information criterion, Akaike information criterion, Hannan-Quinn information criterion, and the Log-likelihood. The top ten best fits for each strain and their corresponding goodness of fit evaluation results are provided in Supplementary Information Appendix Section 3. We then separated the speed distributions arbitrarily into a slow and a fast movement range at an intersection of the fitted probability distribution curves. In addition, we performed the non-parametric Kolmogorov–Smirnov Test to compare the speed distributions and the Kruskal–Wallis tests to compare the mean speed between the KT2440 and UWC1 strains in the slow and fast movement ranges. All statistical analyses and plots were performed using the software Mathematica. The Notebook code is provided in the Supplementary Information.

Results

To establish a mycelial network for the dispersal of bacteria, we first grew the oomycete *P. ultimum* in a "fungal drop" system (Buffi et al. 2023) adapted for high-resolution microscopy. The main adaptation from the original method consisted of the use of ultra-thin coated cover slides instead of treated Petri dishes to enable tracking of individual bacteria cells moving on the liquid film surrounding the hyphae directly in the specific setting of the microscope (mostly regarding focal distance). The oomycete grew into a filamentous hyphal network and connected the two drops after 5 days (Fig. 1a) in all 5 replicates. Two *P. putida* strains, each with a distinct fluorescent tag (KT2440-GFP and UWC1-mCherry), were used to assess the movement of bacteria in the mycelial network. The two strains were able to grow and effectively used the liquid film surrounding the mycelial network of *P. ultimum* to disperse between the two drops (Fig. 1b–d). The fluorescence signals were

detected clearly for both the GFP-tagged (Fig. 1b) and mCherry-tagged strains (Fig. 1d), allowing for accurate tracking and speed measurement for the two strains (Fig. 1c, e).

Because cells were not individually labeled, once they moved in or out of the focal plane, it was impossible to determine if the cells observed corresponded to the same cell or a new one. Therefore, we use the number of independent measurements instead of the number of cells to evaluate the speed distributions of different populations (Table 1). The range of measured speeds for the moving cells of the two strains was similar, from slow-moving (< 1 μm/s) up to over 100 μm/s (Fig. 2a). We fitted the cell movement speed data to different probability distribution functions and evaluated their goodness of fit. The shapes of the speed distribution patterns for the two examined strains were similar in the sense that around 2/3 of the cells moved at relatively low speeds (< 5 μm/s), while a small proportion of cells moved much faster. However, the speed distributions of the two strains had significantly different statistical features. The speed distribution of KT2440 cells (GFP-tagged, hence green) exhibited the best fit to a mixture of a lognormal distribution and a uniform distribution (Fig. 2a, green line; Supplementary Information Section 3). In contrast, the speed distribution of UWC1 cells (mCherry-tagged, hence red) fitted best to a mixture of a Cauchy distribution and a uniform distribution (Fig. 2a, magenta line; Supplementary Information Section 3). More specifically, the difference in distribution meant that a larger fraction of the cells for the KT2440 strain were faster, while cells from strain UWC1 were faster at lower speeds. To test whether the mixed distributions were due to intrinsic features of the data, we split the dataset for each strain at an arbitrarily chosen 60 μm/s into slow and fast subpopulations and fitted each subset of data to probability distribution functions. The top three best-fitting functions for each data subset were still mixed functions,

Table 1 Datasets included in the speed of movement distribution analysis for the UWC1 and KT2240 strains

UWC1	Number of independent speed measurements	Mean slow cells speed (um/s)	Mean fast cells speed (um/s)
rfp_2days022_11fps_2_movement.csv	1476	2.32 ± 1.51	22.34 ± 23.26
rfp_2days025_11fps_2_movement.csv	1473	2.05 ± 1.47	23.24 ± 23.11
rfp_2days026_11fps_2_movement.csv	1501	2.31 ± 1.49	24.56 ± 26.30
rfp_2days028_11fps_2_movement.csv	1463	2.16 ± 1.47	24.54 ± 27.51
rfp_2days031_11fps_2_movement.csv	1211	2.18 ± 1.49	19.21 ± 22.47
Combined data for UWC1	7124	2.20 ± 1.49	22.81 ± 24.54
KT2440	Number of independent speed measurements	Mean slow cells speed (um/s)	Mean fast cells speed (um/s)
gfp_2days002_11fps_2_movement.csv	741	1.54 ± 1.10	42.28 ± 36.60
gfp_2days004_11fps_2_movement.csv	1572	2.03 ± 1.44	24.20 ± 25.81
gfp_2days005_11fps_2_movement.csv	1315	2.04 ± 1.42	27.09 ± 27.88
gfp_2days011_11fps_2_movement.csv	1781	2.28 ± 1.54	24.82 ± 22.06
gfp_2days015_11fps_2_movement.csv	935	2.18 ± 1.50	22.69 ± 29.39
Combined data for KT2440	6344	2.02 ± 1.44	25.06 ± 25.40

The raw data is included in Supplementary Information provided in the Zenodo repository: https://zenodo.org/records/14208231. As cells could not be tracked individually when moving out of focus, we counted the number of individual measurements (N) instead

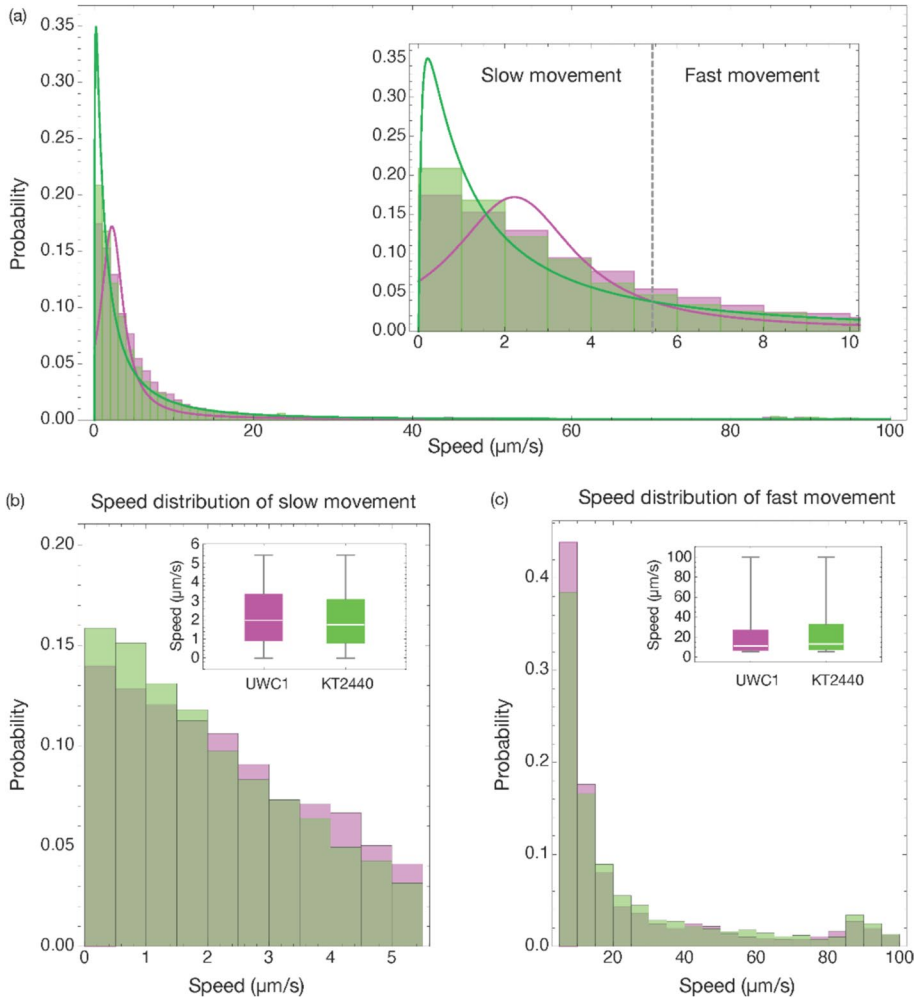

Fig. 2 Speed of movement distribution analysis. **a** Speed distribution of the UWC1 (magenta) and KT2440 (green) cells. The corresponding green and magenta lines are fitted probability distributions. The inset shows a zoomed-in view of the speed distribution below 10 μm/s. We separated the cell speed into slow and fast movement ranges at an intersection of the fitted distribution curves. **b** Speed distributions in the slow movement range; UWC1 cells generally move faster than the KT2440 cells. **c** Speed distributions in the fast movement range; KT2440 cells generally move faster than the UWC1 cells. Details on the best-fitting models and goodness-of-fit analyses are provided in the Supplementary Information provided in the Zenodo repository: https://zenodo.org/records/14208231, Appendix Section 3. For the separate representations of the histograms and the fitted probability distribution curves please see Supplementary Information Appendix Sect. 5

suggesting that the mixed distributions were intrinsic features of the datasets (Supplementary Information Section 4).

Considering the between-individual variation of speed distribution within each strain and the statistically different distributions between the strains, we attempted to compare the movement speed patterns by establishing two categories of movement speed ranges.

For this, we separated the speed distributions arbitrarily into a slow and a fast movement range at an intersection of the fitted probability distribution curves (Fig. 2a, inset) at 5.44 µm/s. In the fast range, KT2440 cells moved faster (mean speed 25.06 µm/s) than UWC1 cells (22.81 µm/s) (Kruskal–Wallis-test p-value = 1.09e-4). In contrast, in the slow range, UWC1 cells moved faster (mean speed 2.20 µm/s) than KT2440 cells (mean speed 2.02 µm/s) (Kruskal–Wallis-test p-value = 2.86e-8).

Discussion

This study represents, to the best of our knowledge, the first successful measurement of speed distributions of individual bacterial cells dispersing on mycelial networks. This was made possible by combining a previously developed method (i.e., fungal drops) designed to better visualize mycelium at the microscale (Buffi et al. 2023) and the use of an inverted widefield fluorescence microscope with an incubation chamber and a high-speed camera. With this approach, we were able to perform the tracking and measurement of the speed of single cells. One interesting result is the maximum speed at which bacteria moved on hyphae. Previous research showed that the speed of different bacterial species during swimming or swarming varies greatly from 15 µm/s for *Escherichia coli* (Mitchell et al. 1995) to more than 100 µm/s (max instantaneous movement up to 500 µm/s) in magnetotactic cocci (Bente et al. 2020). One of the bacterial strains we used in this study, *P. putida* KT2440, has been measured to move at an average speed of 20.9 µm/s and reach a peak velocity of 51.2 µm/s in liquid culture during the exponential growth phase (Davis et al. 2011). However, the speed of individual bacteria dispersing on mycelial networks has not been measured previously. Our results showed that cells from both *P. putida* strains displayed great heterogeneity in their movement speeds in the complex environment of mycelial network compared to the simpler environment of liquid culture. Both strains contained static and very slow-moving cells (mainly in micro-colonies), while a small fraction of cells reached a maximum instantaneous movement speed of up to 100 µm/s (mainly along hyphae connecting distant micro-colonies), which is among the fastest movement speeds described so far. It would be interesting to test whether local cell density influences cell movement speeds in future studies with explicit control for this parameter.

Moreover, our study shed light on how intra-population speed variation may influence the competition outcome between the strains. In previous studies assessing spatial competition between the two *P. putida* strains, conflicting results were obtained under different experimental conditions. In the first study (Kuhn et al. 2022b), the two strains competed on hyphal networks formed on an agar plate, where the UWC1 strain had an advantage and often competitively excluded the other strain. In the second study (Kuhn et al. 2022a), the two strains competed in liquid films formed on an abiotic surface (i.e., the "bacterial bridge" device). In the latter case, the KT2440 strain had an advantage and colonized a distant habitat more efficiently. In both studies, only the bulk dispersal capability of the populations was assessed. Results obtained in the current study suggest that within-strain heterogeneity of dispersal speed can help reconcile those contradicting outcomes. A higher mean speed in the slower range, where a larger fraction of the population was found (67.41% of KT2440 and 65.49% of UWC1), might explain the advantage of the UWC1 strain in hyphae networks on an agar plate, where the movement speed of cells was limited by the low level of water saturation (Kuhn et al. 2022b). By contrast, a higher mean speed in the faster range of the KT2440 strain may have resulted in its competitive advantage

on the abiotic surface, where the degree of water saturation was much higher than in the hyphal networks in an agar plate (Kuhn et al. 2022a). The heterogeneity in the speeds of individual cells suggests that the population mean speed does not reflect the dispersal of individual cells in spatially complex environments, such as soils (Choudoir and DeAngelis 2022) and fermented foods (Louw et al. 2023). We thus speculate that individual variation of dispersal speed serves as a bet-hedging strategy for exploiting diverse spatial niches in complex networks formed by fungi and other mycelial-forming organisms. This hypothesis remains to be tested experimentally, for example, by performing direct competition assays in controlled environments with varying degrees of water saturation, which can be achieved by varying the composition of the media.

By directly measuring the dispersal speed distributions of bacterial cells on hyphal networks, the approach presented here will further our understanding of the characteristics that make bacteria suited to explore spatially complex environments such as soils. For example, it can help us find out if individual cells of the same or closely related bacterial species are equally efficient in using mycelial networks to disperse. The results obtained here suggest this was not the case for the two *P. putida* strains, given their distinct characteristic movement speed distributions under the conditions tested. The fitted probability distribution functions provided a useful statistical description of the heterogeneity in movement speeds, but they revealed no information about the mechanisms causing the difference between the two strains, which remain to be investigated. The heterogeneity of the mycelial network and the resulting liquid paths may select for specific dispersal strategies. Although this has not been investigated in fungal highways, experiments with swarming colonies of *P. aeruginosa* showed that morphological adaptations can influence dispersal success under different degrees of crowdedness. Cells that were genetically modified to express a larger number of pili spread faster at the less crowded colony margins, while cells with fewer pili moved faster under higher cell density (Meacock et al. 2020). A similar diversification of morphological adaptations (with or without a genetic basis) between different species or even within strains of the same species could occur in bacteria moving along fungal highways and other biotic dispersal networks. The mechanisms explaining speed adaptation seem to be largely unexplored. Nevertheless, the flagellum has been suggested to participate in surface sensing in bacteria (Laventie and Jenal 2020), which may help them adjust movement speed according to different surface conditions in the environment. For instance, studies performed in the aquatic bacterium *Vibrio parahaemolyticus* suggested that changes in the rotation speed of flagella upon contact with a surface trigger the expression of lateral flagella for swarming (McCarter et al. 1988). In addition, signaling via c-di-GMP has also been suggested to participate in surface adaptation (Laventie and Jenal 2020). Similar mechanisms might play a role in the speed adaptation in mycelial networks, but this needs to be investigated.

The transport of metabolically resting cells or unrelated microbial species in mono- and multispecies associations within swarming colonies has been considered as a bet-hedging strategy for the colonization of novel habitats under variable environmental conditions (Inghama et al. 2011; Hagai et al. 2014; Finkelshtein et al. 2015). A recent review highlighted the importance of bet-hedging strategies in several categories of microbial lifestyles, including dormancy, resource exploitation, and signaling (Grimbergen et al. 2015). However, the role of speed adaptation as a bet-hedging strategy has not yet been considered as a mechanism for adapting to limited dispersal opportunities in heterogeneous environments. Our method can facilitate future studies addressing this question in complex environments generated by mycelial-forming organisms. For example, by testing whether parameters such as nutrient availability or species composition can affect the features of the

dispersal network (e.g., thickness and composition of the liquid film), which further influences the choice of dispersal strategies. Likewise, hitchhiking dispersal (i.e., non-motile bacteria using motile ones to disperse) is another area of research that can benefit from direct observations and assessment of bacterial movement along fungal highways and other biotic networks (Warmink et al. 2011; Kuhn et al. 2022b). Our new method can facilitate such research by imaging and tracking interacting cells labeled with different fluorescence markers simultaneously. Understanding the causes and consequences of such bet-hedging strategies will prove useful for choosing suitable microbial strains for real-world applications, ranging from biotechnology to ecosystem restoration, plant growth promotion, and engineering (Frey-Klett et al. 2011; Krüger et al. 2019; Steffan et al. 2020; Jiang et al. 2021).

Acknowledgements The authors gratefully acknowledge the ScopeM facility of ETH Zürich for their support & assistance in this work.

Author Contribution MB, SB, XYL, PJ contributed to the study conception and design. Material preparation, data collection and analysis were performed by MB, TK, XYL. The first draft of the manuscript was written by MB, DG, SB, XYL, PJ and all authors commented on previous versions of the manuscript. Resources, funding acquisition, and supervision were provided by PSC, XLY, SB and PJ. All authors read and approved the final manuscript.

Funding Open access funding provided by University of Neuchâtel. This study was funded by the U.S. Department of Energy, Office of Science, Biological and Environmental Research Division, under award number LANLF59T; the Swiss National Science Foundation grants 180145 and 211549 to X-Y.L.R.

Data Availability A supplementary appendix file that includes all supporting materials and links to raw data is provided in the Zenodo repository: https://zenodo.org/records/14208231.

Declarations

Conflict of interest The authors declare no conflict of interest.

References

Banitz T, Johst K, Wick LY, Schamfuß S, Harms H, Frank K (2013) Highways versus pipelines: contributions of two fungal transport mechanisms to efficient bioremediation. Environ Microbiol Rep 5:211–218. https://doi.org/10.1111/1758-2229.12002

Bente K, Mohammadinejad S, Charsooghi MA, Bachmann F, Codutti A, Lefèvre CT, Klumpp S, Faivre D (2020) High-speed motility originates from cooperatively pushing and pulling flagella bundles in bilophotrichous bacteria. Elife. https://doi.org/10.7554/ELIFE.47551

Buffi M, Cailleau G, Kuhn T, Li Richter X-Y, Stanley CE, Wick LY, Chain PS, Bindschedler S, Junier P (2023) Fungal drops: a novel approach for macro- and microscopic analyses of fungal mycelial growth. microLife 4:1–13. https://doi.org/10.1093/FEMSML/UQAD042

Choudoir MJ, DeAngelis KM (2022) A framework for integrating microbial dispersal modes into soil ecosystem ecology. iScience 25:103887. https://doi.org/10.1016/J.ISCI.2022.103887

Custer GF, Bresciani L, Dini-Andreote F (2022) Ecological and evolutionary implications of microbial dispersal. Front Microbiol 13:855859. https://doi.org/10.3389/FMICB.2022.855859/BIBTEX

Davis ML, Mounteer LC, Stevens LK, Miller CD, Zhou A (2011) 2D motility tracking of pseudomonas putida KT2440 in growth phases using video microscopy. J Biosci Bioeng 111:605–611. https://doi.org/10.1016/J.JBIOSC.2011.01.007

Dechesne A, Wang G, Gülez G, Or D, Smets BF (2010) Hydration-controlled bacterial motility and dispersal on surfaces. Proc Natl Acad Sci USA 107:14369–14372. https://doi.org/10.1073/PNAS.1008392107/SUPPL_FILE/SM02.MOV

Finkelshtein A, Roth D, Ben JE, Ingham CJ (2015) Bacterial swarms recruit cargo bacteria to pave the way in toxic environments. Mbio 6:1–10. https://doi.org/10.1128/MBIO.00074-15

Frey-Klett P, Burlinson P, Deveau A, Barret M, Tarkka M, Sarniguet A (2011) Bacterial-fungal interactions: hyphens between agricultural, clinical, environmental, and food microbiologists. Microbiol Mol Biol Rev 75:583–609

Gow NAR, Latge J-P, Munro CA (2017) The fungal cell wall: structure, biosynthesis, and function. Microbiol Spectr 5. https://doi.org/10.1128/MICROBIOLSPEC.FUNK-0035-2016/ASSET/7D28FF9B-A28D-43E9-99DC-2B72E99D94A8/ASSETS/GRAPHIC/FUNK-0035-2016-FIG7.GIF

Grimbergen AJ, Siebring J, Solopova A, Kuipers OP (2015) Microbial bet-hedging: the power of being different. Curr Opin Microbiol 25:67–72. https://doi.org/10.1016/J.MIB.2015.04.008

Hagai E, Dvora R, Havkin-Blank T, Zelinger E, Porat Z, Schulz S, Helman Y (2014) Surface-motility induction, attraction and hitchhiking between bacterial species promote dispersal on solid surfaces. ISME J 8:1147–1151. https://doi.org/10.1038/ISMEJ.2013.218

Inghama CJ, Kalismand O, Finkelshteind A, Ben-Jacob E (2011) Mutually facilitated dispersal between the nonmotile fungus *Aspergillus fumigatus* and the swarming bacterium *Paenibacillus vortex*. Proc Natl Acad Sci USA 108:19731–19736. https://doi.org/10.1073/PNAS.1102097108/-/DCSUPPLEMENTAL/PNAS.201102097SI.PDF

Jiang F, Zhang L, Zhou J, George TS, Feng G (2021) Arbuscular mycorrhizal fungi enhance mineralisation of organic phosphorus by carrying bacteria along their extraradical hyphae. New Phytol 230:304–315. https://doi.org/10.1111/NPH.17081

Junier P, Cailleau G, Palmieri I, Vallotton C, Trautschold OC, Junier T, Paul C, Bregnard D, Palmieri F, Estoppey A et al (2021) Democratization of fungal highway columns as a tool to investigate bacteria associated with soil fungi. FEMS Microbiol Ecol 97:fiab003

Kearns DB (2010) A field guide to bacterial swarming motility. Nat Rev Microbiol 8(9):634–644. https://doi.org/10.1038/nrmicro2405

Kohlmeier S, Smits THM, Ford RM, Keel C, Harms H, Wick LY (2005) Taking the fungal highway: mobilization of pollutant-degrading bacteria by fungi. Environ Sci Technol 39:4640–4646. https://doi.org/10.1021/ES047979Z

Krüger W, Vielreicher S, Kapitan M, Jacobsen ID, Niemiec MJ (2019) Fungal-bacterial interactions in health and disease. Pathogens 8:70

Kuhn T, Buffi M, Bindschedler S, Chain PS, Gonzalez D, Stanley CE, Wick LY, Junier P, Richter XYL (2022a) Design and construction of 3D printed devices to investigate active and passive bacterial dispersal on hydrated surfaces. BMC Biol. https://doi.org/10.1186/S12915-022-01406-Z

Kuhn T, Mamin M, Bindschedler S, Bshary R, Estoppey A, Gonzalez D, Palmieri F, Junier P, Richter XYL (2022b) Spatial scales of competition and a growth–motility trade-off interact to determine bacterial coexistence. R Soc Open Sci. https://doi.org/10.1098/RSOS.211592

Laventie BJ, Jenal U (2020) Surface sensing and adaptation in bacteria. Annu Rev Microbiol 74:735–760. https://doi.org/10.1146/ANNUREV-MICRO-012120-063427/CITE/REFWORKS

Lohberger A, Spangenberg JE, Ventura Y, Bindschedler S, Verrecchia EP, Bshary R, Junier P (2019) Effect of organic carbon and nitrogen on the interactions of *Morchella* spp. and bacteria dispersing on their mycelium. Front Microbiol 10:398464

Losa G, Bindschedler S (2018) Enhanced tolerance to cadmium in bacterial-fungal Co-cultures as a strategy for metal biorecovery from e-waste. Minerals 8:121

Louw NL, Lele K, Ye R, Edwards CB, Wolfe BE (2023) Microbiome assembly in fermented foods. Annu Rev Microbiol 77:381–402. https://doi.org/10.1146/ANNUREV-MICRO-032521-041956

McCarter L, Hilmen M, Silverman M (1988) Flagellar dynamometer controls swarmer cell differentiation of V. parahaemolyticus. Cell 54:345–351. https://doi.org/10.1016/0092-8674(88)90197-3

Meacock OJ, Doostmohammadi A, Foster KR, Yeomans JM, Durham WM (2020) Bacteria solve the problem of crowding by moving slowly. Nat Phys 17(2):205–210. https://doi.org/10.1038/s41567-020-01070-6

Mitchell JG, Pearson L, Dillon S, Kantalis K (1995) Natural assemblages of marine bacteria exhibiting high-speed motility and large accelerations. Appl Environ Microbiol 61:4436–4440. https://doi.org/10.1128/AEM.61.12.4436-4440.1995

Or D, Smets BF, Wraith JM, Dechesne A, Friedman SP (2007) Physical constraints affecting bacterial habitats and activity in unsaturated porous media – a review. Adv Water Resour 30:1505–1527. https://doi.org/10.1016/J.ADVWATRES.2006.05.025

Pion M, Bshary R, Bindschedler S, Filippidou S, Wick LY, Job D, Junier P (2013) Gains of bacterial flagellar motility in a fungal world. Appl Environ Microbiol 79:6862–6867. https://doi.org/10.1128/AEM.01393-13/SUPPL_FILE/ZAM99104851SO1.PDF

R Core Team (2022) R: a language and environment for statistical ## computing

Regenhardt D, Heuer H, Heim S, Fernandez DU, Strömpl C, Moore ERB, Timmis KN (2002) Brief report Pedigree and taxonomic credentials of Pseudomonas putida strain KT2440. Environ Microbiol 4:912–915

Rochat L, Péchy-Tarr M, Baehler E, Maurhofer M, Keel C (2010) Combination of fluorescent reporters for simultaneous monitoring of root colonization and antifungal gene expression by a biocontrol pseudomonad on cereals with flow. Cytometry 23:949–961. https://doi.org/10.1094/MPMI-23-7-0949

Schneider CA, Rasband WS, Eliceiri KW (2012) NIH image to imageJ: 25 years of image analysis. Nat Methods 9(7):671–675. https://doi.org/10.1038/nmeth.2089

Simon A, Bindschedler S, Job D, Wick LY, Filippidou S, Kooli WM, Verrecchia EP, Junier P (2015) Exploiting the fungal highway: development of a novel tool for the in situ isolation of bacteria migrating along fungal mycelium. FEMS Microbiol Ecol 91:fiv116

Simon A, Herve V, Al-Dourobi A, Verrecchia E, Junier P (2017) An in situ inventory of fungi and their associated migrating bacteria in forest soils using fungal highway columns. FEMS Microbiol Ecol 93:fiw217

Steffan BN, Venkatesh N, Keller NP (2020) Let's get physical: bacterial-fungal interactions and their consequences in agriculture and health. J Fungi 6:243

Tinevez J-Y, Perry N, Schindelin J, Hoopes GM, Reynolds GD, Laplantine E, Bednarek SY, Shorte SL, Eliceiri KW (2017) TrackMate: an open and extensible platform for single-particle tracking. Methods 115:80–90

Wadhwa N, Berg HC (2021) Bacterial motility: machinery and mechanisms. Nat Rev Microbiol 20(3):161–173. https://doi.org/10.1038/s41579-021-00626-4

Warmink JA, Nazir R, Corten B, van Elsas JD (2011) Hitchhikers on the fungal highway: the helper effect for bacterial migration via fungal hyphae. Soil Biol Biochem 43:760–765. https://doi.org/10.1016/J.SOILBIO.2010.12.009

Wick LY, Remer R, Würz B, Reichenbach J, Braun S, Schäfer F, Harms H (2007) Effect of fungal hyphae on the access of bacteria to phenanthrene in soil. Environ Sci Technol 41:500–505. https://doi.org/10.1021/ES061407S/ASSET/IMAGES/MEDIUM/ES061407SE00001.GIF

Wong PTW, Griffin DM (1976) Bacterial movement at high matric potentials—II. In Fungal Colonies. Soil Biol Biochem 8:219–223

Xue C, Othmer HG, Erban R (2009) From individual to collective behavior of unicellular organisms: recent results and open problems. AIP Conf Proc 1167:3–14. https://doi.org/10.1063/1.3246413

Zhang Y, Kastman EK, Guasto JS, Wolfe BE (2018) Fungal networks shape dynamics of bacterial dispersal and community assembly in cheese rind microbiomes. Nat Commun 9:336

Supplementary Material Chapter 3

Assessing the speed of individual bacteria dispersing on mycelial networks

Published: 2 January 2025

Evolutionary Ecology

DOI: https://doi.org/10.1007/s10682-025-10329-4

Assessing the speed of individual bacteria dispersing on mycelial networks

Authors: Matteo Buffi[1], Thierry Kuhn[1,2], Diego Gonzalez[1], Saskia Bindschedler[1], Patrick S. Chain[3], Xiang-Yi Li Richter[1,2,4,5]*, Pilar Junier[1]*
Affiliations: 1. Laboratory of Microbiology, University of Neuchâtel, Rue Emile-Argand 11, 2000 Neuchâtel, Switzerland. 2. Laboratory of Eco-ethology, University of Neuchâtel, Rue Emile-Argand 11, 2000 Neuchâtel, Switzerland; 3. Bioscience Division, Los Alamos National Laboratory, Los Alamos, Los Alamos, P.O. Box 1663, NM 87545, New Mexico, USA. 4. Institute of Ecology and Evolution, University of Bern, Baltzerstrasse 6, 3012 Bern, Switzerland. 5. Department of Biology, University of Konstanz, Universitaetsstrasse 10, 78464 Konstanz, Germany.
*Co-corresponding authors: li@evolbio.mpg.de; pilar.junier@unine.ch

Supplementary Information Appendix

1. The tracking speed distribution of the UWC1 strain. The cell movement speeds were obtained directly from the corresponding tracking files, as indicated in each panel. The datasets are provided in the Zenodo repository: https://zenodo.org/records/14161913.
   We set a maximum speed cutoff at 100 μm/s for subsequent analyses, which excluded 1.137% of measurements from the pooled dataset.

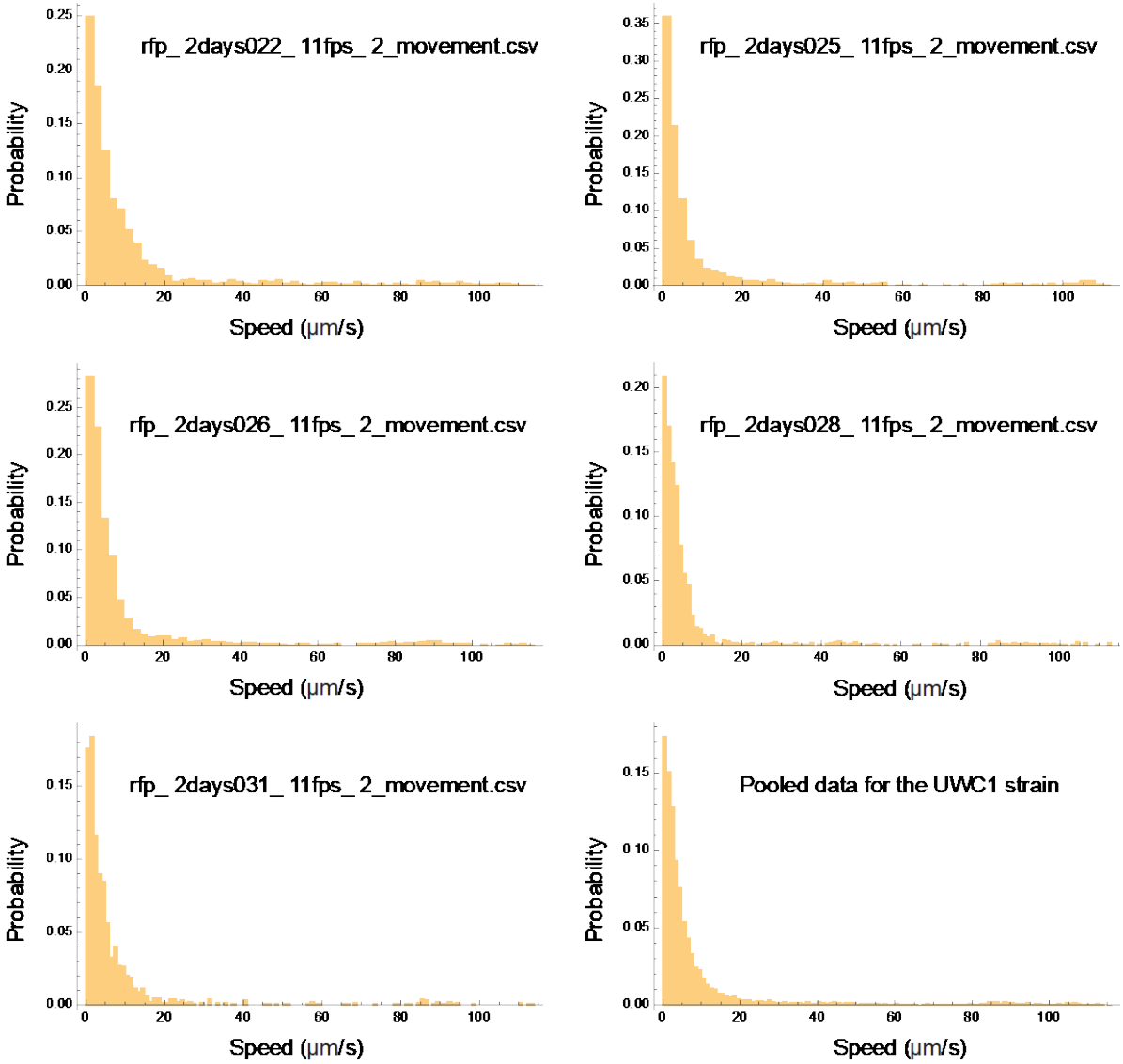

2. The tracking speed distribution of the KT2440 strain. The cell movement speeds were obtained directly from the corresponding tracking files, as indicated in each panel. The datasets are provided in the Zenodo repository: https://zenodo.org/records/14161967.
We set a maximum speed cutoff at 100 μm/s for subsequent analyses, which excluded 0.741% of measurements from the pooled dataset.

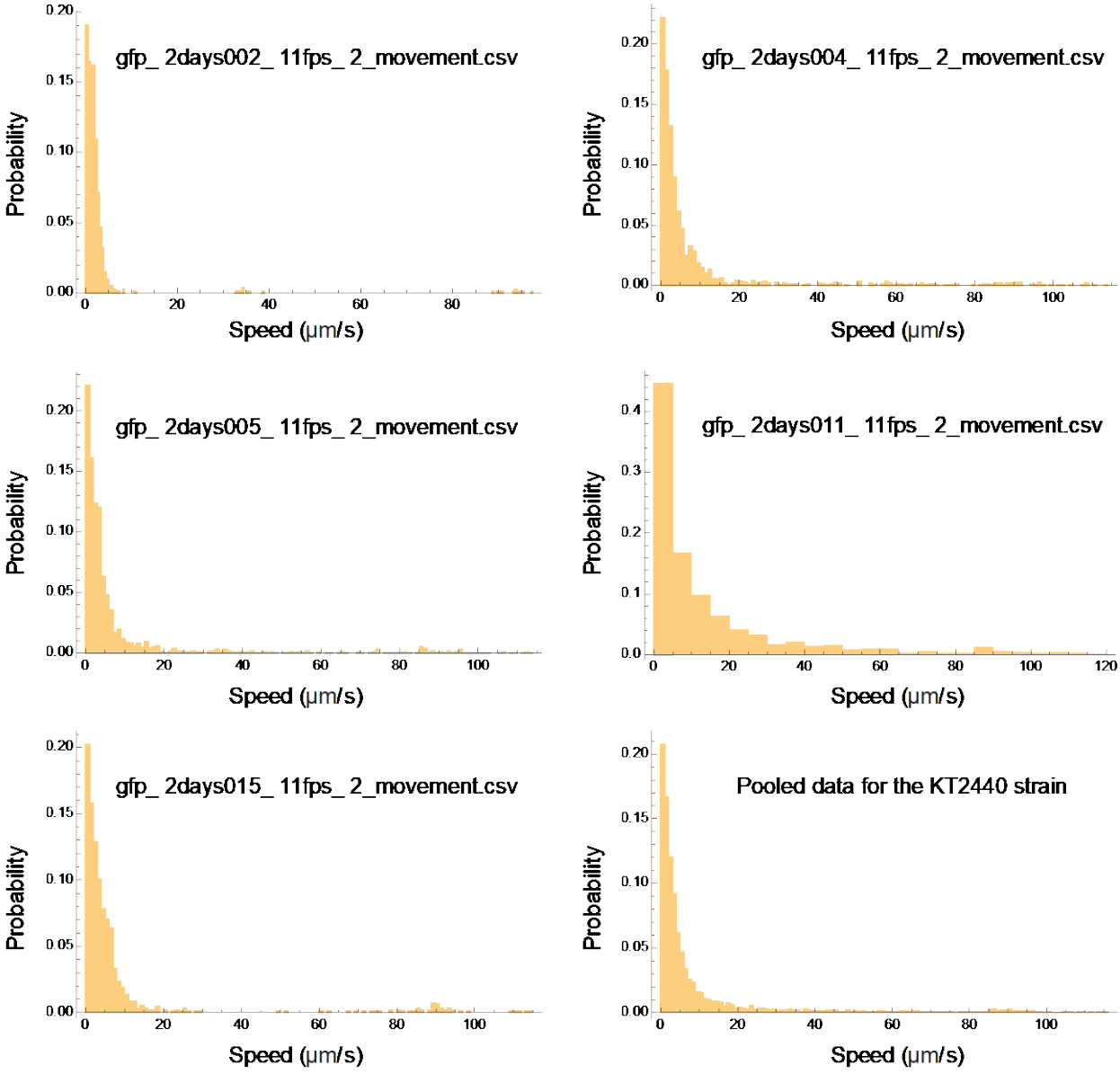

3. The top ten best fits for the speed distribution of UWC1 and KT2440 cells are provided in the supplementary files “rfp-FitTable.csv”, and “gfp-FitTable.csv”, respectively. The datasets are provided in the Zenodo repository: https://zenodo.org/records/14163776.
Detailed descriptions of the goodness-of-fit evaluation criteria and the ranking of fitted functions are provided in the documentation: https://reference.wolfram.com/language/ref/FindDistribution.html

4. To test whether the mixed distributions in the best fits for the speed distributions of the UWC1 and KT2440 cells were due to the intrinsic features of the data, we split the datasets into slow and fast subpopulations at an arbitrarily chosen speed of 60 μm/s, and fitted each subset of data to probability distribution functions. The top three best fits for each subset of data are still mixed distributions. The top ten best fits for the slow and fast subsets of speed distribution data for the two strains are provided in the Zenodo repository: https://zenodo.org/records/14163794.

5. Histograms and the best-fit probability distribution functions of the speed distribution of KT2440 (green) and UWC1 (magenta) strains in different speed ranges.

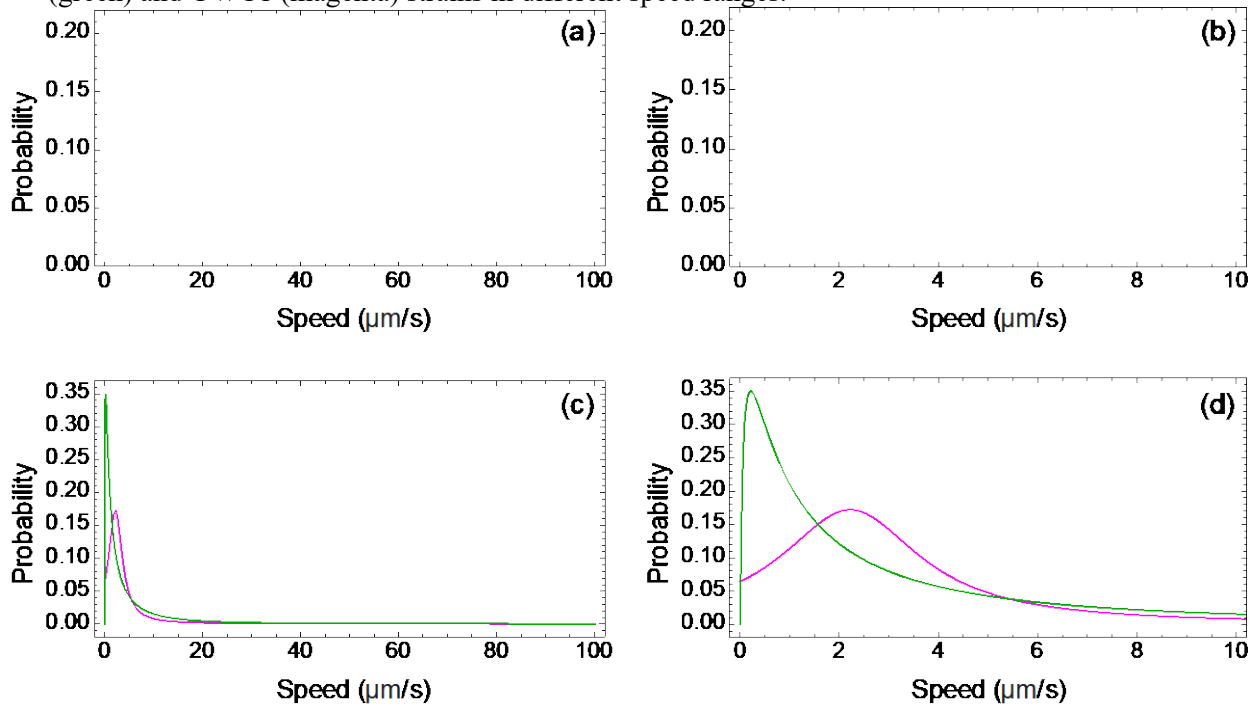

6. The videos we used for tracking the movements of UWC1 and KT2440 cells are provided in the Zenodo repository: https://zenodo.org/records/14163816.

7. The TrackMate output raw data for tracking the movement of UWC1 and KT2440 cells and the R script for calculating the instant movement speed of cells are provided in the Zenodo repository: https://zenodo.org/records/14166147.

8. The TIFF files for the tracking trajectories in Figure 1 of the main text are provided in the Zenodo repository: https://zenodo.org/records/14166198

Chapter 4

Detection of electrical signals in fungal mycelia in response to external stimuli

Publication date: 17 October 2025

CellPress: iScience

DOI: https://doi.org/10.1016/j.isci.2025.113484

Contributions:

Matteo Buffi, contributed to the study conception and design. Material preparation, data collection and analysis and to the writing of the manuscript.

iScience

Article

Detection of electrical signals in fungal mycelia in response to external stimuli

Graphical abstract

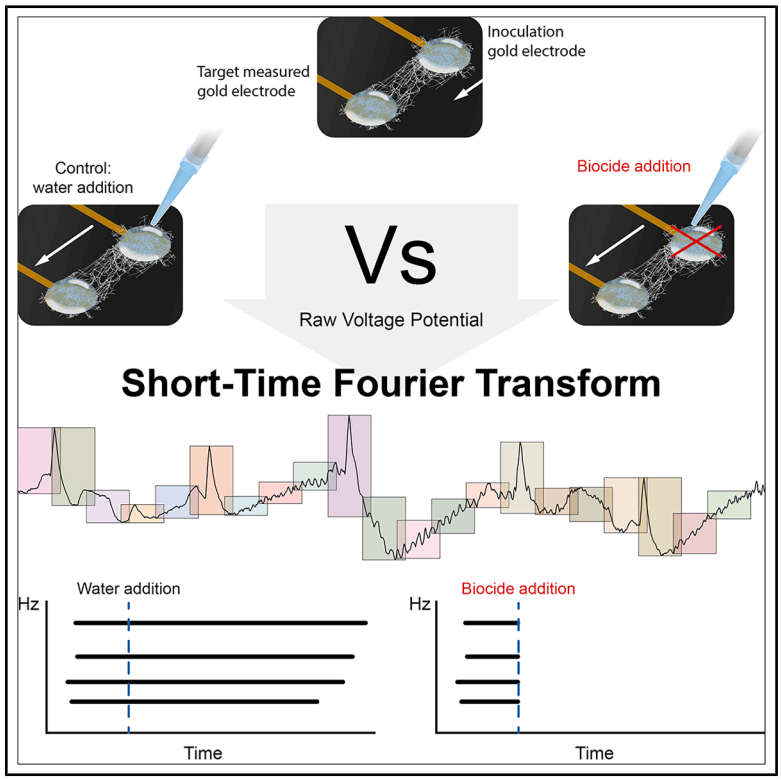

Authors

Matteo Buffi, Silvia Giangaspero, Valerio Foiada, ..., Saskia Bindschedler, Lorenzo Pirrami, Pilar Junier

Correspondence

lorenzo.pirrami@hefr.ch (L.P.), pilar.junier@unine.ch (P.J.)

In brief

Mycology; Biophysics

Highlights

- Development of a tool to study extracellular voltage fluctuations in fungi
- Features minimizing experimental artifacts reducing abiotic and environmental noise
- Application of advanced signal analysis for extraction of frequency patterns
- Robust foundation for further exploration of electrical signaling in fungi

Buffi et al., 2025, iScience *28*, 113484
October 17, 2025
https://doi.org/10.1016/j.isci.2025.113484

CellPress

iScience

CellPress
OPEN ACCESS

Article

Detection of electrical signals in fungal mycelia in response to external stimuli

Matteo Buffi,[1] Silvia Giangaspero,[2] Valerio Foiada,[3] Loïc Puthod,[3] Guillaume Cailleau,[1] Aaron J. Robinson,[4] Julia M. Kelliher,[4] Patrick S.G. Chain,[4] Daniel Oberson,[2] Markus Künzler,[5] Saskia Bindschedler,[1] Lorenzo Pirrami,[2,*] and Pilar Junier[1,6,*]

[1]Laboratory of Microbiology, University of Neuchâtel, 2000 Neuchâtel, Switzerland
[2]iSIS Institute, HEIA-FR, HES-SO University of Applied Sciences and Arts Western Switzerland, 1700 Fribourg, Switzerland
[3]Prototypos Sarl, 1700 Fribourg, Switzerland
[4]Bioscience Division, Los Alamos National Laboratory, Los Alamos, NM 87545, USA
[5]Institute of Microbiology, Department of Biology, ETH Zürich, 8093 Zurich, Switzerland
[6]Lead contact
*Correspondence: lorenzo.pirrami@hefr.ch (L.P.), pilar.junier@unine.ch (P.J.)
https://doi.org/10.1016/j.isci.2025.113484

SUMMARY

Electrical signaling is a crucial mechanism for intercellular communication across diverse biological systems. Despite evidence of electrical activity in fungal mycelia, a standardized, reproducible method for detecting these signals is lacking. In this study, we developed a novel approach using printed circuit boards with embedded differential electrodes to record extracellular voltage fluctuations in mycelium. By incorporating a Faraday cage and short-time Fourier transform analysis, we minimized noise and extracted relevant frequency patterns. Our findings revealed electrical activity correlated with fungal growth that varied with biocide treatments. The results support the biological origin of these signals, suggesting a role in environmental adaptation. This study provides a robust framework for further exploration of fungal electrophysiology, with implications for understanding signaling mechanisms in mycelial networks.

INTRODUCTION

Electrical signaling as a mechanism of inter- and intracellular communication is used by a wide diversity of organisms including animals, plants, and microorganisms.[1–3] Since Luigi Galvani's discovery of so-called "animal electricity,"[4] propagating action potentials have been identified as the principal communication mechanism in the central nervous system of animals.[5] Charles Darwin also observed action-potential-like signals in one of his favorite plants, *Dionaea muscipula*,[6] and it is now widely accepted that many physiological functions in plants rely on action potentials with the same characteristics of those of animals.[7–10] However, given the fundamental differences between animals and plants, additional types of electrical signaling processes have been recognized only in the case of the latter. In plants, variation and systemic potentials are long-distance intercellular electrical signals generated by transient membrane depolarization that coordinate functional responses under stress conditions.[8–11] Electrical signaling has also been recognized as a means of communication in bacterial biofilms, where it facilitates nutrient sharing and aids in the recruitment of distant cells.[3] The diversity of examples of electrical signaling across the entire tree of life suggests the universality of this mechanism of communication. Electrical signaling is the result of a fundamental function of cell membranes: the selective transport of charged molecules that creates a disequilibrium of charge across the membrane, i.e., a membrane potential.[12] This electrochemical gradient is essential for energy production[13] but it also enables communication between adjacent cells, as it can be propagated along the cell membrane via voltage-gated ion channels.[14]

The mycelium of filamentous fungi is a highly plastic network of interconnected cells or hyphae that allows fungi to adapt dynamically to uneven or ephemeral resources in complex environments such as soil or other habitats.[15,16] The architecture of this network depends on multiple factors, but ultimately on the polar growth of hyphal tips, hyphal branching, and hyphal fusion (anastomosis).[17] While the vegetative hyphae of basal fungal clades (i.e., Mucoromycota) are not compartmentalized, hyphae of higher fungi (Dikarya) contain regular septa with pores that regulate exchange and transport among compartments and play a role in differentiation and reproduction.[18,19] Septation also prevents loss of cytoplasm after hyphal damage[20,21] or in response to attack[22,23] but restricts the propagation of chemical signals via cytoplasmic bulk flow. In contrast, the continuity of the cellular membrane, even across plugged septal pores, offers a mechanism by which electrical signaling could allow for communication between distant hyphal compartments. Moreover, the membrane is surrounded by the cell wall that is comprised of components that can act as electrical insulators analogously to myelin in neurons.[24–26]

Filamentous fungi are known to produce electrical currents in their hyphal tips.[27,28] Pioneering work using internal electrodes

iScience 28, 113484, October 17, 2025

has shown action-potential-like spikes in rhizomorphs or loose mycelium of *Armillaria bulbosa* and *Pleurotus ostreatus* exposed to a wood block (complex source of carbon) or in response to mechanical pressure.[29] These currents or membrane potential changes were low in voltage (nV to μV).[28–30] More recently, several studies using needle electrodes inserted into fruiting bodies[31–36] recorded action-potential-like spikes in various fungi and suggested a type of species-specific frequency code in the signal.[32] Even though these studies offer an initial insight into the production and potential role of electrical signaling in filamentous fungi, a reproducible method to detect these signals and confirm their biological origin is still lacking.[37] Furthermore, since not all fungi produce macrostructures such as fruiting bodies or rhizomorphs, it is necessary to confirm the existence of membrane potential fluctuations at the level of vegetative mycelium or single hyphae and to extend the observations beyond Basidiomycetes, which have been the subject of most studies conducted thus far.

RESULTS

Development of an experimental setup for recording of electrical signals in filamentous fungi

We designed the fungal potential card (FPC) for the extracellular recording of electrical signals produced by filamentous fungi. The FPCs are printed circuit boards with pairs of embedded differential electrodes to measure extracellular changes in voltage of a growing mycelium (Figures 1 and S1). Droplets containing medium with or without fungal spores were deposited on the electrodes in a manner consistent with previously described methods.[38] The spores were inoculated onto one of the electrodes in each pair, and, upon germination and hyphal growth, the mycelium was expected to create a connection with the second electrode in the pair. Moreover, as the system is open, stimuli can be added to validate the biological origin of the signal (Figure 1A). The FPC was placed inside an incubation chamber designed to maintain humidity and prevent evaporation of the inoculation droplets during the experiments (Figure 1B). The system was placed inside a Faraday cage to decrease external noise and artifacts. This experimental setup successfully maintained optimal conditions for growth, while also permitting the collection of nearly noise-free recordings.

Validation of the experimental setup

To validate the method, we selected *Fusarium oxysporum*, an ascomycete that is ubiquitous in soils,[39–41] has a fast growth rate, and can easily be propagated through spores, making it ideal for the inoculation approach employed in this study. As a first step, we tested the biocompatibility of the electrodes as well as the impact of the electrode size and distance between electrode pairs on hyphal growth. For this, *F. oxysporum* was grown on FPCs with different electrode sizes (1, 2, 3, and 4 mm) placed 1 cm apart (center to center). We selected gold-covered electrodes because gold is considered an inert non-toxic material.[42,43] The smallest electrode size (1 mm) resulted in inconsistent colonization and was difficult to inoculate accurately. For larger electrode sizes (3 and 4 mm), the fungus did not consistently colonize the second electrode. In contrast,

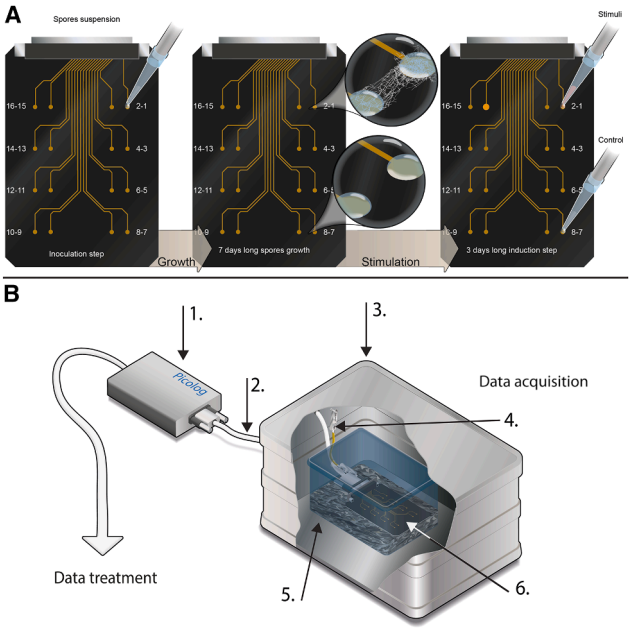

Figure 1. Schemes showing the development of the fungal potential card (FPC), an optimized system for the recording of electrical signals in filamentous fungi

(A) The system is based on printed circuit boards (PCBs) with pairs of embedded differential electrodes to measure voltage changes. In this system, the fungus is inoculated as a spore suspension (left image) on one of the electrodes. The fungus is allowed to grow and colonize the second electrode as shown in the bubble in the middle of the figure. After this, the effect of different stimuli can be assessed (right image).

(B) For recording, the system is placed in a custom-made incubator. The components of the incubation system included (1) data logger; (2) shielded cable; (3) Faraday cage; (4) crocodile head cable connected to the PCB; (5) filter for gas exchange; and (6) moistened vermiculite at the bottom to maintain optimal growth conditions.

with 2 mm electrodes, the fungus was able to consistently colonize and connect the two electrodes on the FPCs, and therefore, this electrode size was selected for all of the following experiments (Figure S2).

Development of a method for data interpretation

Interpretation of the recorded data can be challenging, and this was considered when analyzing the data collected on the selected 2-mm electrode FPCs. The use of a Faraday cage makes it impossible to assess the density of hyphae connected to each electrode, which is a feature required for characterization of raw voltage measurements as action-potential-like signals. Therefore, the changes in voltage were broken down to their frequency components using a short-time Fourier transform (STFT). This type of analysis results in a spectrogram that displays frequencies over time (Figure 2A). In contrast to raw recordings, which only show how the signal behaves in the time domain, STFT enables the analysis of both time and frequency simultaneously. This is particularly useful for identifying patterns in the data that may evolve or shift over time and would be hard to detect using the raw voltage data alone. For instance, the colonization of the second electrode by the growing hyphae

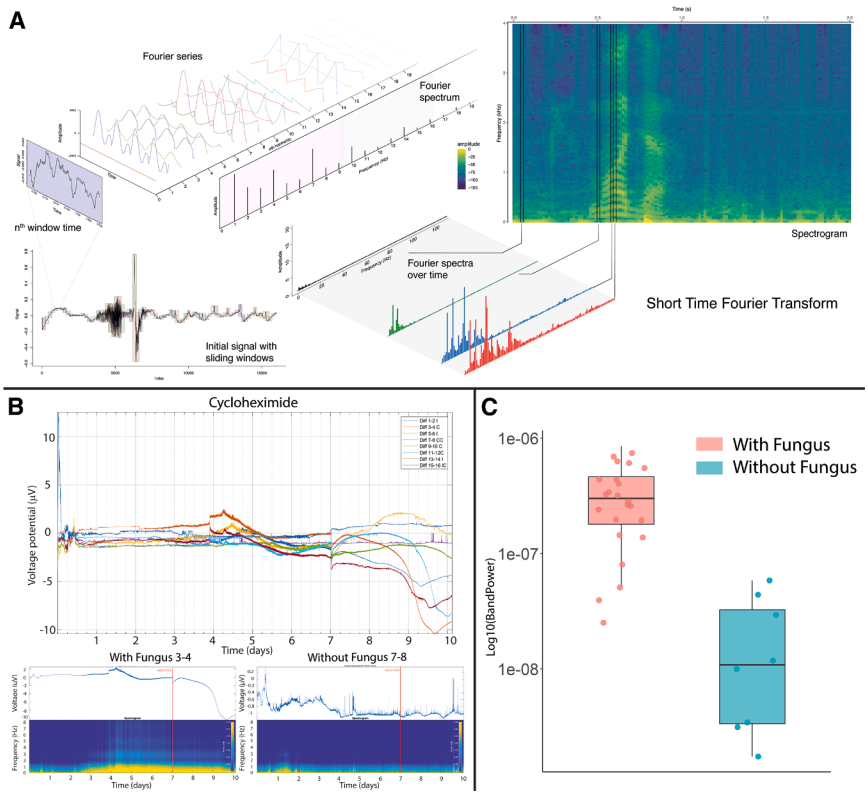

Figure 2. Transformation of raw signals into frequencies for data analysis

(A) The signal is recorded as voltage change between the inoculated electrodes and a reference electrode. The signal is further transformed into frequencies using a short-time Fourier transform (STFT). This procedure results in a spectrogram that represents the signals' component frequencies over time and allows for comparison against controls.

(B) In the example shown here, the top panel represents the raw voltage measurements. After STFT, the pattern in the spectrogram on the left (corresponding to the inoculated electrode) is clearly distinct from the background in the uninoculated controls (right image). The change starts at 3 days after inoculation, but it is more pronounced after 4 days.

(C) To quantitatively assess the difference in the STFT pattern between conditions, a power analysis was performed by integrating the power spectral density (PSD) comparing inoculated (with fungus) and non-inoculated (without fungus) electrode pairs. This difference was significant (p value < 0.001).

was expected to result in a change in the STFT data pattern. To test this, we grew the fungus for seven days and recorded the voltage changes between the two electrodes. Controls without inoculation were also included in these experiments. Based on previous experiments with this isolate of *F. oxysporum*, we estimated that the mycelium would take 3–4 days to connect the pair of electrodes.[38] The use of a Faraday cage prevented the direct monitoring of the colonization, but a change in the STFT pattern was consistently observed four days post-inoculation, which is consistent with the previously observed colonization time.[38] The signal profiles from inoculated electrode pairs were visually distinct; in the non-inoculated controls, a background signal with a frequency below 1 Hz was recorded (yellow color in the STFT frequency). The signals from electrode pairs connected by the fungal mycelium also contained this low-frequency component prior to day four, but after this period, additional frequencies above 1.5 Hz were detected (Figure 2B). To further characterize the data, we calculated the power spectral density (PSD), which quantifies the strength or intensity of a signal at different frequencies but results in a single cumulative value. This allowed us to compare how the bulk frequency signal changed comparing the inoculated electrodes versus the control electrodes without the fungus. The results showed a 1,604% PSD increase in the inoculated electrodes compared to the non-inoculated electrodes, which was significant (Figure 2C; Table 1). This suggests that our setup records electrical signals generated by the colonizing mycelium. However, further evidence was needed to confirm the biological origin of the observed signals.

Evaluation of the biological origin of electrical signals

To assess the biological origin of the detected electrical signals, we tested the effect of different chemicals that are known to negatively affect hyphal physiology (Figure 3). For this, we ran experiments with eight electrode pairs at a time. As controls, non-inoculated electrode pairs were also subjected to the applied chemical and chemical carrier (e.g., solvent or Milli-Q water). First, we tested the biocide cycloheximide, confirming that the fungus was sensitive to it by culturing both spores and mycelium in the presence of this antibiotic. Cycloheximide (20 mg/mL) fully inhibited spore germination (Figure 3A) and partially inhibited mycelial growth (Figure S3). The addition of cycloheximide reduced the frequency content under 1.5 Hz to a minimum and eliminated the signals above 1.5 Hz (Figure 3B). In contrast, the addition of the carrier (Milli-Q water) did not alter the frequency content. The frequency content under 1.5 Hz remained unchanged, and the signals above 1.5 Hz (specially the one at 2 Hz) were still observable (Figures 3B and S3). The PSD showed a reduction of 74.21% in the treated pairs compared to the untreated controls but this difference was not significant (Table 1). Next, we tested voriconazole, a second antibiotic. In contrast to cycloheximide, voriconazole (12.5 μg/mL) was shown not to be toxic on a plate assay (Figures 3C and S4). The STFT pattern after addition of voriconazole showed a minor dent in the measurements compared to the carrier (i.e., Milli-Q water; Figures 3D and S4). The PSD increased by 1,201%, but this result was not significant (Table 1). In addition, increased hyphal branching was observed following treatment with voriconazole (Figure S5).

We also tested the antibiotic Calcimycin. In this case, the solvent dimethyl sulfoxide (DMSO) was used as carrier. Since

Table 1. Summary of the results of the power spectral density (PSD) analysis across the tested experimental conditions

Fungi vs. no fungi before induction	Replicates	Fungi mean	No fungi mean	*p* value	% change
Fungi/No fungi	24 f/8 nf	3.44429E-07	2.0204E-08	0.000*	1,604.752
Drug/control before induction	**Replicates**	**Drug mean**	**Control mean**	***p* value**	**% change**
Cycloheximide/MQwater	3	5.98197E-07	3.13556E-07	0.317	90.779
Voriconazole/MQwater	3	2.72814E-07	3.41486E-07	0.786	−20.110
Calcimycin/DMSO	3	4.50667E-07	2.51333E-07	0.179	79.310
Sodium Azide/MQwater	3	3.5809E-07	1.69289E-07	0.286	111.526
Induction					
Cycloheximide/MQwater	3	1.81389E-06	7.03443E-06	0.327	−74.214
Voriconazole/MQwater	3	3.53236E-06	2.71344E-07	0.391	1,201.803
Calcimycin/DMSO	3	1.58093E-06	9.97417E-07	0.580	58.503
Sodium Azide/MQwater	3	3.41499E-06	2.34075E-07	0.116	1,358.933

PSD values were extracted from three days before and after the induction. Each row represents an individual condition, with PSD values computed on a logarithmic scale (Log10) over a three-day period following induction or control treatment. The analysis was performed exclusively for conditions with sufficient replicates, while controls without fungi were excluded due to the availability of only a single replicate per sample. Additionally, the table reports the percentage change (increase or decrease) in PSD values between the induction and control conditions for each treatment. All data processing and table generation were conducted using RStudio (2024.09.1 Build 394; Document S2). For the fungi/no fungi comparison, f = fungi and nf = no fungi (replicate number). MQwater = Milli-Q water. * = significant *p* value (<0.001).

DMSO has been reported to be toxic under some conditions,[44] we assessed the toxicity of both Calcimycin and DMSO in a plate assay. Calcimycin inhibited spore germination and hyphal growth, whereas DMSO had no obvious impacts on germination or growth (Figure S6). The addition of Calcimycin (1.3 mg/mL) in DMSO also reduced the detected frequencies to a minimum, but DMSO alone produced an identical result (Figure S6). As the effect observed on the signal was not due to DMSO toxicity, it is

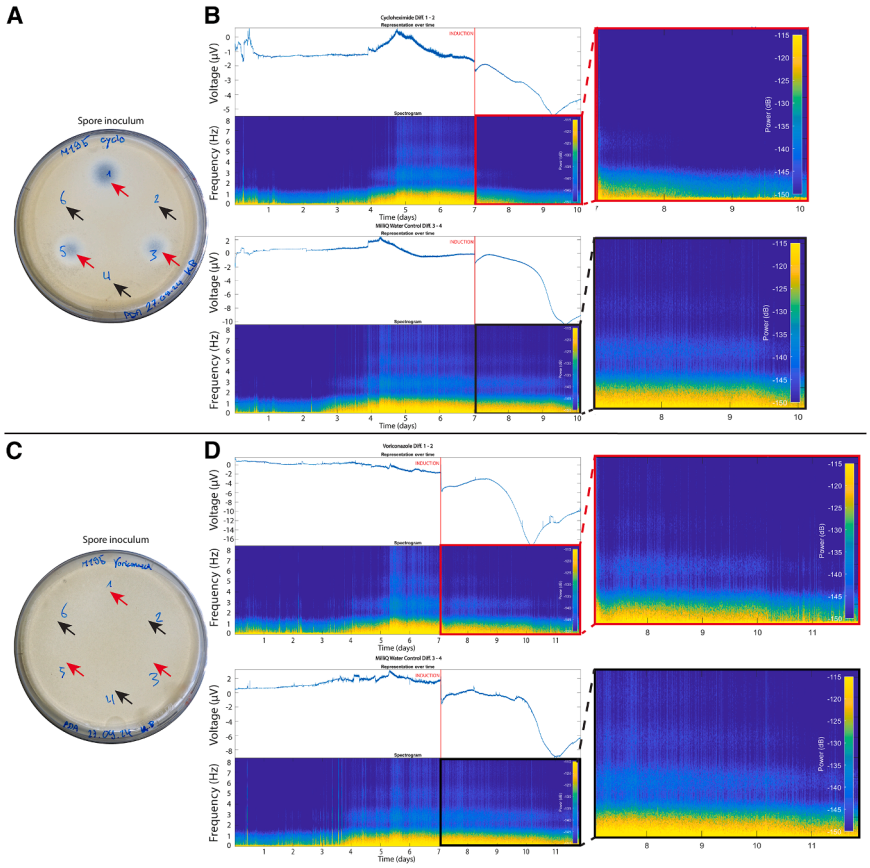

Figure 3. Frequency change analysis of electrical recordings in *Fusarium oxysporum* in response to cycloheximide and voriconazole

(A and C) To evaluate the effect of the two biocides, susceptibility tests were performed on spores (for tests on mycelium please see Figures S3 and S4). The site of application of the biocides is shown by the red arrows (cycloheximide in A and voriconazole in C). Black arrows show the addition of Milli-Q water, which is the carrier solvent of the two biocides and acted as a control.

(B and D) Examples of voltage plots and their respective interpretation in frequency patterns obtained by STFT analysis (see Figure 2B) for cycloheximide (B) and voriconazole (D). In both cases, the stimuli are shown on the top panel, and the carrier (Milli-Q water) is shown on the bottom panel. The time of application of the stimuli is shown by the red line. The effect of the biocides is shown on the window indicated by the red (biocide) and black (Milli-Q water) squares. The images on the right show a magnification of the frequency pattern after addition of the biocides and Milli-Q water to highlight the effect of the stimuli on the electrical signal produced by the mycelium.

more likely that DMSO interfered with the gold-plated electrodes.[45] Three days after the addition of Calcimycin or DMSO, a signal was detectable again in some replicates (Figure S6), suggesting a recovery process. Finally, sodium azide had a substantial impact on spore germination but had a lower impact on established mycelium (Figure S7A). The application of sodium azide (6.5 mg/mL) reduced the signal for about 18 h, before returning to a signal equivalent to the control treatments with Milli-Q water (Figures S7B and S7C). The addition of Milli-Q water in the control resulted in a decrease of the frequency signal in one of the three replicates for a short duration (about 5–6 h) (Figures S7C and S7D), but as all other Milli-Q water controls did not result in a reduced signal, this is likely an artifact. In the case of Calcimycin and sodium azide, the comparison of the PSD showed an increase of the signal after the induction, but the differences were not significant (Table 1).

DISCUSSION

The recording of voltage changes in fruiting bodies using needle electrodes[31–36] triggered the development of techniques to accurately measure voltage in growing mycelium. However, hitherto attempts suffered from flaws in the experimental design, leading to the recording of artifacts and the lack of confidence on the biological origin of the measured signals. These shortcomings have been highlighted by other authors.[37] To overcome these problems, we established a setup based on the design and construction of the FPC, a printed circuit board in which the differential electrodes were embedded and allowed for the omission of agar-containing media, which can be prone to the development of abiotic electrochemical gradients that can be mistakenly interpreted as true electrical signals.[37]

The use of a Faraday cage was also an essential addition for the improvement of the setup. This feature has been missing in previous studies,[31,32] and this has been a common criticism and indicated as an experimental flaw of previous studies.[37] The addition of the Faraday cage reduced the effect of external noise and artifacts for accurate measurements of voltage changes in the order of microvolts. In previous studies lacking a Faraday cage and employing the same recording instrument, the presence of people walking near the incubator or even the automatic closing of window shades affected voltage measurements.[46] This issue was eliminated in the current setup.

In addition to an improved experimental setup, we also used a signal analysis methodology that allows us to observe changes in the frequency of electrical signals over time. Previous studies have relied on the characterization of action-potential-like signals directly from the changes in voltage to infer electrical signaling in fungi.[32,33] However, the use of a Faraday cage makes it impossible to assess the density of hyphae connected to each electrode, which is a feature required for characterization of action-potential-like signals.[27,35] Moreover, action potentials are transmembrane potentials that arise between the intracellular and extracellular space and are generally measured with microelectrodes placed inside living cells. Instead, extracellular electrodes record field potentials (i.e., local voltage changes) when placed close to or in contact with excitable cells. This type of indirect measure of cellular activity reflects the synchronous electric behavior of multiple cells.[37,47] To obtain a signal that corresponded to this synchronous behavior, the changes in voltage were broken down into their frequency components using an STFT. This analysis is akin to the analysis of electroencephalographic signals in studies of human physiology,[48] but in this case, it was applied to the changes in voltage produced upon colonization of the second electrode in the FPC. The STFT, an adaptation of the fast Fourier transform (FFT) algorithm,[49] is useful in this case because it allows for the extracting of the non-stationary frequency content from noisy signals,[50] which better correspond to those expected by the non-coordinated expansion of a mycelial network.

A set of signature frequencies above 1.5 Hz were recorded in the time frame in which colonization of the second electrode was to be expected according to previous studies with the same fungus.[38] The observed range of frequencies (1.5–8 Hz) is consistent with previous studies using internal electrodes, in which frequencies ranging from 0.5 to 5 Hz were recorded.[29] For comparison, the animal central neuronal system acts at much higher frequencies (up to 200–300 Hz).[51] However, frequencies in other organs such as the heart (1 Hz for the normal heartbeat) or the intestine (slow waves 0.05–0.2 Hz) are lower.[52] Similarly, electrical communication in plants depend on signals at lower frequencies.[2,53] For instance, the fast cell movement required for the closing of marginal tentacles in the carnivorous plant *Drosera capensis*[54] is triggered by two action potentials in less than 30 s (4 Hz).[55] In contrast, other types of signals are thought to use frequencies below 0.2 Hz.[56] The range of frequencies observed for the mycelium of *F. oxysporum* appears to be compatible with the speed of signal integration required in a digestive system (i.e., intestinal movement), a heartbeat, or to the one existing for fast cell movement in plants. This offers potential for comparative studies across organisms. However, it is still unclear if the signal conveys information or if it is the result of periodic ion redistribution in growing hyphae. Nevertheless, if this mechanism allows intracellular communication, it could contribute to the fast adaptation and the dynamic response of the mycelium to external stimuli, in combination with other processes such as bulk transport of chemical signals.[57]

The comparison of the effect of different biocides with different mechanisms of action on mycelial growth or spore germination suggests that the recorded signals have a biological origin. The effect of cycloheximide, which was confirmed to be toxic in culture assays, suggests that the signal is generated by the active growth of the fungus. Cycloheximide is a biocide of bacterial origin that affects protein synthesis, and it is widely used as a fungicide.[58] Cycloheximide was toxic, and its addition reduced the frequency content under 1.5 Hz and eliminated the signals above 1.5 Hz. The rapid decrease of electrical signals confirms that those are not merely noise, but rather a physiological indicator reflecting the cellular activity of the mycelium. Voriconazole is also a commonly used fungicide that stops ergosterol production, resulting in an initial stop of growth followed by the destruction of the membrane.[59] However, voriconazole was not toxic for *F. oxysporum* on a plate assay. In contrast to cycloheximide, voriconazole resulted only on a minor dent in the signal that could be the result of temporary cytosol leaking in the affected hyphae.

However, mechanisms ensuring survival, such as the plugging of septal pores,[20,21] could be responsible for the fast recovery and are consistent with the observed hyphal branching.

In the future, the use of the FPC could be complemented by monitoring ion fluctuations at a single hyphal level using fluorescent voltage-dependent dyes or tagged ions in combination with fluorescence microscopy. Likewise, the use of knockout mutants or the silencing of genes coding for putative voltage or ion-gated membrane channels is compatible with the method presented here. All the above will increase our knowledge and understanding of the mechanisms involved in the fluctuations of membrane potentials in fungi and help to determine if these fluctuations contribute to cell-to-cell communication conveying information in fungal networks.

Limitations of the study

Future experiments should focus on the dissection of the molecular mechanisms generating the detected signals by identifying the ions and ion-gated membrane channels involved in this mechanism of electrical signaling. Unfortunately, the first experiments performed in this direction using Calcimycin were inconclusive due to the interaction of DMSO with the electrodes. Calcimycin is an ionophore for divalent cations across biological membranes and leads to Ca^{2+}-dependent cell death in Gram-positive bacteria.[60] Influx and efflux of Ca^{2+} via Ca^{2+}-dependent membrane channels have been involved in thigmotropism and galvanotropism in fungi, relaying topologic information during hyphal growth.[61–63] In addition, a study in *Aspergillus nidulans* showed a highly localized Ca^{2+} movement that caused a wave of voltage measurements with variable frequency in response to stress.[64] Accordingly, we expected that the treatment with Calcimycin would further support the role of Ca^{2+} in fungal electrophysiology. However, Calcimycin was highly toxic, and its effect could not be differentiated from its solvent (DMSO). Future experiments need to consider other solvents to evaluate the role of Ca^{2+} using this antibiotic. Electrical signaling in other microbial systems such as bacterial biofilms has been associated with K^+ transport, in both Gram-positive and Gram-negative bacteria.[3,65,66] K^+-gated channels have been detected and characterized in fungi[67] and could be also tested in the future using the FPCs. Additional experiments could consider testing multiple stimuli such as combining ionophores with sodium azide, which is known to stop the production of ATP[68] and applied alone had a limited effect on the signal.

RESOURCE AVAILABILITY

Lead contact

Further information and requests for resources and reagents should be directed to and will be fulfilled by the lead contact, Pilar Junier (pilar.junier@unine.ch).

Materials availability

The FPC were produced by prototypos SARL (prototypos.ch).

Data and code availability

All data are available in the main text or the supplemental information. The original unprocessed data are available in Mendeley Data under the https://doi.org/10.17632/srkxbkh6sp.1. The code for analysis is provided in the Method S1.

ACKNOWLEDGMENTS

We would like to thank Diego Gonzalez for his comments on early versions of this manuscript, Lukas Wick for insightful discussion during the development of the idea, and Ilona Palmieri for technical help.

This research was supported by a Science Focus Area Grant from the US Department of Energy (DOE), Biological and Environmental Research (BER), Biological System Science Division (BSSD) under the grant number LANLF59T to P.S.C., and the Swiss National Science Foundation Grant 310030_212435 to M.K.

AUTHOR CONTRIBUTIONS

Conceptualization, M.B., S.B., and P.J.; methodology, M.B., S.G., A.J.R., J.M.K., M.K., D.O., S.B., L.P., and P.J.; investigation, M.B., S.G., V.F., and L.P.; visualization, M.B., S.G., G.C., L.P., and P.J.; funding acquisition, A.J.R., P.S.G.C., M.K., S.B., and P.J.; project administration, A.J.R., P.S.G.C., and P.J.; supervision, S.B., L.P., and P.J.; writing—original draft, M.B., S.G., M.K., and P.J.; writing—review & editing, M.B., S.G., A.J.R., J.M.K., M.K., S.B., and P.J.

DECLARATION OF INTERESTS

The authors declare no conflict of interest.

STAR★METHODS

Detailed methods are provided in the online version of this paper and include the following:

- KEY RESOURCES TABLE
- EXPERIMENTAL MODEL AND STUDY PARTICIPANT DETAILS
- METHOD DETAILS
  - Inocula preparation
  - Measurement set-up
  - Testing of electrode sizes
- QUANTIFICATION
  - Signal recording
  - Induction testing on fungal drop setup
  - Short-time Fourier transform
  - Statistical analysis

SUPPLEMENTAL INFORMATION

Supplemental information can be found online at https://doi.org/10.1016/j.isci.2025.113484.

Received: June 6, 2025
Revised: July 14, 2025
Accepted: August 29, 2025
Published: September 2, 2025

REFERENCES

1. Hille, B. (1978). Ionic channels in excitable membranes. Current problems and biophysical approaches. Biophys. J. *22*, 283–294. https://doi.org/10.1016/S0006-3495(78)85489-7.
2. Fromm, J., and Lautner, S. (2007). Electrical signals and their physiological significance in plants. Plant Cell Environ. *30*, 249–257. https://doi.org/10.1111/j.1365-3040.2006.01614.x.
3. Prindle, A., Liu, J., Asally, M., Ly, S., Garcia-Ojalvo, J., and Süel, G.M. (2015). Ion channels enable electrical communication in bacterial communities. Nature *527*, 59–63. https://doi.org/10.1038/nature15709.
4. Piccolino, M. (1998). Animal electricity and the birth of electrophysiology: the legacy of Luigi Galvani. Brain Res. Bull. *46*, 381–407. https://doi.org/10.1016/s0361-9230(98)00026-4.

5. Curtis, H.J., and Cole, K.S. (1942). Membrane resting and action potentials from the squid giant axon. J. Cell. Comp. Physiol. *19*, 135–144. https://doi.org/10.1002/jcp.1030190202.

6. Burdon-Sanderson, J.S. (1873). I. Note on the electrical phenomena which accompany irritation of the leaf of *Dionæa muscipula*. Proc. Roy. Soc. Lond. *21*, 495–496. https://doi.org/10.1098/rspl.1872.0092.

7. Król, E., Dziubinska, H., and Trebacz, K. (2010). What do plants need action potentials for. Action Potential: Biophysical and Cellular Context. In Initiation, Phases and Propagation, 26, M.L. DuBois, ed., p. 1.

8. Zimmermann, M.R., Maischak, H., Mithöfer, A., Boland, W., and Felle, H. H. (2009). System potentials, a novel electrical long-distance apoplastic signal in plants, induced by wounding. Plant Physiol. *149*, 1593–1600. https://doi.org/10.1104/pp.108.133884.

9. Davies, E. (2006). Electrical signals in plants: facts and hypotheses. In Plant electrophysiology: theory and methods (Springer), pp. 407–422.

10. Hedrich, R., Salvador-Recatalà, V., and Dreyer, I. (2016). Electrical Wiring and Long-Distance Plant Communication. Trends Plant Sci. *21*, 376–387. https://doi.org/10.1016/j.tplants.2016.01.016.

11. Vodeneev, V., Akinchits, E., and Sukhov, V. (2015). Variation potential in higher plants: Mechanisms of generation and propagation. Plant Signal. Behav. *10*, e1057365. https://doi.org/10.1080/15592324.2015.1057365.

12. Höber, R. (1905). Über den Einfluss der Salze auf den Ruhestrom des Froschmuskels. Archiv für die gesamte Physiologie des Menschen und der Tiere *106*, 599–635.

13. Mitchell, P. (1961). Coupling of phosphorylation to electron and hydrogen transfer by a chemi-osmotic type of mechanism. Nature *191*, 144–148. https://doi.org/10.1038/191144a0.

14. Katz, B. (1961). How cells communicate. Sci. Am. *205*, 209–220. https://doi.org/10.1038/scientificamerican0961-209.

15. Fricker, M.D., Heaton, L.L., Jones, N.S., and Boddy, L. (2017). The mycelium as a network. In The Fungal Kingdom, pp. 335–367.

16. Hutchings, M.J., and John, E.A. (2004). The effects of environmental heterogeneity on root growth and root/shoot partitioning. Ann. Bot. *94*, 1–8. https://doi.org/10.1093/aob/mch111.

17. Fischer, M.S., and Glass, N.L. (2019). Communicate and Fuse: How Filamentous Fungi Establish and Maintain an Interconnected Mycelial Network. Front. Microbiol. *10*, 619. https://doi.org/10.3389/fmicb.2019.00619.

18. Fischer, R. (1999). Nuclear movement in filamentous fungi. FEMS Microbiol. Rev. *23*, 39–68. https://doi.org/10.1111/j.1574-6976.1999.tb00391.x.

19. Abadeh, A., and Lew, R.R. (2013). Mass flow and velocity profiles in *Neurospora* hyphae: partial plug flow dominates intra-hyphal transport. Microbiology (Read.) *159*, 2386–2394. https://doi.org/10.1099/mic.0.071191-0.

20. Markham, P. (1994). Occlusions of septal pores in filamentous fungi. Mycol. Res. *98*, 1089–1106. https://doi.org/10.1016/S0953-7562(09)80195-0.

21. Steinberg, G., Harmer, N.J., Schuster, M., and Kilaru, S. (2017). Woronin body-based sealing of septal pores. Fungal Genet. Biol. *109*, 53–55. https://doi.org/10.1016/j.fgb.2017.10.006.

22. Gimeno, A., Stanley, C.E., Ngamenie, Z., Hsung, M.H., Walder, F., Schmieder, S.S., Bindschedler, S., Junier, P., Keller, B., and Vogelgsang, S. (2021). A versatile microfluidic platform measures hyphal interactions between *Fusarium graminearum* and *Clonostachys rosea* in real-time. Commun. Biol. *4*, 262. https://doi.org/10.1038/s42003-021-01767-1.

23. Schmieder, S.S., Stanley, C.E., Rzepiela, A., van Swaay, D., Sabotič, J., Nørrelykke, S.F., deMello, A.J., Aebi, M., and Künzler, M. (2019). Bidirectional Propagation of Signals and Nutrients in Fungal Networks via Specialized Hyphae. Curr. Biol. *29*, 217–228.e4. https://doi.org/10.1016/j.cub.2018.11.058.

24. Wosten, H.A., and de Vocht, M.L. (2000). Hydrophobins, the fungal coat unravelled. Biochim. Biophys. Acta *1469*, 79–86. https://doi.org/10.1016/s0304-4157(00)00002-2.

25. Kulkarni, S., Nene, S., and Joshi, K. (2017). Production of Hydrophobins from fungi. Process Biochemistry *61*, 1–11. https://doi.org/10.1016/j.procbio.2017.06.012.

26. Linder, M.B., Szilvay, G.R., Nakari-Setälä, T., and Penttilä, M.E. (2005). Hydrophobins: the protein-amphiphiles of filamentous fungi. FEMS Microbiol. Rev. *29*, 877–896. https://doi.org/10.1016/j.femsre.2005.01.004.

27. Gow, N.A.R. (1989). Relationship Between Growth and the Electric Current of Fungal Hyphae. Biol. Bull. *176*, 31–35. https://doi.org/10.2307/1541645.

28. Gow, N.A.R., and Morris, B.M. (1995). The electric fungus. Bot. J. Scotl. *47*, 263–277.

29. Olsson, S., and Hansson, B.S. (1995). Action potential-like activity found in fungal mycelia is sensitive to stimulation. Naturwissenschaften *82*, 30–31. https://doi.org/10.1007/BF01167867.

30. Gow, N.A. (1984). Transhyphal electrical currents in fungi. J. Gen. Microbiol. *130*, 3313–3318. https://doi.org/10.1099/00221287-130-12-3313.

31. Adamatzky, A. (2023). Fungal Machines: Sensing and Computing with Fungi (Springer Nature).

32. Adamatzky, A. (2022). Language of fungi derived from their electrical spiking activity. R. Soc. Open Sci. *9*, 211926. https://doi.org/10.1098/rsos.211926.

33. Adamatzky, A. (2018). On spiking behaviour of oyster fungi *Pleurotus djamor*. Sci. Rep. *8*, 7873. https://doi.org/10.1038/s41598-018-26007-1.

34. Adamatzky, A. (2018). Towards fungal computer. Interface Focus *8*, 20180029. https://doi.org/10.1098/rsfs.2018.0029.

35. Adamatzky, A., and Gandia, A. (2021). On Electrical Spiking of Ganoderma resinaceum. Biophys. Rev. Lett. *16*, 133–141. https://doi.org/10.1142/s1793048021500089.

36. Mayne, R., Roberts, N., Phillips, N., Weerasekera, R., and Adamatzky, A. (2023). Propagation of electrical signals by fungi. Biosystems *229*, 104933. https://doi.org/10.1016/j.biosystems.2023.104933.

37. Blatt, M.R., Pullum, G.K., Draguhn, A., Bowman, B., Robinson, D.G., and Taiz, L. (2024). Does electrical activity in fungi function as a language? Fungal Ecology *68*, 101326. https://doi.org/10.1016/j.funeco.2023.101326.

38. Buffi, M., Cailleau, G., Kuhn, T., Li Richter, X.Y., Stanley, C.E., Wick, L.Y., Chain, P.S., Bindschedler, S., and Junier, P. (2023). Fungal drops: a novel approach for macro- and microscopic analyses of fungal mycelial growth. Microlife *4*, uqad042. https://doi.org/10.1093/femsml/uqad042.

39. Fravel, D., Olivain, C., and Alabouvette, C. (2003). *Fusarium oxysporum* and its biocontrol. New Phytol. *157*, 493–502. https://doi.org/10.1046/j.1469-8137.2003.00700.x.

40. Gordon, T.R. (2017). *Fusarium oxysporum* and the Fusarium Wilt Syndrome. Annu. Rev. Phytopathol. *55*, 23–39. https://doi.org/10.1146/annurev-phyto-080615-095919.

41. Joshi, R. (2018). A review of *Fusarium oxysporum* on its plant interaction and industrial use. J. Med. Plants Stud. *6*, 112–115.

42. Zamani, M., Klapperich, C.M., and Furst, A.L. (2023). Recent advances in gold electrode fabrication for low-resource setting biosensing. Lab Chip *23*, 1410–1419. https://doi.org/10.1039/d2lc00552b.

43. Islam, M.S., Banik, S., and Collinson, M.M. (2023). Recent Advances in Bimetallic Nanoporous Gold Electrodes for Electrochemical Sensing. Nanomaterials *13*, 2515. https://doi.org/10.3390/nano13182515.

44. Basch, H., and Gadebusch, H.H. (1968). In vitro antimicrobial activity of dimethylsulfoxide. Appl. Microbiol. *16*, 1953–1954.

45. Al-Mualem, Z., Lorenz-Ochoa, K., Pan, L., Ren, H., and Baiz, C. (2023). Water DMSO Cosolvent Mixtures Modulate Hydrogen Bonding at a Gold Electrode Interface. https://doi.org/10.26434/chemrxiv-2023-9x6ht.

46. Buffi, M., Kelliher, J.M., Robinson, A.J., Gonzalez, D., Cailleau, G., Macalindong, J.A., Frau, E., Schintke, S., Chain, P.S.G., Stanley, C.E., et al. (2025). Electrical signaling in fungi: past and present challenges. FEMS Microbiol. Rev. *49*, fuaf009. https://doi.org/10.1093/femsre/fuaf009.

47. Buzsaki, G., Anastassiou, C.A., and Koch, C. (2012). The origin of extracellular fields and currents–EEG, ECoG, LFP and spikes. Nat. Rev. Neurosci. *13*, 407–420. https://doi.org/10.1038/nrn3241.

48. Akinci, T.C., Seker, S., Türkpençe, D., Korkmaz, U., and Kalin, F. (2020). Detection of Epileptic Seizure Using STFT and Statistical Analysis. In Advances in Neural Signal Processing, R. Vinjamuri, ed.. https://doi.org/10.5772/intechopen.89026.

49. Heideman, M., Johnson, D., and Burrus, C. (1984). Gauss and the history of the fast Fourier transform. IEEE ASSP Mag. *1*, 14–21.

50. Goyal, D., and Pabla, B.S. (2015). Condition based maintenance of machine tools—A review. CIRP J. Manuf. Sci. Technol. *10*, 24–35.

51. Hausser, M., Raman, I.M., Otis, T., Smith, S.L., Nelson, A., du Lac, S., Loewenstein, Y., Mahon, S., Pennartz, C., Cohen, I., and Yarom, Y. (2004). The beat goes on: spontaneous firing in mammalian neuronal microcircuits. J. Neurosci. *24*, 9215–9219. https://doi.org/10.1523/JNEUROSCI.3375-04.2004.

52. Guyton, A., and Hall, J. (2006). Textbook of Medical Physiology (Elsevier Saunders), p. 323.

53. Mudrilov, M., Ladeynova, M., Grinberg, M., Balalaeva, I., and Vodeneev, V. (2021). Electrical Signaling of Plants under Abiotic Stressors: Transmission of Stimulus-Specific Information. Int. J. Mol. Sci. *22*, 10715. https://doi.org/10.3390/ijms221910715.

54. Krausko, M., Perutka, Z., Šebela, M., Šamajová, O., Šamaj, J., Novák, O., and Pavlovič, A. (2017). The role of electrical and jasmonate signalling in the recognition of captured prey in the carnivorous sundew plant Drosera capensis. New Phytol. *213*, 1818–1835. https://doi.org/10.1111/nph.14352.

55. Bohm, J., Scherzer, S., Krol, E., Kreuzer, I., von Meyer, K., Lorey, C., Mueller, T.D., Shabala, L., Monte, I., Solano, R., et al. (2016). The Venus Flytrap *Dionaea muscipula* Counts Prey-Induced Action Potentials to Induce Sodium Uptake. Curr. Biol. *26*, 286–295. https://doi.org/10.1016/j.cub.2015.11.057.

56. Li, J.H., Fan, L.F., Zhao, D.J., Zhou, Q., Yao, J.P., Wang, Z.Y., and Huang, L. (2021). Plant electrical signals: A multidisciplinary challenge. J. Plant Physiol. *261*, 153418. https://doi.org/10.1016/j.jplph.2021.153418.

57. Lew, R.R. (2011). How does a hypha grow? The biophysics of pressurized growth in fungi. Nat. Rev. Microbiol. *9*, 509–518. https://doi.org/10.1038/nrmicro2591.

58. Baliga, B.S., Pronczuk, A.W., and Munro, H.N. (1969). Mechanism of cycloheximide inhibition of protein synthesis in a cell-free system prepared from rat liver. J. Biol. Chem. *244*, 4480–4489.

59. Desai, C. (2016). Meyler's Side Effects of Drugs: The International Encyclopedia of Adverse Drug Reactions and Interactions (Medknow).

60. Pal, S., Manjunath, B., Ghorai, S., and Sasmal, S. (2018). Benzoxazole alkaloids: occurrence, chemistry, and biology. Alkaloids - Chem. Biol. *79*, 71–137.

61. Brand, A., and Gow, N.A.R. (2009). Mechanisms of hypha orientation of fungi. Curr. Opin. Microbiol. *12*, 350–357. https://doi.org/10.1016/j.mib.2009.05.007.

62. Brand, A., Shanks, S., Duncan, V.M.S., Yang, M., Mackenzie, K., and Gow, N.A.R. (2007). Hyphal orientation of Candida albicans is regulated by a calcium-dependent mechanism. Curr. Biol. *17*, 347–352. https://doi.org/10.1016/j.cub.2006.12.043.

63. Kumamoto, C.A. (2008). Molecular mechanisms of mechanosensing and their roles in fungal contact sensing. Nat. Rev. Microbiol. *6*, 667–673. https://doi.org/10.1038/nrmicro1960.

64. Itani, A., Masuo, S., Yamamoto, R., Serizawa, T., Fukasawa, Y., Takaya, N., Toyota, M., Betsuyaku, S., and Takeshita, N. (2023). Local calcium signal transmission in mycelial network exhibits decentralized stress responses. PNAS Nexus *2*, pgad012. https://doi.org/10.1093/pnasnexus/pgad012.

65. Meysman, F.J.R. (2018). Cable Bacteria Take a New Breath Using Long-Distance Electricity. Trends Microbiol. *26*, 411–422. https://doi.org/10.1016/j.tim.2017.10.011.

66. Humphries, J., Xiong, L., Liu, J., Prindle, A., Yuan, F., Arjes, H.A., Tsimring, L., and Süel, G.M. (2017). Species-Independent Attraction to Biofilms through Electrical Signaling. Cell *168*, 200–209.e12. https://doi.org/10.1016/j.cell.2016.12.014.

67. Houdinet, G., Guerrero-Galán, C., Rose, B.D., Garcia, K., and Zimmermann, S.D. (2023). Secrets of the fungus-specific potassium channel TOK family. Trends Microbiol. *31*, 511–520. https://doi.org/10.1016/j.tim.2022.11.007.

68. Hall, A.H. (2007). Cyanide and related compounds—Sodium azide. In Haddad and Winchester's Clinical Management of Poisoning and Drug Overdose (Elsevier), pp. 1309–1316.

STAR★METHODS

KEY RESOURCES TABLE

REAGENT or RESOURCE	SOURCE	IDENTIFIER
Biological samples		
Fusarium oxysporum	Laboratory of Microbiology	NEU 195
Chemicals, peptides, and recombinant proteins		
Cycloheximide (20 mg/ml),	Thermo Fisher Scientific	357420050
Voriconazole (12,5 μg/ml)	Sandoz®	65064
Calcimycin (1.3 mg/ml)	Merck	CAS 52665-69-7
Sodium azide (6.5 mg/ml)	Merck	45/Kit-No 78374
Deposited data		
Raw Data recordings	This work	https://doi.org/10.17632/srkxbkh6sp.1
Software and algorithms		
Code for STFT analysis	This work	Document S2
Other		
PCB card for recordings	Prototypos.ch	This Work
ADC-24 data logger	https://www.picotech.com	-
Shielded armoured cable D-Sub	(Phoenix Contact, mouser.ch	651-2302146

EXPERIMENTAL MODEL AND STUDY PARTICIPANT DETAILS

The experimental model corresponded to *Fusarium oxysporum* Neu 195, a fungal strain obtained from the fungal and bacterial collection of the laboratory of microbiology, University of Neuchâtel, Switzerland.

METHOD DETAILS

Inocula preparation

For the regular maintenance, the organism was plated on Malt Extract Agar (12g/l malt extract [“Support Is Our Success”; SIOS® homebrew, Switzerland, Ref: XE201], 15g/l Technical Agar [Biolife, Japan, Ref: 4110254], 1 l deionized water). *F. oxysporum* was grown for 2 weeks on Potato Dextrose Agar (39 g/l PDA stock powder [CARLROTH®, Germany, Ref: AE92.2]) to induce spore production, spores were then collected washed and re-suspended in 50ml MQ water and stored at 4°C for use. Prior to the experiment, 100 μl of the spore suspension were added to 900 μl of liquid Potato Dextrose Broth (4g/l Potato infusion [MERCK Sigma-Aldrich, Germany, Ref: 52424], 20g/l D[+] Glucose monohydrate [CARLROTH®, Germany, Ref: 6887.1], 1 l deionized water) and well mixed. Then 20 μl of the suspension were deposited on the electrodes (1, 3, 5, 9, 11, 13) at a final concentration of around 350 spores for each drop.

Measurement set-up

A high-resolution data logger ADC-24 (Pico Technology, UK) was used to measure voltage potential changes in fungal mycelium. Instead of the sub dermal needles used in previous studies we designed the fungal potential card (FPC), a printed circuit board card with 8 couples of embedded ENIG Electro-less Nickel / Immersion Gold electrodes (Figure S1). The FPC was designed and produced by prototypos SARL (prototypos.ch). The card was connected to the ADC-24 via a shielded armoured cable D-Sub (Phoenix Contact, 651-2302146, mouser.ch) for noise-free recordings. The card was placed inside a tailored-made incubator to keep the system at above 80% humidity. For this, a plastic storage container (l: 21.5, w: 12.5, h: 9.5 cm) was used. A dent (height 2.5 cm) was open on one of the short sides of the box to insert one end of the shielded cable. The remaining space was closed with aquarium silicon to avoid water evaporation and contamination. A 1 cm hole was created on the lid and plugged with a hydrophobic filter to permit gas exchange without reduction of humidity. Inside the incubator, a cylindrical piece of plastic was glued to the bottom to act as a holder of the FPC card (1.5 cm height). Vermiculite was deposited on the bottom of the box (covering one 1 cm) and moistened with sterile MilliQ water to keep high humidity. In addition to the plastic holder, to avoid the card from touching the vermiculate, two rubber caps were fixed between the card and the plastic box to block the FPC in place. A second dent was created in between the lid and the box to pass the grounding cable and attach it from the armoured cable to the Faraday cage. The Faraday cage was made from an aluminium box (ALUTEC aluminium box classic 30, l: 40, w: 30, h: 25 cm). We removed the rubber band separating the lid from

the box. A hole of 1.5 cm between the lid and the box was cut to pass the cable inside the box. The conductivity of the Faraday cage was tested from the lid (box closed) to the end of the cable attached to the ADC-24 with the aid of a multimeter.

Testing of electrode sizes

Different sizes of electrode were tested (1, 2, 3, 4 mm diameter). A single FPC with the four sizes were produced and tested. Each line was of a different size for a total of 2 couples of electrodes per size. In each case, one of the couples was used as an empty control, on which only the medium (PDB) was added. The second electrode pair was inoculated with a spore suspension on PDB.

QUANTIFICATION

Signal recording

Once the optimal electrode size to be used in the FPC cards was defined (2 mm; Figure S2), several experiments were designed to evaluate the biological origin of the recorded signals. For this, five different chemicals were used, including four antimicrobial agents: cycloheximide (20 mg/ml), voriconazole (12.5 μg/ml), calcimycin (1.3 mg/ml), and sodium azide (6.5 mg/ml). To add the stimuli, the fungus was inoculated on the first electrode and left to colonize the target electrode for seven days. At this point the ADC-24 was paused to avoid noise recording, because to add the stimuli the faraday cage and the incubator needed to be open. With the aid of a micropipette 2 μl of the stimuli (2.5 μl for Voriconazole to attend the good final concentration of 12.5 ug/ml) were added to one of the empty controls (drops without spores) and to the target drop of 3 inoculated electrode pairs. As an additional control, the solvent in which the compounds were dissolved was added to the second empty control and to the target drop of the remaining three inoculated electrode pairs. The solvent was respectively MilliQ water for cycloheximide, voriconazole, and sodium azide; DMSO for calcimycin. After addition of the stimuli, the ADC-24 recording was restarted immediately and the recording continued for another three days to measure the reaction of the fungus. At the end of the experiment pictures of all the boards were taken with a stereoscope (NIKON SMZ18) to confirm the colonisation of the second electrode.

Induction testing on fungal drop setup

As the system is currently a black box with no possibilities to observe directly fungal development, we performed the induction experiment in cell culture treated Petri dishes.[38] For this the same media and spore suspension were used as described above. As *F. oxysporum* grows faster in this system compared to PCB cards, the stimuli were added after five days and not seven as in the electrical measurement. Microscopical pictures were taken in between the drops and inside the target drops using an inverted microscope (EVOS FL, EVOS M5000, Invitrogen) before the addition of the stimuli and two days after addition to observe the outcome.

Short-time Fourier transform

Measurements from the ADC-24 Precision Data Logger (Pico Technology, UK) were acquired using the PicoLog 6 Software (Pico Technology, UK), exported in HDF5 format and analysed in MATLAB R2024a. The signal was sampled with a conversion time per channel of 60 ms and thus a sampling frequency of approximately 17 Hz. The potential on the electrodes was analysed both over time and in a time-frequency representation to analyse the frequency spectrum of the signals as they changed over time. After reading the HDF5 files, Not-a-Number (NaN) values were removed from all channels, caused by the loss of some acquisition samples and by the ADC-24 Precision Data Logger pausing during the stimuli addition phase. For time-frequency domain representation, the short-time Fourier transform (STFT) of each signal was calculated. Calculating a STFT means running small time windows along the signal and calculating the fast Fourier transform (FFT) in each time segment. This gives the frequency content of the signal in the time enclosed in the window. The squared amplitude of the STFT is represented in a time-frequency diagram, i.e., the spectrogram. The STFT was calculated using a Blackman – Harris window with a length of 1024 samples and a window overlap percentage of 80% to improve temporal resolution.

Statistical analysis

To conduct a quantitative comparative analysis and associate each spectrum of the different channels with a unique value, the average power was calculated by integrating the power spectral density (PSD). The signals were extracted before and after induction, segmented into intervals of 3 days each. To avoid aliasing phenomena, a low-pass filter was applied that limited the spectrum to 4 Hz; since the spectral content is mainly concentrated below 4 Hz, the signals were subsampled to 8 Hz. The PSD was calculated in each time window (after induction), allowing the average power to be determined. The average power values obtained from the three "Fungi + Induction" channels were subsequently averaged with each other. Similarly, the same operation was performed for the "Fungi + Control" channels. To compare the extracted PSD values, all pairwise comparisons were performed using Welch's t-test, which does not assume equal variances between groups, after confirming the normality of the data using the Shapiro–Wilk test (Table 1). We did not include comparisons with the controls without fungi, as only a single replicate was available for each card in this condition. Additionally, we calculated the percentage increase or decrease in PSD values from the Induction condition to the Control for each experimental condition. Furthermore, to quantify the presence/colonization of the fungus, we pooled similar conditions before the induction and compared those with the controls for all electrodes. This was done as described before and a t-test was used to compare the two groups.

Supplementary Material Chapter 4

Detection of electrical signals in fungal mycelia in response to external stimuli

Publication date: 17 October 2025

CellPress: iScience

DOI: https://doi.org/10.1016/j.isci.2025.113484

iScience, Volume *28*

Supplemental information

Detection of electrical signals in fungal mycelia in response to external stimuli

Matteo Buffi, Silvia Giangaspero, Valerio Foiada, Loïc Puthod, Guillaume Cailleau, Aaron J. Robinson, Julia M. Kelliher, Patrick S.G. Chain, Daniel Oberson, Markus Künzler, Saskia Bindschedler, Lorenzo Pirrami, and Pilar Junier

Supplemental items

This PDF file includes:

Figs. S1 to S7

Method S1- code for analysis

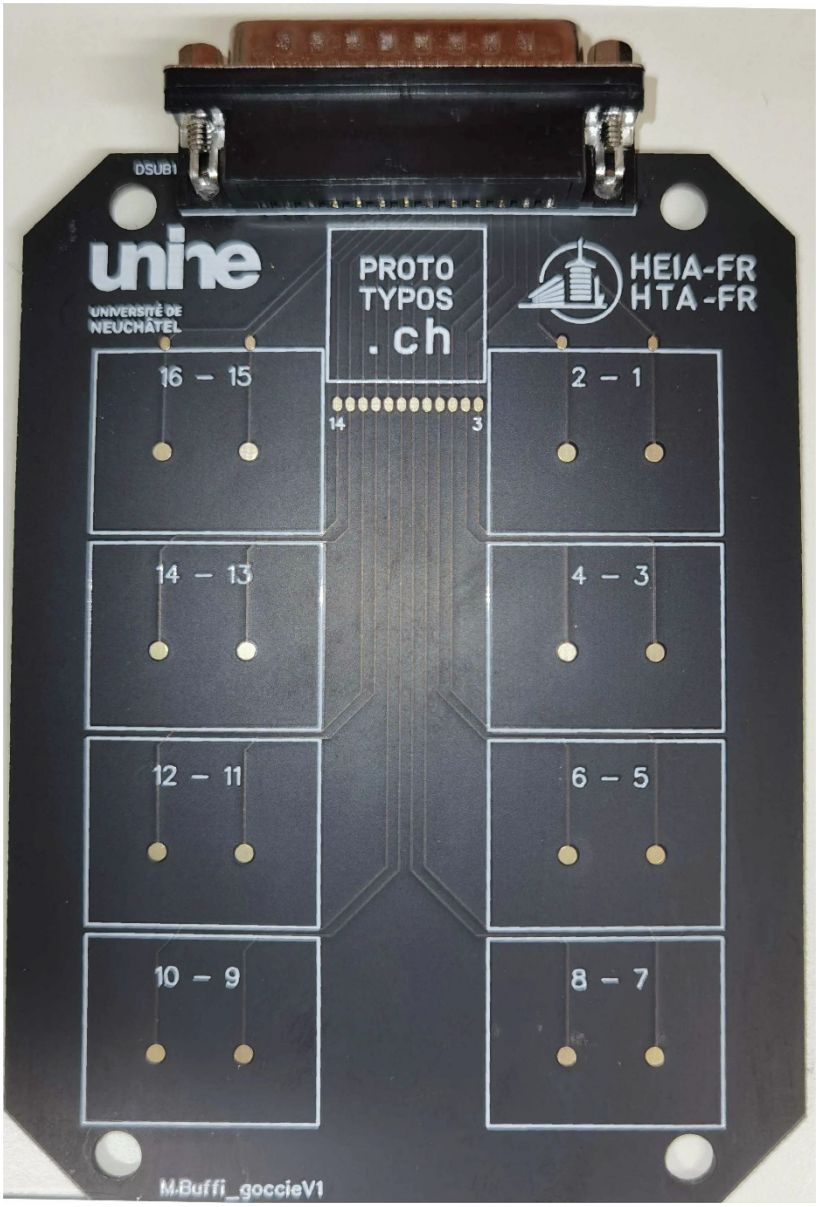

Fig. S1. Image of a printed circuit board (PCB) with embedded gold covered electrodes. Couples of electrodes (1-2, 3-4, 5-6, 7-8, 9-10, 11-12, 13-14, 15-16) are used for the differential measurements resulting in voltage changes between the two electrodes. The PCB were designed by Valerio Foiada, prototypos.ch.

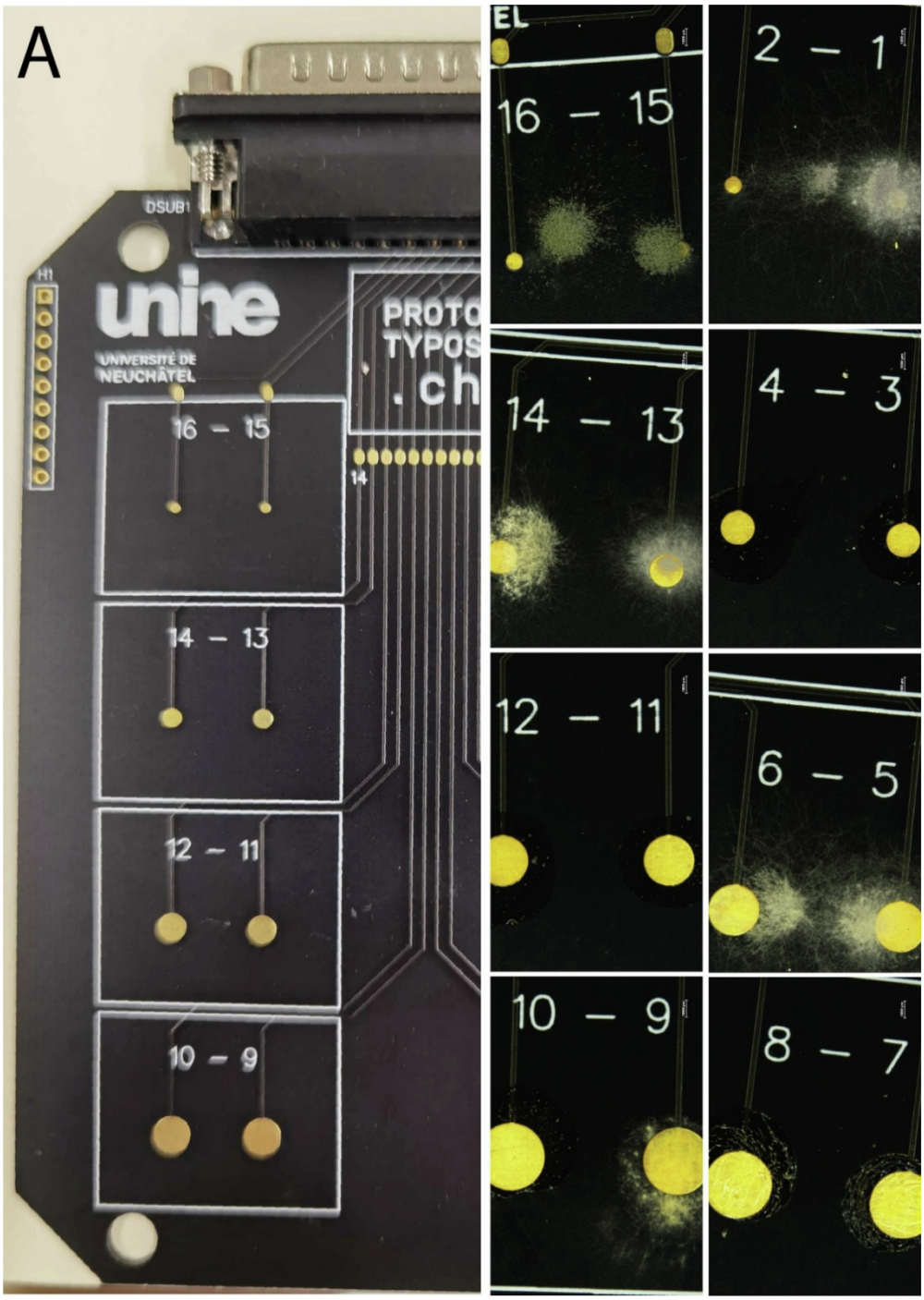

Fig. S2. Testing of optimal electrode size for colonization and recording using circuit board (PCB) with different size electrodes. Empty PCB with embedded gold covered electrodes of different size (from the top electrode sizes of 1, 2, 3 and 4 mm). The pictures on the right show the results obtained during the testing for the growth of *Fusarium oxysporum* on electrodes of different size.

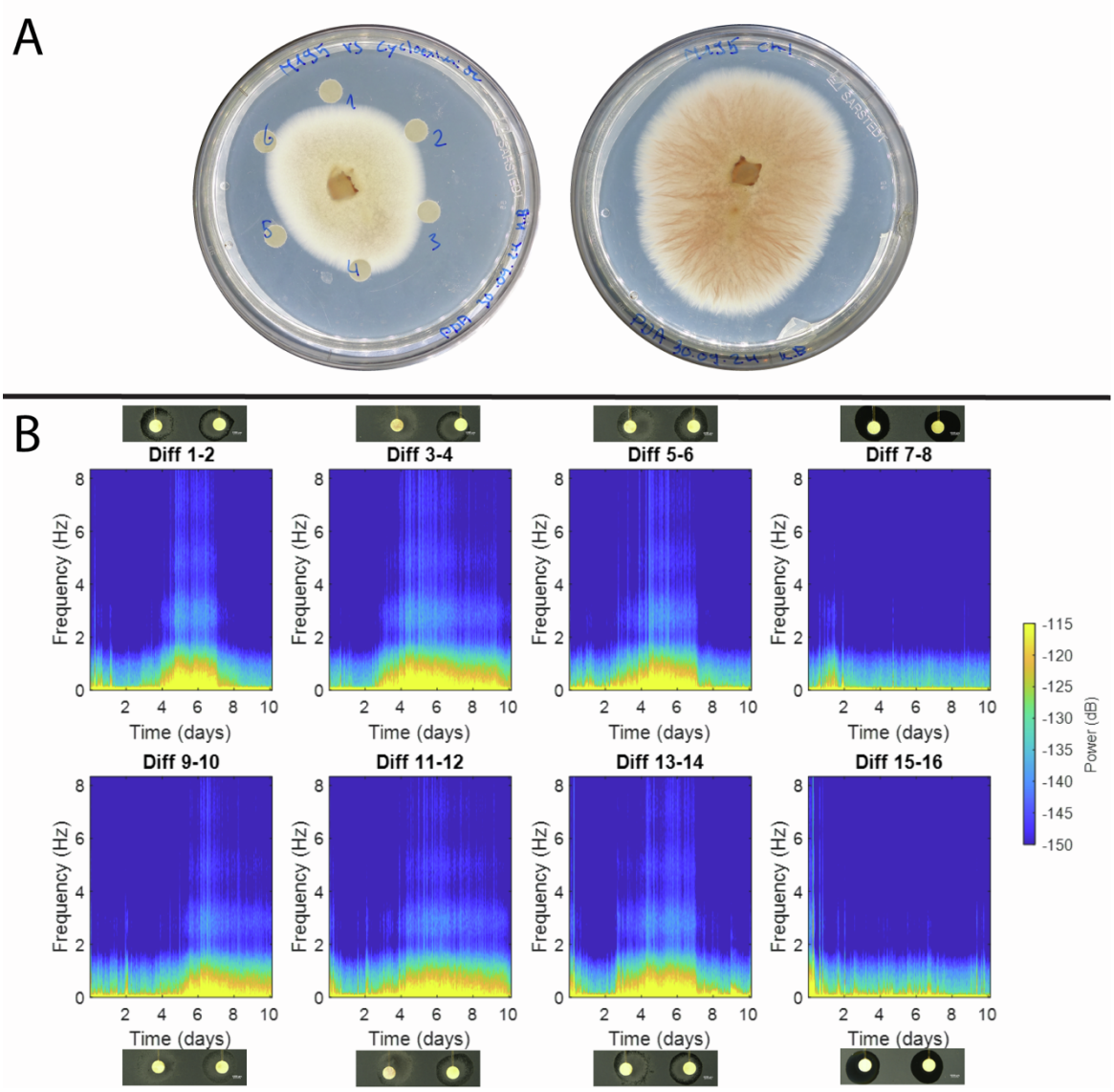

Fig. S3. Effect of cycloheximide on electrical signaling. (**A**) Susceptibility test for cycloheximide and MilliQ water (carrier). The antifungal was applied in the discs 1, 3, and 5 and compared to MilliQ water (discs 2, 4, and 6 (image on the left). Growth on the absence of the discs is shown on the right. (**B**) Differential electrodes colonized by *Fusarium oxysporum* for stimulation with addition of cycloheximide (1-2, 5-6, 13-14, 15-16) or Milli-Q water (3-4, 7-8, 9-10, 11-12), respectively. Electrodes 7-8 and 15-16 were non-inoculated and acted as controls. Pictures were taken with a stereoscope (NIKON SMZ18). All the replicates were performed in the same PCB. The addition of either Cycloheximide (1-2, 5-6, 13-14, 15-16) or Milli-Q water (3-4, 7-8, 9-10, 11-12) was performed at day 7. The images were created with MatLab.

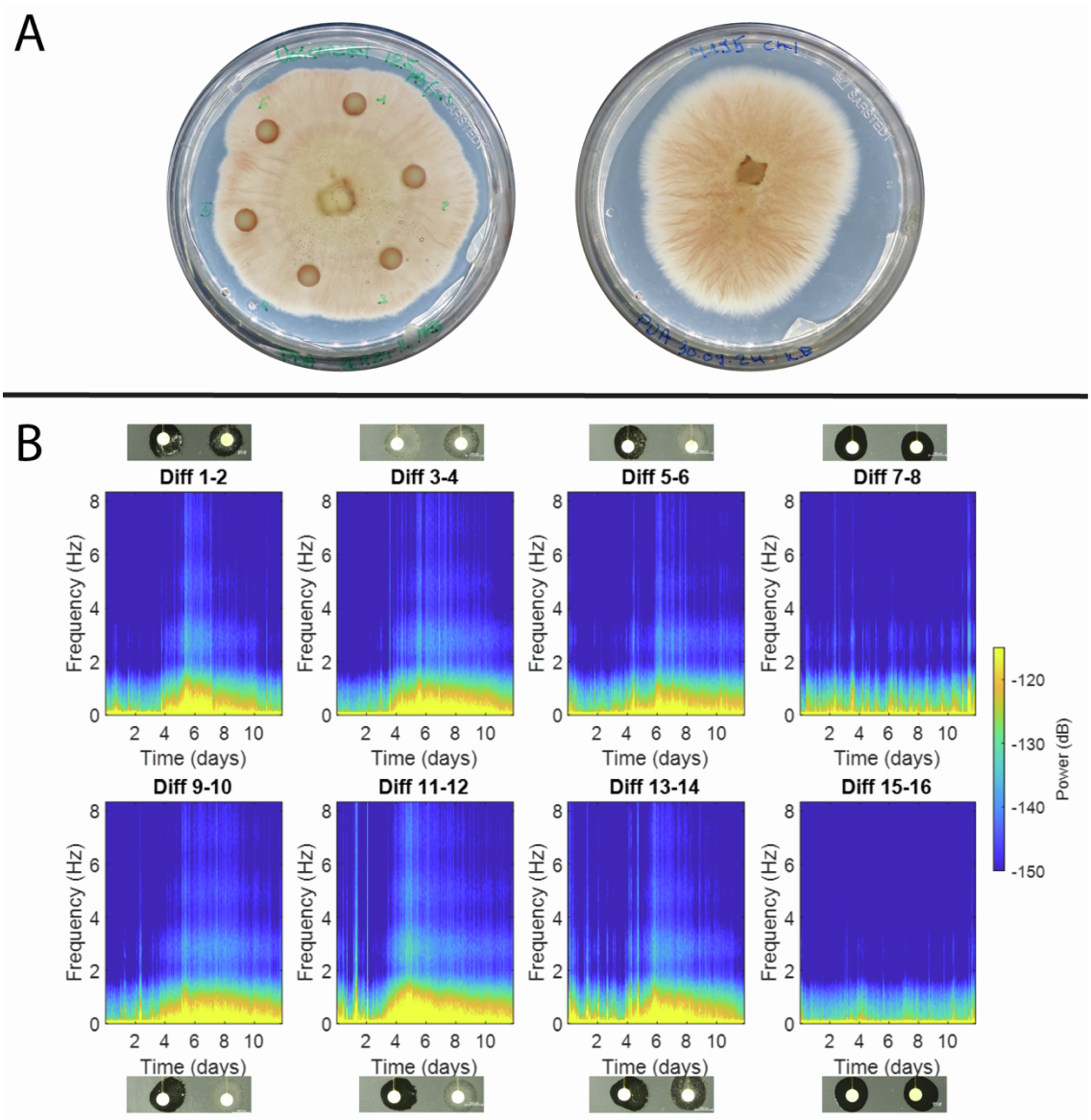

Fig. S4. Effect of voriconazole on electrical signaling. (**A**) Susceptibility test for voriconazole and MilliQ water (carrier). The antifungal was applied in the discs 1, 3, and 5 and compared to MilliQ water (discs 2, 4, and 6 (image on the left). Growth on the absence of the discs is shown on the right. (**B**) Differential electrodes colonized by *Fusarium oxysporum* for stimulation with addition of either voriconazole (1-2, 9-10, 11-12, 15-16) or Milli-Q water (3-4, 5-6, 7-8, 13-14), respectively. Electrodes 7-8 and 15-16 were non-inoculated and act as a control. Pictures were taken with a stereoscope (NIKON SMZ18). All the replicates were performed in the same PCB. The addition of either calcimycine (1-2, 9-10, 11-12, 15-16) or DMSO (3-4, 5-6, 7-8, 13-14) was performed at day 7. The images were created with MatLab.

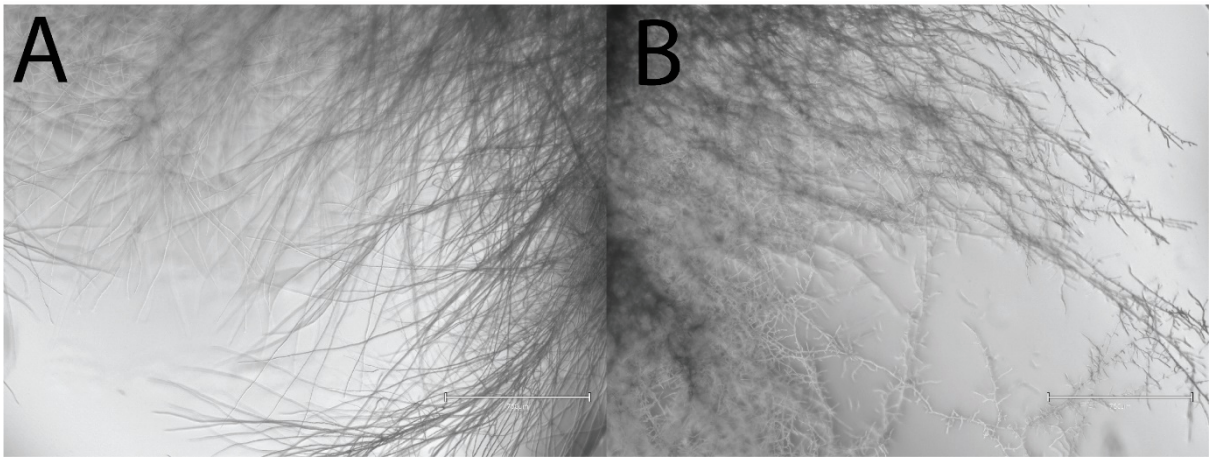

Fig. S5. Effect of voriconazole on growth. Observation of *F. oxysporum* 3 days after the addition of Voriconazole in a drop system. (A) Normal growth after addition of Milli-Q water. (B) Branching of hyphae after addition of Voriconazole. Microscopical pictures were performed with an inverted microscope (Invitrogen, EVOS FL, EVOS M5000).

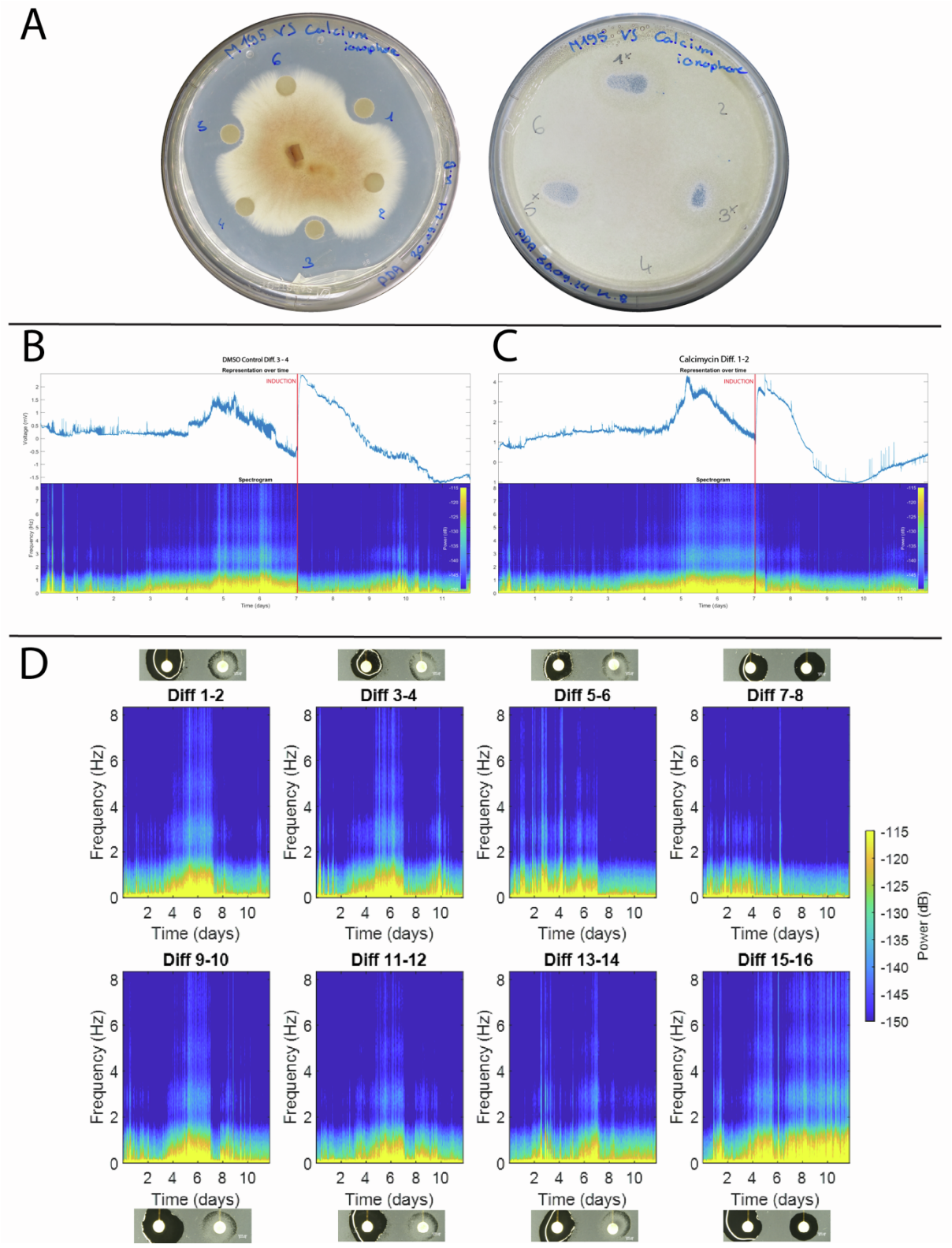

Fig. S6. Effect of calcimycin on electrical signaling. (**A**) Susceptibility test for calcimycin and its solvent (DMSO). On the left *Fusarium oxysporum* was placed using an agar plug on standard potato dextrose agar (PDA); on the right column the fungus was inoculated as spores (final concentration 2 mio) mixed with soft PDA (PDA with only 6 g.l- 1of agar) and poured on a bottom layer of normal PDA. Induction was performed by placing 5 µl of either the tested drug (calcimycin) in 3 different places around the inoculum/center of the Petri dish in positions 1, 3 and 5. The solvent (DMSO) was added in position 2, 4 and 6. The inhibitory effect of calcimycin on both mycelial growth and spore inoculum was observed after 2 days post inoculation. (**B - C**) Frequency change analysis of electrical recordings in *F. oxysporum* in response to calcimycin and DMSO.

Representative recordings for the control carrier (DMSO, **B**) or the corresponding stimulant (calcimycin, **C**) are shown. After 7 days, the recording was stopped (red line) and the stimulant was added to the system. The recording continued after stimulation. (**D**) Differential electrodes colonized by *F. oxysporum* for the testing of either calcimycin (1-2, 5-6, 7-8, 13-14) or DMSO (3-4, 9-10, 11-12, 15-16), respectively. Electrodes 7-8 and 15-16 are non-inoculated and act as a control. Pictures were taken with a stereoscope (NIKON SMZ18). All the replicates were performed in the same PCB. The addition of either voriconazole (1-2, 5-6, 7-8, 13-14) or Milli-Q water (3-4, 9-10, 11-12, 15-16) was performed at day 7. The images were created with MatLab.

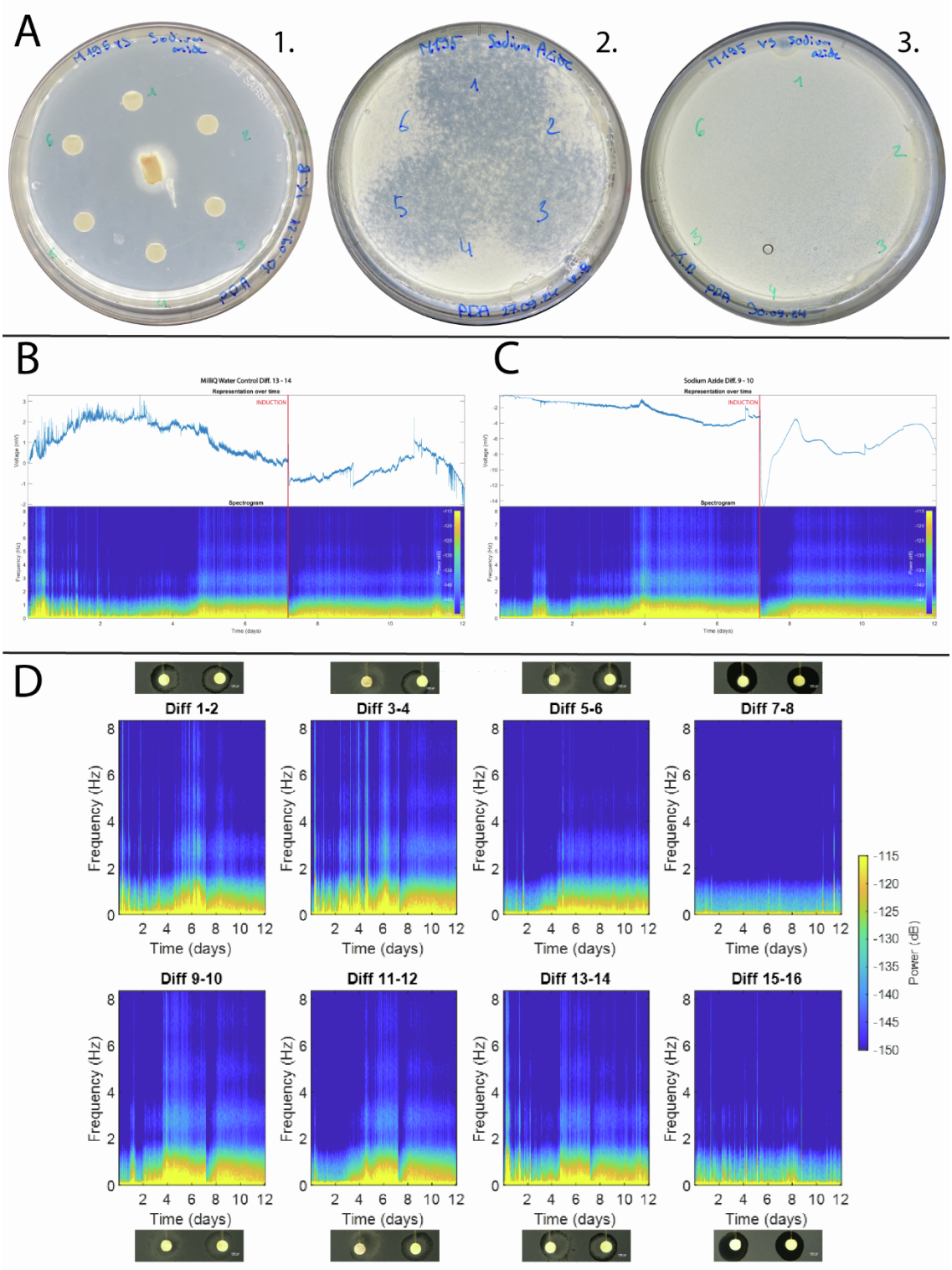

Fig. S7. Effect of sodium azide on electrical signaling. (**A**) Susceptibility test for sodium azide and its solvent (MilliQ water). On the left column (A.1.) *Fusarium oxysporum* was placed using an agar plug on standard potato dextrose agar (PDA); on the right (A.2., A.3.) the fungus was inoculated as spores (final concentration 2 mio) mixed with soft PDA (PDA with only 6 g.l- 1of agar) and poured on a bottom layer of normal PDA. Induction was performed by placing 5 µl of either the tested drug (sodium azide) in 3 different places around the inoculum/center of the Petri dish in positions 1, 3 and 5. The solvent (MilliQ water) was added in position 2, 4 and 6. The stimulant was added with the inoculum for the first two (A.1., A.2.) and at 6 dpi for the last one (A.3.) The inhibitory effect of sodium azide on both mycelial growth and spore inoculum was observed after 2 days post inoculation (A.1., A.2.) or post stimuli addition (A.3.). For controls refer to Supplementary Figure 4A. (**B - C**) Frequency change analysis of electrical recordings in *F. oxysporum* in

response to sodium azide and MilliQ water, representative recordings for the control carrier (MilliQ water, **B**) or the corresponding stimulant (sodium azide, **C**) are shown. After 7 days, the recording was stopped (red line) and the stimulant was added to the system. The recording continued after stimulation. (**D**) Differential electrodes colonized by *F. oxysporum* for the testing with addition of either sodium azide (3-4, 9-10, 11-12, 15-16) or Milli-Q water (1-2, 5-6, 7-8, 13-14), respectively. Electrodes 7-8 and 15-16 are non-inoculated and act as a control. Pictures were taken with a stereoscope (NIKON SMZ18). All the replicates were performed in the same PCB. The addition of either sodium azide (3-4, 9-10, 11-12, 15-16) or Milli-Q water (1-2, 5-6, 7-8, 13-14) was performed at day 7. The images were created with MatLab.

Method S1- Detailed procedure for STFT analysis

Table of Contents


```
clc;
clear;
close all;

infostrings = ["Diff 1-2" "Diff 3-4" "Diff 5-6"...
                "Diff 7-8" "Diff 9-10" "Diff 11-12"...
                 "Diff 13-14" "Diff 15-16"];

dt        = 60e-3;                  % temporal resolution (s)
fs        = 1/dt;                   % sampling frequency (Hz)

% ------------------------------------------------------------------------
% CHANGE
%
% 1) FILENAME with PATH TO THE HDF5 FILE
%
% 2) SUBSTANCE with NAME OF INJECTED SUBSTANCE
% ------------------------------------------------------------------------

substance = "Cycloheximide";

filename = "";

% ------------------------------------------------------------------------

%h5disp(filename)

data.diff1_2 = h5read(filename,'/Differenziale 1 - 2');
data.diff3_4 = h5read(filename,'/Differenziale 3 - 4');
data.diff5_6 = h5read(filename,'/Differenziale 5 - 6');
data.diff7_8 = h5read(filename,'/Differenziale 7 - 8');
data.diff9_10 = h5read(filename,'/Differenziale 9 - 10');
data.diff11_12 = h5read(filename,'/Differenziale 11 - 12');
data.diff13_14 = h5read(filename,'/Differenziale 13 - 14');
data.diff15_16 = h5read(filename,'/Differenziale 15 - 16');

fields = fieldnames(data);
numchann = length(fields);
N = length(data.(fields{1}));
time = linspace(1, N*dt-dt, N); % in seconds
```

Removing NaNs

```
% Find the channel with the most NaN values
maxNaN = -1;
maxNaNChannel = '';
for i = 1:numchann
    numNaN = sum(isnan(data.(fields{i})));
    if numNaN > maxNaN
        maxNaN = numNaN;
        maxNaNChannel = fields{i};
    end
end

disp(['Channel with the most NaN values: ', maxNaNChannel]);

nanIndices = find(isnan(data.(maxNaNChannel)));

% Remove NaN indices from other channels to match lengths
for i = 1:numchann
        data.(fields{i})(nanIndices) = [];
end

time(nanIndices) = [];
N = length(time);

disp('NaN values have been removed and channels have been aligned.');

% %% Downsampling at 8 Hz
%
% fsNew = 8;          % new sampling frequency (Hz)
% dtNew = 1/fsNew;    % new temporal resolution (s)
%
% factorDown = round(fs/fsNew);
% timeDown = downsample(time, factorDown);
% Ndown = length(timeDown);
%
% % downsampling
% for i = 1 : numchann
%     dataDown.(fields{i}) = downsample(data.(fields{i}), factorDown);
% end
```

Plot raw data

```
figure
for i = 1 : numchann
    plot(time/(60*60*24), data.(fields{i})*1e3);
    hold on;
end
title(substance)
legend(infostrings)
xlabel('Time (days)'); ylabel('Voltage potential (mV)');
axis tight
```

```
grid on;
ax = gca;
ax.GridAlpha = 0.3;  % Set grid transparency to make it lighter
ax.XGrid = 'on';
ax.XMinorGrid = 'on';
ax.XMinorTick = 'on';
ax.XAxis.MinorTickValues = time(1)/(60*60*24):1/4:time(end)/(60*60*24); % Set
minor ticks for every 6 hours
```

Short - Time Fourier Transform

```
% Parameters
win = blackmanharris(1024);         % Increased window length
Overlap = 800;                      % Increased overlap
FFTLength = 2048;                   % Increased FFT length

for i = 1:numchann

    figure
    tile_l = tiledlayout(2, 1, 'TileSpacing', 'none', 'Padding', 'compact');

    % Plot the time-domain signal (downsampled)
    ax1 = nexttile;
    plot(time/(60*60*24), data.(fields{i})*1e3);
    axis tight;
    ylabel('Voltage (mV)');
    title('Representation over time');
    set(gca, 'XTick', []);

    % Calculate and plot the spectrogram
    ax2 = nexttile;
    [~,F,T,P] = spectrogram(data.(fields{i})-mean(data.(fields{i})), win,
Overlap, FFTLength, fs, 'yaxis', 'power');

    % Smooth the spectrogram with a 2D Gaussian filter
    sigma = 2; % Standard deviation of the Gaussian kernel
    P_smoothed = imgaussfilt(10*log10(P + eps), sigma);

    imagesc(T/(60*60*24), F, P_smoothed);

    axis xy;
    ylabel('Frequency (Hz)');
    xlabel('Time (days)');
    title('Spectrogram');
    % Modified Colorbar Placement
    h = colorbar('east', 'Color', 'white');
    h.Label.String = 'Power (dB)';
    clim([-150 -115]);

    % Add overall title
    title(tile_l, sprintf('%s - %s', substance, infostrings(i)), 'FontSize',
12);
```

```
end

% Create a single figure for all STFT plots
figure

for i = 1:numchann
    % Calculate the spectrogram for each channel
    subplot(2, 4, i);
    [~, F, T, P] = spectrogram(data.(fields{i}) - mean(data.(fields{i})),
win, Overlap, FFTLength, fs, 'yaxis', 'power');

    % Smooth the spectrogram with a 2D Gaussian filter
    sigma = 4; % Standard deviation of the Gaussian kernel
    P_smoothed = imgaussfilt(10*log10(P + eps), sigma);

    imagesc(T/(60*60*24), F, P_smoothed);
    axis xy;
    ylabel('Frequency (Hz)');
    xlabel('Time (days)');
    title(infostrings(i));

    % Emphasize color differences and smooth representation
    clim([-150 -115]); % Set the range of colors for better emphasis
end

% Adjust colorbar to cover all subplots
colorbar;

% Add colorbar label
h = colorbar;
h.Label.String = 'Power (dB)';

% Add an overall title to the figure
sgt = sgtitle(substance);
sgt.FontSize = 10;
```

Published with MATLAB® R2024b

General Discussion

1. Revisiting Electrophysiology in Fungi: A Need for New Tools

The core objective of this thesis was to identify a clear, ideally visual, method for observing electrical signals within the mycelium. Historically, techniques adapted from animal electrophysiology were used to study fungal hyphae. These included glass electrodes inserted directly into hyphae (Slayman & Slayman, 1962) and extracellular vibrating microelectrodes (Jaffe & Nuccitelli, 1974), all discussed in chapter one. Our approach aimed to update these methods while being as non-invasive as possible, to preserve the system in a state as close as possible to its natural condition. Personally, I believe that fungi—accustomed to regulating their networks in natural environments—may block or reroute signals when disrupted by an electrode or high-frequency vibration. Moreover, as someone without a background in electrical engineering or classical electrophysiology, I aimed to find a method that made sense from a biological perspective. In an ideal scenario, such signals could be visualized through fluorescent dyes or membrane proteins that respond to changes in membrane potential (Grinvald et al., 1982). To pursue this goal, I tested various approaches: measuring resistance changes using microrobotics (Imina), recording extracellular signals via high-density multi-electrode arrays (3Brain, Switzerland), applying fluorescent voltage-sensitive dyes such as Thioflavin T, and using subdermal electrodes with a datalogger (ADC24, Pico Technology) to capture signals in macrostructures like fructifications. Additionally, we searched for homologues of known ion channel genes involved in electrical signaling in other organisms. These genes appear conserved across most of the species examined, though functional validation through gene knockout studies remains necessary. However, their presence may point to a shared evolutionary origin for electrical signaling, even if these genes likely served entirely different functions millions of years ago. Our largely negative results, summarized in chapter one, nevertheless confirmed key hypotheses—such as the insulating role of the fungal cell wall—and highlighted the challenges of applying traditional electrophysiological methods to fungi. The lack of established protocols and reference data made it difficult to know what signals to expect, or even how to recognize them. Despite years of inconclusive or null results, this process led to the development of a new methodology for investigating electrical activity in fungi. As the saying goes, not all bad things come to harm.

2. Spatial Control and the Architecture of Fungal Networks

In this thesis, I aimed to understand how filamentous fungi regulate their mycelium in response to their surrounding environment. One of the first challenges was to gain control over where and how filamentous organisms grow. As previously introduced, filamentous fungi continuously reorganize their mycelium while exploring new areas. This dynamic restructuring allows, for instance, mycorrhizal fungi to optimize exchanges between the foraging site and the area of contact with tree roots (Oyarte Galvez et al., 2025). Previous studies suggest the existence of trunk hyphae—larger filaments connected by a network of smaller hyphae—which act as primary channels for nutrient exchange and potentially for coordination signals (Schmieder et al., 2019). Although specialized hyphae have not been confirmed in all species, the absence of evidence is not the evidence of absence. Therefore, it was essential to develop a system that enabled localized fungal growth from one area (e.g., a nutrient pool) to another (e.g., a sink), with a clear physical separation between the two. This setup was necessary to investigate whether electrical signals exist within the mycelium and whether they facilitate growth or nutrient absorption as hypothesized. If such signals do occur, they must pass through the mycelium connecting the two zones in order to re-organize the network.

3. Mycelial Responses to Local Stimuli: Growth and Nutrient Sensing

The second chapter of this thesis addressed the development of such a system. Through a simple droplet-based setup, I observed how fungi explored their environment and whether directional growth occurred in response to different stimuli or nutrient sources. The experiments presented in the article, along with additional unreported observations, showed that our organisms are indeed capable of growing toward, and reinforcing connections with, droplets containing higher nutrient concentrations. The results of this second chapter, support the idea of learning, in this case growing towards the source with more nutrients after discovering all of them, and a "basal cognition" in fungi as in other studies (Aleklett & Boddy, 2021).

4. Highways and Hitchhikers: Tracking Bacteria on Fungal Networks

To further explore the utility of this system, we also looked at how bacteria interact with the fungal mycelium. In chapter three, we extended this work to include bacterial dynamics on the mycelium. This thesis presents one of the first methodologies for observing the movement of individual bacteria along the hyphae of a pseudo-fungus, i.e. *Pythium ultimum*. Pseudo-fungi are organisms that morphologically resemble filamentous fungi but differ significantly in their composition and genetics. A key distinction relevant to this study is that Oomycetes, a prominent group of pseudo-fungi, do not contain chitin as a major component of their cell walls, whereas true fungi do. Our aim was to better understand the conditions under which bacterial transport occurs and how different strains may exhibit different colonisation strategies. In a simple experiment, we were able to observe how differences in movement speed between two strains of the same bacterium could underlie distinct strategies for colonizing new areas. This aligns with previous studies (De Boer et al., 2005; Junier et al., 2021; Ritz & Young, 2004; Simon, 2016), which emphasize the role of filamentous organisms as social architects of the soil. A deeper understanding of these interactions is crucial to assess the ecological consequences of a decline in these organisms. Such knowledge could also be instrumental in designing microbial consortia for bioremediation that are capable of self-propagation within the soil. It may also benefit biotechnological applications involving interactions between filamentous fungi and other microorganisms, such as in industrial fermentation, natural product synthesis, or environmental remediation (Frey-Klett et al., 2011; Kohlmeier et al., 2005; Zhang et al., 2018).

5. Building the Fungal-Potential-Cards: A New Experimental Platform

In chapter four, we integrated insights gained throughout the project to create the Fungal-Potential-Cards (FPC). This new system, developed with electronic engineers and data scientists, allows for reproducible, non-invasive signal detection. Instead of penetrating the mycelium, electrodes are positioned underneath it. Each card includes two nutrient droplets (stimulus and response zones) separated by an inert area, with electrodes placed directly beneath the droplets. Spores inoculated on Electrode A consistently led to mycelial growth toward Electrode B, following directional patterns established in earlier experiments. The eight-replicate layout and standardized conditions improved reproducibility. This open system also permits the application of external stimuli, enhancing its experimental flexibility.

Future improvements may include optimizing electrode materials, refining signal detection sensitivity, and integrating additional analytical tools.

6. From Waves to Meaning: Signal Processing and Frequency Analysis

One of the major challenges of this approach was data processing. With measurements taken every 60 milliseconds over the span of a week, the volume of data generated was immense. Traditional approaches to voltage analysis often search for action potential-like spikes—rapid depolarizations followed by hyperpolarization and refractory periods. While insightful in neuronal systems, this model is reductive when applied to fungi. The anthropocentric view of action potentials is relevant mainly to specialized structures like neurons and is much less common in other organs or organisms (Lee & Calvo, 2023). For instance, plants employ additional mechanisms such as system potentials, which are much slower and consist of a single voltage wave propagating throughout the organism (Zimmermann et al., 2009). Action potentials similar to those observed in animals are only found in organisms requiring rapid reactions, such as carnivorous plants (Böhm et al., 2016; Krausko et al., 2017). For other functions, the signaling process is likely slower. However, if fast electrical signals do exist in fungi, they could be involved in rapid processes such as the closing of nematode traps—structures requiring immediate action. For most other physiological or ecological roles, however, slower signaling mechanisms are likely more relevant. Fungi, like plants, may instead rely on slower electrical signals such as system potentials. The "all-or-nothing" principle of action potentials is better suited to organisms that require rapid response times. It seems unlikely that fungi operate using the same mechanism. Still, they may encode information in a different way: through frequency. Frequency coding—akin to Morse code—is a powerful model where meaning is conveyed not by the shape of a signal, but by the timing and frequency of impulses. Even in animal neurons, this principle is fundamental(Jadeja, 2021). We hypothesized that fungal electrical signals could be similarly decoded. To test this, we applied frequency analysis tools such as the Fourier Transform (FT) and Short-Time Fourier Transform (STFT). While FT provides a breakdown of frequency components, STFT allowed us to visualize how these frequencies evolve over time—especially important for non-stationary signals like those generated by fungal systems (Zhou et al., 2023). Initial results revealed clear differences in signal patterns between colonized and uncolonized electrodes. While more advanced signal processing techniques—such as wavelet transforms or empirical mode decomposition (EMD)—could further

enhance resolution (Manjula & Sarma, 2012), our results mark an important first step. In future studies, combining these tools with machine learning could significantly improve signal classification (Bhamare & Suryawanshi, 2018).

7. Applications and Outlook: From Biomedicine to Bioremediation

Although this thesis did not fully define a mechanism for fungal network coordination, I am proud to have introduced frequency analysis as a valuable tool for studying fungal electrophysiology. I hope that researchers across fields—from plant biology to microbial ecology—can build upon these findings to explore how frequency coding may underpin physiological processes in non-neuronal organisms. This research could also serve as a basis for high-throughput screening systems to assess fungal responses to antifungal agents or environmental stressors. For example, targeting ion channels or membrane proteins involved in electrical signaling could uncover new therapeutic strategies. Likewise, evaluating how pollutants like microplastics or heavy metals affect electrical responses may offer novel ways to monitor soil health and ecosystem resilience. Moreover, the integration of fluorescent biosensors with microfluidic systems may allow real-time visualization of signal propagation within the mycelium. Combined with machine learning and refined data filtering methods, such tools could unlock the complexity of fungal communication. Ultimately, as fungal biology continues to gain attention across disciplines—from ecology and medicine to biotechnology and materials science—this is the ideal moment to invest/support in innovative methods for their study. By advancing how we observe, measure, and interpret fungal behaviour, we may not only unravel the logic behind mycelial networks but also gain new insights into the evolutionary roots of biological coordination across life forms.

8. Final Reflections

The process of writing this thesis has profoundly changed the way I see my subject of study. What began as a journey into a relatively underexplored area—often met with scepticism—soon became an immersion into the infinite complexity of the mycelial network. From the beginning, I was convinced that fungi are underestimated, and I set out, perhaps naively, to help demonstrate the existence of an electrical communication system within them. At first, I imagined the fungus as an organism with a thousand hands, convinced it must generate action potentials, perhaps driven by potassium given its abundance in soil. Now, six years

later, I often think back to those early philosophy courses where we were introduced to Socrates' famous words: "I know that I know nothing." I find myself completely identifying with that sentiment. Throughout the years, I held onto my project—sometimes with confidence, other times with doubt, and the journey has been like a rollercoaster. Many disagreed with my hypotheses, and yet, that resistance only strengthened my determination. I still know that I do not know—but if I may venture a thought—I no longer see the fungus as a body with a thousand hands, but rather as a body with a thousand heads, much like the mythological Hydra. It would not surprise me if, in the future, a central role in fungal electrical communication were attributed to the Spitzenkörper, with septa contributing to signal maintenance. Even if these two structures are not present in all fungi. Perhaps the Spitzenkörper itself could one day be recognized as the elusive "head" or "brain" of the fungus—something we so instinctively look for when we try to understand organisms through an animal-centric lens. As for the mechanisms involved, I believe we must remain open to discovery. Given the evolutionary convergence that often occurs in fungi, the underlying mechanisms of this communication may not only vary between different fungal groups but even among species—yet still serve the common goal of managing the extraordinarily complex mycelium. With the methods and reflections presented in this thesis, I sincerely hope to support other researchers in exploring fungal electrical communication—not only in detail, but with a mindset open to the unknown and to the possibility of mechanisms that complement what we already know. This work would never have been possible without interdisciplinary collaboration spanning biology, physics, chemistry, and mathematics. For this reason, I would like to emphasize the importance of fostering cross-disciplinary partnerships in future research. From my perspective, complex networks resemble one another through the appearance of a seemingly unstructured web. This pattern is evident in neurons, the internet, street and trade routes, social networks, and, of course, mycelium. A recent image of the universe gas filaments connecting "galaxies" (Tornotti et al., 2025) reminded me of the many hours I spent observing my networks under the microscope.

To me, these resemblances are not merely coincidental. So I ask: *what does truly make a complex network complex?*

Bibliography

Aleklett, K., & Boddy, L. (2021). Fungal behaviour: a new frontier in behavioural ecology. *Trends in Ecology & Evolution*, *36*(9), 787–796. https://doi.org/10.1016/J.TREE.2021.05.006

Bhamare, D., & Suryawanshi, P. (2018). Review on Reliable Pattern Recognition with Machine Learning Techniques. In *Fuzzy Information and Engineering* (Vol. 10, pp. 362–377). Taylor and Francis Ltd. https://doi.org/10.1080/16168658.2019.1611030

Böhm, J., Scherzer, S., Krol, E., Kreuzer, I., Von Meyer, K., Lorey, C., Mueller, T. D., Shabala, L., Monte, I., Solano, R., Al-Rasheid, K. A. S., Rennenberg, H., Shabala, S., Neher, E., & Hedrich, R. (2016). The venus flytrap dionaea muscipula counts prey-induced action potentials to induce sodium uptake. *Current Biology*, *26*(3), 286–295. https://doi.org/10.1016/J.CUB.2015.11.057/ATTACHMENT/0552DDBD-CEE1-4737-A8D4-B90AC7A3BFC7/MMC2.PDF

De Boer, W., Folman, L. B., Summerbell, R. C., & Boddy, L. (2005). Living in a fungal world: impact of fungi on soil bacterial niche development. *FEMS Microbiology Reviews*, *29*(4), 795–811. https://doi.org/10.1016/J.FEMSRE.2004.11.005

Frey-Klett, P., Burlinson, P., Deveau, A., Barret, M., Tarkka, M., & Sarniguet, A. (2011). Bacterial-Fungal Interactions: Hyphens between Agricultural, Clinical, Environmental, and Food Microbiologists. *Microbiology and Molecular Biology Reviews*, *75*(4), 583–609. https://doi.org/10.1128/MMBR.00020-11/ASSET/8F9A1F3A-704F-4404-A4F4-81F9A4240E1F/ASSETS/GRAPHIC/ZMR9990922840007.JPEG

Grinvald, A., Hildesheim, R., Farber, I. C., & Anglister, L. (1982). Improved fluorescent probes for the measurement of rapid changes in membrane potential. *Biophysical Journal*, *39*(3), 301–308. https://doi.org/https://doi.org/10.1016/S0006-3495(82)84520-7

Jadeja, N. M. (2021). Frequencies and Rhythms. *How to Read an EEG*, 32–39. https://doi.org/10.1017/9781108918923.008

Jaffe, L. F., & Nuccitelli, R. (1974). AN ULTRASENSITIVE VIBRATING PROBE FOR MEASURING STEADY EXTRACELLULAR CURRENTS. *Journal of Cell Biology*, *63*(2), 614–628. https://doi.org/10.1083/jcb.63.2.614

Junier, P., Cailleau, G., Palmieri, I., Vallotton, C., Trautschold, O. C., Junier, T., Paul, C., Bregnard, D., Palmieri, F., Estoppey, A., Buffi, M., Lohberger, A., Robinson, A., Kelliher, J.

M., Davenport, K., House, G. L., Morales, D., Gallegos-Graves, L. V., Dichosa, A. E. K., … Chain, P. S. G. (2021). Democratization of fungal highway columns as a tool to investigate bacteria associated with soil fungi. *FEMS Microbiology Ecology*, *97*(2). https://doi.org/10.1093/FEMSEC/FIAB003

Kohlmeier, S., Smits, T. H. M., Ford, R. M., Keel, C., Harms, H., & Wick, L. Y. (2005). Taking the Fungal Highway: Mobilization of Pollutant-Degrading Bacteria by Fungi. *Environmental Science and Technology*, *39*(12), 4640–4646. https://doi.org/10.1021/ES047979Z

Krausko, M., Perutka, Z., Šebela, M., Šamajová, O., Šamaj, J., Novák, O., & Pavlovič, A. (2017). The role of electrical and jasmonate signaling in the recognition of captured prey in the carnivorous sundew plant Drosera capensis. *New Phytologist*, *213*(4), 1818–1835. https://doi.org/10.1111/NPH.14352

Lee, J., & Calvo, P. (2023). The potential of plant action potentials. *Synthese*, *202*(6), 1–30. https://doi.org/10.1007/S11229-023-04398-7/METRICS

Manjula, M., & Sarma, A. V. R. S. (2012). Comparison of empirical mode decomposition and wavelet based classification of power quality events. *Energy Procedia*, *14*, 1156–1162. https://doi.org/10.1016/j.egypro.2011.12.1069

Oyarte Galvez, L., Bisot, C., Bourrianne, P., Cargill, R., Klein, M., van Son, M., van Krugten, J., Caldas, V., Clerc, T., Lin, K. K., Kahane, F., van Staalduine, S., Stewart, J. D., Terry, V., Turcu, B., van Otterdijk, S., Babu, A., Kamp, M., Seynen, M., … Shimizu, T. S. (2025). A travelling-wave strategy for plant–fungal trade. *Nature 2025 639:8053*, *639*(8053), 172–180. https://doi.org/10.1038/s41586-025-08614-x

Ritz, K., & Young, I. M. (2004). Interactions between soil structure and fungi. *Mycologist*, *18*(2), 52–59. https://doi.org/10.1017/S0269915X04002010

Schmieder, S. S., Stanley, C. E., Rzepiela, A., van Swaay, D., Sabotič, J., Nørrelykke, S. F., deMello, A. J., Aebi, M., & Künzler, M. (2019). Bidirectional Propagation of Signals and Nutrients in Fungal Networks via Specialized Hyphae. *Current Biology*, *29*(2), 217-228.e4. https://doi.org/https://doi.org/10.1016/j.cub.2018.11.058

Simon, A. (2016). *Highways and subways : a story of fungi and bacteria in soils*. Université de Neuchâtel, Faculté des sciences. http://data.rero.ch/01-R008430461/html?view=NJ_V1 http://doc.rero.ch/record/278339

Slayman, C. L., & Slayman, C. W. (1962). Measurement of Membrane Potentials in Neurospora. *Science*, *136*(3519), 876–877. https://doi.org/10.1126/SCIENCE.136.3519.876

Tornotti, D., Fumagalli, M., Fossati, M., Benitez-Llambay, A., Izquierdo-Villalba, D., Travascio, A., Arrigoni Battaia, F., Cantalupo, S., Beckett, A., Bonoli, S., Dayal, P., D'Odorico, V., Dutta, R., Lusso, E., Peroux, C., Rafelski, M., Revalski, M., Spinoso, D., & Swinbank, M. (2025). High-definition imaging of a filamentary connection between a close quasar pair at z = 3. *Nature Astronomy*. https://doi.org/10.1038/s41550-024-02463-w

Zhang, Y., Kastman, E. K., Guasto, J. S., & Wolfe, B. E. (2018). Fungal networks shape dynamics of bacterial dispersal and community assembly in cheese rind microbiomes. *Nature Communications 2018 9:1*, *9*(1), 1–12. https://doi.org/10.1038/s41467-017-02522-z

Zhou, B., Song, Y., & Ai, J. (2023). Time-frequency analysis of non-stationary signals based on short-time Fourier transform. *ACM International Conference Proceeding Series*, 245–248. https://doi.org/10.1145/3654446.3654490

Zimmermann, M. R., Maischak, H., Mithöfer, A., Boland, W., & Felle, H. H. (2009). System Potentials, a Novel Electrical Long-Distance Apoplastic Signal in Plants, Induced by Wounding. *Plant Physiology*, *149*(3), 1593–1600. https://doi.org/10.1104/pp.108.133884

Collaborations

Here is a list of publications generated by collaborations during my Ph.D thesis:

Robinson, Aaron J., et al. "Widespread bacterial diversity within the bacteriome of fungi." *Communications biology* 4.1 (2021): 1168.

DOI: https://doi.org/10.1038/s42003-021-02693-y

Junier, Pilar, et al. "Democratization of fungal highway columns as a tool to investigate bacteria associated with soil fungi." *FEMS microbiology ecology* 97.2 (2021): fiab003.

DOI: https://doi.org/10.1093/femsec/fiab003

Kuhn, Thierry, et al. "Design and construction of 3D printed devices to investigate active and passive bacterial dispersal on hydrated surfaces." *BMC biology* 20.1 (2022): 203.

DOI: https://doi.org/10.1186/s12915-022-01406-z

Périat, Claire, et al. "Host and nonhost bacteria support bacteriophage dissemination along mycelia and abiotic dispersal networks." *Microlife* 5 (2024): uqae004.

DOI: https://doi.org/10.1093/femsml/uqae004

Oral presentations

Zurich mycology symposium 10.06.2022:

Title: Fungal drops: a novel method for the observation of fungal modularity and coordination

Swiss Society for Microbiology 31.08.2022:

Title: Fungal drops: a novel method for the observation of fungal modularity and coordination

8th. Swiss Microbial Ecology Meeting 19.01.2023:

Title: Development of an inexpensive and fast method to study and quantify modularity in filamentous fungi at both the mycelial and hyphal scales

(Winner of best oral presentation)

MATTEO BUFFI

Mobile: +41 76 349 69 24
E-mail: buffi91@gmail.com
Linkedin

About me

I am trained as a biologist with a specialization in microbiology, chemical ecology, and sustainable agriculture. My main interest lies in the protection and maintenance of natural systems, with a focus on plant-fungus interactions. My doctoral research not only led to the development of innovative methods for studying mycetes but also fostered interdisciplinary collaborations, underscoring the value of cross-disciplinary synergy and knowledge exchange. These experiences have honed my leadership abilities, project management skills, and have instilled a profound appreciation for the power of collaborative innovation. As a sociable, inquisitive individual with a passion for problem-solving, strategy and innovation, I am keenly interested in all sciences and perpetually eager to absorb new knowledge. I am particularly enthusiastic about leveraging my scientific background and interdisciplinary approach in management roles, aiming to bridge gaps between scientific research and practical, sustainable solutions. I am interested in challenges outside of my academic background.

Skills

Lab skills	Microbial cultures, strain isolation, molecular methods (DNA extraction, DNA quantification, PCR, gel electrophoresis), biochemistry methods basics
Personal Skills	Autonomous, strategic, reliable, problem solving, coaching, supervision, teaching, communication to different audiences.
IT	Microsoft Office Suite, RStudio. Adobe Illustrator, Image J, Python (basics), Linkedin, OpenAI, and other Ai tools
Languages	Italian (native), French (fluent, Bachelor in French), English (fluent, MSc and Ph.D. in English, public presentations).

Education

2019 – Present	**PhD thesis in microbiology,** Laboratory of microbiology**,** University of Neuchâtel**,** ongoing (Defence 13 May)
2017 – 2019	**Student in Master of Science in Biology**. *Cum laude.* Specialization: Chemical Ecology, Sustainable Agriculture, Laboratory of Microbiology. University of Neuchâtel, switzerland.
2014 – 2017	**Bachelor of Science in Biology**. University of Neuchâtel, Switzerland.
2008 – 2012	**High School degree (SSS) in Biology-Chemistry**, Liceo di Locarno, Ticino, Switzerland.

Continuous learning

Patenting in life sciences and chemistry
Innosuisse business concept

Research experience

2019 – Present	**PhD thesis in microbiology,** Laboratory of microbiology**,** University of Neuchâtel**,** ongoing.
2018 – 2019	**Master thesis in Microbiology,** Laboratory of Microbiology, University of Neuchâtel.

	"Old ideas new methods: Re-discovering Filamentous fungi electrical communication".
Apr. – May 2014	**Problem-based learning in Eco-ethology**, Laboratory of Eco-Ethology, University of Neuchâtel. "House sparrow responses to Carrion crow vocalizations".
Mar. – Apr. 2014	**Problem-based learning in parasitology**, Laboratory of Parasitology, University of Neuchâtel. "Food choice in malaria vector *Anopheles gambiae* after infection by *Plasmodium berghei*".
Feb. – Mar. 2017	**Problem-based learning in microbiology**, Laboratory of Microbiology, University of Neuchâtel. "Biocontrol of pathogenic fungi with the utilization of oxalotrophic bacteria".

Teaching experience

Ph.D.	**PhD student assistant** for the practical of Microbiology for 2nd year Biology students, Laboratory of Microbiology, University of Neuchâtel. **PhD student assistant** for the Problem-based learning in Microbiology for 3rd year Biology students, Laboratory of Microbiology, University of Neuchâtel. **PhD student assistant** for the practical of Molecular Biology for 1st year Master BGS students, Laboratory of Microbiology, University of Neuchâtel. **PhD student assistant** for the course of Biostatistics for 3rd year Biology students, Laboratory of Parasitology, University of Neuchâtel.
Master	**Student-Assistant** for the practical of Histology for 1st year biology students, Laboratory of Microbiology, University of Neuchâtel. **Student-Assistant** for the practical of Molecular Biology and Biochemistry for 3rd year biology students, Laboratory of Microbiology, University of Neuchâtel. **Student-Assistant** for the excursions of microbiology for the 1st year biology students, Laboratory of Microbiology, University of Neuchâtel.

Conferences

19 Jan. 2023	**Swiss Microbial Ecology Meeting**; SUPSI Mendrisio, Switzerland; **presentation** title: "Development of an inexpensive and fast method to study and quantify modularity in filamentous fungi at both the mycelial and hyphal scales".
31 Aug. 2022	**Swiss Society for Microbiology**, EPFL, Lausanne, Switzerland, **presentation** title: "Fungal drops: a novel method for the observation of fungal modularity and coordination".
10 Jun. 2022	**Zürich Mycology Symposium**; Neuchâtel University, Switzerland; **presentation** title: "Fungal drops: a novel method for the observation of fungal modularity and coordination".
Jul. 2019	**AFMBioMed summer school** 2018, Marseille, France.
Mar. 2019	**Electromicrobiology 2019**, Aarhus University, Denmark. Travel grant for **poster** presentation: "Electric signaling in filamentous fungi".

Prizes and subventions

January 2023	**Best oral presentation** at the **Swiss Microbial Ecology Meeting**, SUPSI Mendrisio.
March 2019	Travel grant for **Electromicrobiology symposium** at Aahrus University, Denmark.

Supervising experiences

2021 – 2022	**Co-advising** of Junna Frei (Master student), Laboratory of Microbiology, University of Neuchâtel.
2021 – 2022	**Co-advising** of Margaux Leisi (Master student), Laboratory of Microbiology, University of Neuchâtel.
2021	**Co-advising** of Matys Constantino (Biology technician trainee), Laboratory of Microbiology, University of Neuchâtel.
2021	**Co-advising** of Laura Blanco Pérez (Bachelor student), Laboratory of Microbiology, University of Neuchâtel.
2019	**Advising** for laboratory practices of the new master students in Mycology.

Event organization:

Sep. 2022	**Co-organizer** of the annual Ph.D meeting of the university of Neuchâtel at the Natural history Museum, Neuchâtel. Title: Science and Society.

External collaborations / public mandates:

Translator French – Italian, English – Italian for the Service Learning "Microbes go to school".
Fungal and Bacterial identifications for private and public mandates.
In charge for the preparation and signal registration of carpophores for the art exposition: "I wanna say a word" by Maëlle Gross 27-29 October, Berlin, Germany (to be performed also at the Natural History Museum, Neuchâtel).
Partecipation to the work group charged of improving the Master in Biology at the University of Neuchâtel.

Media:

May 2023	« Le langage subtil des champignons » Avis d'expert, CQFD, RTS. **Interview**
Mar. 2023	« Subtilités de langage : Secrets de Champignons », En Direct journal, Université de Franche-Comté. **Article**
28 Jul. 2022	« Les ondes électriques des champignons », Les bonnes ondes, RTS. **Interview**
2 Dec. 2021	"Les champignons champions de la transaction écologique », Avis d'expert, CQFD, RTS. **Interview**

Publications:

Published	Matteo Buffi, Guillaume Cailleau, Thierry Kuhn, Xiang-Yi Li Richter, Claire E Stanley, Lukas Y Wick, Patrick S Chain, Saskia Bindschedler, Pilar Junier, **Fungal drops: a novel approach for macro- and microscopic analyses of fungal mycelial growth**, *microLife*, Volume 4, 2023, uqad042, https://doi.org/10.1093/femsml/uqad042
Published	Buffi, M., Kuhn, T., Gonzalez, D. *et al.* **Assessing the speed of individual bacteria dispersing on mycelial networks.** *Evol Ecol* (2025). https://doi.org/10.1007/s10682-025-10329-4

Published

Matteo Buffi, Julia M Kelliher, Aaron J Robinson, Diego Gonzalez, Guillaume Cailleau, Justine A Macalindong, Eleonora Frau, Silvia Schintke, Patrick S G Chain, Claire E Stanley, Markus Künzler, Saskia Bindschedler, Pilar Junier, **Electrical signaling in fungi: past and present challenges,** *FEMS Microbiology Reviews*, 2025; fuaf009, https://doi.org/10.1093/femsre/fuaf009

Submitted:

Matteo Buffi, Silvia Giangaspero, Valerio Foiada, Loïc Puthod, Guillaume Cailleau, Aaron J. Robinson, Julia M. Kelliher, Patrick S.G. Chain, Daniel Oberson, Markus Künzler, Saskia Bindschedler, Lorenzo Pirrami, Pilar Junier, **Detection of electrical signals in fungal mycelia in response to external stimuli,** Submitted the 11.04.2025

References

On request